# BERWICK BANK WIND FARM
# **OFFSHORE ENVIRONMENTAL IMPACT ASSESSMENT**

# APPENDIX 7.1: PHYSICAL PROCESSES TECHNICAL REPORT

**EOR0766**
**Environmental Impact Assessment – Appendix 7.1**
**Final**

## Document Status

| Version | Purpose of Document | Authored by | Reviewed by | Approved by | Review Date |
|---|---|---|---|---|---|
| FINAL | Final | RPS | RPS | RPS | November 2022 |

## Approval for Issue

| | | |
|---|---|---|
| Sarah Edwards | S Edwards | 30 November 2022 |

| | |
|---|---|
| Prepared by: | **RPS** |
| Prepared for: | **SSE Renewables** |
| Checked by: | **Douglas Watson** |
| Accepted by: | **Ross Hodson** |
| Approved by: | **Sarah Edwards** |



The report has been prepared for the exclusive use of our client.

The report has been compiled using the resources agreed with the client and in accordance with the scope of work agreed with the client. No liability is accepted by RPS for any use of this report, other than the purpose for which it was prepared. The report does not account for any changes relating to the subject matter of the report, or any legislative or regulatory changes that have occurred since the report was produced and that may affect the report. RPS does not accept any responsibility or liability for loss whatsoever to any third party caused by, related to or arising out of any use or reliance on the report.

RPS accepts no responsibility for any documents or information supplied to RPS by others and no legal liability arising from the use by others of opinions or data contained in this report. It is expressly stated that no independent verification of any documents or information supplied by others has been made.

RPS has used reasonable skill, care and diligence in compiling this report and no warranty is provided as to the report's accuracy.

# CONTENTS



## TABLES



## FIGURES

# 1. INTRODUCTION

1. This Physical Processes Technical Report provides information relating to the physical environment and coastal processes for the offshore components of the Berwick Bank Wind Farm (hereafter referred to as the “Proposed Development”). It describes the current baseline conditions and quantifies the potential changes due to the installation and presence of the Proposed Development. This report is divided into two main sections:

- baseline conditions – describing current hydrography and sedimentology; and
- environmental variations – describing changes to baseline arising from the installation and presence of the Proposed Development.

2. For the purposes of this Physical Processes Technical Report physical processes are defined as encompassing the following elements:

- tidal elevations and currents;
- waves;
- bathymetry;
- seabed sediments;
- suspended sediments; and
- sediment transport.

3. The physical processes modelling presented in this technical report relates to the Proposed Development site boundary as described in volume 1, chapter 3 of the Offshore Environmental Impact Assessment (EIA) Report, which supports an Application for development consent submitted in December 2022. In June 2022, this (‘the current Proposed Development site boundary’) was reduced from the previous Berwick Bank Wind Farm boundary (as detailed in SSER, 2021a), but contains the same proposed infrastructure.

# 2. STUDY AREA

4. The physical processes study area for the Proposed Development is illustrated in Figure 2.1 and defined as the:

- Proposed Development array area (i.e. the area in which the wind turbines will be located);
- Proposed Development export cable corridor;
- landfall area; and
- seabed and coastal areas that may be influenced by changes to physical processes due to the Proposed Development, based on the outputs of the physical processes modelling which will encompass a wider domain including the Firth of Forth Banks Complex.

5. It is however noted that the physical processes study area forms the focus for the assessment and that the numerical model extent is not limited to this region. The physical processes study area extends in excess of one tidal excursion from the Proposed Development boundary and would therefore encapsulate the distance suspended sediment is transported prior to being carried back on the returning tide. It includes all banks within the Firth of Forth Bank Complex namely, Berwick Bank, Marr Banks, Montrose and Scalp Banks along with Wee Bankie. The modelling study would therefore also identify potential impacts beyond the physical processes study area.

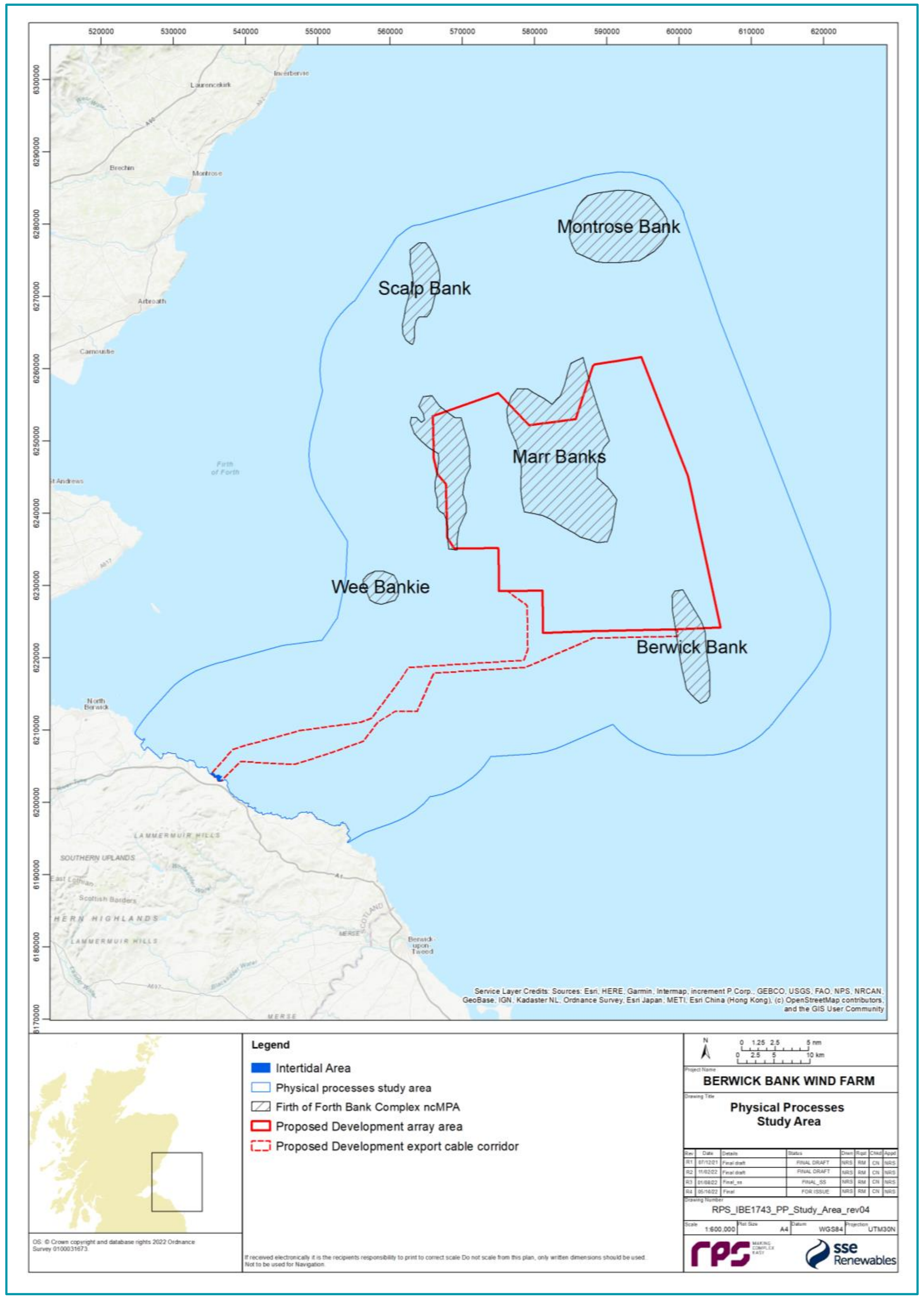


Figure 2.1: Physical Processes Study Area

# 3. METHODOLOGY

## 3.1. NUMERICAL MODELLING

6. Numerical modelling techniques were used to describe tide, wave and sediment transport regimes. The MIKE suite of software was employed, as a single model mesh could be used to simulate these processes both individually and in combination. The model domain is shown in Figure 3.1. The MIKE suite of models is a widely used industry standard modelling suite developed by the Danish Hydraulic Institute (DHI). It has been approved for use by industry and government bodies including the Scottish Environmental Protection Agency (SEPA). The MIKE suite is a modular system that contains a number of different but complementary modules encompassing different physical processes: these are summarised in Table 3.1 and described in further detail within the relevant sections.

**Table 3.1: MIKE Suite of Models**

| Simulation | Model | Description |
|---|---|---|
| Baseline and post-construction tidal flow | MIKE21 Flexible Mesh (FM) modelling system | The FM Module is a 2-dimensional, depth averaged hydrodynamic model which simulates the water level variations and flows in response to a variety of forcing functions in lakes, estuaries and coastal areas. The water levels and flows are resolved on a mesh covering the area of interest when provided with bathymetry, bed resistance coefficient, wind field, hydrodynamic boundary conditions, etc. |
| Baseline and post-construction wave climate | MIKE21 Spectral Wave (SW) | The wave modelling was undertaken using the spectral wave model, MIKE21 SW. The waves were computed on the same grid as the tidal flows. The model resolves the wave field by simulating wind generation of waves within the model domain and the propagation of externally generated swell waves through the domain. The model setup ensured that the detail of both locally generated wind waves and swell conditions from further afield were captured. |
| Baseline and post-construction littoral currents | MIKE21 FM and SW | The MIKE suite facilitates the coupling of models. The depth averaged hydrodynamic model, used for the tidal modelling, coupled with the spectral wave model, provides a full wave climate incorporating the impact of water levels and currents on waves and wave breaking. Using this, the littoral currents (i.e. those currents driven by tidal, wave and meteorological forces) were examined. |
| Baseline and post-construction sediment transport | MIKE21 Sand Transport (ST) | This module enables assessment of bed sediment transport rates and initial rates of bed level change for non-cohesive sediment resulting from currents or combined wave-current flows. It was used to determine the sediment transport pattern on and around all the bank features within the physical processes study area as shown in Figure 2.1. The model combines inputs from both the hydrodynamic model and, if required, the wave propagation model. It uses sediment size and gradation to determine the bed level changes and sediment transport rates. |
| Foundation installation | MIKE21 Mud Transport (MT) | A sample of three representative pile installations were simulated to cover the range of conditions across the Proposed Development array area both in terms of water depth and tidal currents. The MIKE MT module allows the modelling of erosion, transport and deposition of cohesive and cohesive/granular sediments. This model is suited to sediment releases in the water column and allows sediment sources which may vary spatially and temporally. |
| Cable installation | MIKE21 Particle Tracking (PT) | The PT module was implemented for cable installation as it has the advantage that it could be used to describe the transport of material released in a specific part of the water column. In this way, the dispersion would not be over-estimated, or the corresponding sedimentation underestimated. |

7. Following the establishment of baseline conditions, a number of scenarios were modelled to determine the environmental variations arising from the installation and presence of the Proposed Development. These are outlined in Table 3.2.

**Table 3.2: Summary of Modelled Environmental Variation Scenarios**

| Variation/Operation | Description | Parameter Modelled |
|---|---|---|
| Hydrography<br><br>Section 5.2 | Models updated to take account of the installation of the Proposed Development and associated features to quantify:<br>• changes to tidal currents;<br>• changes to wave climate; and<br>• changes to littoral currents. | • Wind turbine infrastructure: 179 x 24 MW installations with 20 m caisson foundations diameter with scour protection 2 m in height and 80 m diameter. Additionally, structures with four legs per site with 5 m diameter spaced 60 m apart were included within the water column.<br>• Offshore substation platforms (OSPs)/Offshore Convertor Station Platforms: Eight High Voltage Alternating Current (HVAC) converters each with 6 jacket legs comprising suction caissons of 15 m in diameter with associated scour protection of 60 m diameter and a height of 2 m. The 6 legs of 4 m diameter spaced 40 m apart at the seabed were also included within the water column.<br>• Additionally, 2 High Voltage Direct Current (HVDC) converters each with 8 jacket legs comprising suction caissons of 15 m in diameter with associated scour protection of 60 m diameter and a height of 2 m. The 8 legs of 5 m diameter spaced 80 m apart at the seabed were also included within the water column.<br>• Cable protection to a height of 3 m for 15% of inter-array/interconnector cables and areas along the Proposed Development export cable corridor with limited burial depth. |
| Sedimentology<br><br>Section 5.3 | Models updated to take account of the installation of the Proposed Development and associated features to quantify:<br>• changes to sediment transport characteristics. | As above with the addition of:<br>• scour protection simulated using an area of fixed bed around each structure. |
| Seabed features clearance<br><br>Section 6.1 | Sample dredging operation:<br>• dredging and disposal is undertaken in a cycle along sample routes; and<br>• clearance is undertaken along sample cable routes of a width of 25 m with dredging undertaken at 10,000 $m^3$/h with a spill rate of 3%. | • offshore cable clearance is undertaken to an average depth of 5 m on a 2.5 hour cycle;<br>• inter-array cable clearance is undertaken to an average depth of 1.3 m over a 75 minute cycle; and<br>• released through water column. |
| Augured pile installation<br><br>Section 6.2 | Three sample locations are presented:<br>• piles are 5.5 m in diameter and 16 m deep representing 20% of total depth; and<br>• two adjacent operations occurring simultaneously. | • drilling undertaken at 0.5 m/h;<br>• drilling is undertaken over a 32 hour period;<br>• 380 $m^3$ of material mobilised per pile; and<br>• released throughout water column. |
| Inter-array cabling<br><br>Section 6.3.1 | • trenching is undertaken along a 78 km sample inter-array cable route crossing the Proposed Development array area; and<br>• trench is a slot 2 m wide and 3 m deep. | • dredge trenching is undertaken at 500 m/h;<br>• the route is trenched over a period of 6.5 days; and<br>• circa 469,000 $m^3$ material displaced near bed. |
| Offshore export cables trenching<br><br>Section 6.3.2 | • trenching is undertaken from the Proposed Development array area towards the landfall; and<br>• trench is a slot 2 m wide and 3 m deep. | • dredge trenching is undertaken at 500 m/h;<br>• the route is trenched over a period of circa 5.5 days; and<br>• circa 400,000 $m^3$ material displaced near bed for each route. |

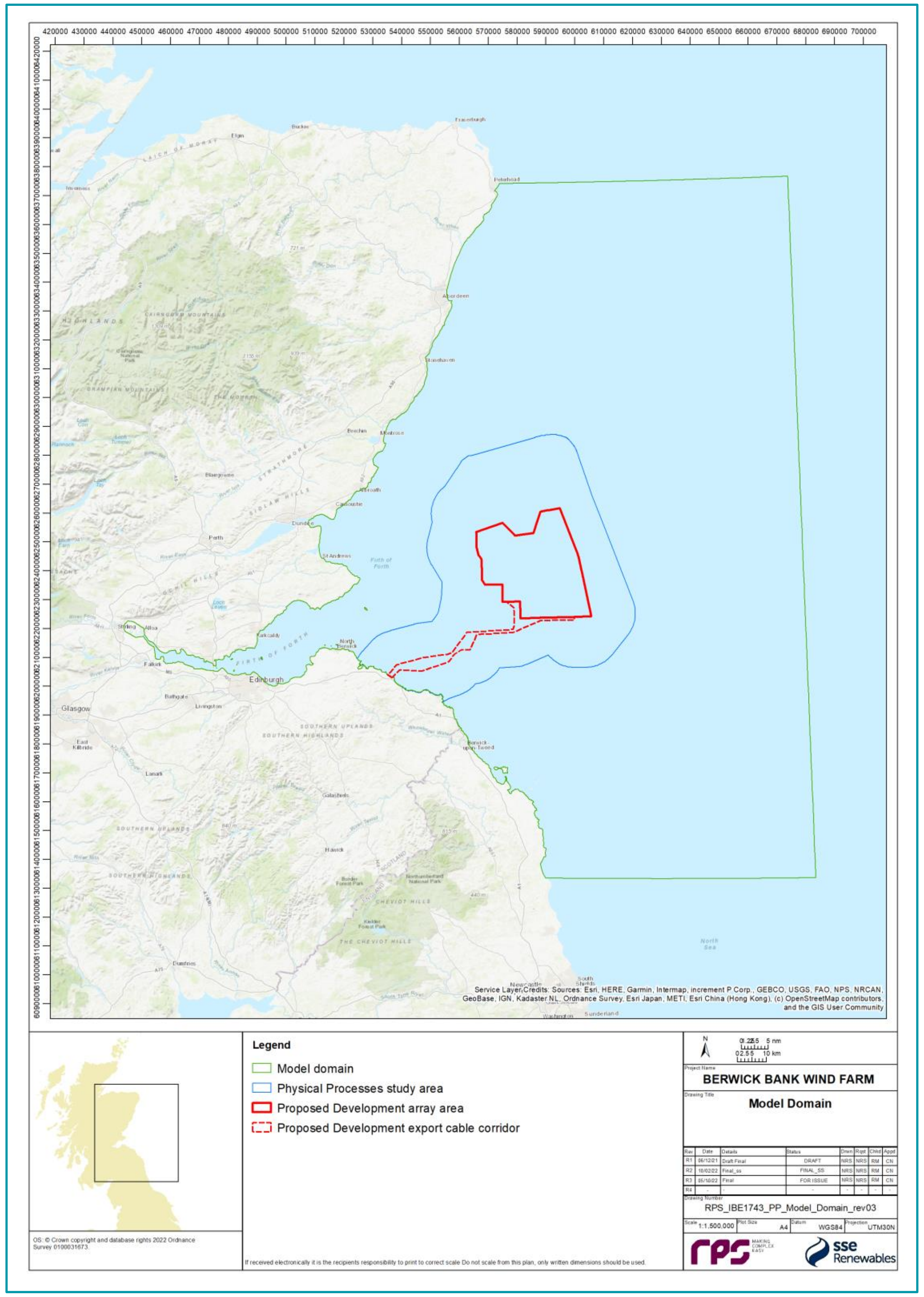


**Figure 3.1: Model Domain (Green Outline)**

## 3.2. DATA SOURCES

8. Information on the physical environment within the physical processes study area and beyond to the model domain was collected through a detailed desktop review of existing studies and datasets. These are summarised in Table 3.3.

**Table 3.3: Summary of Key Resources**

| Source | Coverage | Data Provision |
|---|---|---|
| Marine Environmental Data Information Network (MEDIN) including Admiralty Marine Data Portal | UK Waters | Bathymetry data |
| European Centre for Medium-range Weather Forecast (ECMWF) | European Waters | Historic and contemporary pressure, wind speed and wave datasets. |
| European Marine Observation and Data Network (EMODnet) | European Waters | Bathymetry, geology; and seabed substrate and classifications |
| Centre for Environment Fisheries and Aquaculture Science (Cefas) Offshore observation data | UK Waters | Salinity, seawater temperature and turbidity. |
| Cefas Climatology Data (Cefas, 2016) (https://data.cefas.co.uk/view/18133) | UK Waters | Suspended sediment concentrations (SSC) |
| British Oceanographic Data Centre (BODC) UK tide gauge network. Database of current observation | UK Waters | Tidal levels, current speed and current direction. |
| United Kingdom Hydrographic Office (UKHO) - Published Charts and Tide tables | UK Waters | Charts 1407 1:200000 and 175 1:75000 incorporating tidal diamonds with current stream data |
| Summary of Seagreen Firth of Forth Metocean Surveys to Date (Intertek Metoc, 2012) | Former Firth of Forth Zone | Wave data, current data, water level data, seawater temperature and turbidity. |
| Firth of Forth Zone Development: Metocean survey (Fugro GEOS, 2011) | Former Firth of Forth Zone | Metocean data. |
| UK Round 3 Offshore Wind Farm Zone 2 Firth of Forth: Wave Height Spells for Survey Operability (Metoc, 2010) | Former Firth of Forth Zone | Metocean data. |
| Dynamic Coast (https://www.dynamiccoast.com) | Scottish Waters | Coastal change maps and resources. |
| JNCC mapping data (https://jncc.gov.uk/mpa-mapper/) | UK Waters | Spatial data for Marine Protected Areas (MPA) incl. Special Protection Area (SPA), Site of Special Scientific Interest (SSSI) and conservation zones. |
| Marine Science Scotland Scottish Shelf model (http://marine.gov.scot/information/wider-domain-scottish-shelf-model, https://data.marine.gov.scot/dataset/climatology-surface-and-near-bed-temperature-and-salinity-north-west-european-continental and Berx 2009) | UK Waters | Climatology: temperature, salinity and current speed characteristics. |

| Source | Coverage | Data Provision |
|---|---|---|
| Marine Scotland mapping data (https://marinescotland.atkinsgeospatial.com/nmpi/) | Scottish Waters | Spatial data for physical characteristics, metocean, climate change, bathing waters and marine activities. |

## 3.3. SITE-SPECIFIC SURVEYS

9. A summary of the surveys undertaken of relevance to physical processes is outlined in Table 3.4.

**Table 3.4: Summary of Surveys Undertaken to Inform Physical Processes**

| Title | Extent of Survey | Overview of Surveyor | Surveyor Contractor | Date | Reference to Further Information |
|---|---|---|---|---|---|
| 00338 SSE Berwick Bank Lot 1 and 2 Operations and Results Report | Proposed Development export cable corridor. | Geophysical study to establish bathymetry, seabed geology, morphology and sediments | XOCEAN Ltd. | 2021 | XOCEAN (2021) |
| Geophysical survey | Proposed Development array area and Proposed Development export cable corridor. | Geophysical study to establish bathymetry, seabed geology, morphology and sediments | Fugro | 2020 | Fugro (2020a) and Fugro (2020b) |
| Benthic subtidal survey | Proposed Development array area and Proposed Development export cable corridor. | Grab and Drop-Down Video (DDV) sampling with chemical analysis and particle sieve analysis | Ocean Ecology Ltd. | 2021 | See volume 3, appendix 8.1 |
| SSE Berwick and Marr Bank Metocean | Proposed Development array area | Waverider buoy deployments | Partrac | 2020 | Partrac (2020) |

# 4. BASELINE ENVIRONMENT

10. This section outlines the numerical modelling undertaken in order to determine the baseline conditions. It describes the physical processes in terms of sea state and sediment transport regimes.

## 4.1. BATHYMETERY

11. The bathymetry of the Proposed Development array area is influenced by the presence of large scale morphological bank features, including the Marr Bank and the northern extent of the Berwick Bank. These two bank features are defined as Shelf Banks and Mounds and are part of the Firth of Forth Banks Complex.

12. Geophysical data collected in 2019 suggests the water depth within the Proposed Development array area varies between 32.8 m and 68.5 m relative to Lowest Astronomical Tide (LAT), and average depths of generally 51 m below LAT. Minimum water depths of approximately 38 m below LAT are found on top of the western central part of the Proposed Development array area and maximum depth around 68 m below LAT in the east of the banks. Figure 4.1 illustrates the bathymetry recorded across the Proposed Development array area during the 2019 geophysical survey.

13. The bathymetry of the Proposed Development export cable corridor is relatively variable, from the intertidal zone to 69.8 m below LAT at the time of geophysical investigation. This variance in depth is influenced by the seafloor typography which slopes gently, reaching 60 m depth below LAT approximately 20 km from landfall, before decreasing to circa 40 m below LAT in the area of the Proposed Development export cable corridor which extends to the western margin of Berwick Bank. Water depths in the far east extent of the route extends to 64 m below LAT.

14. The model domain had full bathymetry data coverage and was populated using a combination of data sources. The site-specific geophysical survey undertaken in 2019 and the resulting bathymetry data was used to populate the model. The survey data provided to LAT vertical datum was converted to model mean sea level datum using reference values published by Admiralty. Where additional data was required for the model extent beyond the survey area, bathymetry data was sourced from the EMODnet as illustrated in Figure 4.2. This database is available under the European Inspire Directive and provides access to data in a variety of formats, datums and resolutions based on a combination of survey datasets. Data was extracted to mean sea level datum at the finest resolution in the vicinity of the physical processes study area with a resolution of at least three times the mesh resolution to ensure that coastal features were represented within the numerical modelling.

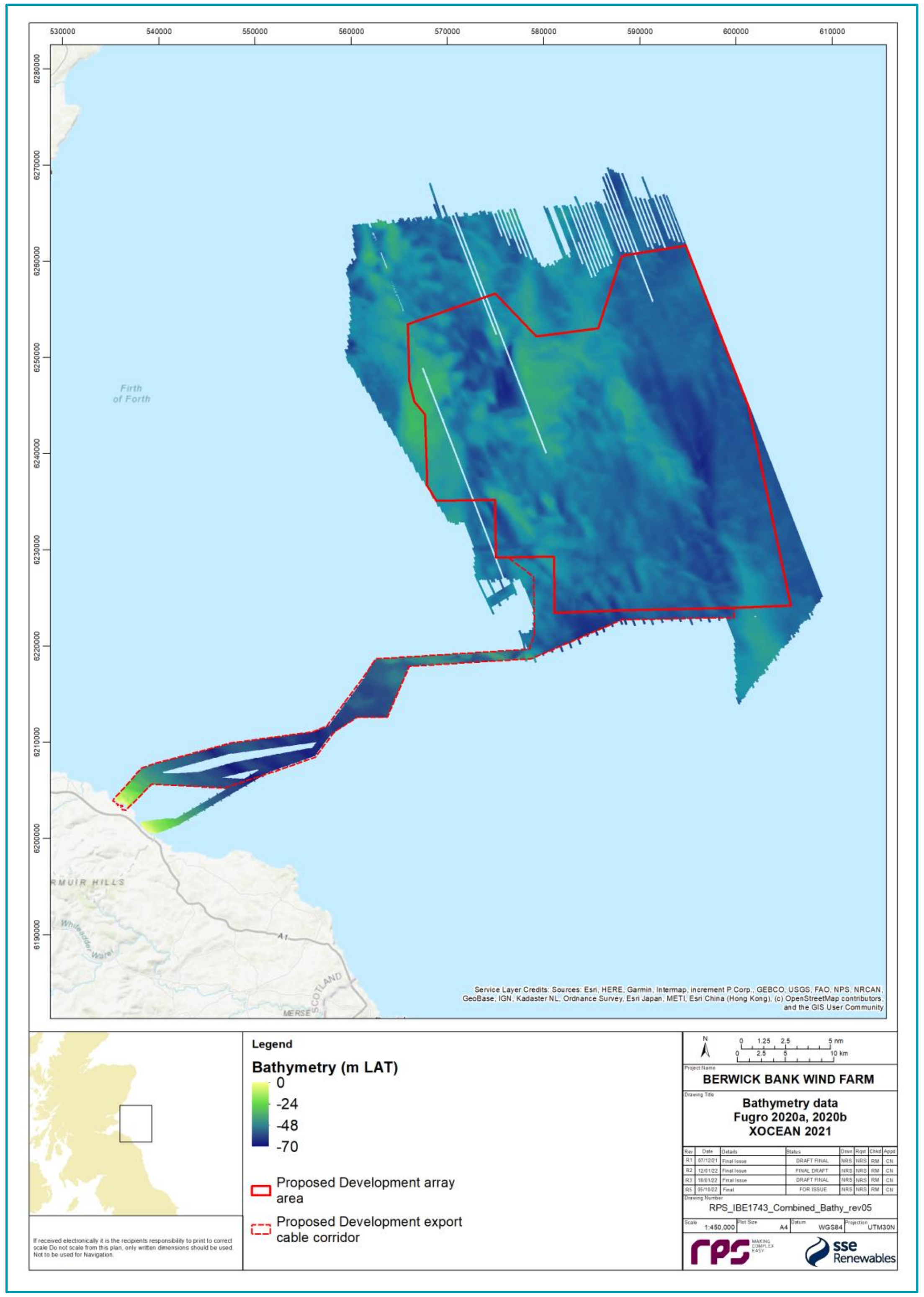


Figure 4.1: Bathymetric Data Fugro Survey 2019 and XOCEAN 2021

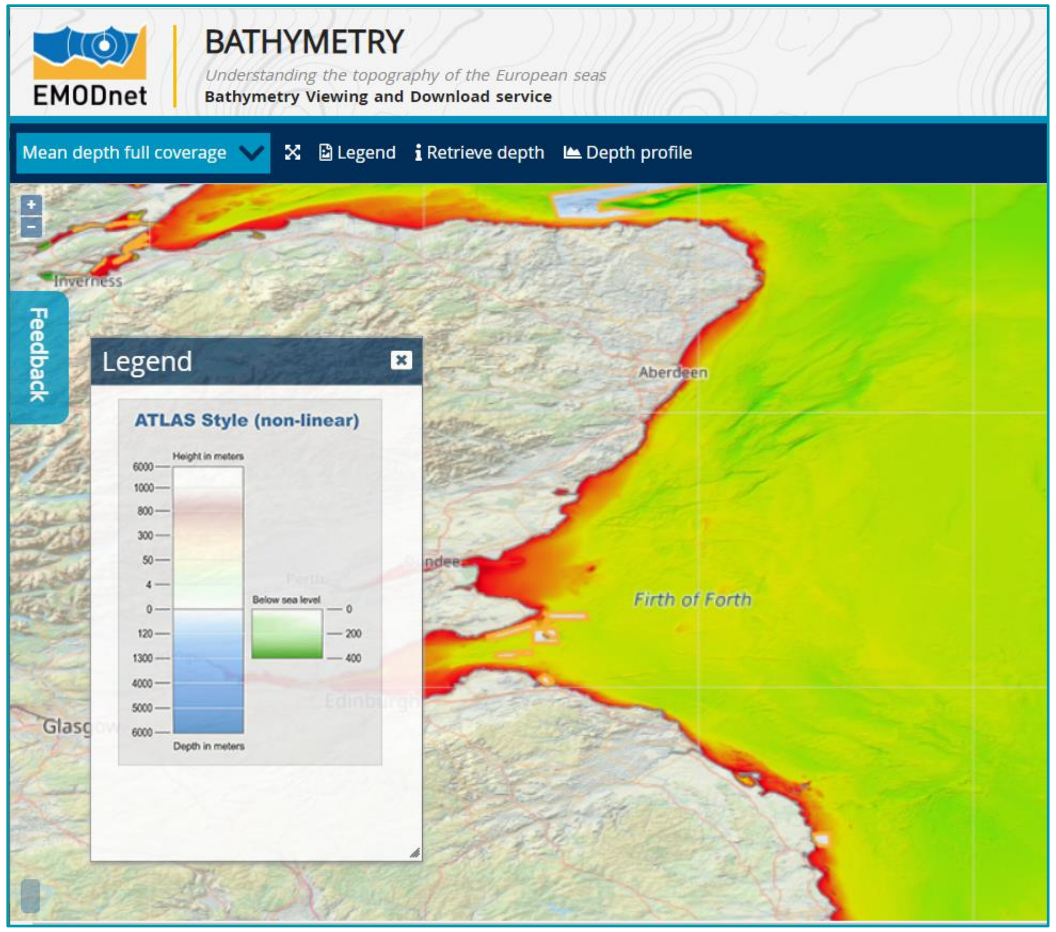


Figure 4.2: Bathymetric Data EMODnet Data Portal

15. The resolution of the model bathymetry was designed to reflect variations in water depth and bed forms for the accurate simulation of tidal currents as shown in Figure 4.3. Additional model resolution was also included to incorporate the installation of the Proposed Development. This enabled the same cell arrangement to be used for the baseline and post-construction assessment, thereby avoiding the introduction of any numerical mesh effects into the assessment. Across the Proposed Development array area, the resolution varied between circa 50 m down to 5 m in order that the influence of scour protection on the tidal flow and sediment transport for the Proposed Development could be quantified. With increasing distance from the physical processes study area, the cell size was increased but maintained at a level which retained model accuracy. Figure 4.4 illustrates the mesh resolution with an inset of the mesh within the Proposed Development array area.

16. The extent of the domain was designed to provide the basis for a model which could be utilised for tide, wave and sediment transport modelling. The focus of the study is a tidal excursion from the Proposed Development to quantify any changes due to the installation however a larger domain is required to develop wave fields and ensure that tidal currents are simulated. The model extends north, south and offshore beyond the adjacent banks to ensure that any influence on the Firth of Forth Banks Complex is included in the detailed model.

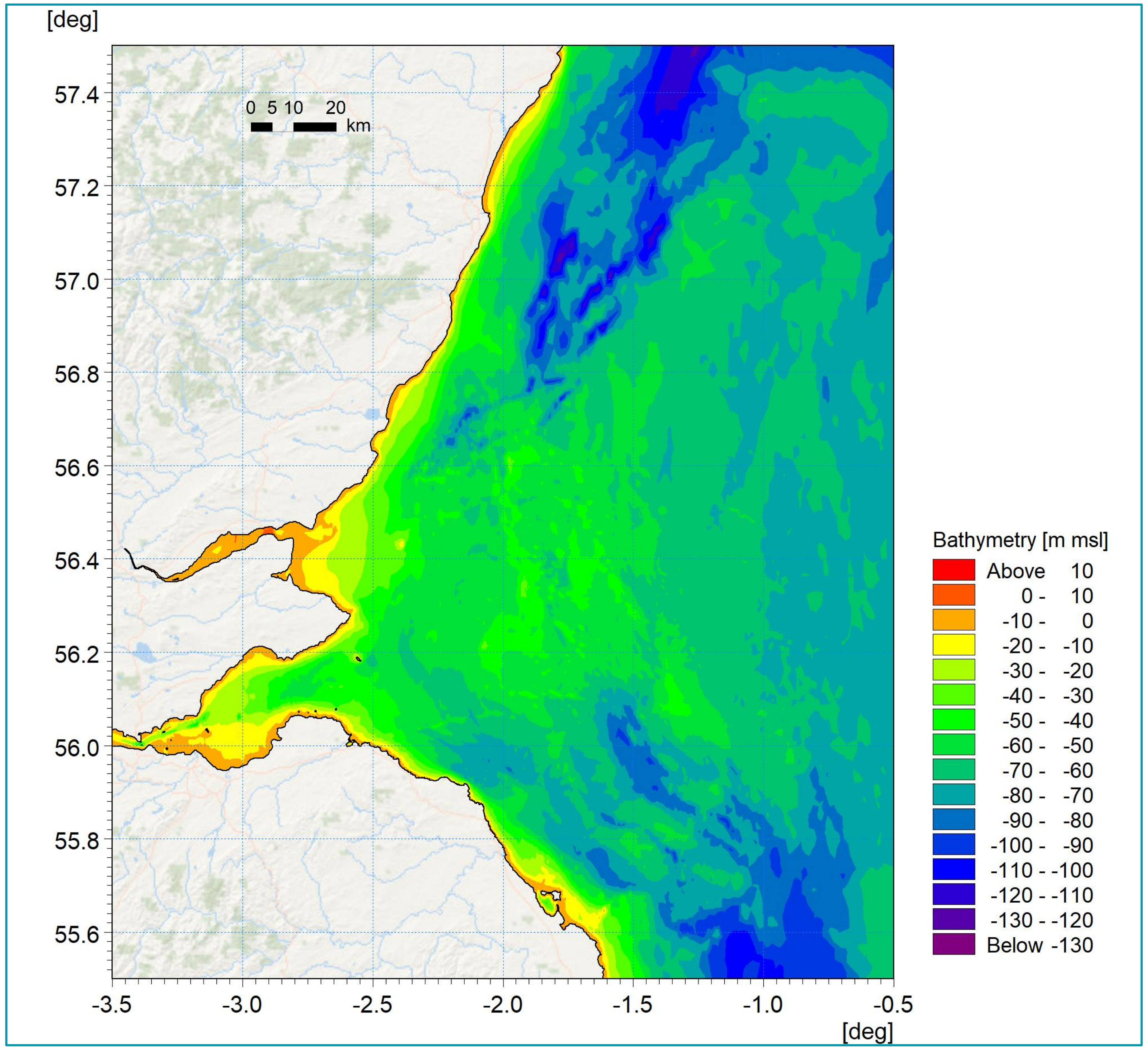


**Figure 4.3: Model Bathymetry**

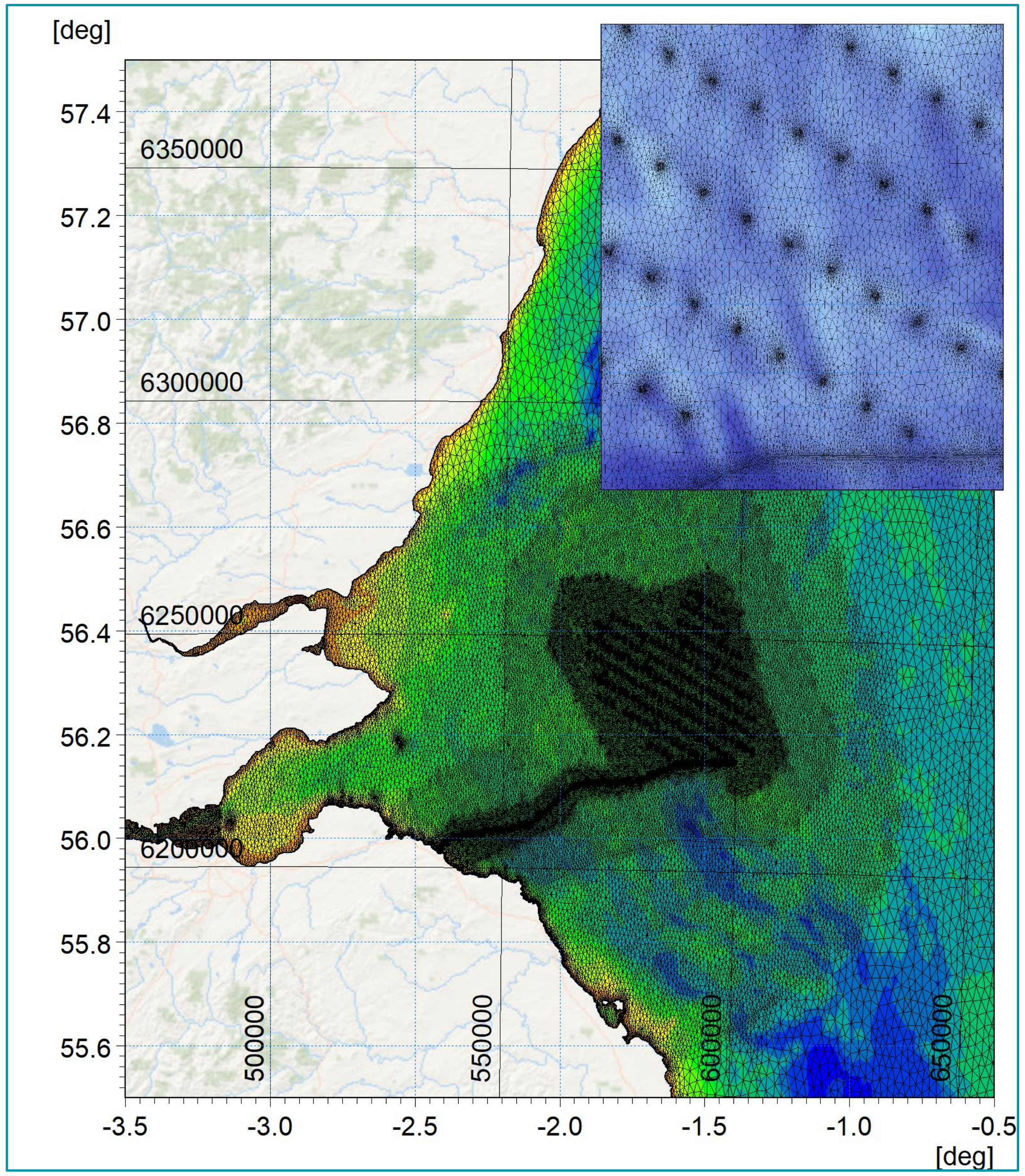


**Figure 4.4: Model Mesh with Section of Proposed Development Array Area Inset**

## 4.2. HYDROGRAPHY

17. The UKHO states that the mean tidal range at the Standard Port of Leith is approximately 3.6 m whilst the Standard Port at Montrose is 3 m. The two sites have the tidal characteristics shown in Table 4.1 in metres referenced to Chart Datum (CD):

**Table 4.1: Tidal Levels at Standard Ports**

| Tidal Level (m CD) | Leith | Montrose |
|---|---|---|
| Lowest Astronomical Tide (LAT) | -0.1 | 0.2 |
| Mean Low Water Springs (MLWS) | 0.8 | 0.8 |
| Mean Low Water Neaps (MLWN) | 2.0 | 1.9 |
| Mean Sea Level (MSL) | 3.2 | 2.9 |
| Mean High Water Neaps (MHWN) | 4.4 | 3.8 |
| Mean High Water Springs (MHWS) | 5.6 | 4.9 |
| Highest Astronomical Tide (HAT) | 6.3 | 5.6 |

18. Tidal elevations across the outer Firth of Forth are governed by a southerly directed flood tide which moves along the eastern coastline of Scotland into the Firth of Forth and around Fife Ness (HR Wallingford, 2009). Across the mouth of the Firth, the flood tidal stream has a general east-southeast pattern, whilst the ebb tidal stream runs in a west-north-west direction. The main peak flood tide occurs approximately two hours before high water (HW), with the main peak ebb tide occurring approximately four hours after HW (HR Wallingford, 2009). Tidal processes are often characterised by the natural tidal elevation of an area. The Firth of Forth Zone is characterised by a tidal regime which is semi-diurnal with variable mean spring tidal ranges, based on the metocean data collated within the 2011 survey campaign (HR Wallingford, 2012).

19. The tidal flow simulations which form the basis of the study were undertaken using the MIKE21 FM modelling system. The FM Module is a 2-dimensional, depth averaged hydrodynamic model which simulates the water level variations and flows in response to a variety of forcing functions in lakes, estuaries and coastal areas. The water levels and flows are resolved on a mesh covering the area of interest when provided with bathymetry, bed resistance coefficient, wind field, hydrodynamic boundary conditions, etc.

20. The tidal model was driven using boundary conditions extracted from the DHI global tidal model which is based on the DTU10 ocean model developed by the National Space Institute of Denmark. These boundaries were fully defined 'flather' boundaries for which both surface elevation and current vectors are specified. The model was calibrated using the following data sources:

- metocean data collected for Seagreen;
- Admiralty tidal harmonics;
- Admiralty tidal diamonds; and
- data sourced from the British Oceanographic Data Centre (BODC).

21. A large amount of hydrometric data was available across the model domain, a selection of the principal resources is illustrated in Figure 4.5. A sample of this calibration data is presented in this report, Figure 4.6 presents the location of the selected data. The site 1407R relates to the tidal diamond "R" from the Admiralty chart number 1407 which is located to the south of the Proposed Development export cable corridor. The labelling of the other site references the locations as reported (Fugro, 2011 and Partrac 2020).

22. Figure 4.7 shows the comparison of the modelled (blue) and Admiralty tidal levels predicted from harmonic analysis (red). The model correlated well through both spring and neap tidal phases. The comparative study undertaken to quantify the potential changes in tidal currents was undertaken during spring tides to ensure a wide range of tidal conditions were applied in the modelling. The validation data presented is therefore focussed on specific spring tidal periods. Short periods are presented for clarity along with representative data records to demonstrate the range and variability of monitored data.

23. Figure 4.8 through to Figure 4.18 show the measured data during the Seagreen 1 campaign at a number of locations across the physical processes study area for both spring and neap tidal states. Figure 4.8 to Figure 4.11 show comparison of current speed and direction for spring and neap tides respectively at monitoring point B in the Fugro campaign. In each case three traces are included from the monitored data, these being representative of near bed, mid depth and near surface flow conditions whilst the depth averaged model has a single trace (shown in red). For completeness, further data is presented for a spring-neap cycle at this location in Figure 4.12. The average of the value recorded through the water column is presented (red trace) along with the range of values from which this has been calculated (envelope formed between the green traces), whist the modelled value is shown by the blue trace. This plot illustrates that whilst there is a wide range of current speeds within the water column the modelled depth average value is representative of the average currents, particularly for spring tidal conditions during which the model was implemented.

24. Further locations are presented in Figure 4.13 to Figure 4.18 and at each location the modelled data lies within the range of the measured data indicating that tidal currents are well represented particularly in terms of timing which is important in the area which exhibits tidal skew (i.e. where slack water does not correspond with high and/or low tide). It should be noted the measured data will also include the influence of meteorological conditions whilst the numerical tidal model calibration was driven by astronomical forces alone.

25. Figure 4.19 to Figure 4.21 relate to Admiralty tidal diamonds for locations within the domain. This data is published in a generalised format (i.e. there are 14 sets of hourly current speed data each referenced to high water Leith for spring and neap tides and a single set of current direction values). These values therefore do not relate to a known time period or specific tidal range. The Admiralty data (shown by points) correlate well with the modelled current directions and current speeds. These datasets are generally used as a cross reference as current speeds are not consistent across all neap or spring tides due to the varying tidal range. Generally, the field data supporting the diamonds was collected using drogues which often measure the higher surface current speeds than those simulated in a depth averaged model.

26. The calibration data demonstrates that the numerical model simulates the tidal currents in the region. This includes the representation of the skew tide where peak flood and ebb flows are typically one to two hours prior to high and low water respectively. Figure 4.22 illustrates tidal patterns during peak flood on a spring tide whilst Figure 4.23 illustrates the ebb tide. These points in the tidal cycle are used as reference for the assessment of potential impacts and changes to tidal flows due to the Proposed Development. The period selected for the comparative study represents a spring tide on the upper end of the range experienced in the region; this was to ensure the study included the greatest variation in tidal conditions (i.e. water depth and current speed). Residual tidal flows and how they drive sediment transport regimes are examined in section 4.6.

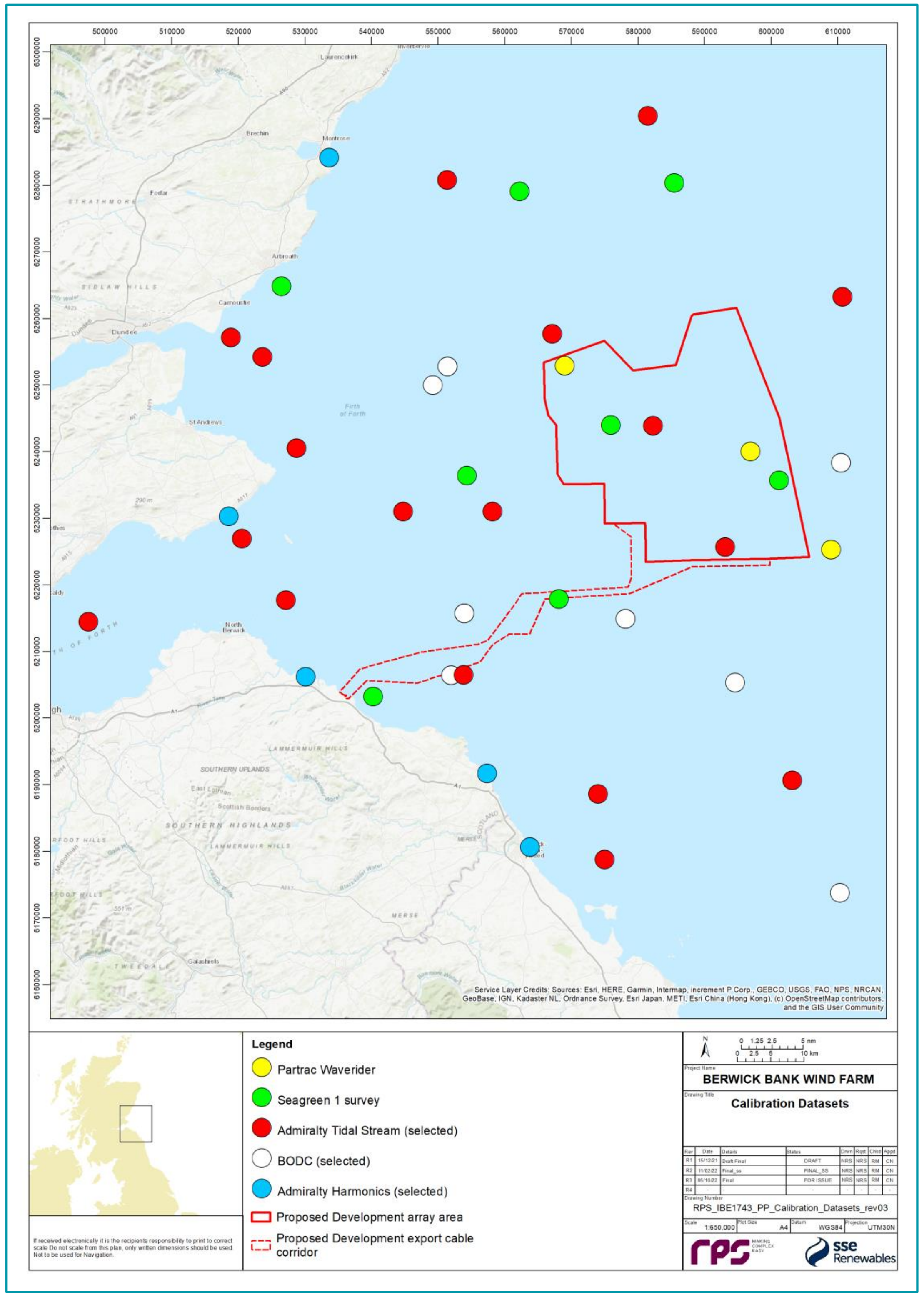


**Figure 4.5: Location of Selected Calibration Datasets Available**

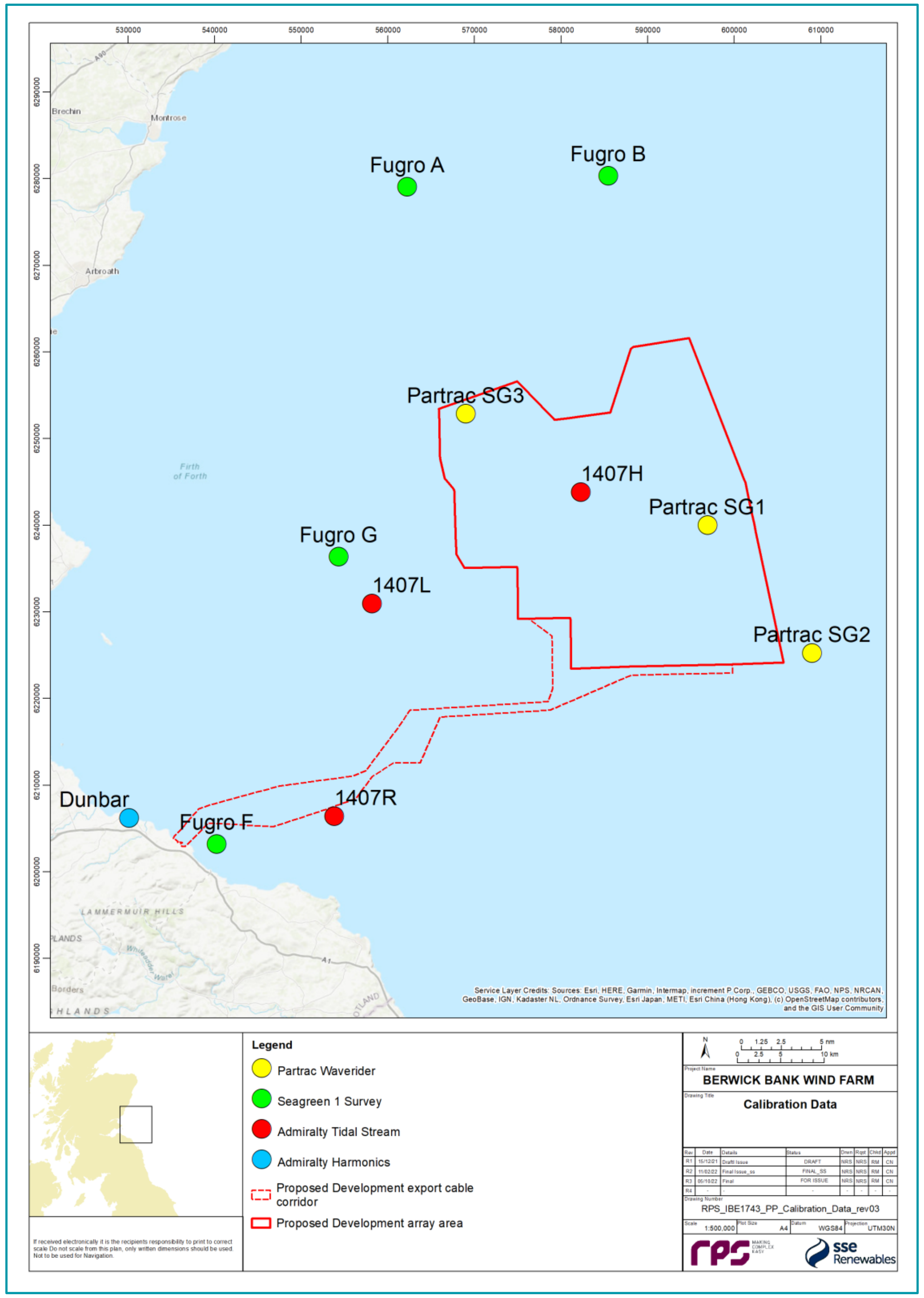


**Figure 4.6: Location of Calibration Data Presented**

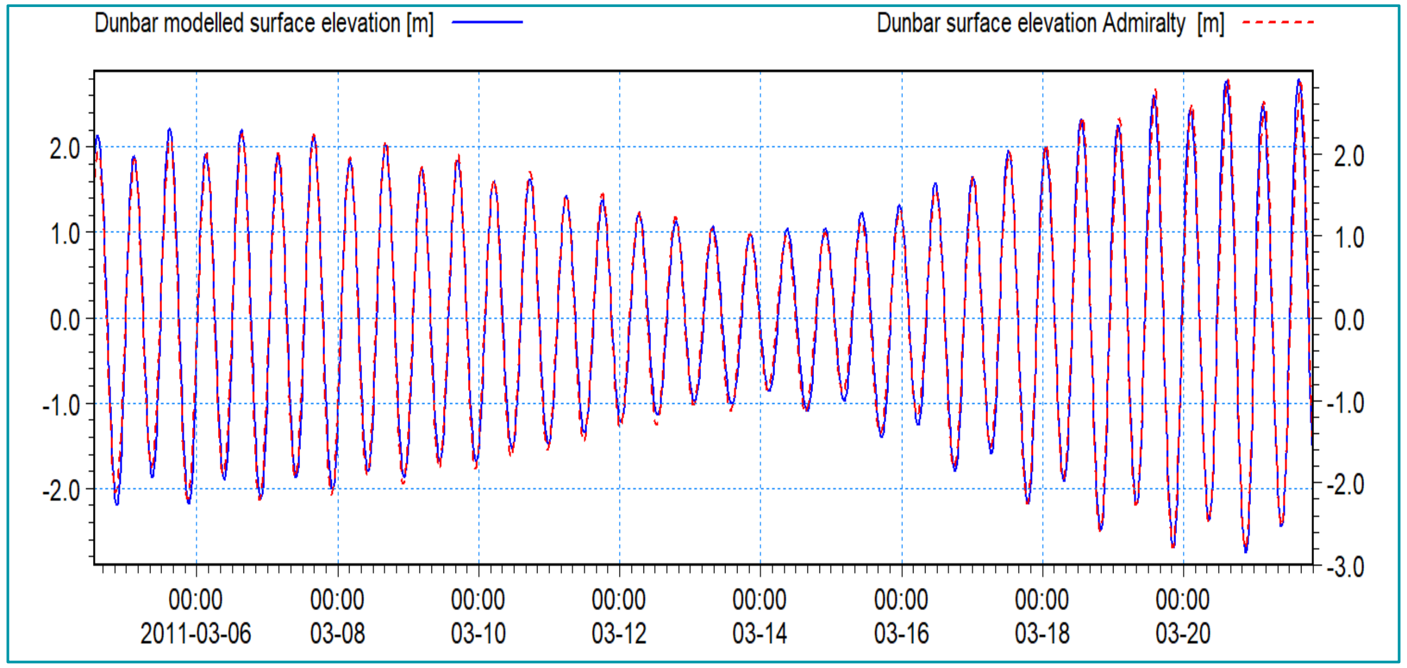


**Figure 4.7: Comparison of Model and Admiralty Harmonic Tide Data for Dunbar**

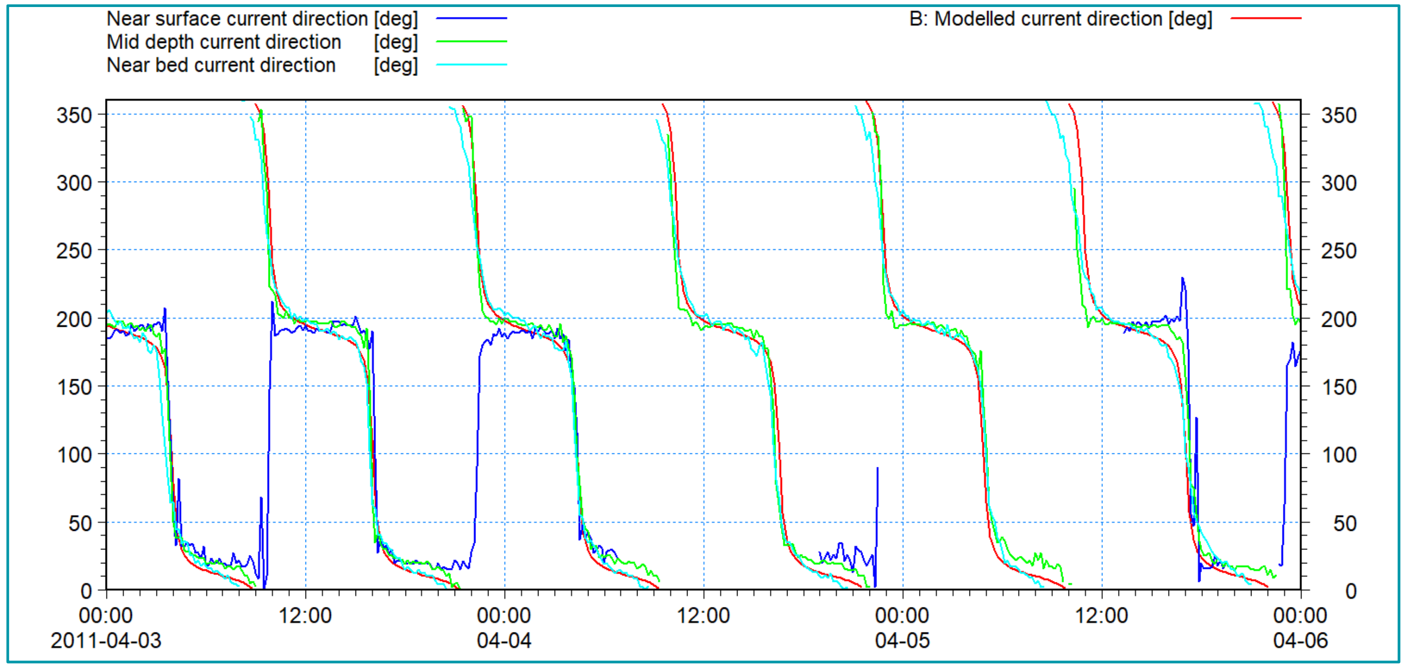


**Figure 4.9: Comparison of Model and Recorded Data Fugro Location B – Current Direction Spring**

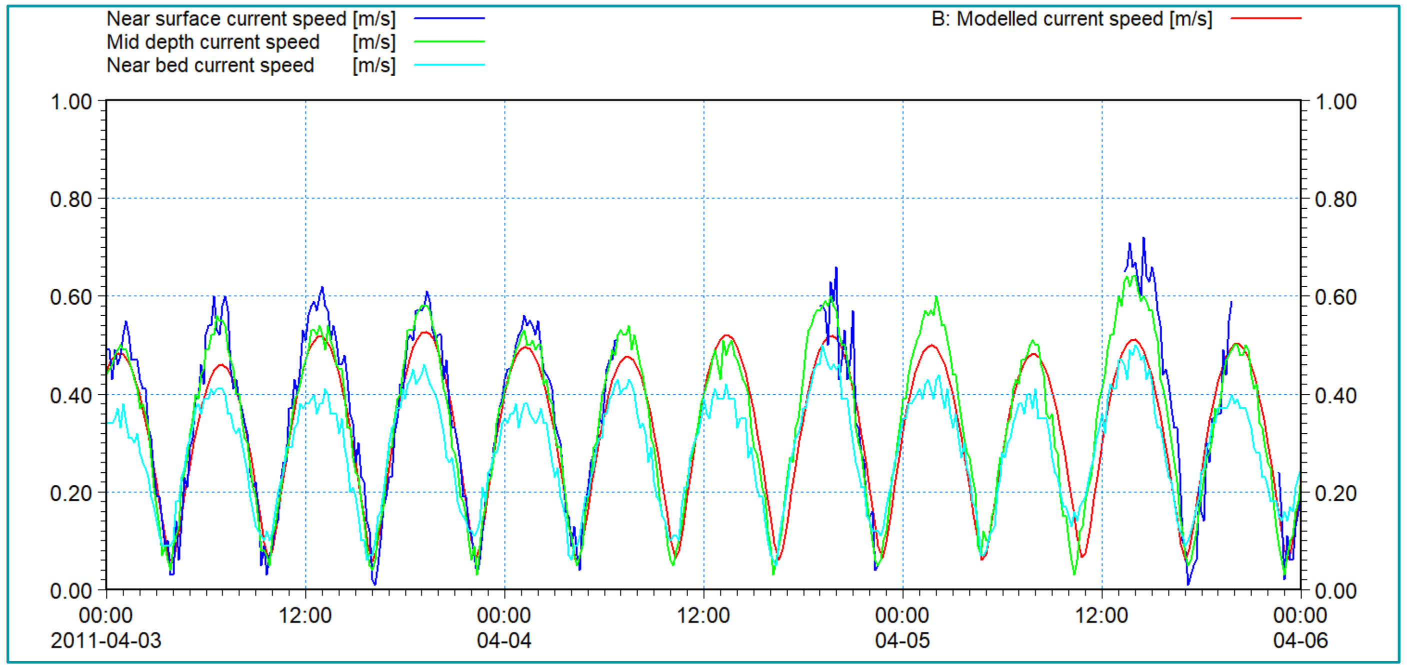


**Figure 4.8: Comparison of Model and Recorded Data Fugro Location B – Current Speed Spring**

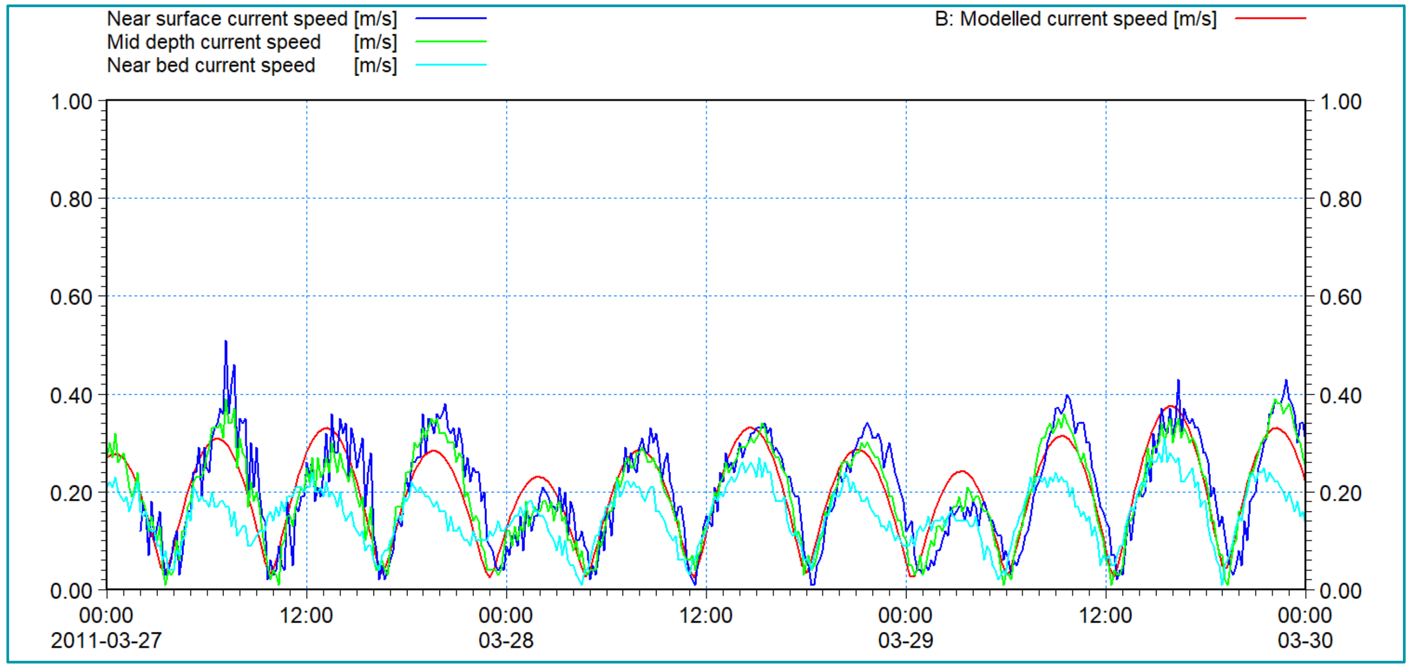


**Figure 4.10: Comparison of Model and Recorded Data Fugro Location B – Current Speed Neap**

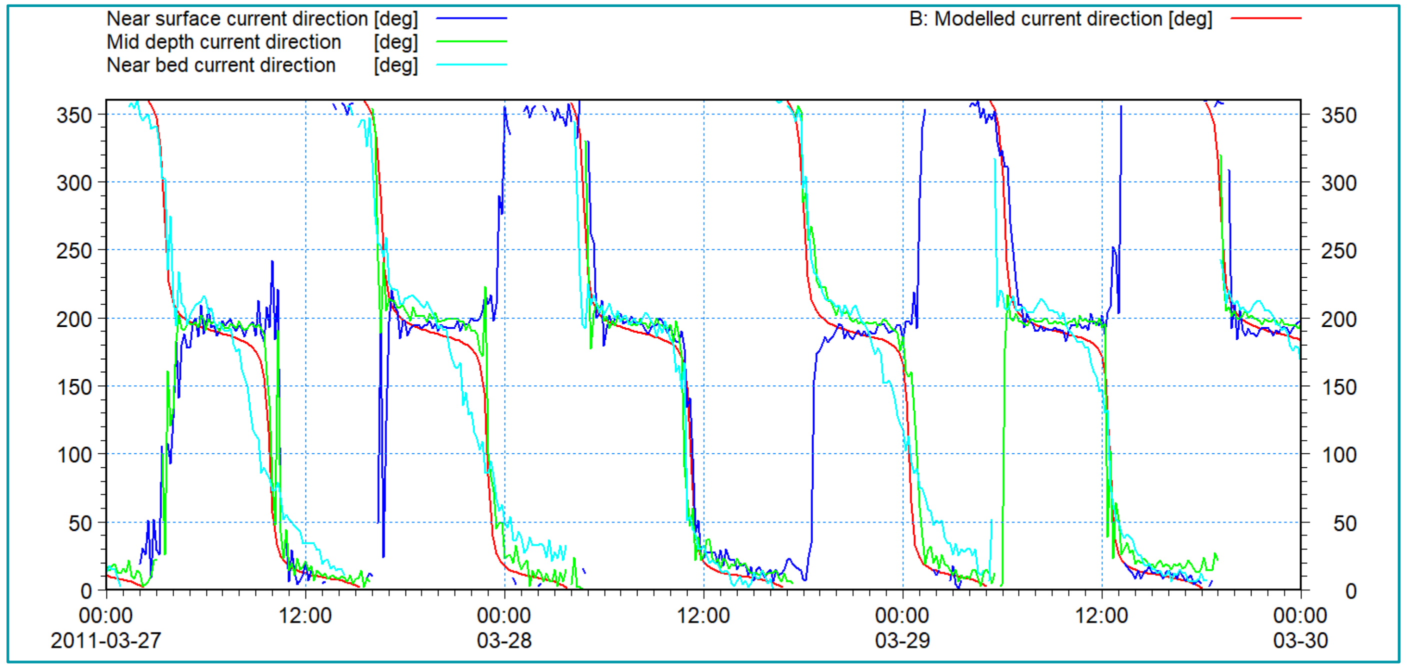


**Figure 4.11: Comparison of Model and Recorded Data Fugro Location B – Current Direction Neap**

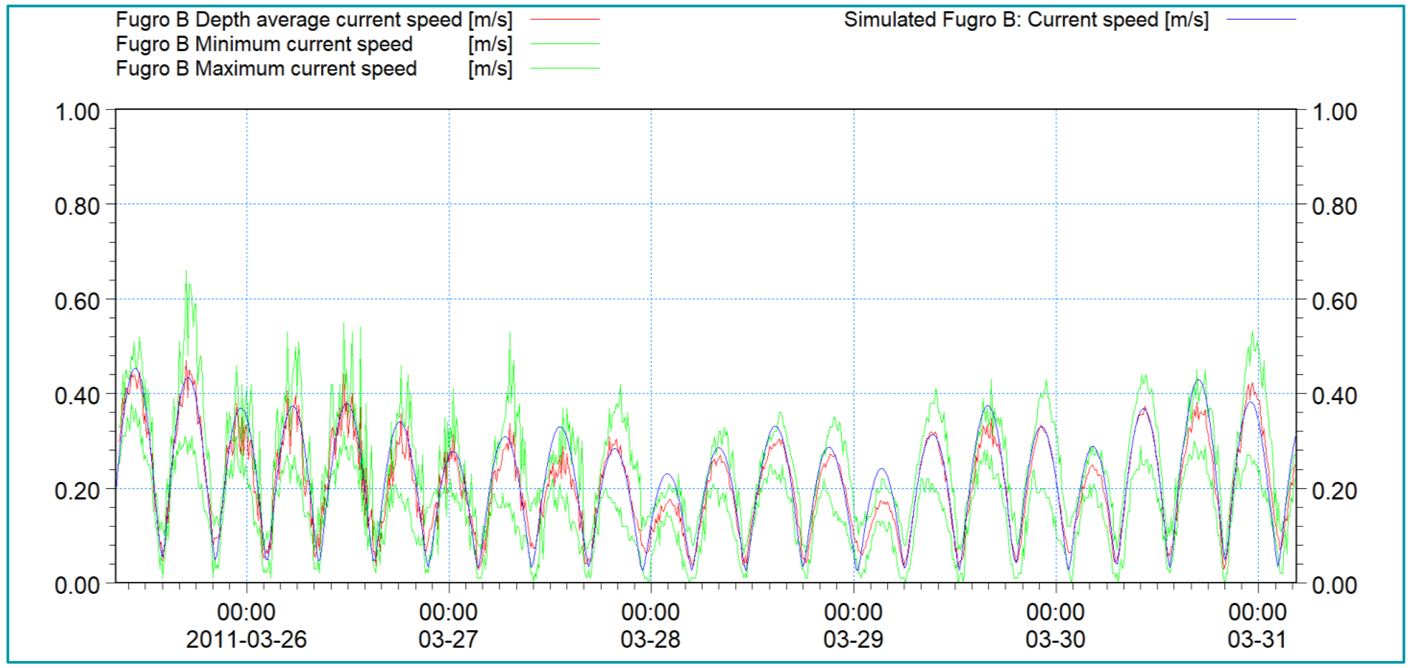


**Figure 4.12: Comparison of Model and Recorded Data Fugro Location B – Current Speed Spring - Neap Cycle**

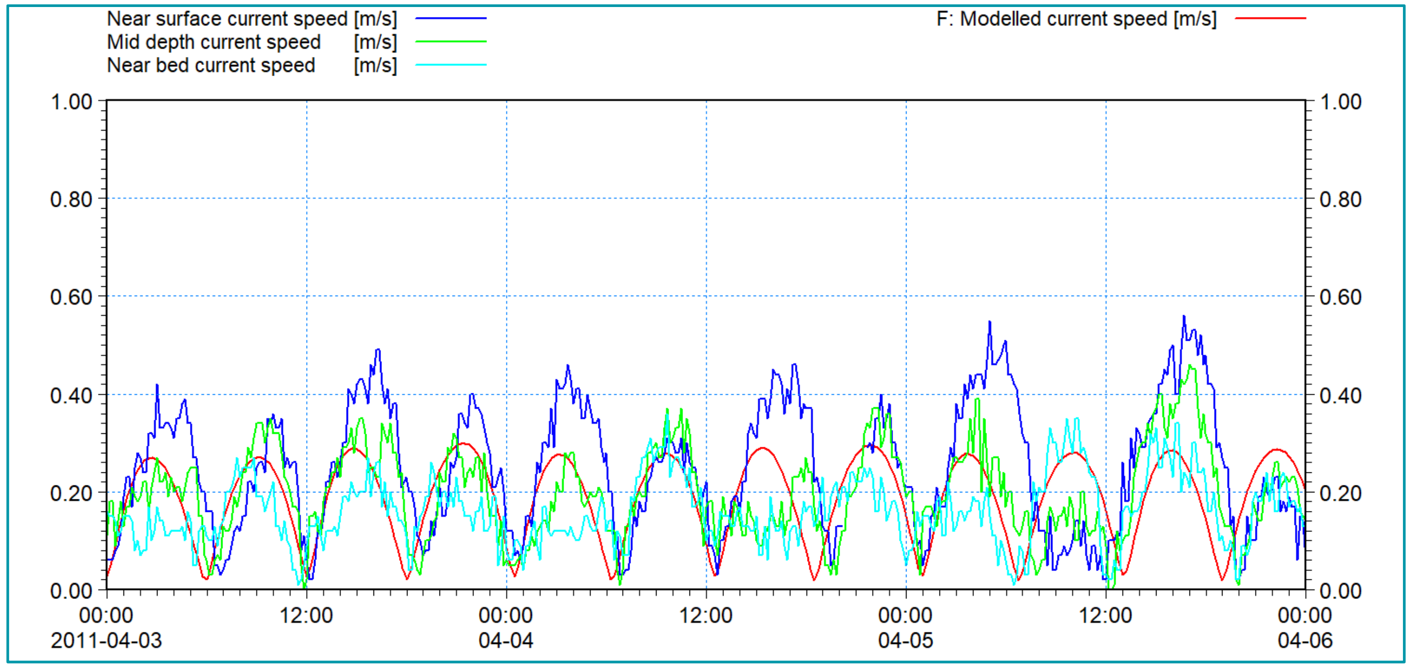


**Figure 4.13: Comparison of Model and Recorded Data Fugro Location F – Current Speed Spring**

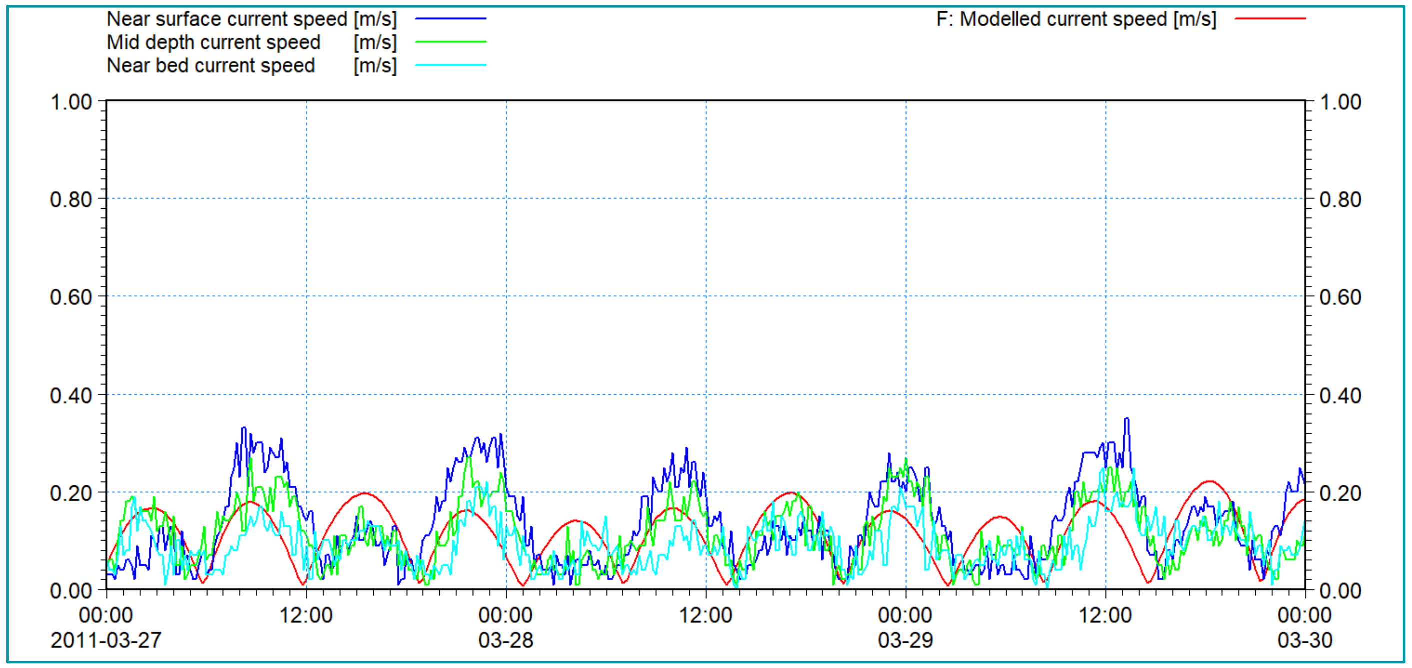


**Figure 4.14: Comparison of Model and Recorded Data Fugro Location F – Current Speed Neap**

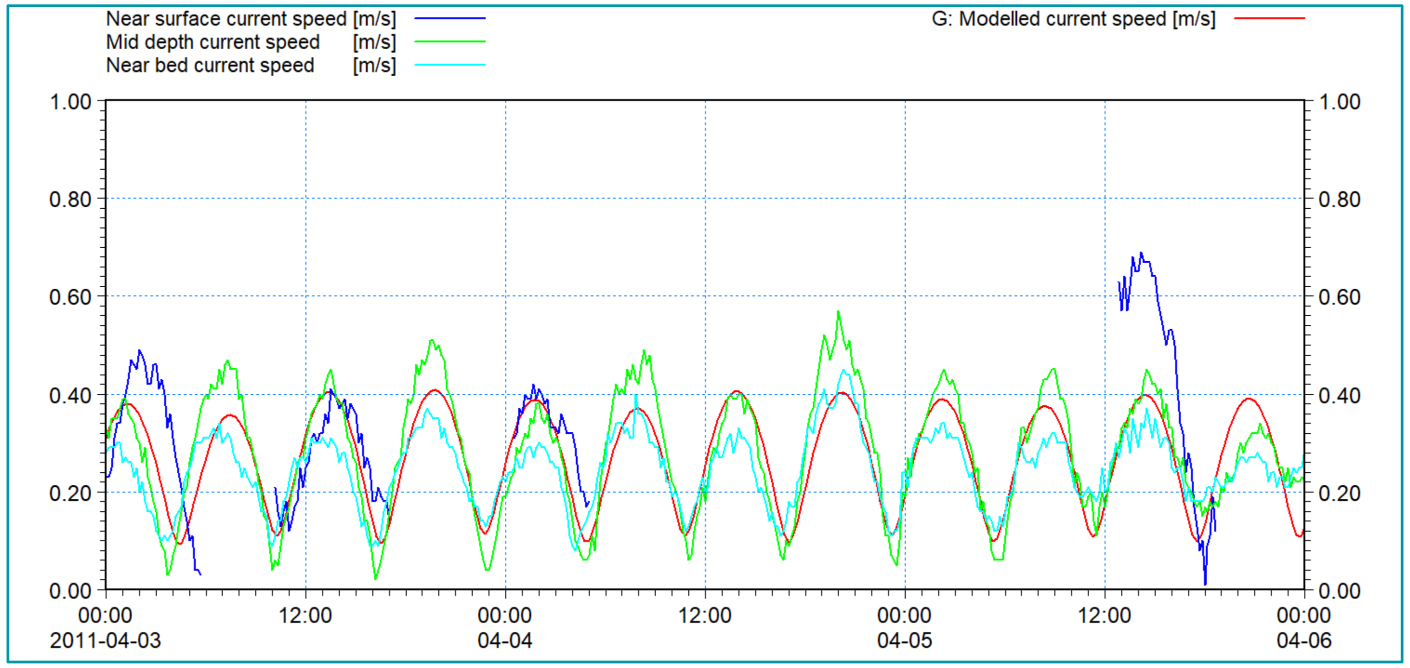


Figure 4.15: Comparison of Model and Recorded Data Fugro Location G – Current Speed Spring

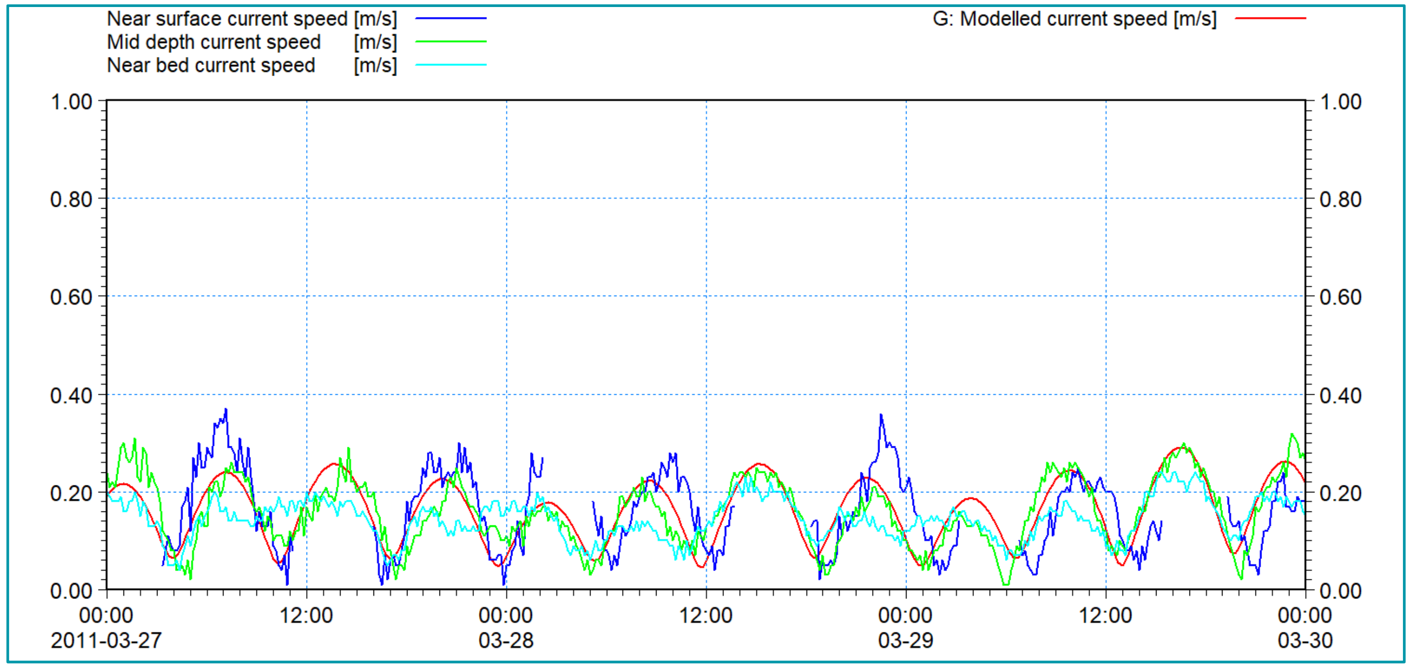


Figure 4.17: Comparison of Model and Recorded Data Fugro Location G – Current Speed Neap

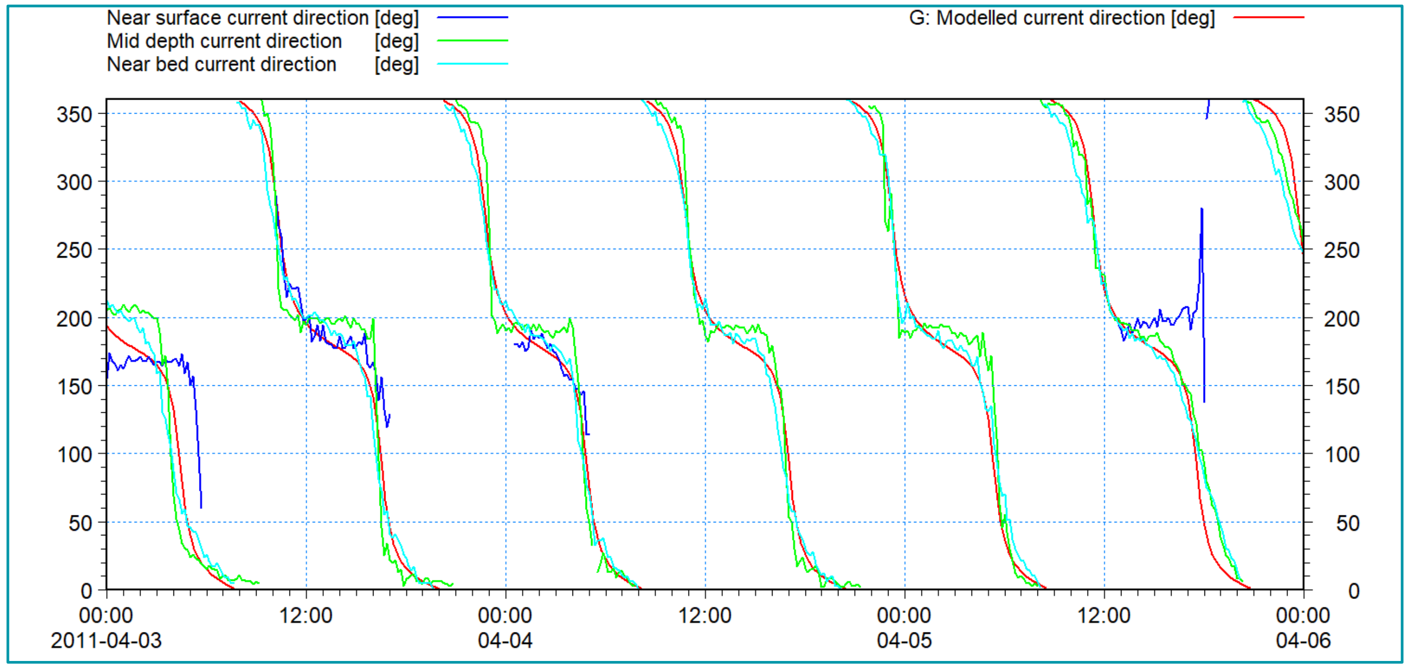


Figure 4.16: Comparison of Model and Recorded Data Fugro Location G – Current Direction Spring

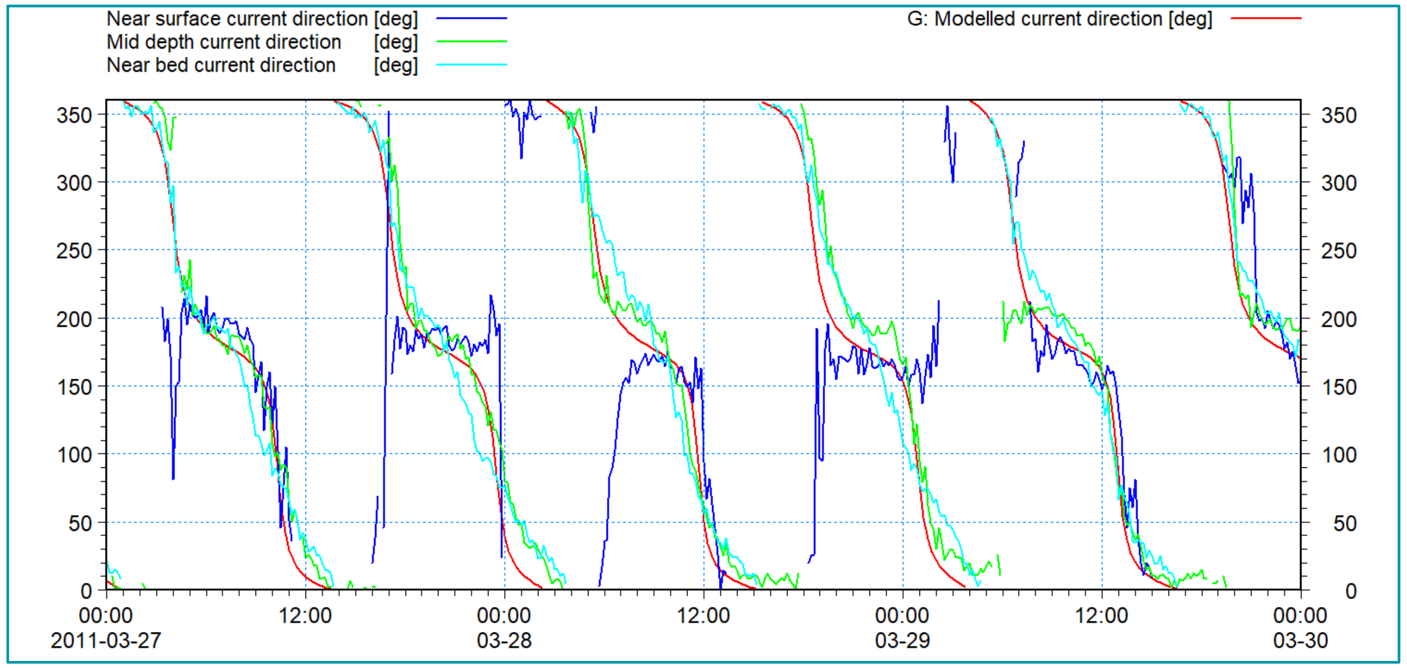


Figure 4.18: Comparison of Model and Recorded Data Fugro Location G – Current Direction Neap

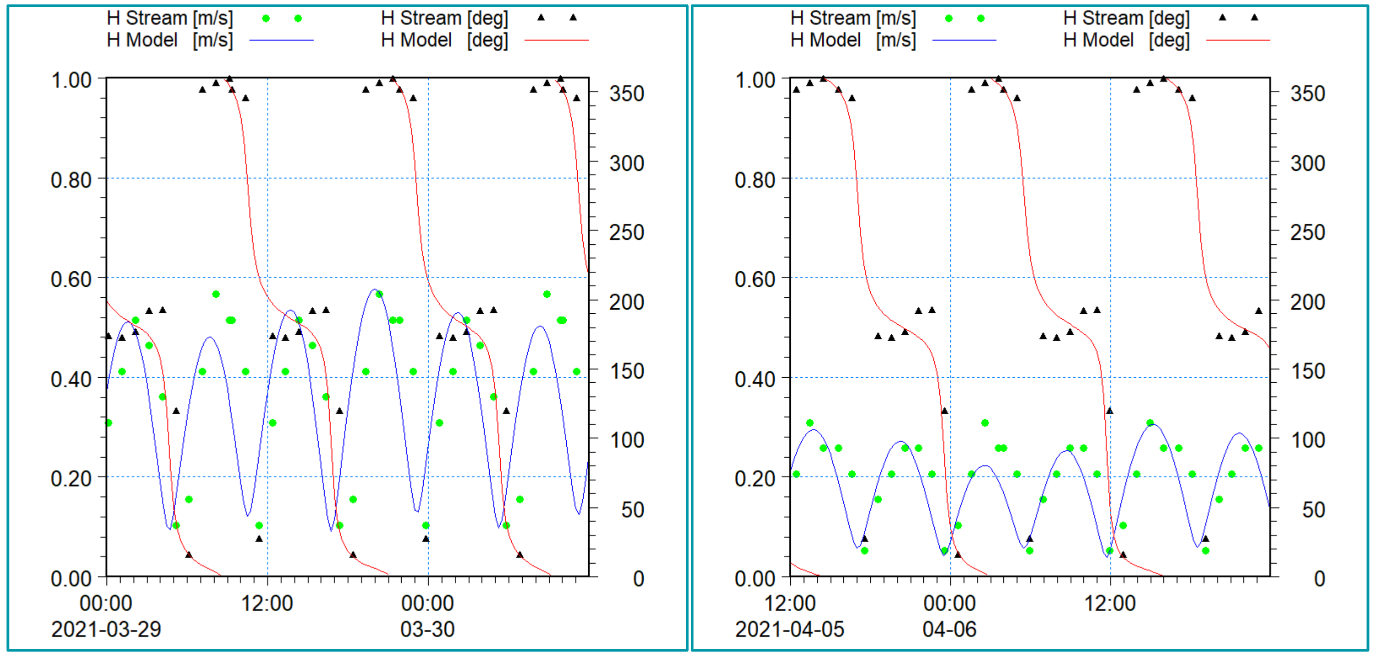


**Figure 4.19: Comparison of Model and Recorded Data Admiralty Diamond Location 1407H (Spring Left, Neap Right)**

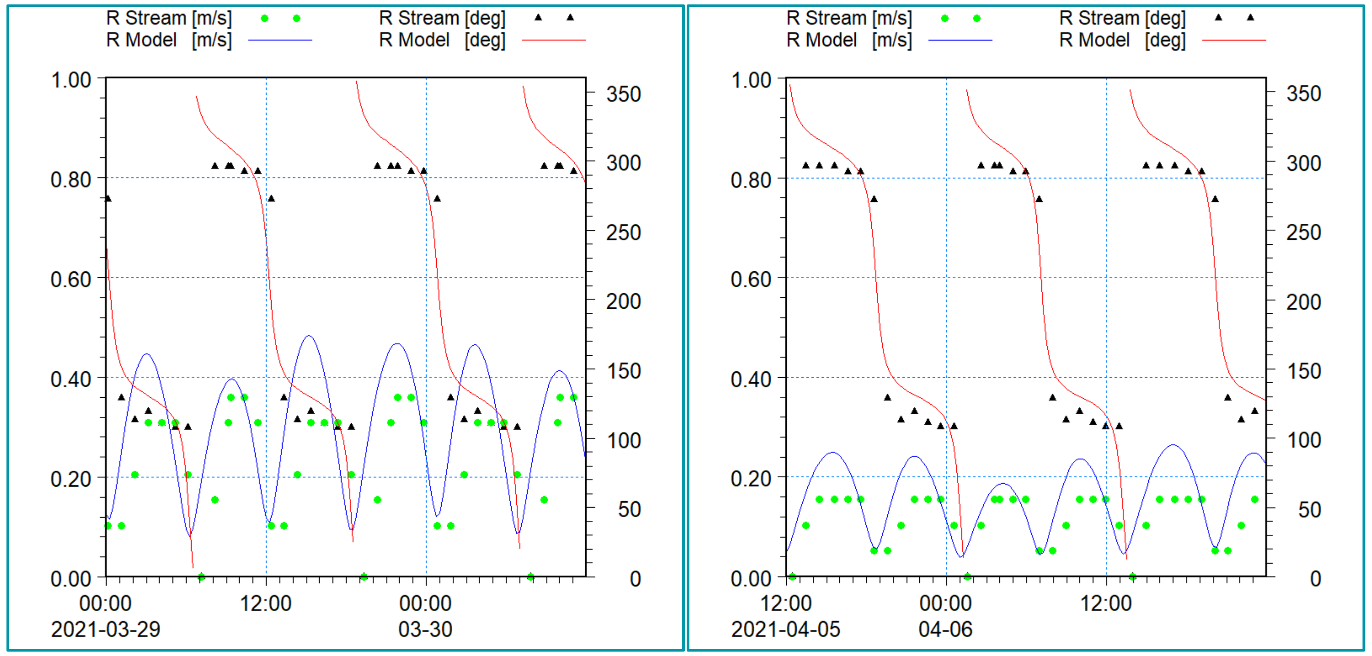


**Figure 4.21: Comparison of Model and Recorded Data Admiralty Diamond Location 1407R (Spring Left, Neap Right)**

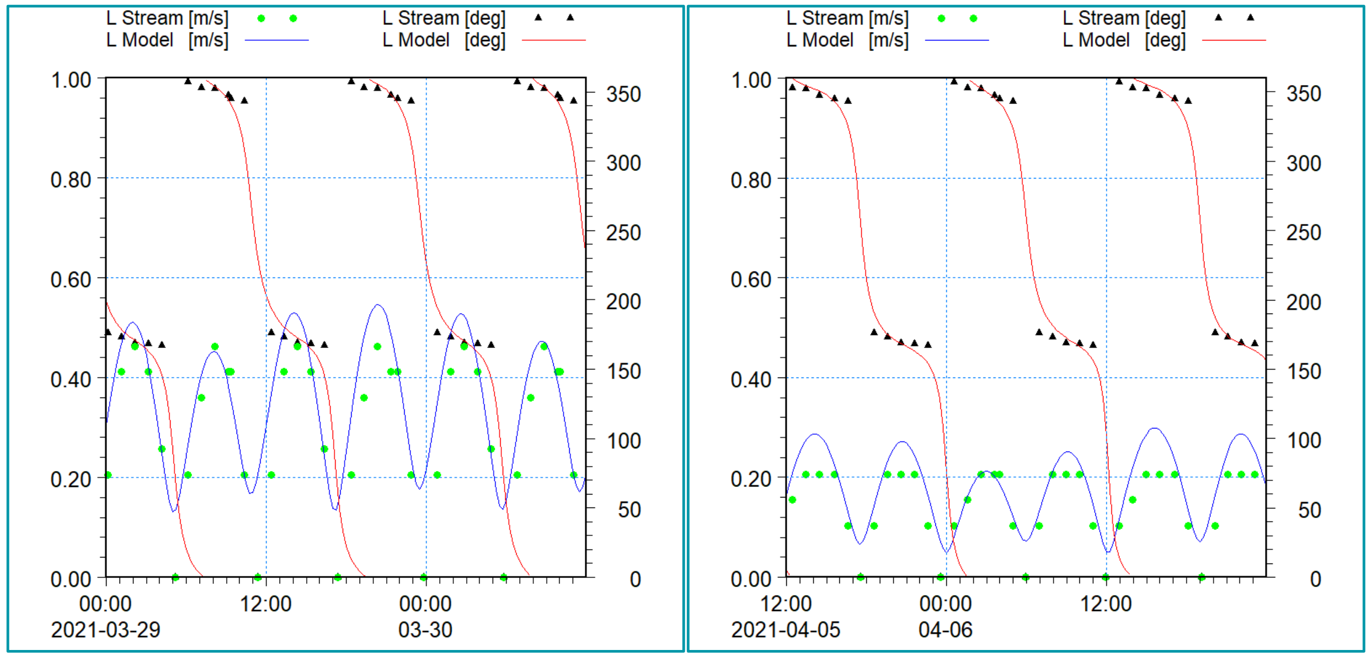


**Figure 4.20: Comparison of Model and Recorded Data Admiralty Diamond Location 1407L (Spring Left, Neap Right)**

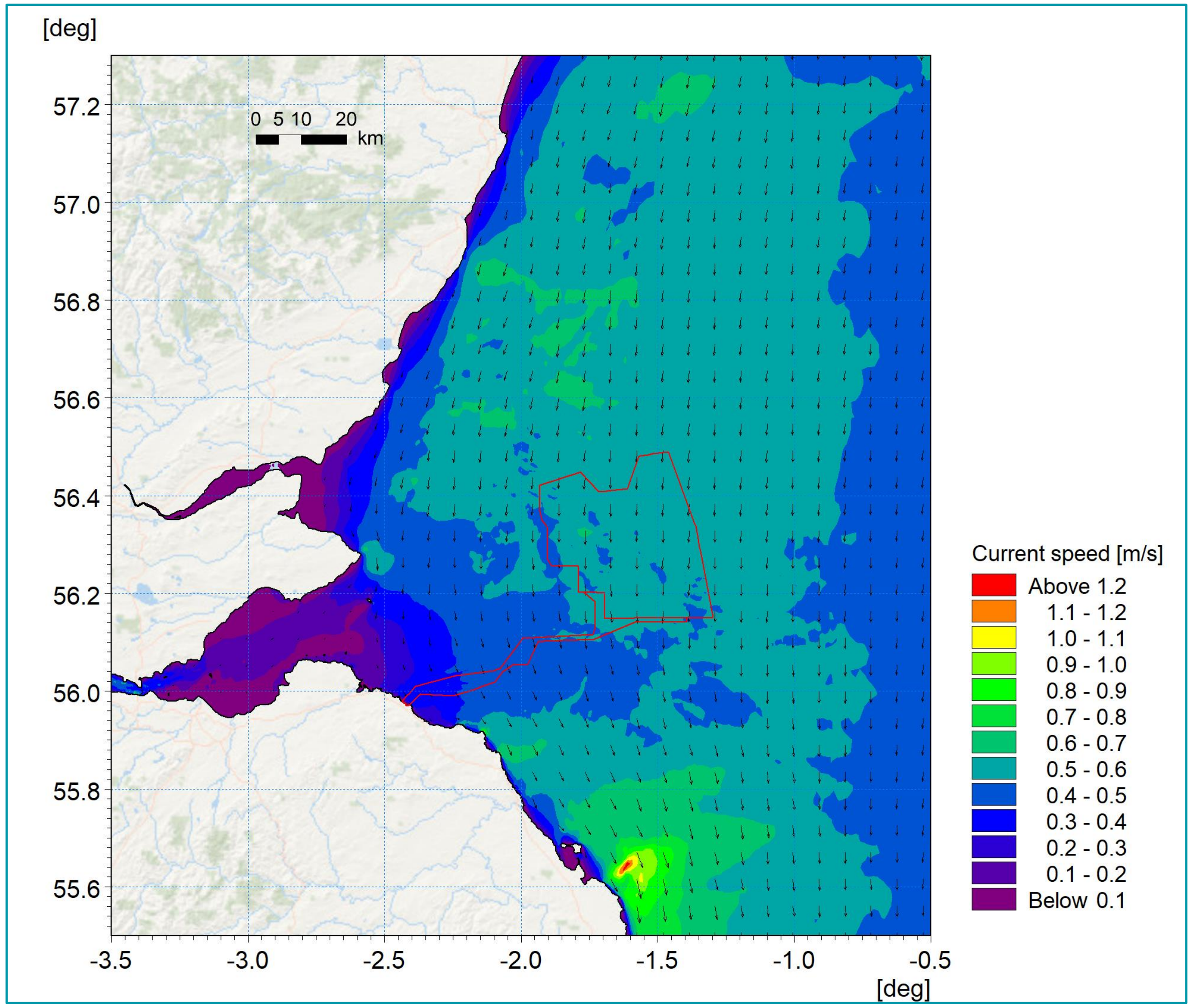


**Figure 4.22: Tidal Flow Patterns – Peak Flood (HW-1 Hour)**

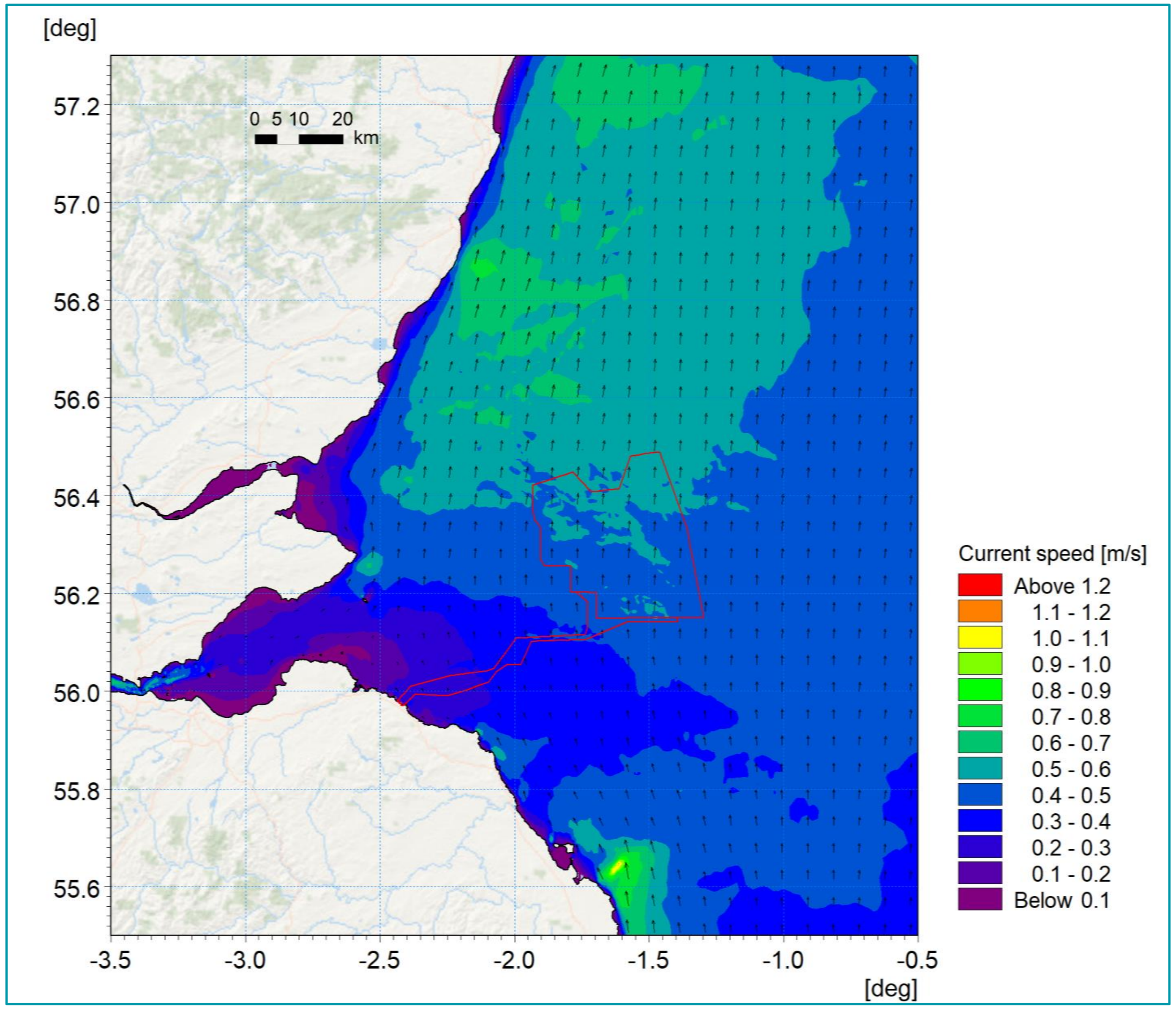


**Figure 4.23: Tidal Flow Patterns – Peak Ebb (LW-1 Hour)**

## 4.3. WAVE CLIMATE

27. Throughout the North Sea, strong winds can occur with wave heights varying greatly due to fetch limitations and water depth effects. Waves in the northern North Sea can be generated either by local winds or from remote wind systems (swell waves). East of the mouth of the River Tay, the dominant wave conditions approach from between 20ºN and 60ºN. However, extreme wave conditions (> 4 m) can be experienced from the entire eastern sector (0º to 180º) (HR Wallingford, 2012).

28. Metocean surveys conducted across the former Firth of Forth Zone to characterise the zone provide an overview of the wave regime within the physical processes study area. During the stormiest event over the 18-month wave buoy deployment, a significant wave height of 6.7 m was recorded in January 2012, which correlated with a one in one year sea wave climate return period event (Fugro, 2012).

29. As offshore waves transfer from the deep offshore water to shallower coastal areas (e.g. Proposed Development export cable corridor to landfall), a number of important modifications may result due to interactions of offshore deep water waves with the seabed, with the resultant modifications producing shallow water waves. These physical 'wave transformation' interactions include:

- shoaling and refraction (due to both depth and current interactions with the wave);
- energy loss due to breaking;
- energy loss due to bottom friction; and
- momentum and mass transport effect.

30. In addition to the data collected during the Seagreen 1 field study, longer term data was used in order to evaluate the baseline wave climate for more extreme events to enable assessment of the Proposed Development over a wider range of conditions. For this assessment the 22 year ECMWF Operational Wave model database was used. Figure 4.24 shows the wave rose from this dataset for a location at the centre of the Proposed Development array area. As noted from the field data even though the largest proportion of the waves are combined wind and swell from northerly sectors, there is sufficient fetch in the east to enable a wave field to develop.

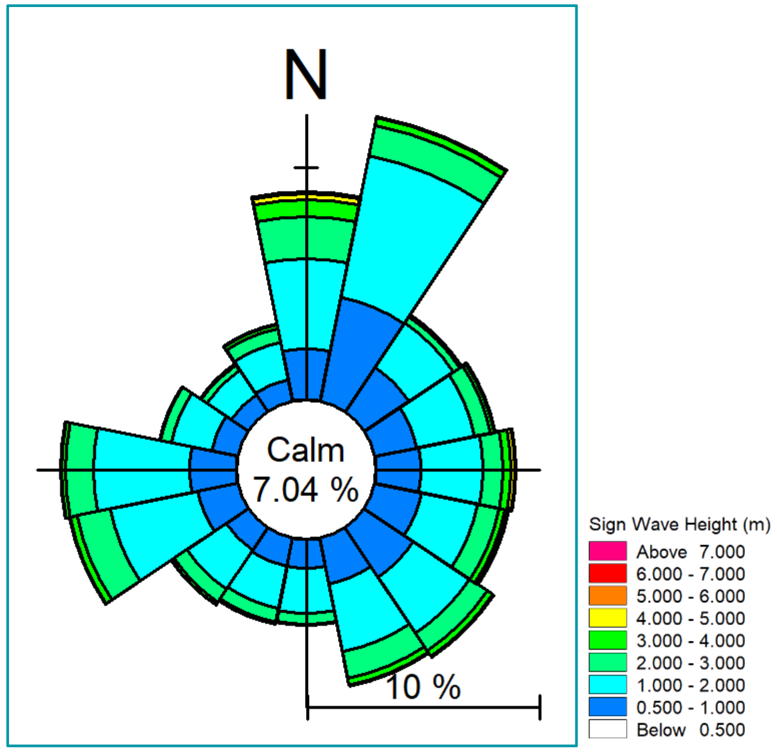


**Figure 4.24: Wave Rose for Proposed Development Array Area – 22 Year ECMWF**

31. In order to evaluate the potential changes in wave climate due to the Proposed Development, a comparative study was carried out. This meant that baseline wave climate was required; due to the comparative nature of the assessment, a full metocean study was not essential however representative sea-states were required.

32. An analysis was undertaken to determine the offshore conditions for which waves reach the site from all directions. Twenty-two years of data were obtained from the ECMWF's operational dataset for multiple locations on the north, east and southern boundaries of the model domain. The wave roses for these sites are presented in Figure 4.25 overlain on the model domain at the locations to which they relate. Extreme value analysis using peak over threshold was undertaken for the principal sectors to determine the one in one and 1 in 20 year offshore wave climate. These were then used as boundary conditions within the wave modelling to determine the resultant wave climate at the site and across the physical processes study area.

33. In addition to boundary wave data, it was necessary to analyse the wind field to include the contribution of local wind seas. For this, a representative point for each of the key directions, was identified and utilised from the ECMWF ten year dataset, as for the relevant sectors, the variation in wind speed was found to have consistency across the domain. The wind rose for this period is presented in Figure 4.26. This was analysed on the same sectoral basis as the wave data to give an indication of the return period wind speed.

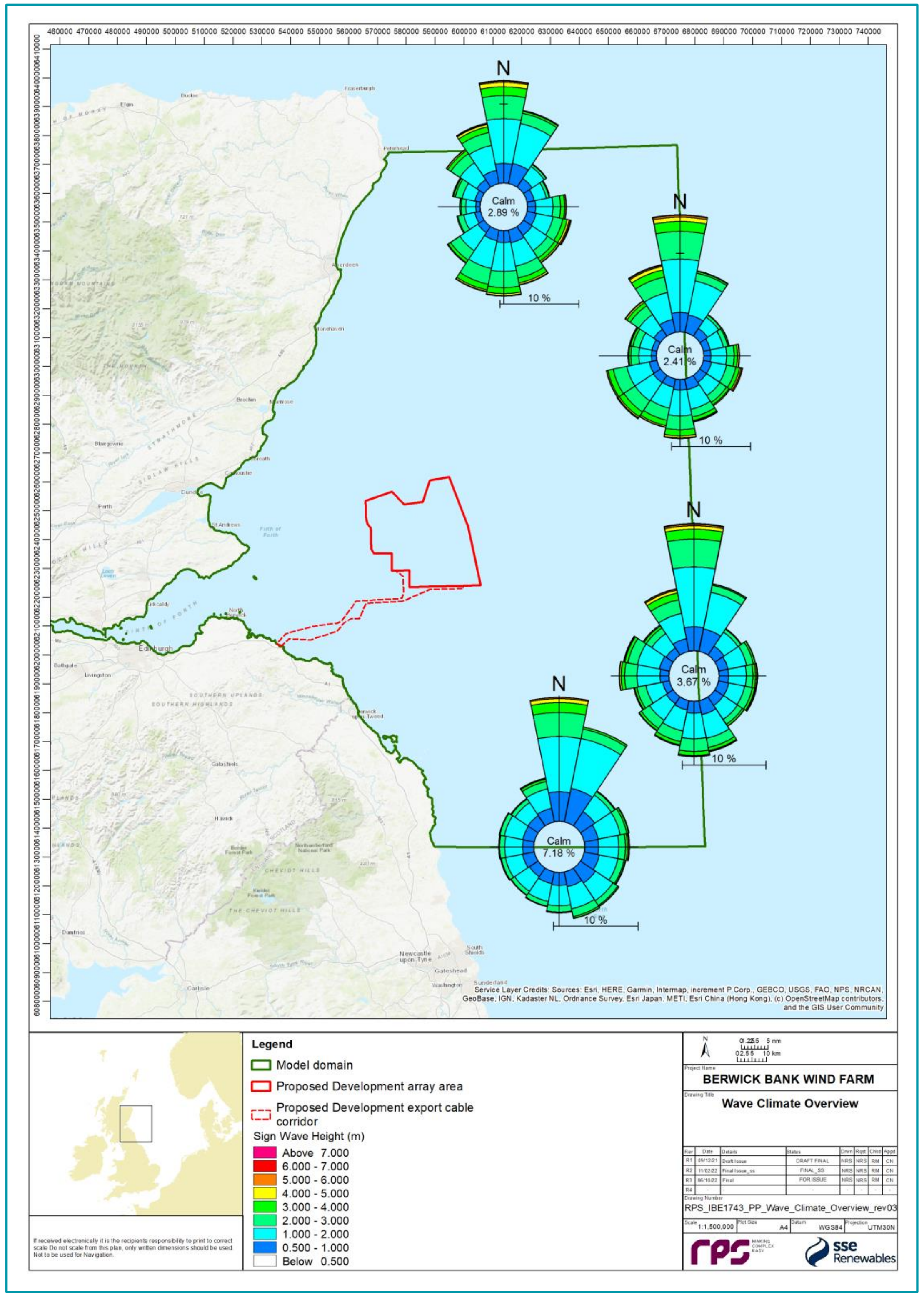


**Figure 4.25: Wave Roses for Model Boundaries – 22 Year ECMWF Dataset**

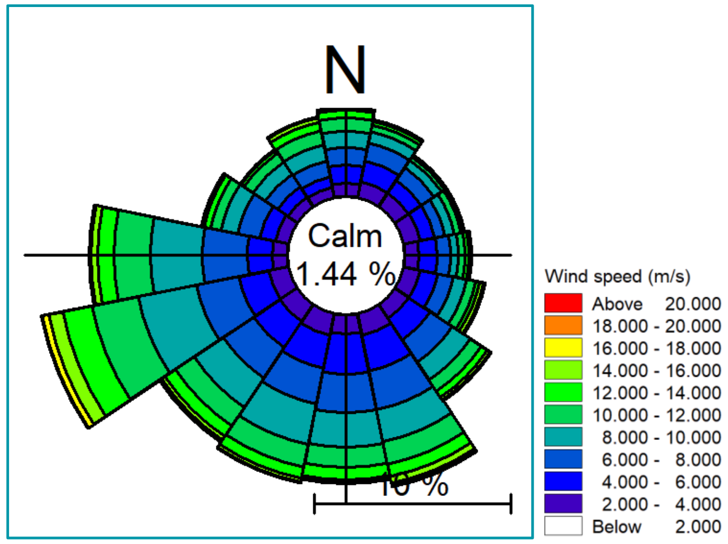


**Figure 4.26: Wind Rose for Proposed Development Array Area – Ten Year ECMWF**

34. The wave modelling was undertaken using the spectral wave model, MIKE21 SW, to provide a full wave climate and wave breaking across the physical processes study area. The model used a quasi stationary formulation which meant that for each event the wave field fully established over a number of numerical iterations until convergence was reached. The waves were computed on the same grid as the tidal flows. The model resolves the wave field by simulating wind generation of waves within the model domain and the propagation of externally generated swell waves through the domain. The model setup ensured that the detail of both locally generated wind waves and swell conditions from further afield were captured.

35. The following set of figures show the wave climate for four one in one year return period events; from approximately a northerly (000°), north-easterly (045°), easterly (090º) and south-easterly (135°) direction. These sectors were selected to be representative of the different characteristics of the wave climate and also for sectors for which the Proposed Development may potentially affect marine processes along the coastline. Although the modelling was undertaken throughout the tidal cycle the variation in wave climate was limited therefore the figures presented relate to mean sea level mid flood tide.

36. Figure 4.27 shows the waves approaching from the north and demonstrates, as anticipated, the largest waves approach from this sector. Figure 4.28 and Figure 4.29 show the climates from 045º and 090º respectively and demonstrates that although significant waves may approach from the north-east sector, they are less common, giving rise to lower wave heights for the same return period. Figure 4.30 indicates that there is sufficient fetch to develop a wind sea. The resulting magnitude of the waves transformed from offshore correlate with those recorded during the measurement campaign. Three Waverider Buoy datasets captured during 2020 were used for comparison with data produced from the model, during a key northerly storm event in June. The location of the three buoys SG1, SG2 and SG3 are shown in Figure 4.6 and a number of model validation plots for Significant Wave Height, Peak Wave Period and Mean Wave Direction are presented in Figure 4.35 to Figure 4.39. As can be seen the modelled storm event correlates well with the recorded data, taking account of the spatial and temporal resolution of atmospheric and wave data input to the model.

37. A second set of figures are presented relating to the 1 in 20 year return period. Figure 4.31 to Figure 4.34 present the data for the same sectors and tidal height as the one in one year return period. They have been introduced to ensure that the baseline for a more arduous conditions is established for assessment of the potential effect of the Proposed Development on wave climate.

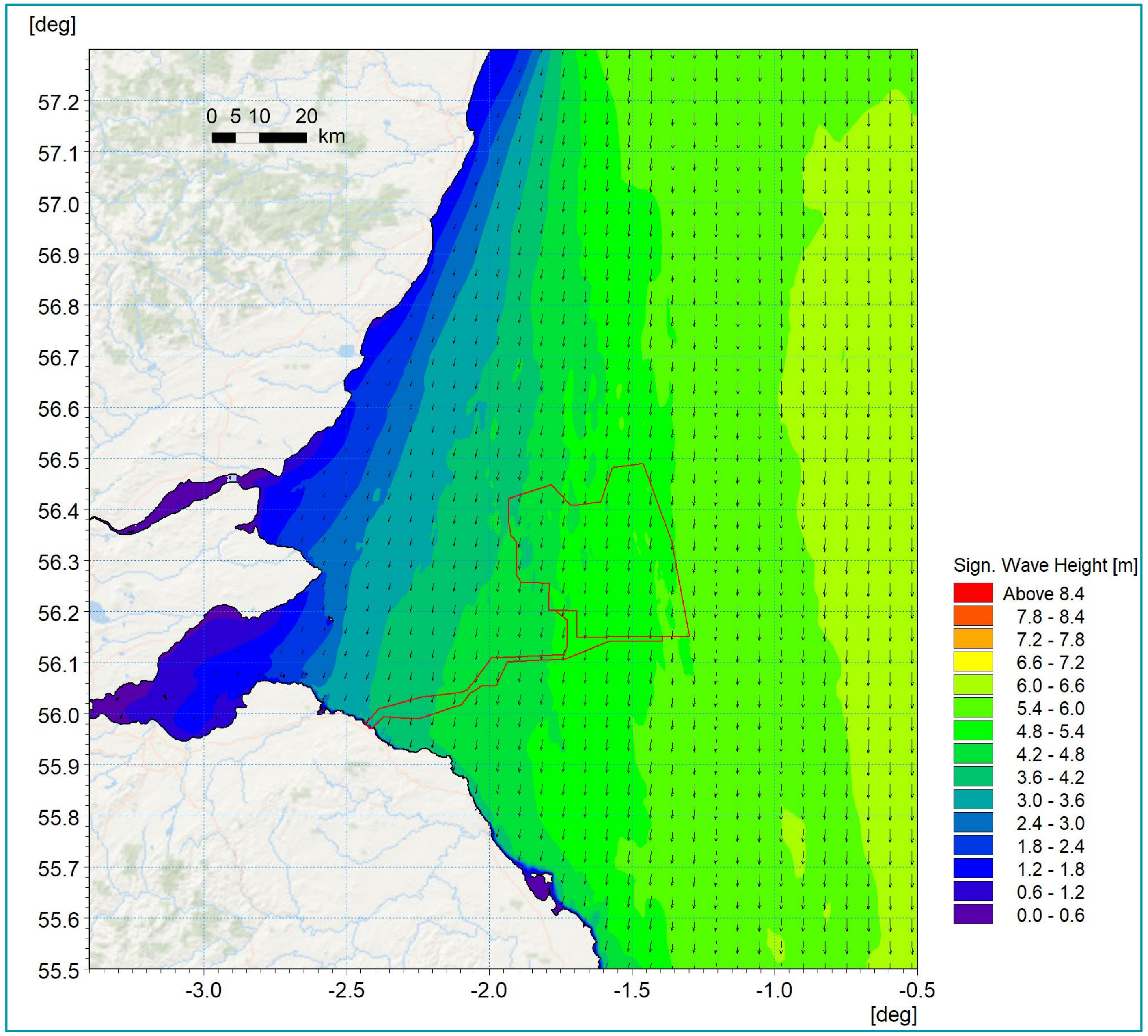


**Figure 4.27: Wave Climate 1:1 Year Storm from 000° at Mid-Tide**

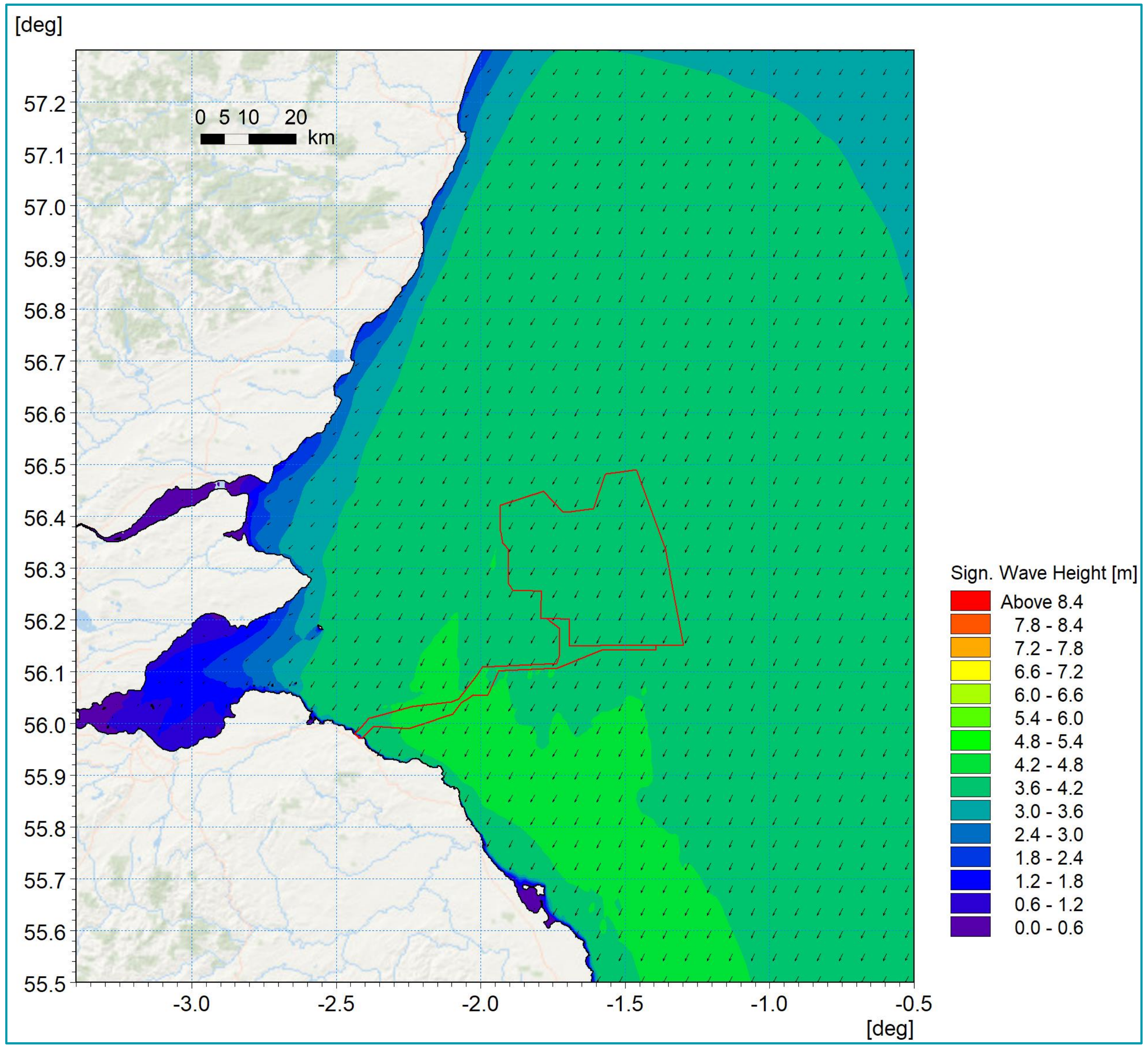


**Figure 4.28: Wave Climate 1:1 Year Storm from 045° at Mid-Tide**

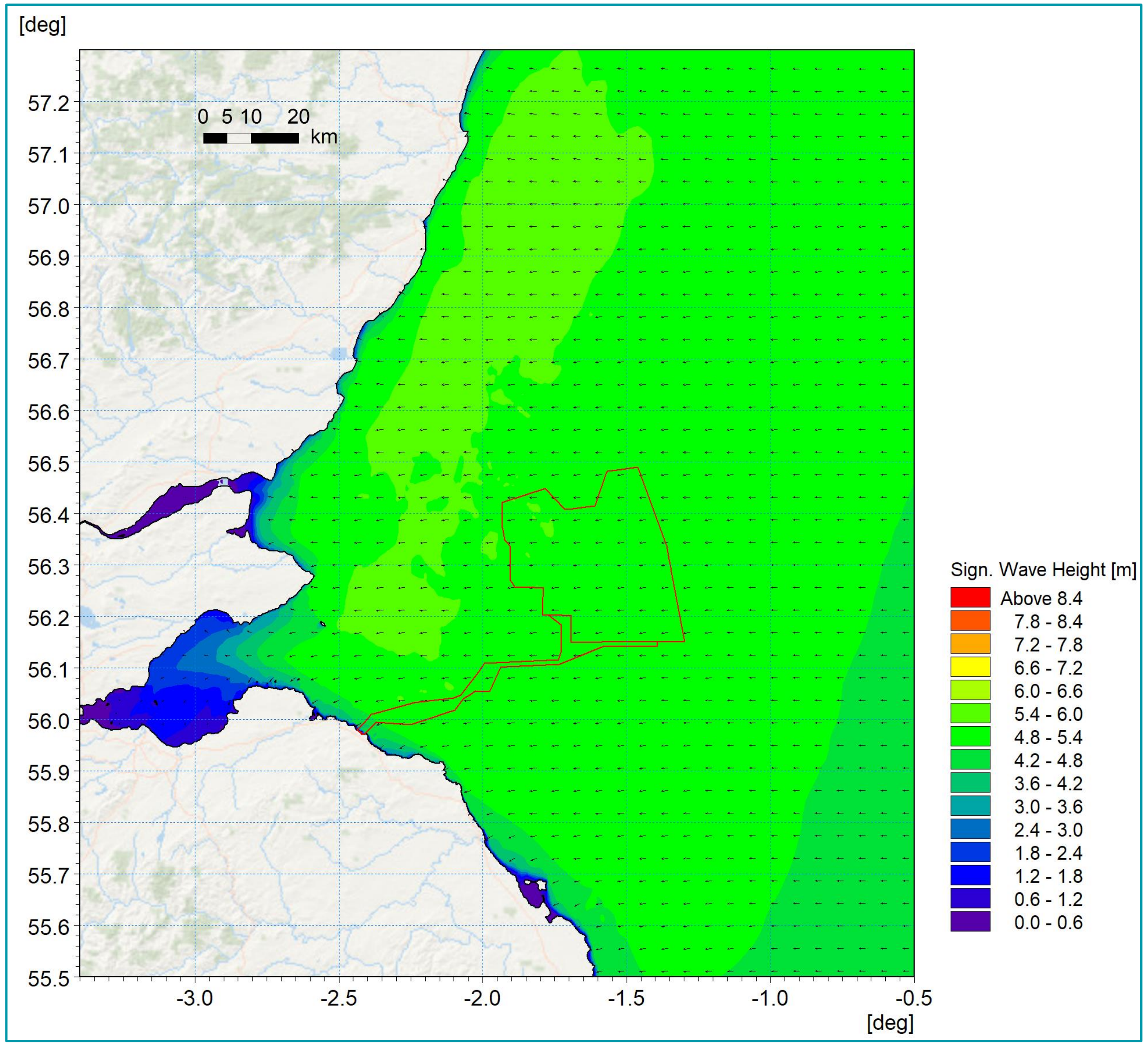


**Figure 4.29: Wave Climate 1:1 Year Storm from 090° at Mid-Tide**

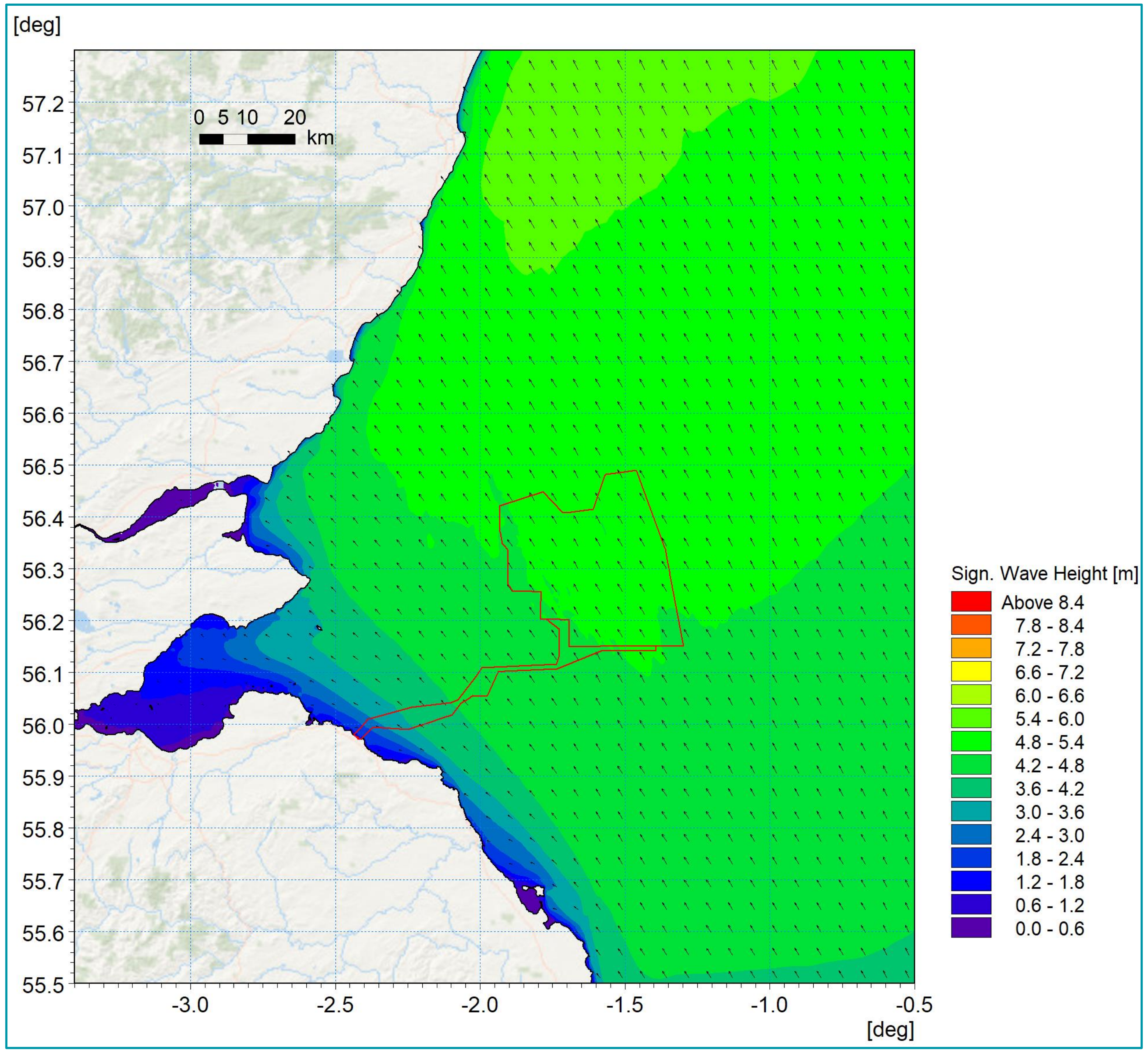


**Figure 4.30: Wave Climate 1:1 Year Storm from 135° at Mid-Tide**

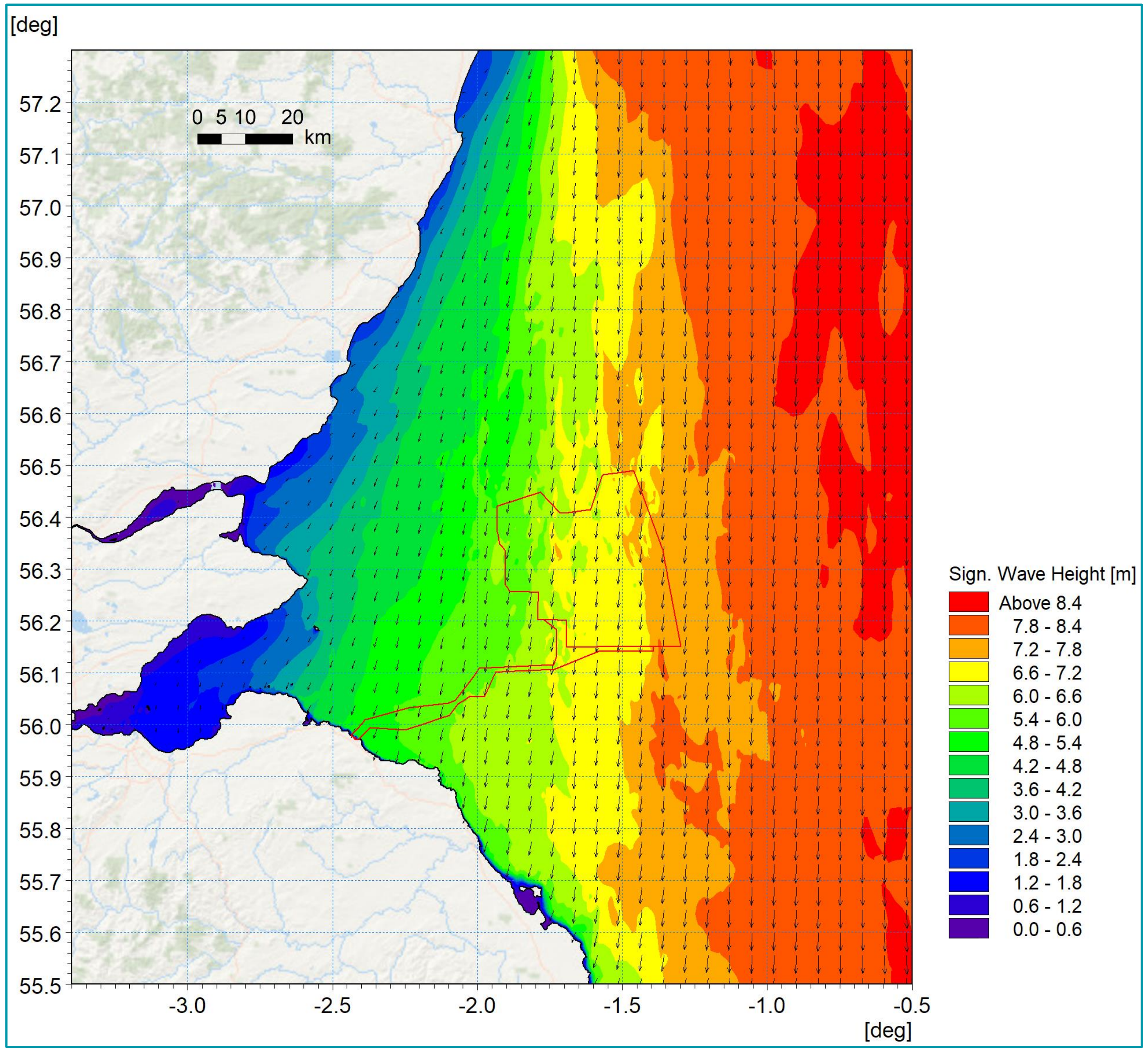


**Figure 4.31: Wave Climate 1:20 Year Storm from 000° at Mid-Tide**

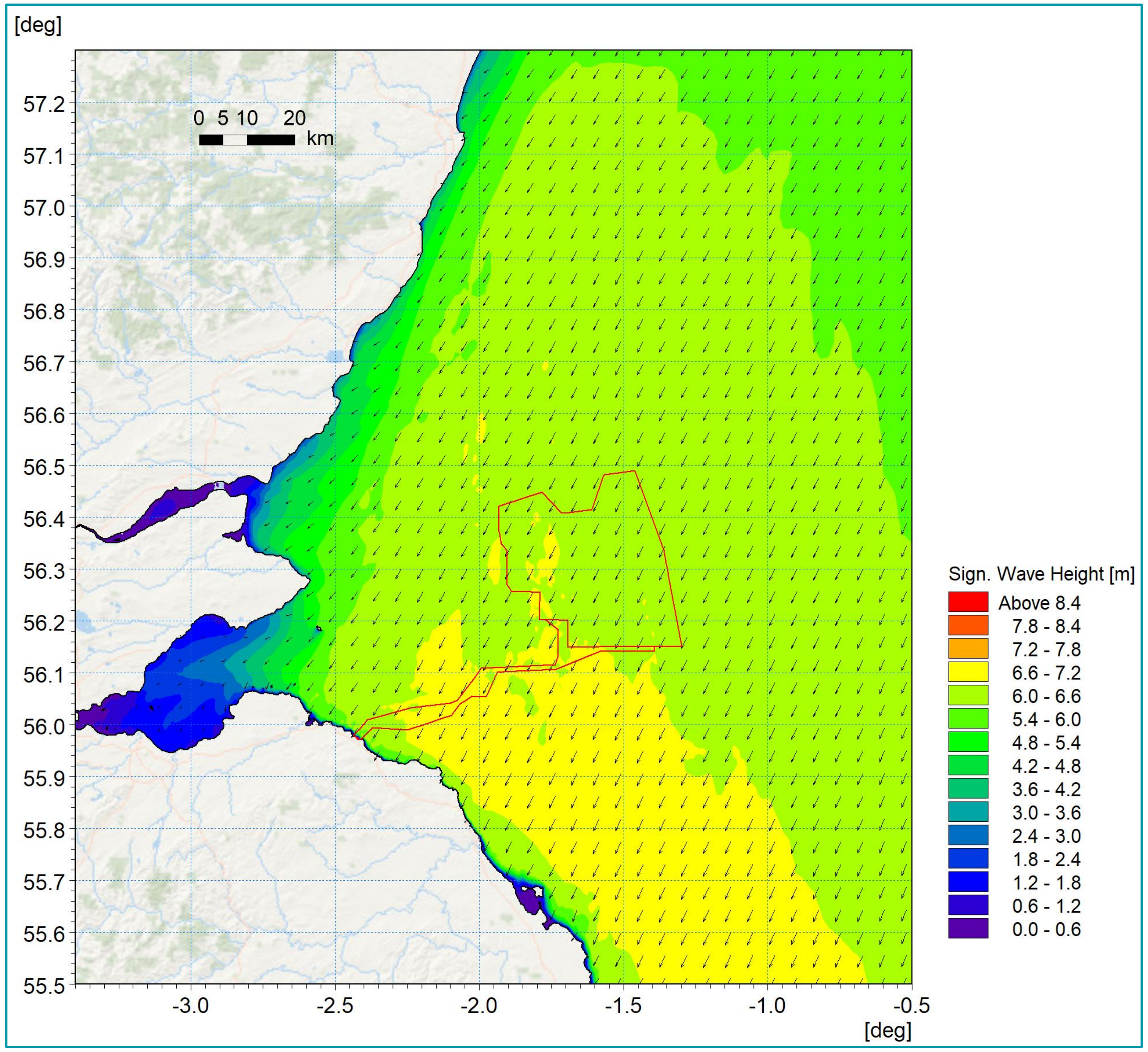


**Figure 4.32: Wave Climate 1:20 Year Storm from 045° at Mid-Tide**

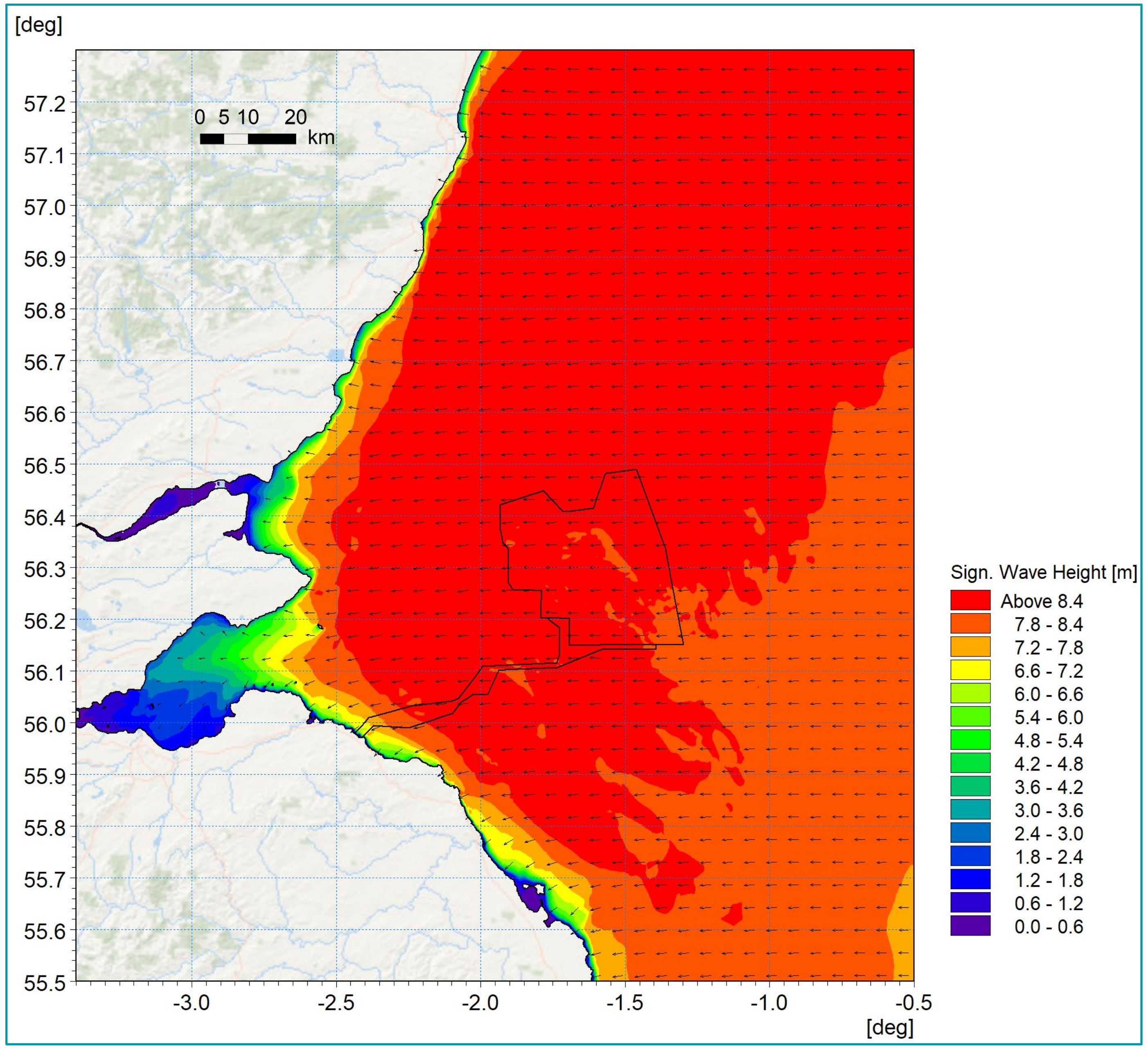


**Figure 4.33: Wave Climate 1:20 Year Storm from 090° at Mid-Tide**

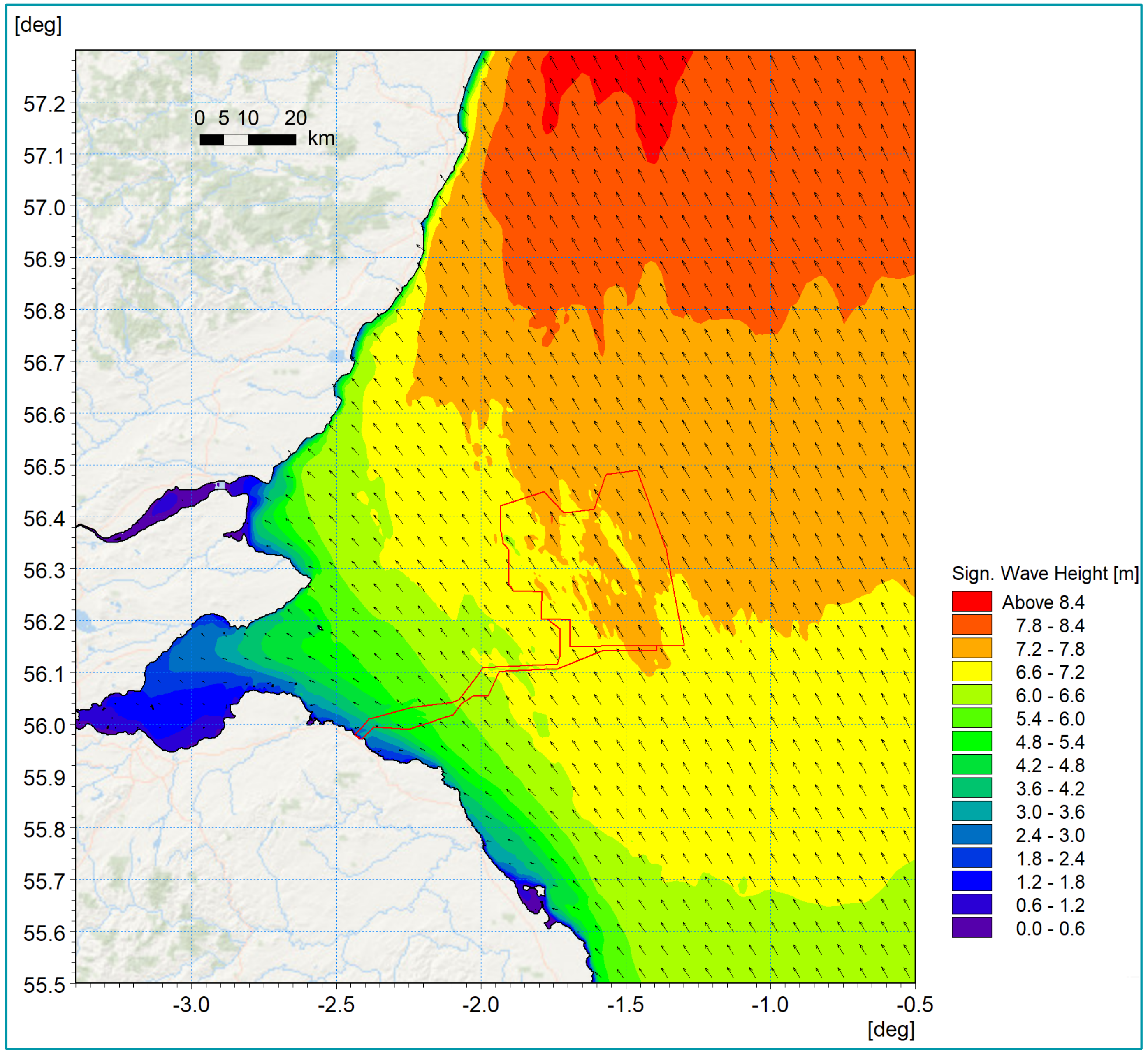


**Figure 4.34: Wave Climate 1:20 Year Storm from 135° at Mid-Tide**

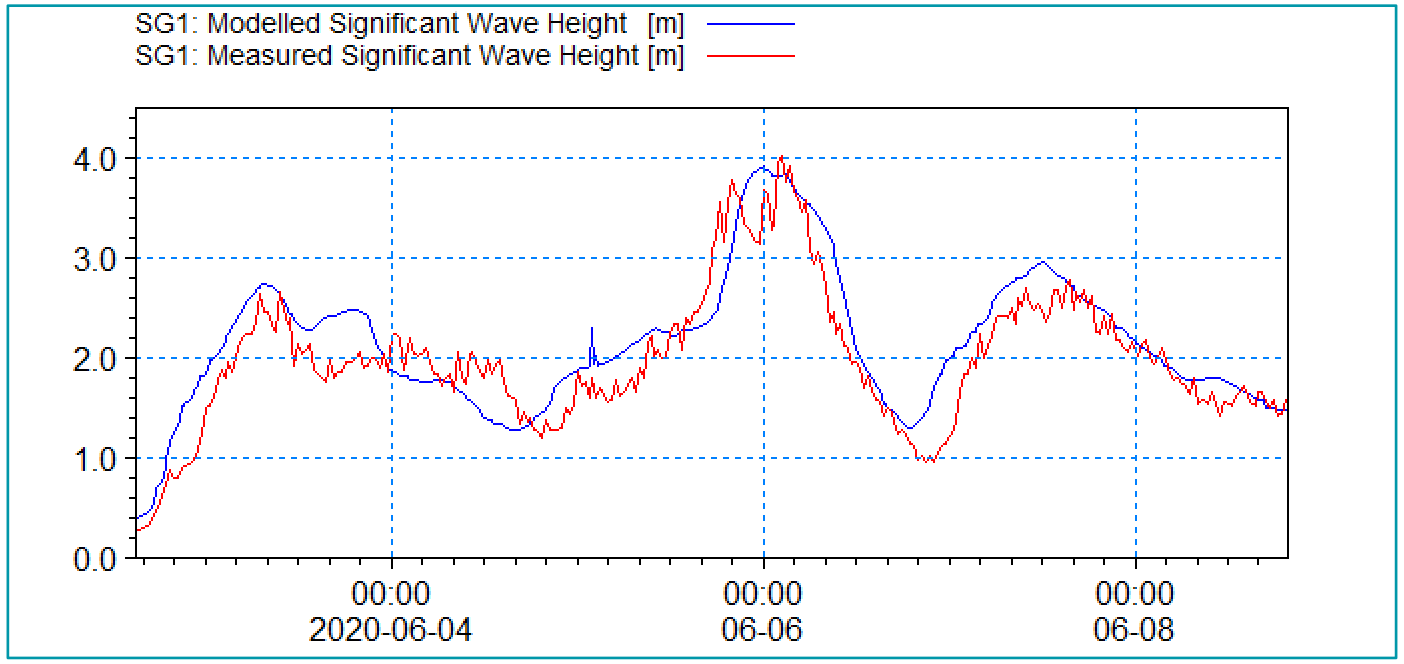


**Figure 4.35: Validation of Modelled Significant Wave Height with Measured Data at SG1**

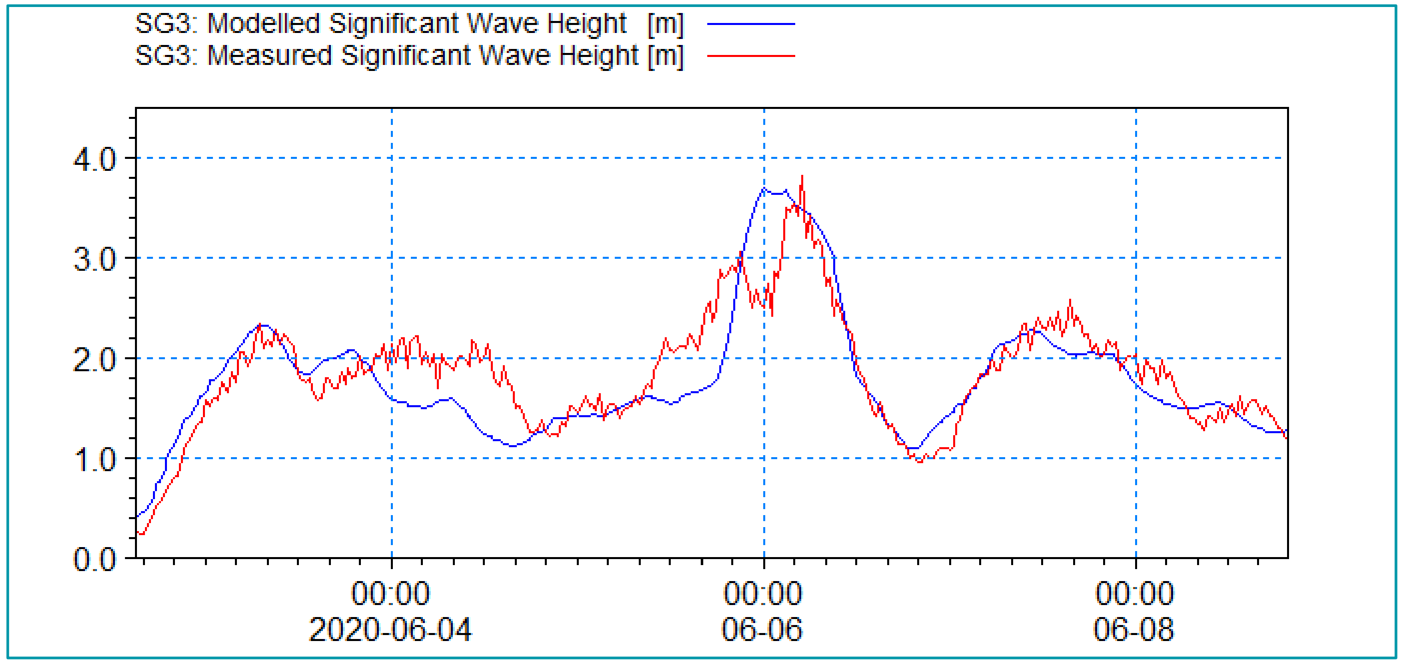


**Figure 4.37: Validation of Modelled Significant Wave Height with Measured Data at SG3**

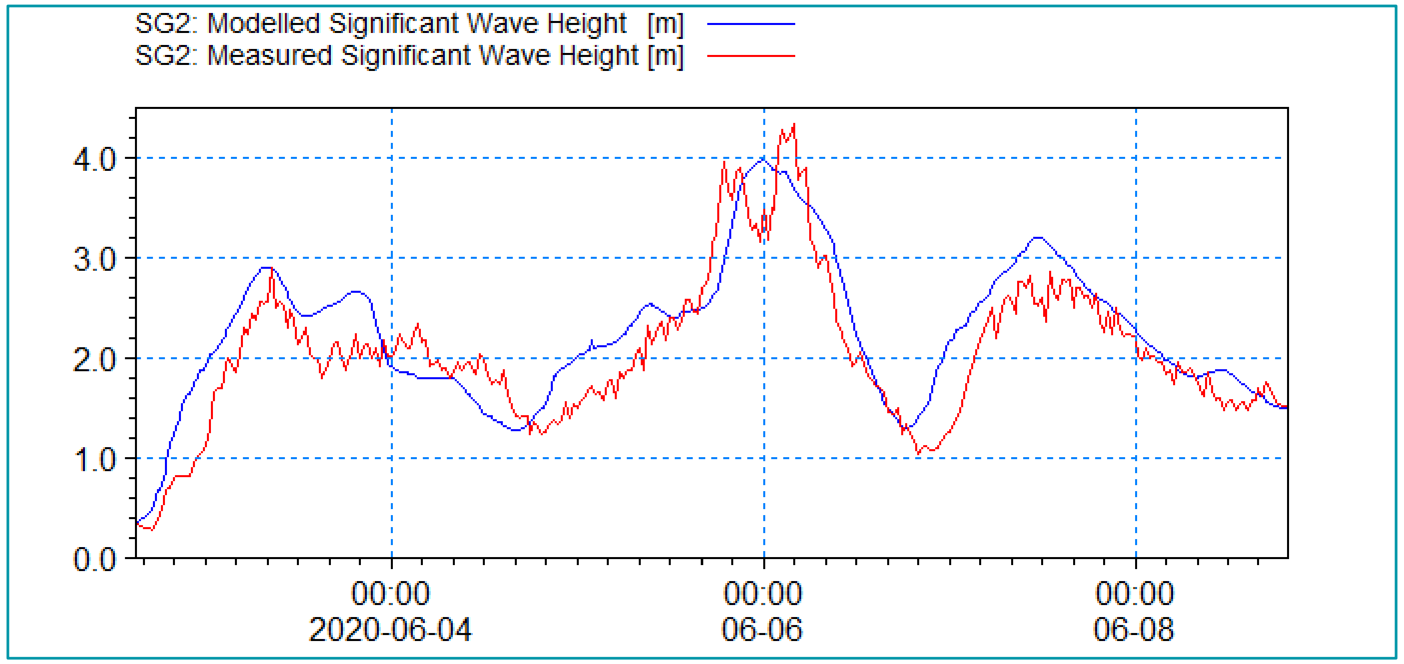


**Figure 4.36: Validation of Modelled Significant Wave Height with Measured Data at SG2**

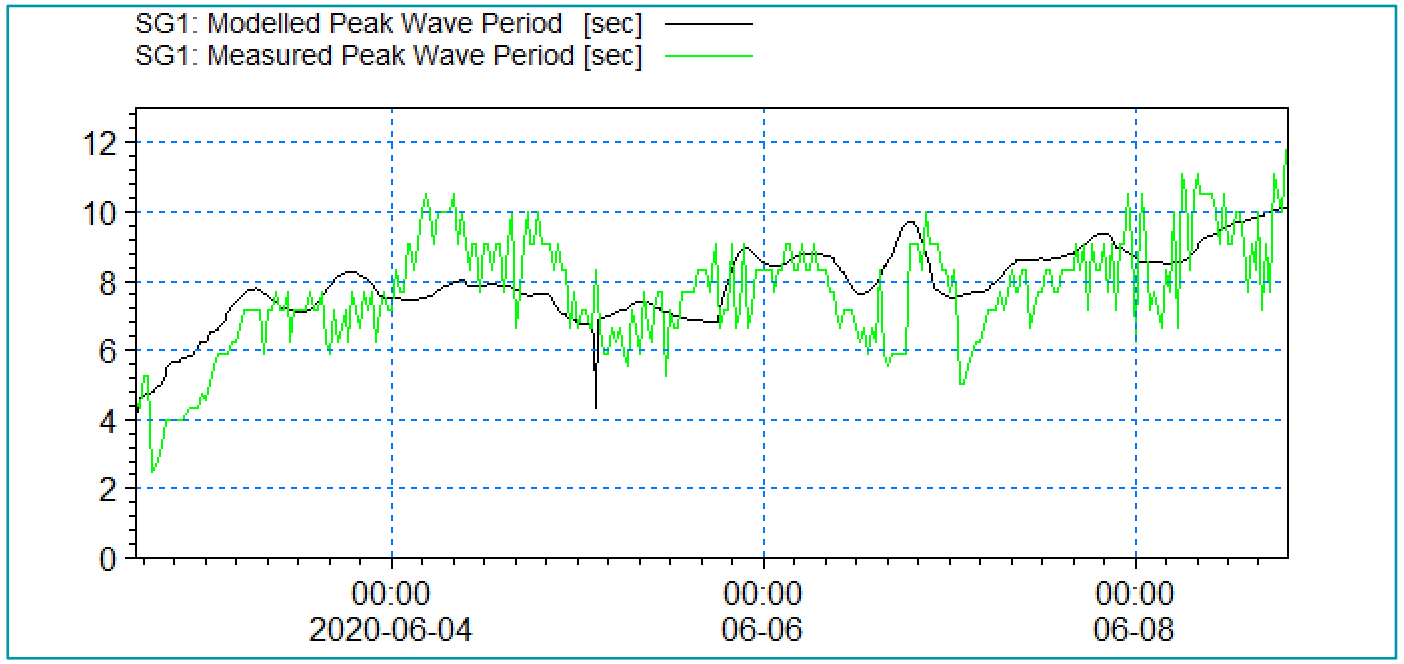


**Figure 4.38: Validation of Modelled Peak Wave Period with Measured Data at SG1**

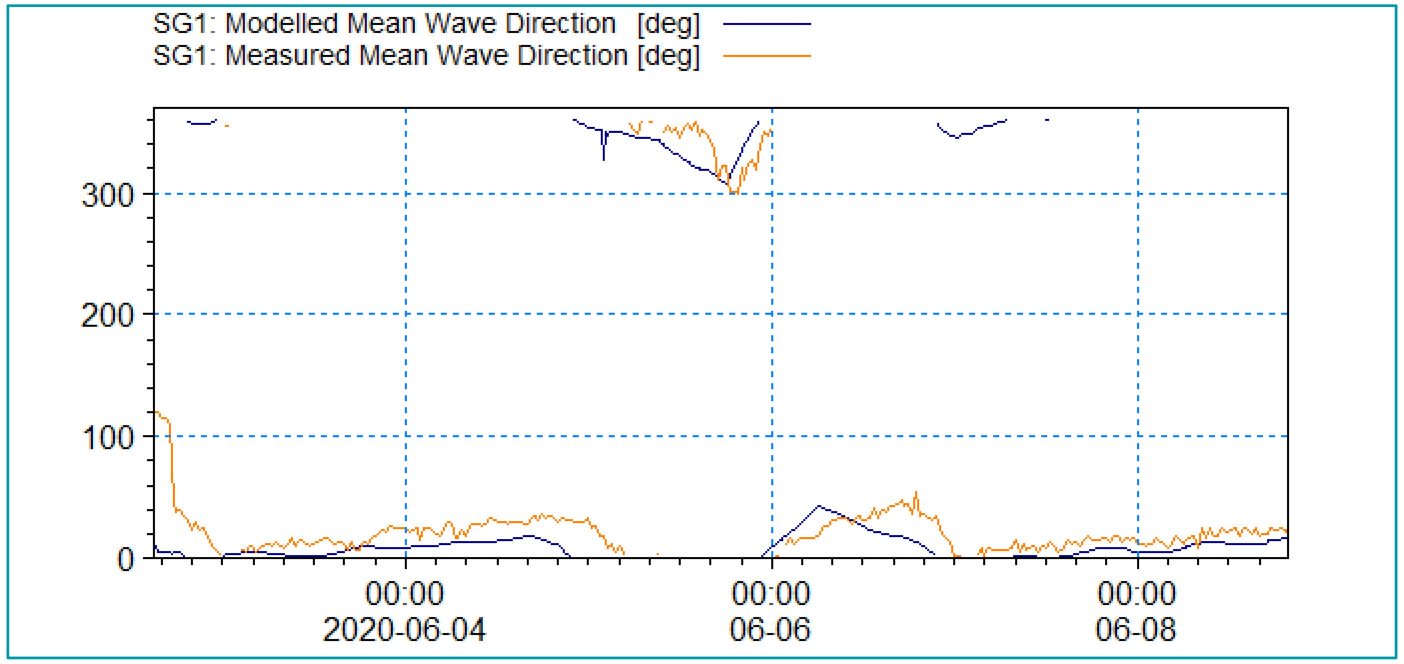


**Figure 4.39: Validation of Modelled Mean Wave Direction with Measured Data at SG1**

## 4.4. LITTORAL CURRENTS

38. The MIKE suite facilitates the coupling of models. The depth averaged hydrodynamic model, used for the tidal modelling, coupled with the spectral wave model, provides a full wave climate incorporating the impact of water levels and currents on waves and wave breaking. Using this, the littoral currents (i.e. those currents driven by tidal, wave and meteorological forces) were examined.

39. The one in one year storm from 000° sector was simulated with the inclusion of large spring tides to include a wide range of tidal conditions and the resulting peak flood and peak ebb currents are presented in Figure 4.40 and Figure 4.41 respectively. These correspond with the (calm) tidal plots presented in Figure 4.22 and Figure 4.23. As expected, the presence of the south going waves increase the currents on the flood tide whilst reducing them on the ebb.

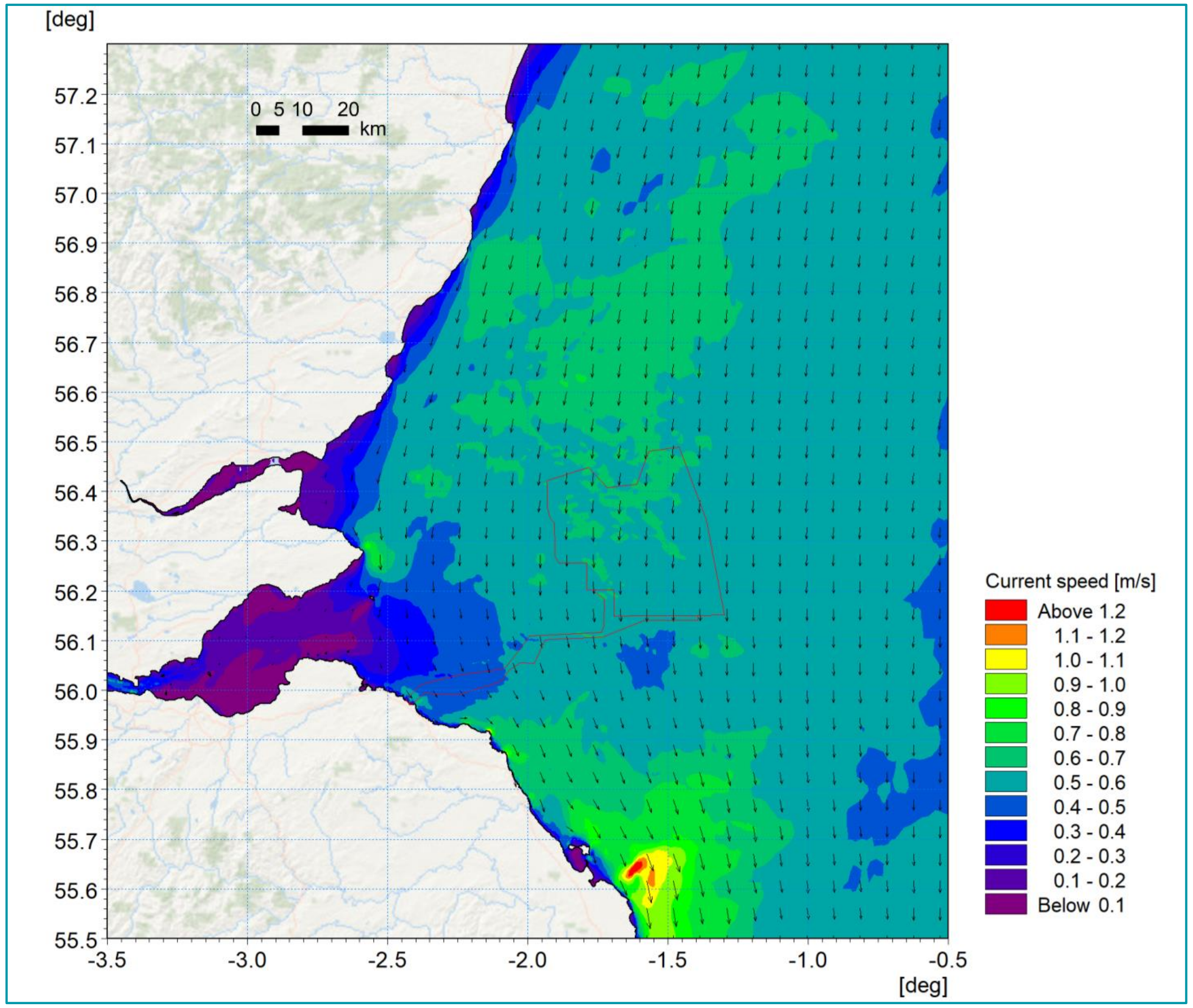


**Figure 4.40: Littoral Current 1:1 Year Storm from 000° - Flood Tide (HW -1 Hour)**

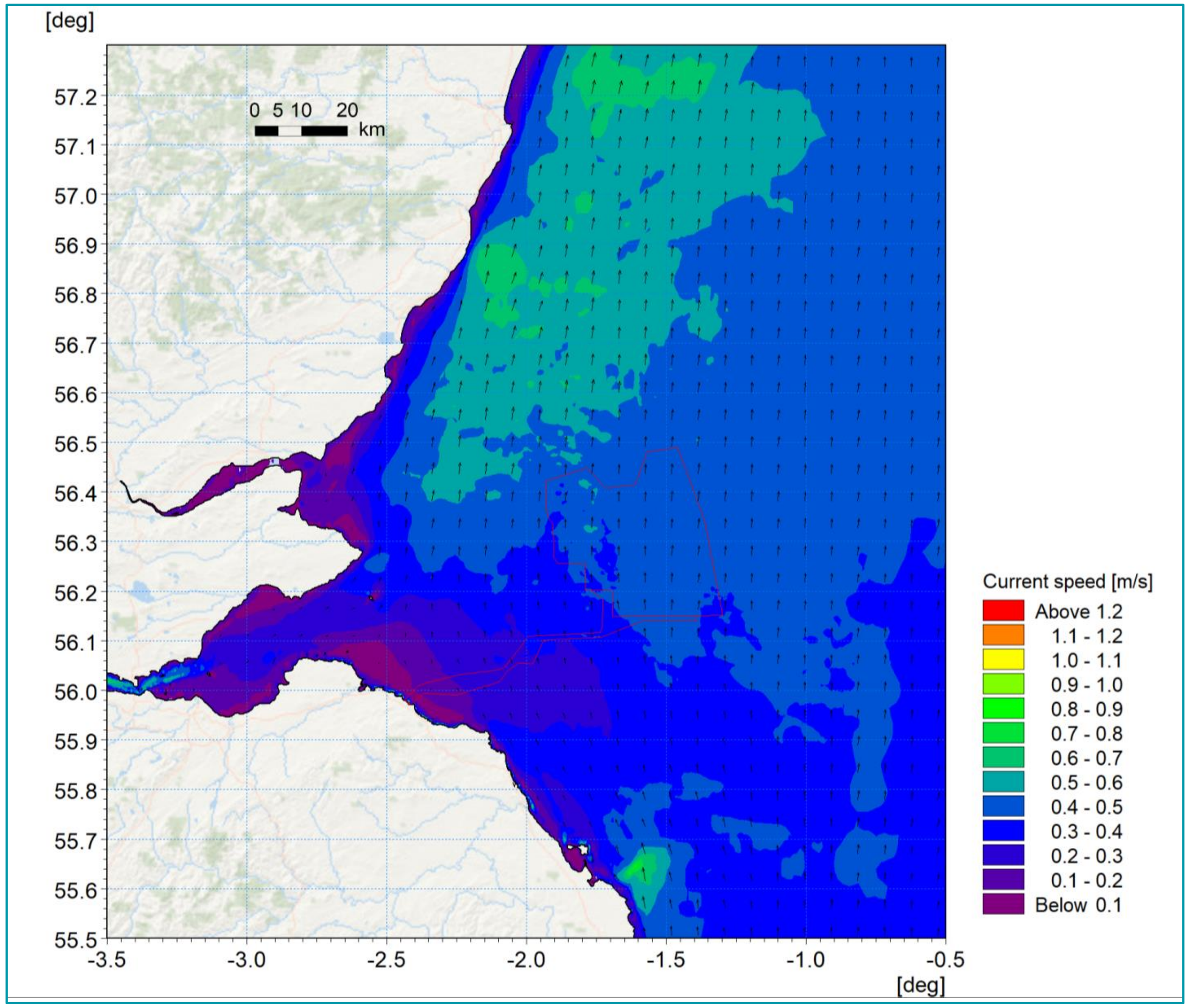


**Figure 4.41: Littoral Current 1:1 Year Storm from 000° - Ebb Tide (LW – 1 Hour)**

## 4.5. SEDIMENTOLOGY

### 4.5.1. GEOLOGY

40. Information on the geology of the Proposed Development allows for an understanding of the origin and stability of the seabed, and the geology which will be encountered during the installation of wind turbines, offshore platform foundations, inter-array cables and offshore export cables.

41. The Proposed Development array area is part of a dynamic landscape where quaternary and pre-quaternary formations have been shaped as erosional surfaces by different geomorphic factors and continue to be shaped and modelled by the present day offshore marine conditions (Fugro, 2020a). The morphology features present are due to advances and rapid retreats consistent with an oscillating and dynamic ice margin during British Ice Sheet (BIS) deglaciation (Graham *et al*., 2009).

42. Subsequent sea level rise without new sediments led to the deepening and eroding of the sea mounds and banks present in the area. Seabed bottom currents have been actively mobilising and redistributing surficial sediments, developing bedforms and filling up both depressions and channels.

43. The seafloor morphology within the Proposed Development array area is very varied and can be classified into four types of morphological features:

- large scale banks (the Marr Bank and the Berwick Bank);
- arcuate ridges;
- incised valleys, relic glacial lakes and channels; and
- bedforms.

44. The seabed within the Proposed Development export cable corridor is variable with morphological features which are framed by relic pre-Holocenic landscape, and secondary morphological features characterised by bedforms and boulder fields formed by reworked and redeposition of available material in present-day shallow marine conditions.

45. Geophysical surveys observed that the bedforms in the Proposed Development export cable corridor are comprised of principally flow-transverse structures (subaqueous dunes: ripples, megaripples); locally the bedforms can be linear, braided and lobe-shaped (bars and ribbons). The seabed within the Proposed Development export cable corridor can be classified into several types of morphological features, which include:

- primary morphological features:
  - outcrops and erosional surfaces and platforms;
  - ridges; and
  - high topographic mounds and incised valleys and channels.
- secondary morphological features:
  - subaqueous dunes;
  - irregularity of the seafloor;
  - features related to anthropogenic activity; and
  - boulder fields.

### 4.5.2. SEABED SUBSTRATE

46. An overview of surficial sediment geology and the seabed features is presented in this section, based on interpretation undertaken of the side-scan sonar (SSS) data collected during the recent geophysical surveys. An understanding of seabed substrate types is required to assess the potential impacts which may arise due to the installation of wind turbines, offshore platform foundations, inter-array cables and offshore export cables. Figure 4.42 illustrates the seabed substrates present across the Proposed Development. The recent geophysical survey of the Proposed Development array area and Proposed Development export cable corridor identified that it is comprised of several distinctive features:

- boulders and boulder fields;
- areas of ripples;
- areas of megaripples and sand waves; and
- areas of trawl marks.

47. The majority of the Proposed Development array area seabed is 'featureless' however the southern and north-western extent of the Proposed Development array area are dominated by megaripples, sand waves, ribbons and bars. Boulders are also prevalent across the area and are either represented as isolated boulders or as clusters. Seabed sediments present in the Proposed Development array area can be classified into several groups:

- coarse gravel, shelly gravelly sand with boulders;
- mixed sediment;
- mixed sediments with patchy coarse material or boulders; and
- muddy sand.

48. The seabed within the Proposed Development export cable corridor was recorded as smooth with very few observed primary morphological features (such as high reliefs or ridges), while secondary morphological features such as ripples and megaripples, sand bars and ribbons characterise the seabed morphology. Seabed sediments present in the Proposed Development export cable corridor can be classified into several groups:

- hard substrate: coarse sediment with cobbles, boulders and rock outcropping or sub outcropping characterised by high reflectivity signature in the side-scan data;
- gravelly sand and coarse sediments with medium reflectivity; and
- sandy sediments including fine sand and muddy sand with low reflectivity.

49. The Skateraw landfall is sited on the East Lothian coast and is characterised by a foreshore which is mostly made up of rock with areas of sand deposits, where the top of the beach is lined with a mixture of sand, pebbles, and small boulders. The seabed morphology comprises a rocky undulating Carboniferous platform with patches of megarippled sands where sediment has accumulated within larger channels. Extending offshore, the undulating rocky seabed becomes flatter, with areas of sediment with boulders interpreted as sediment overlaying rock, (XOCEAN, 2021).

50. To inform the modelling study seabed sediment information was required beyond the extent of the survey data and the EMODnet Geology database was utilised. The seabed classification shown in Figure 4.43 also corresponds with the interpretation of the most recent study, particularly with respect to the location of the nearshore rocky outcrops, sandy regions of the Proposed Development export cable corridor and the mixed sediments within the Proposed Development array area.

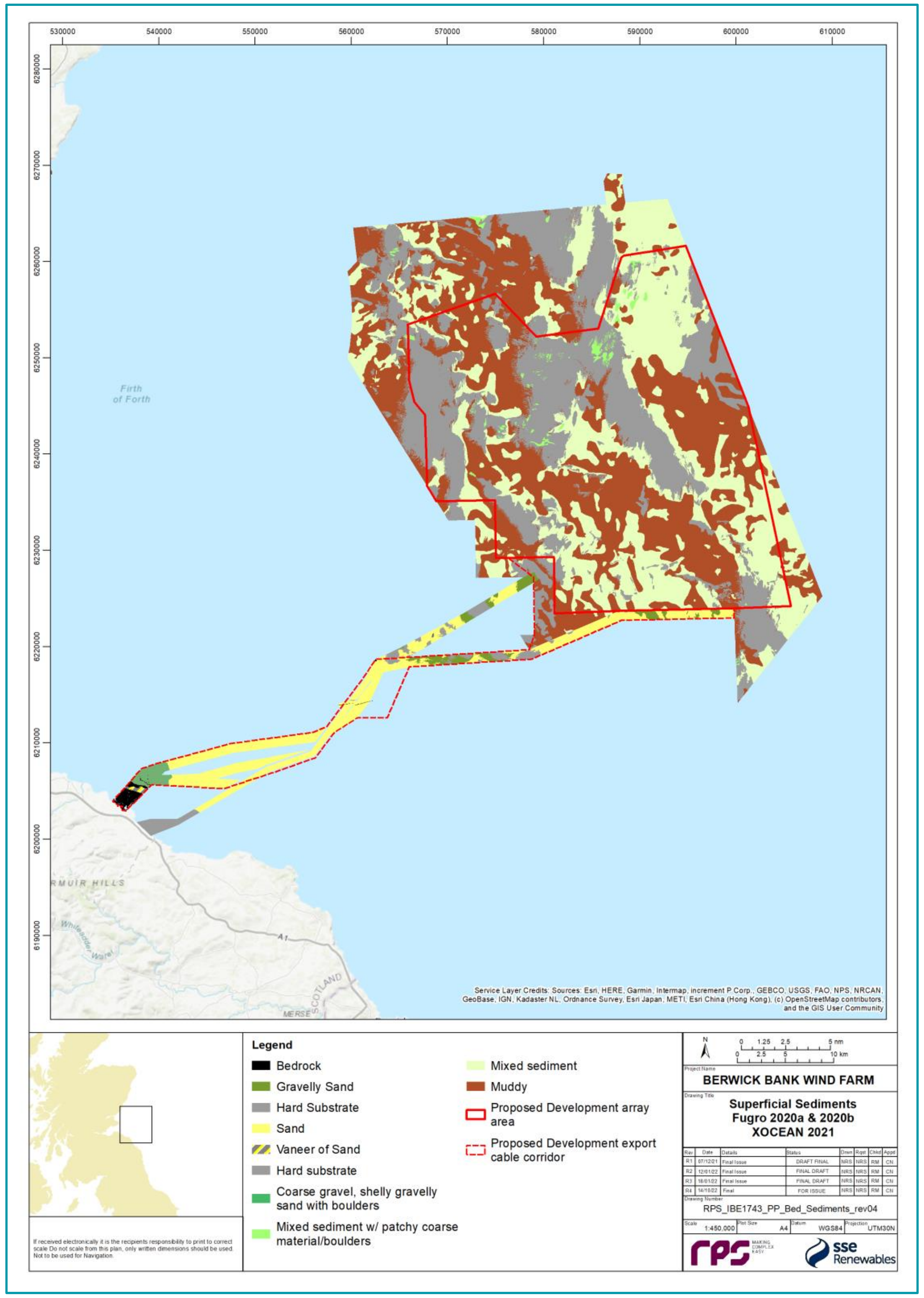


**Figure 4.42: Seabed Classification Fugro 2019 Survey and XOCEAN 2021**

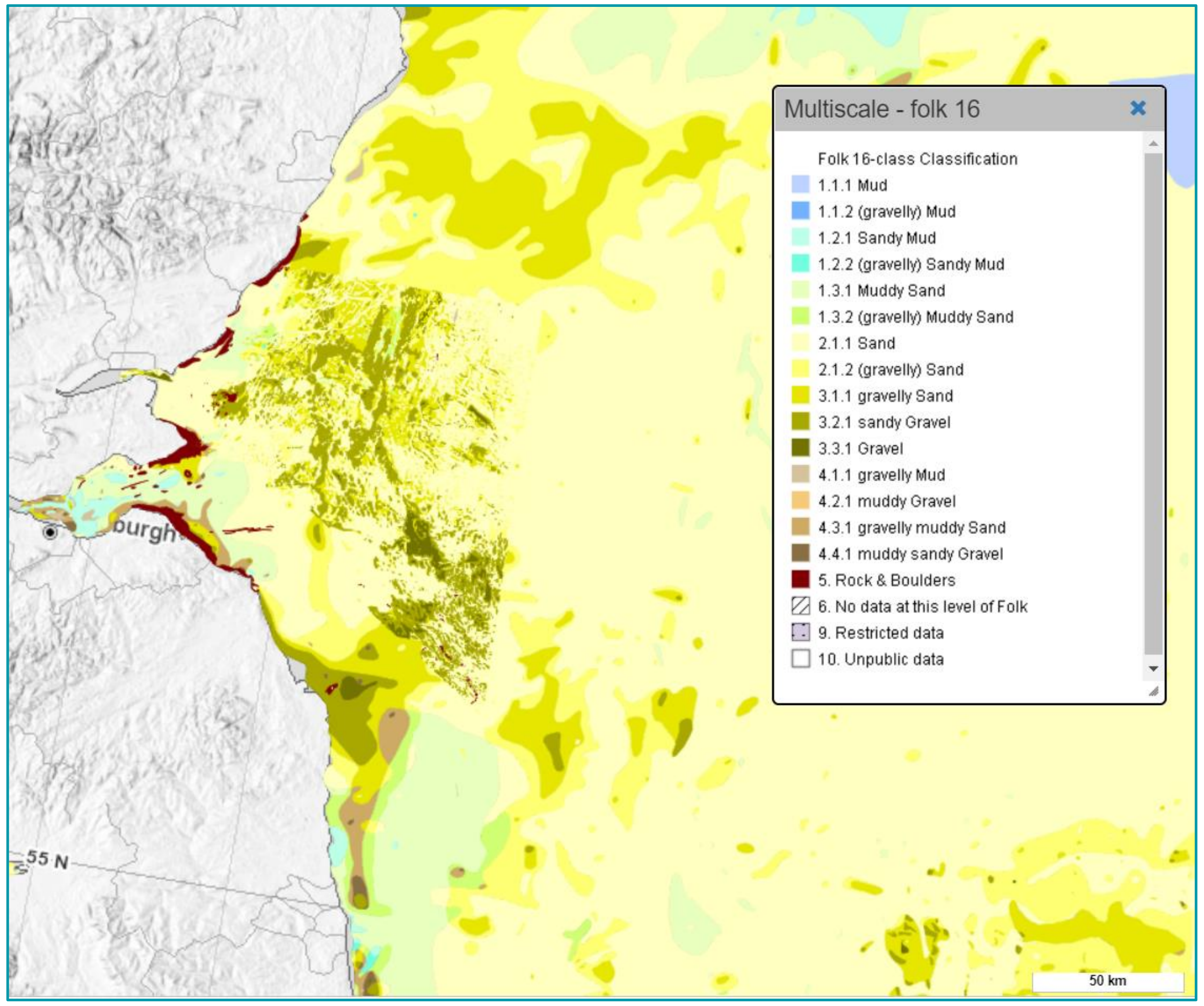


**Figure 4.43: EMODnet Geology Seabed Substrate**

## 4.6. SEDIMENT TRANSPORT

51. The MIKE21 Sediment Transport module enables assessment of bed sediment transport rates and initial rates of bed level change for non-cohesive sediment resulting from currents or combined wave current flows. It was used to determine the sediment transport pattern within the model domain. The model combines inputs from both the hydrodynamic model and, if required, the wave propagation model. It used sediment characteristics provided by the recent survey and EMODnet data as presented in the previous section to determine the sediment transport characteristics. It is noted that for a detailed sediment transport study greater detail of sediment characteristics across the model domain and along the coastline would be required. In the context of a comparative study to identify the impact of the Proposed Development infrastructure on sediment transport patterns the sediment characteristics identified within the survey and sampling were interpolated to those areas in the EMODnet data with similar sediment classifications.

52. The model domain was set up with a layer of mobile bed material as described by the survey data. In areas where sediment is present an initial layer depth was set to 3 m and tapered to zero in the areas of rocky outcrops to ensure that sediment was not exhausted during the simulated events. Two sediment transport scenarios were examined, one relating to calm conditions and a second relating to the one in one year return period event from 000°. In each case the evaluations were undertaken over the course of two spring tides. These simulations included a period for the hydrodynamics and wave fields to stabilise and develop across the domain prior to sediment transport being enabled (i.e. a “warm-up” period).

53. For each scenario three aspects were examined:

- residual current, which is the net flow over the course of the tidal cycle. This is effectively the driving force of the sediment transport;
- potential sediment transport over this period; and
- rate of change of the bed during flood and ebb tides. This provides information for a ‘snap-shot’ in time to enable the process to be illustrated.

54. For the tidal current alone, the residual current is presented in Figure 4.44. It is characterised by low residual current speeds within the Proposed Development area which are borne out by the low transport rates shown in Figure 4.45. The transport plot includes a log scale palette as the values within the offshore banks are several orders of magnitude smaller than those along the coastline. The mechanism is more clearly illustrated in Figure 4.46 and Figure 4.47, where the bed levels are reduced at certain locations during the flood tide and increase to the same degree on the return tide. This corresponds with the sand ripples that are evident in the area. A log scale was also applied in these figures to encompass the range of values at the coast and across the offshore banks and at peak currents these changes are of the order of a fraction of a millimetre per day. This indicates that although the bed is mobile the area is stable.

55. When a storm approaches from the north, the flood tide currents are enhanced by the wave climate. This is reflected in an increase in the residual currents and thus an increase in the sediment transport capacity on the flood tide as illustrated in Figure 4.48 and Figure 4.49. Similarly, the figures showing the changes in bed level peak tide indicate rates of change for both flood and ebb tide, Figure 4.50 and Figure 4.51. It is however noticeable that the increases and decreases in bed levels remain largely in opposition during the storm event indicating that tidal factors remain dominant under these circumstances.

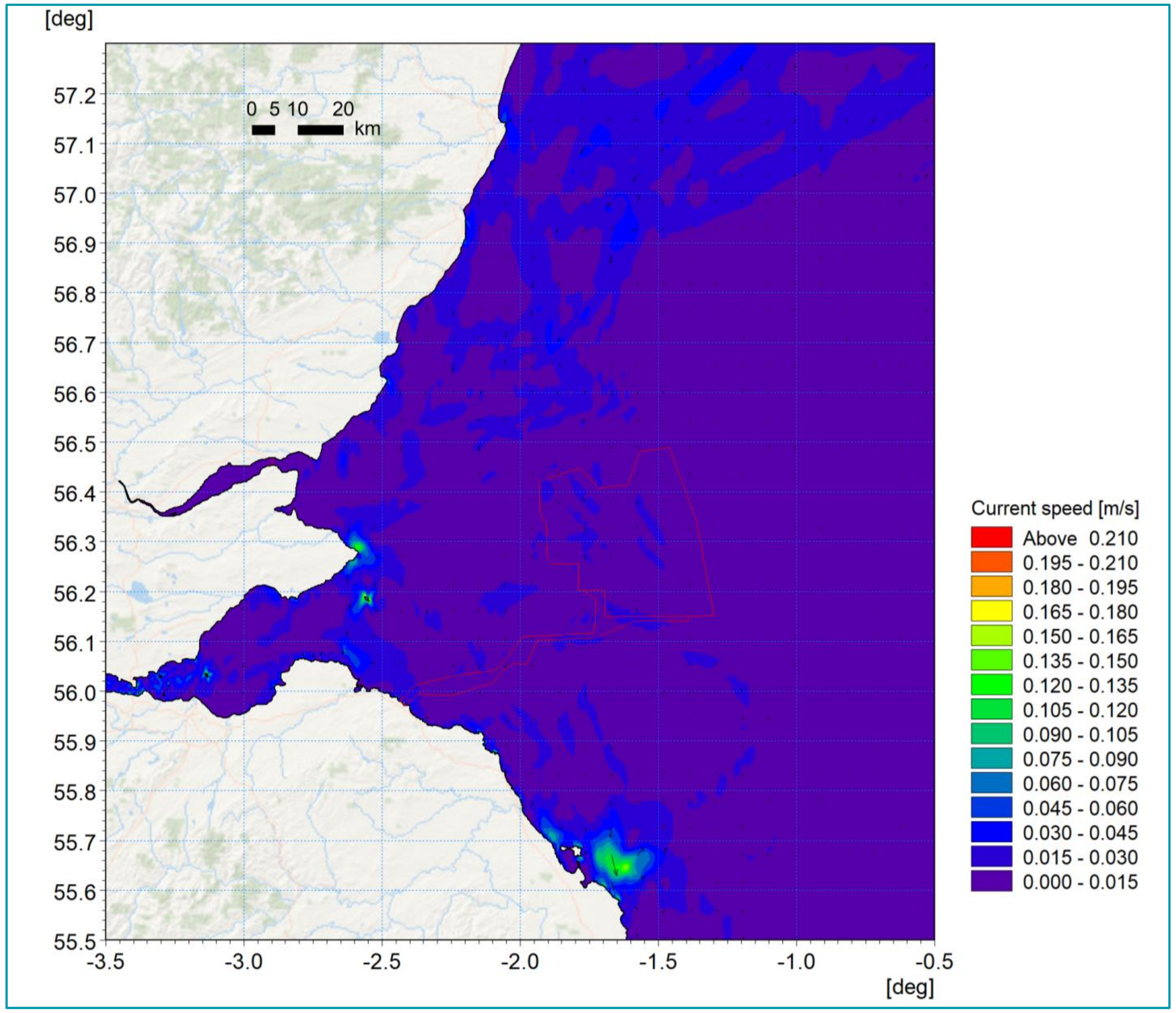


**Figure 4.44: Residual Current Spring Tide**

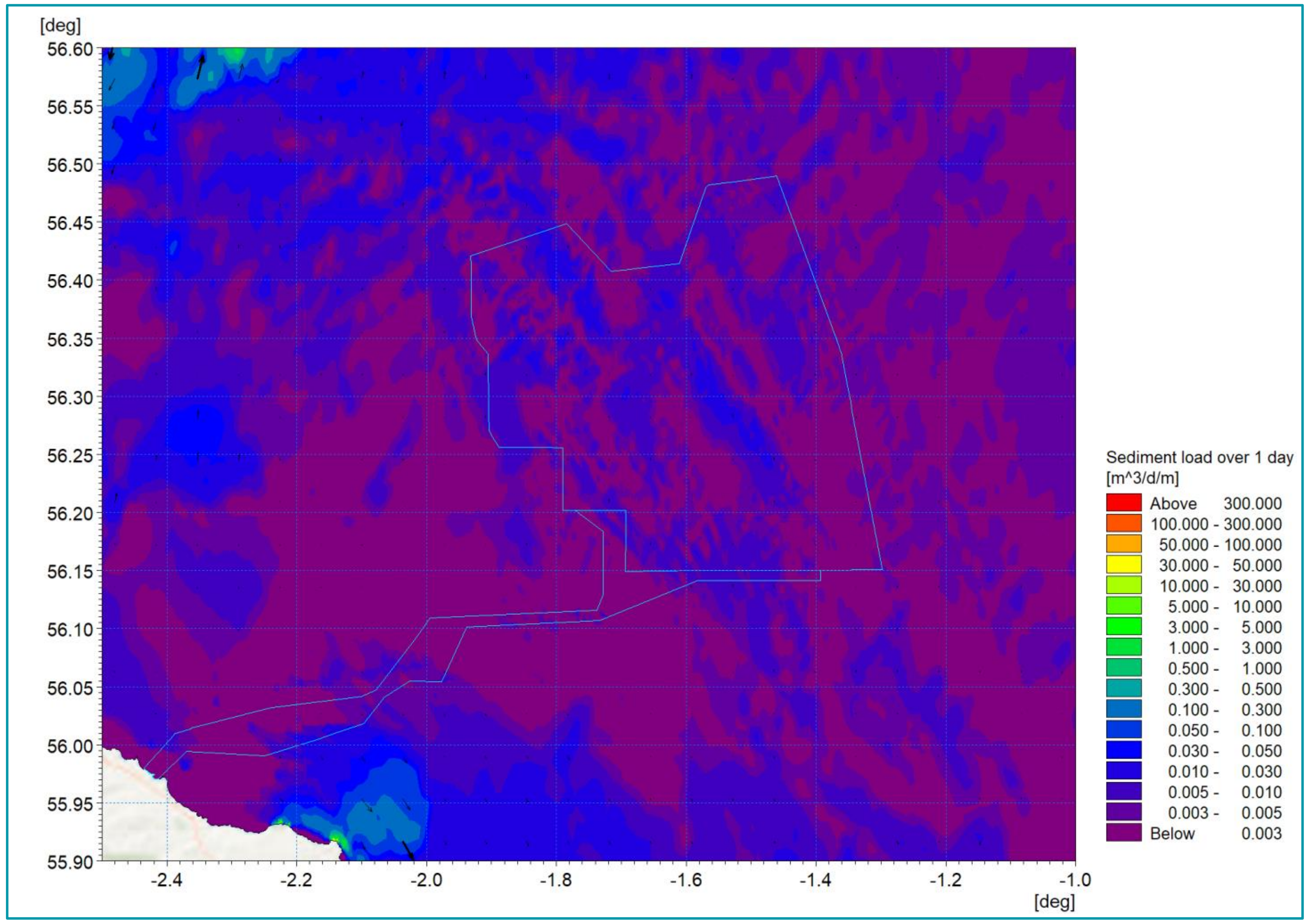


**Figure 4.45: Potential Sediment Transport over the Course of One Day (Two Tide Cycles)**

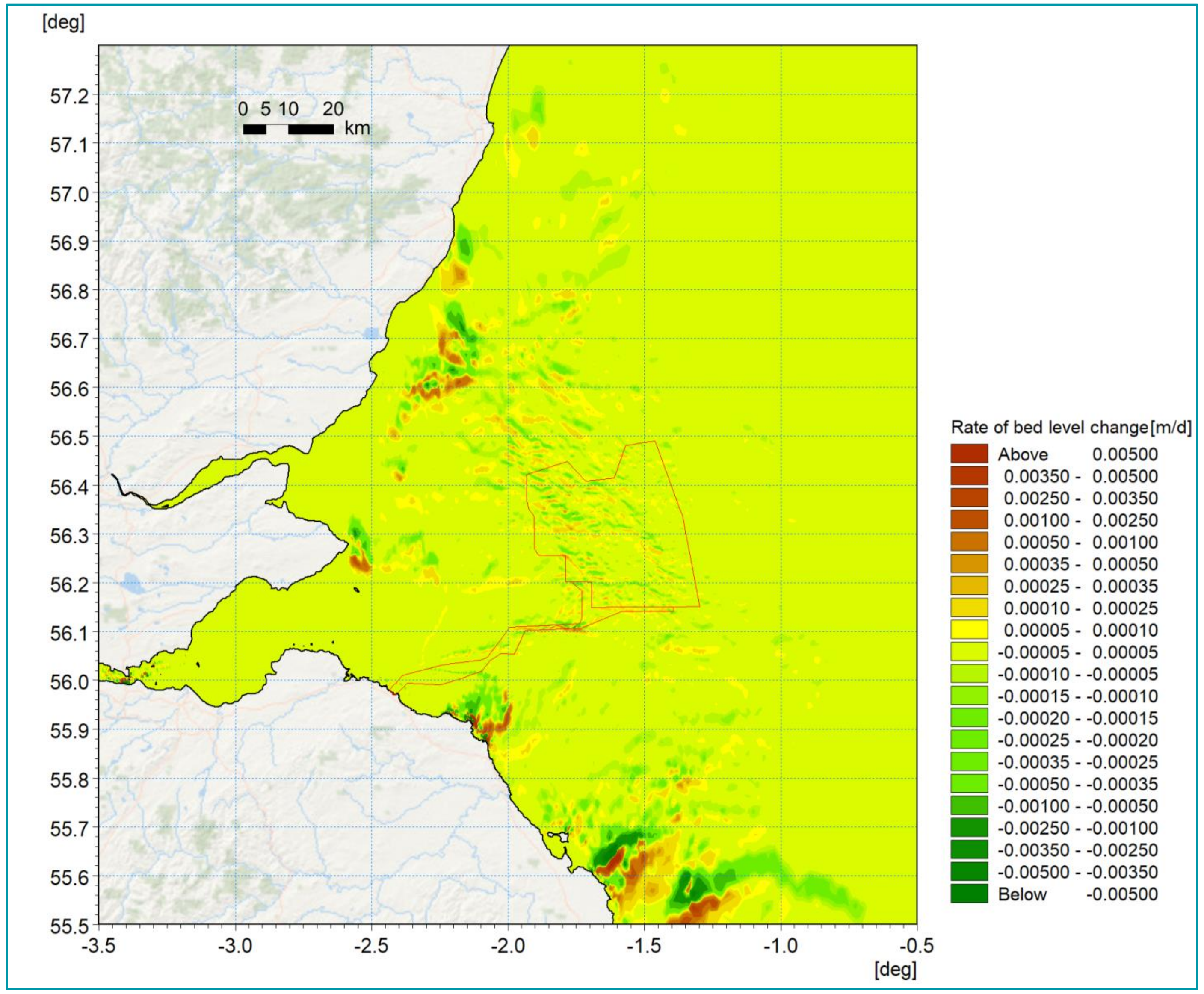


**Figure 4.46: Rate of Bed Level Change – Peak Flood Tide**

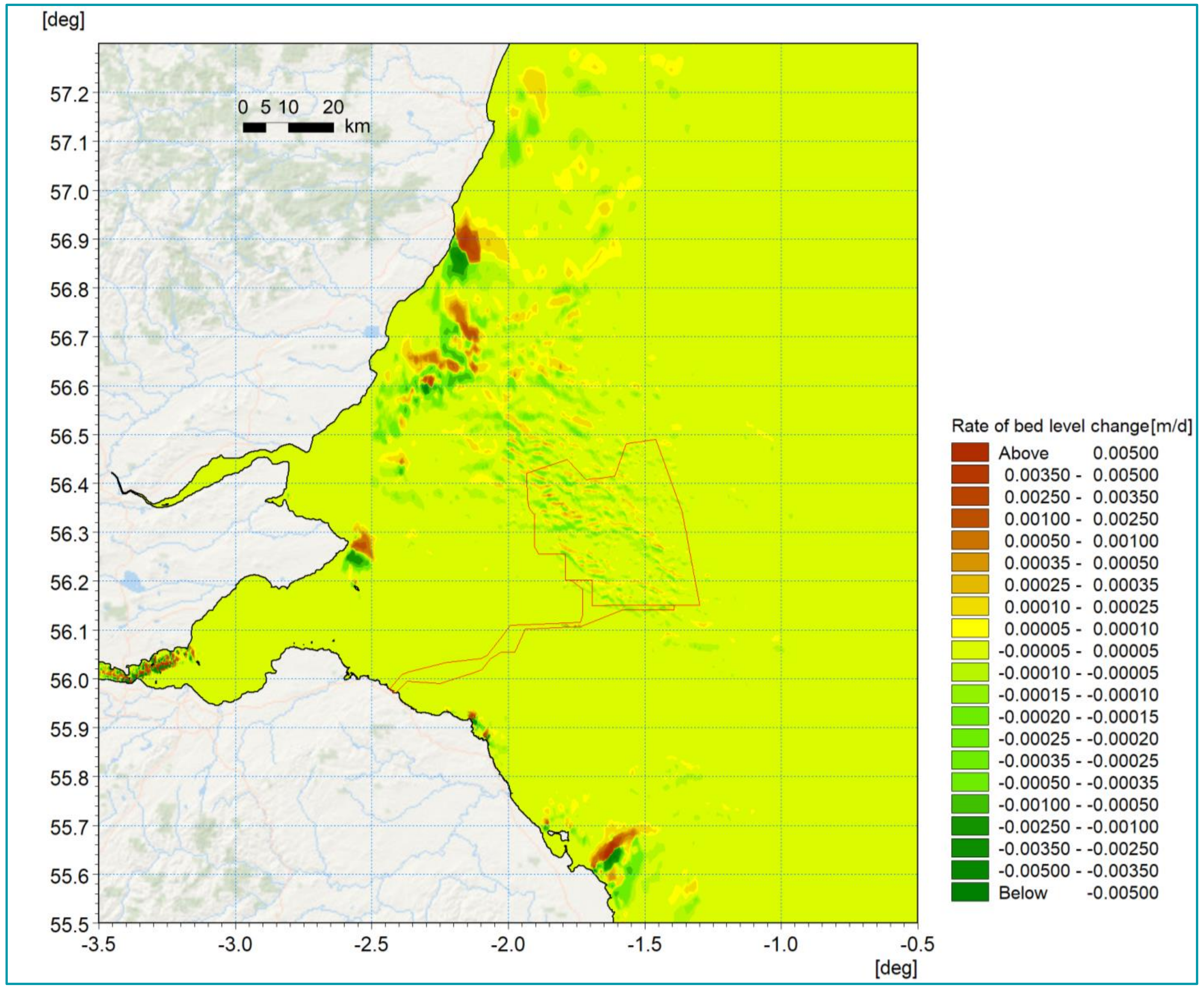


**Figure 4.47: Rate of Bed Level Change – Peak Ebb Tide**

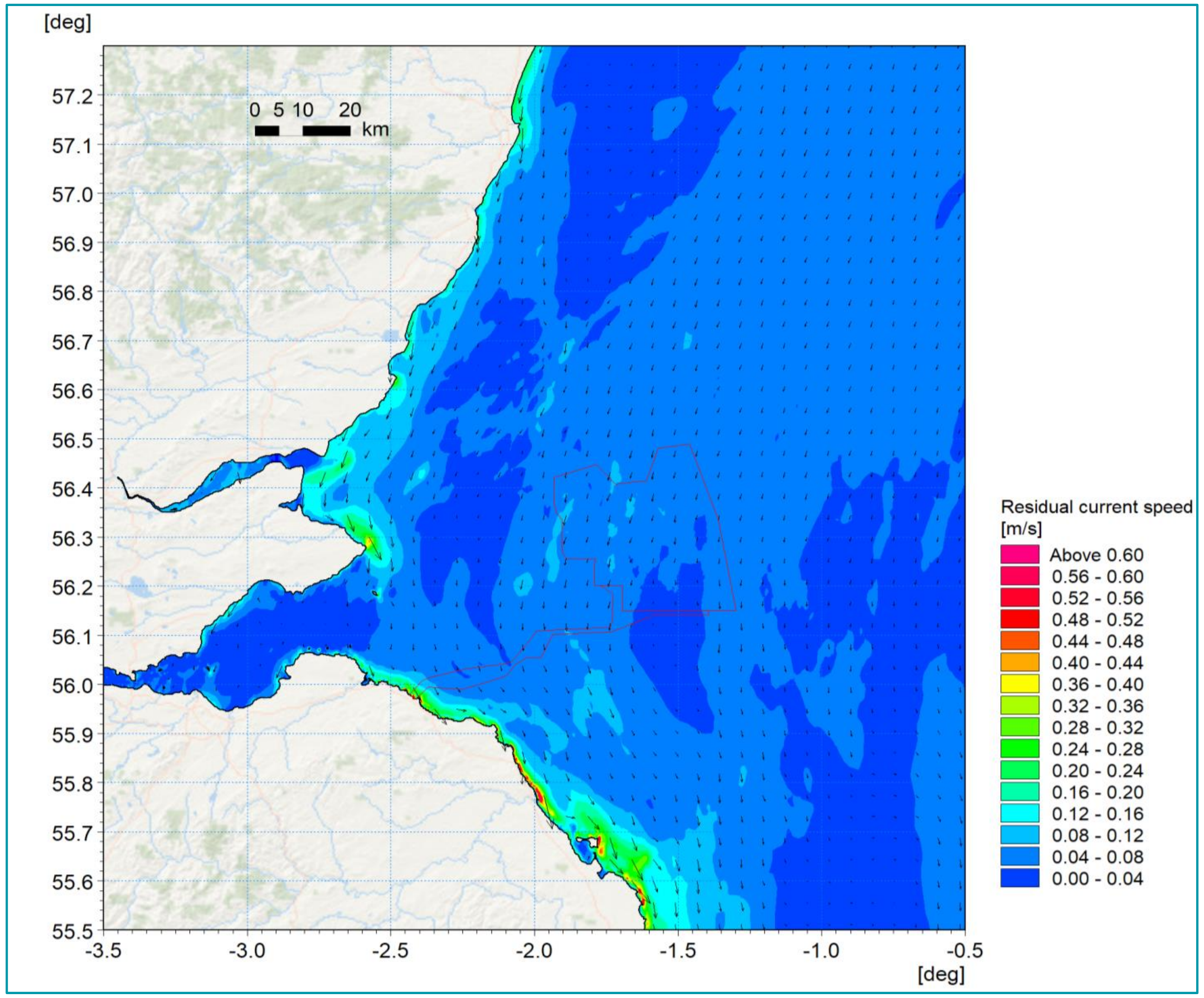


**Figure 4.48: Residual Current Spring Tide with 1:1 Year Storm from 000º**

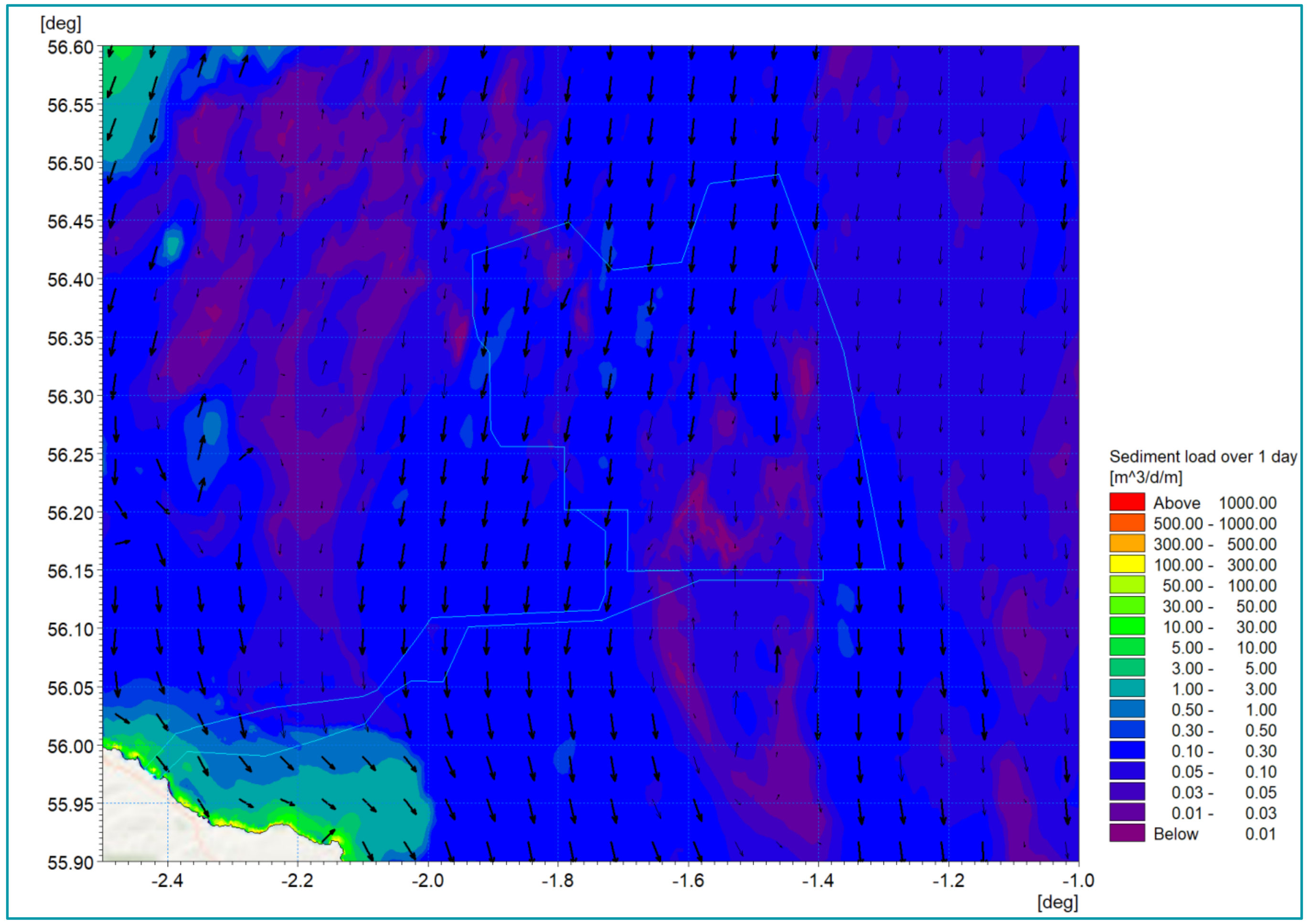


**Figure 4.49: Potential Sediment Transport over the Course of One Day with 1:1 Year Storm from 000º**

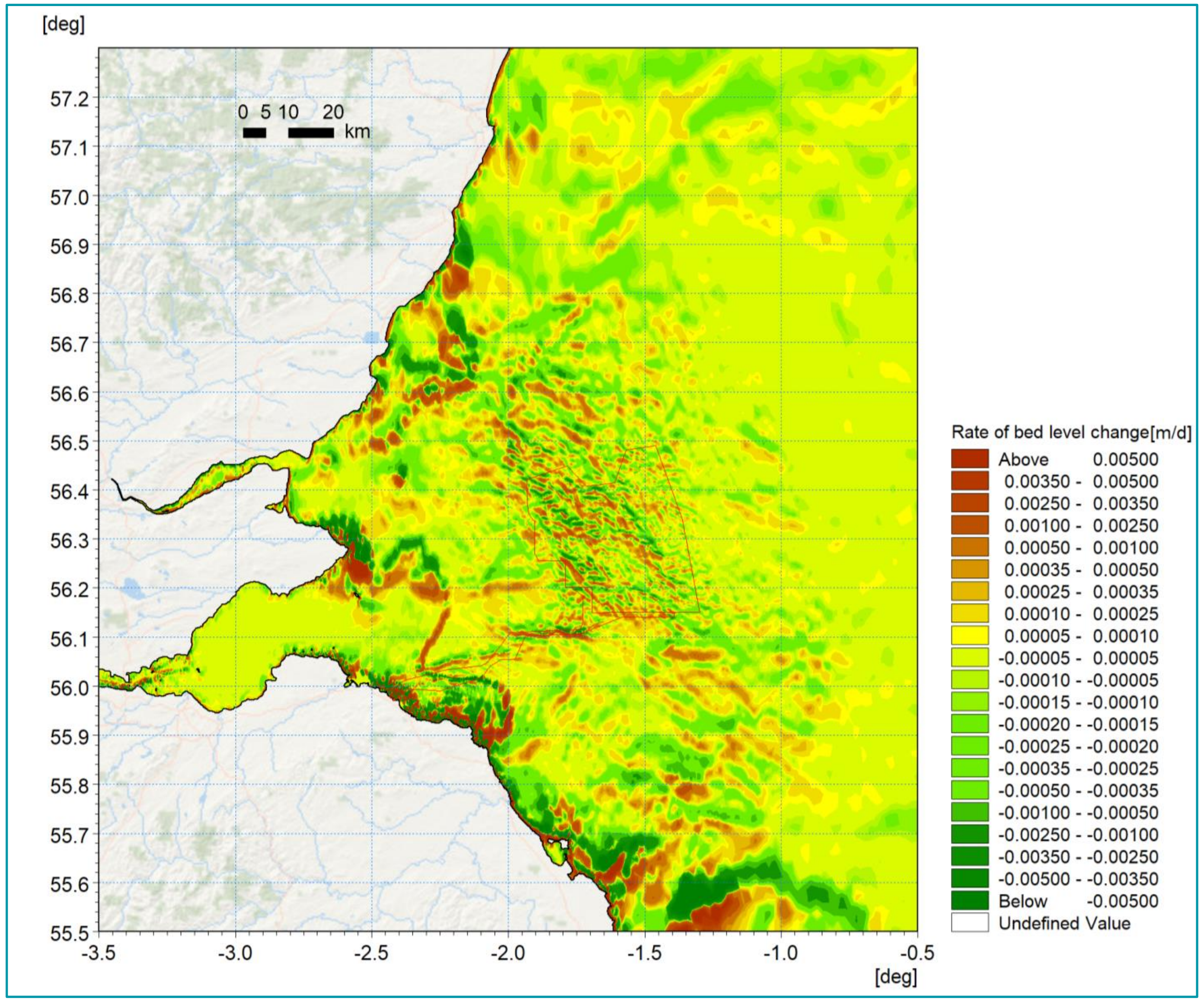


**Figure 4.50: Rate of Bed Level Change – Peak Flood Tide with 1:1 Year Storm from 000°**

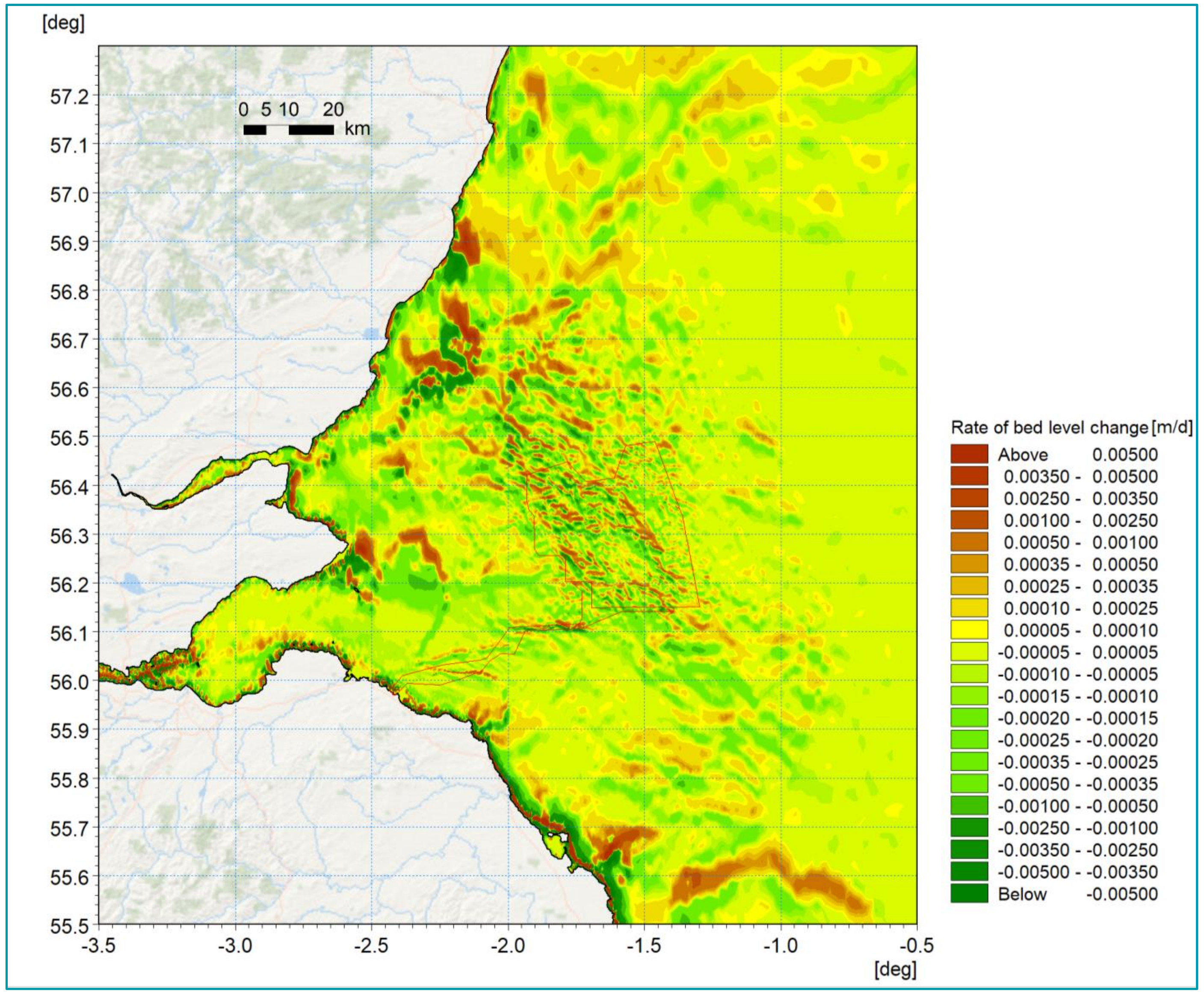


**Figure 4.51: Rate of Bed Level Change – Peak Ebb Tide with 1:1 Year Storm from 000°**

## 4.7. SUSPENDED SEDIMENTS

56. The principal mechanisms governing SSC in the water column are tidal currents, with fluctuations observed across the spring-neap cycle and across the different tidal stages (high water, peak ebb, low water, peak flood) observed throughout both datasets. It is key to note that SSCs can also be temporarily elevated by wave-driven currents during storm events. During high-energy storm events, levels of SSC can rise considerably, both near bed and extending into the water column. Following storm events, SSC levels will gradually decrease to baseline conditions, regulated by the ambient regional tidal regimes. The seasonal nature and frequency of storm events supports a broadly seasonal pattern for SSC levels.

57. Sampling was conducted at an offshore station for Seagreen 1 in March and June 2011, suggesting Total Suspended Solids (TSS) to be low. The samples collected illustrated a TSS of < 5 mg/l with a maximum reading of 10 mg/l during March 2011 (Fugro, 2012). Although all values are low, a slight increase in TSS was observed in March. Further monitoring at a nearshore location south of the proposed landfall (shown in Figure 4.6) captured how SSC can increase substantially due to meteorological conditions. Figure 4.52 shows the SSCs are generally < 5 mg/l (blue trace) however during storm conditions these may be increased to over 100 mg/l when wave heights are increased (black trace). Counter to this, in deeper water such as Fugro site A (Figure 4.6), turbidity and hence SSC (which are of the same order of magnitude) are not influenced by the wave climate to the same degree. Figure 4.53 shows the turbidity levels (red trace) and corresponding significant wave height (black trace). Turbidity levels remain low even during periods of increased wave activity.

58. For more generalised conditions the Cefas Climatology Report 2016 (Cefas, 2016) and associated dataset provides the spatial distribution of average non-algal Suspended Particulate Matter (SPM) for the majority of the United Kingdom Continental Shelf (UKCS). Between 1998 and 2005, the greatest plumes are associated with large rivers such as those that discharge into the Thames Estuary, The Wash and Liverpool Bay, which show mean values of SPM above 30 mg/l. Based on the data provided within this study, the SPM associated with the Proposed Development has been estimated as approximately 0 mg/l to 1 mg/l over the 1998 to 2005 period, Figure 4.54. Higher levels of SPM are experienced more commonly in the winter months; however, due to the tidal influence, even during summer months the levels remain elevated.

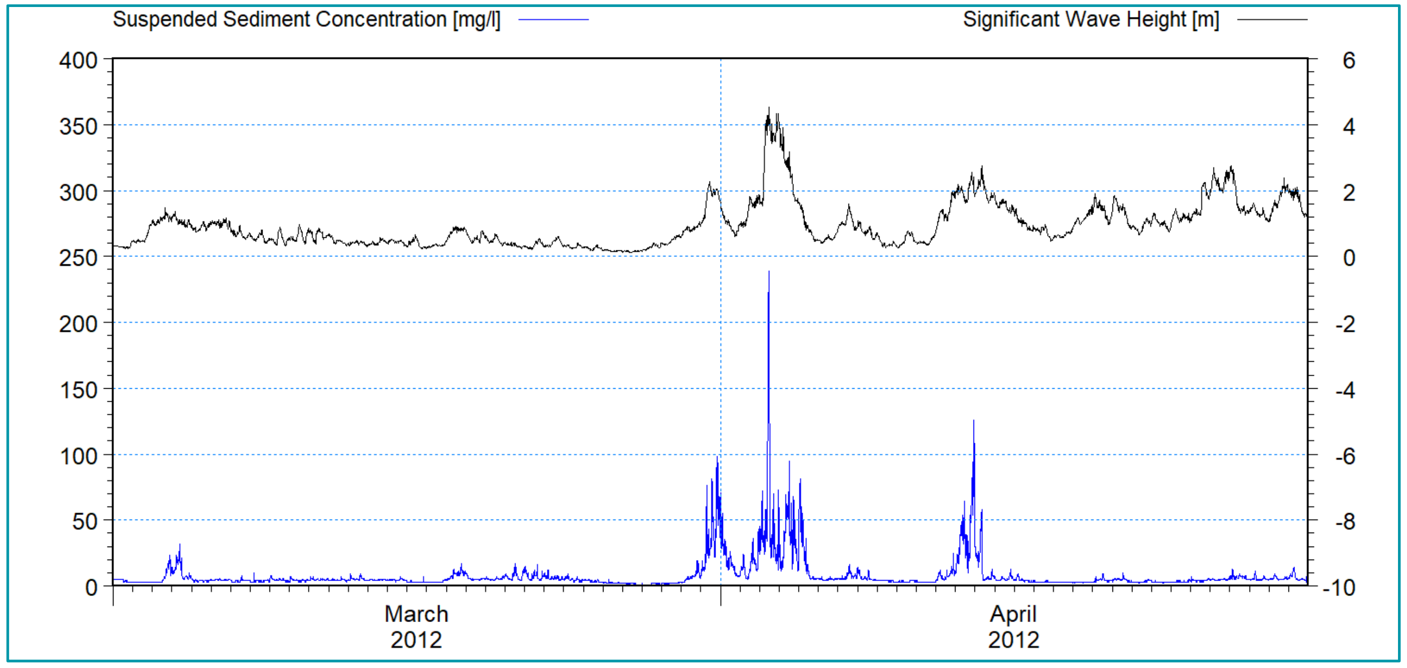


**Figure 4.52: Measured Suspended Sediment Concentrations at Fugro Site F**

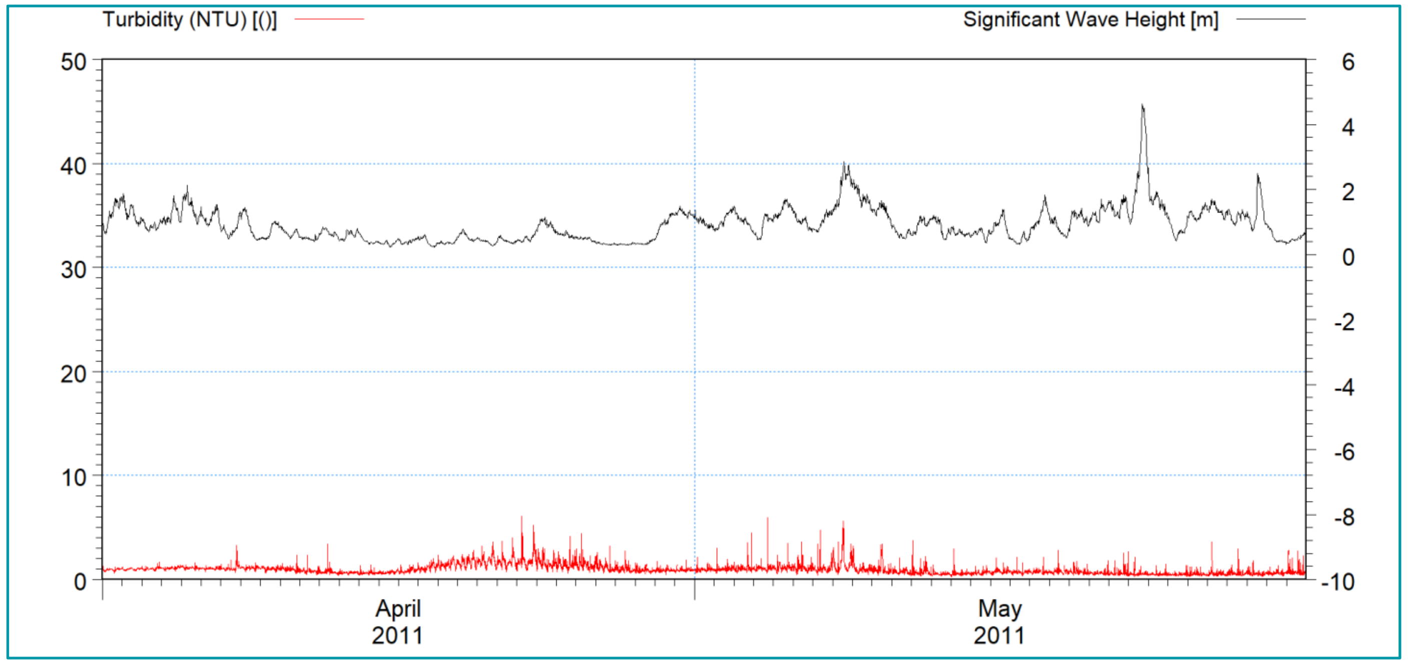


**Figure 4.53: Measured Turbidity at Fugro Site A**

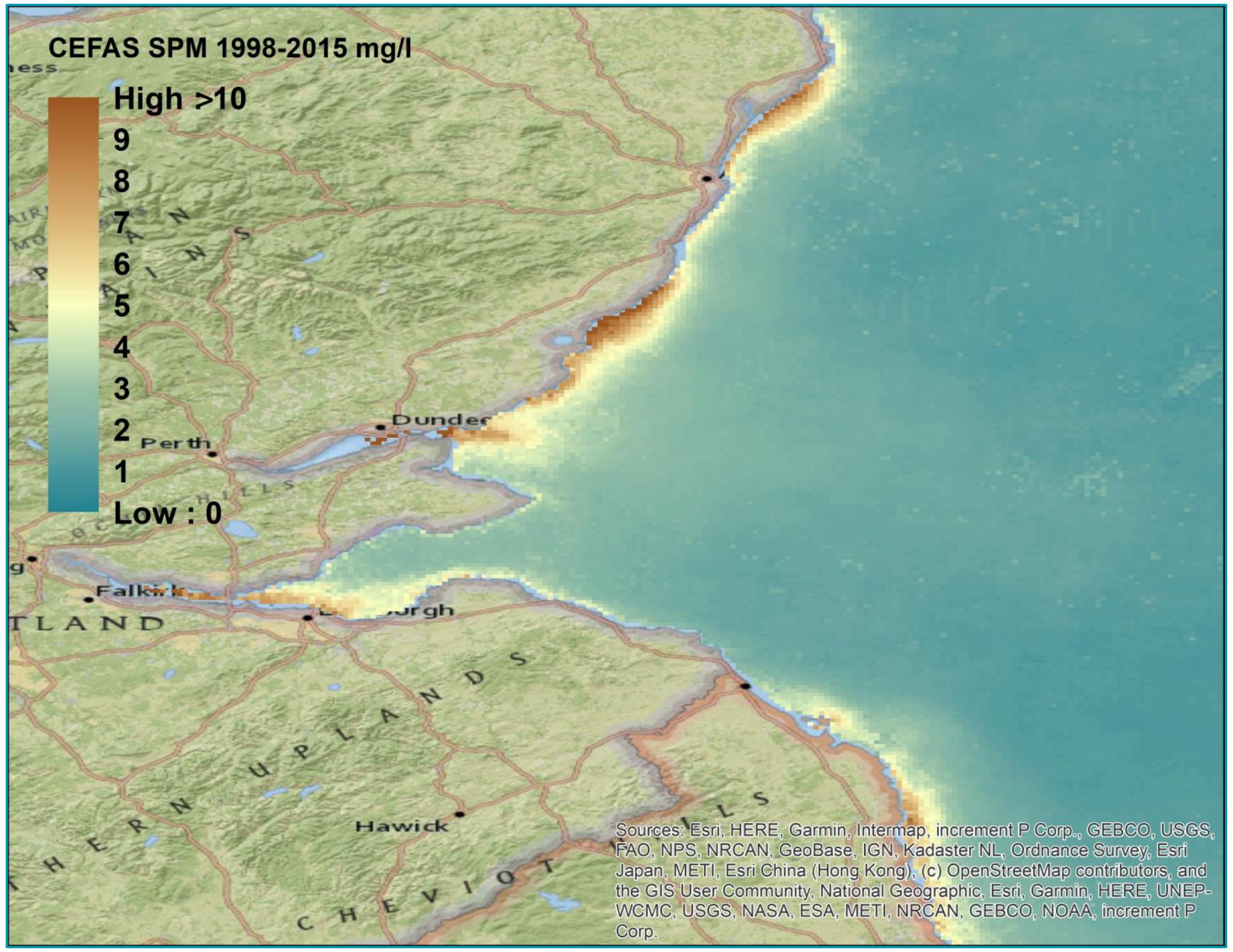


**Figure 4.54: Distribution of Average Non-algal Suspended Particulate Matter - CEFAS**

# 5. POTENTIAL ENVIRONMENTAL CHANGES

## 5.1. OVERVIEW

59. The potential changes to the baseline hydrographic conditions as a result of the installation and presence of the Proposed Development are quantified in the following sections. These changes relate to the presence of the infrastructure within the water column and seabed and are therefore associated with wind turbine legs along with cable and scour protection. The potential changes to sea state and sediment transport regimes were established by repeating the modelling undertaken in the previous section with the inclusion of the Proposed Development. The modelling was undertaken using an indicative layout which included the following changes in line with the maximum design scenario for physical processes:

- leg structures 5 m in diameter relating to 179 wind turbine structures each comprising four legs;
- scour protection 80 m diameter and 2 m in height associated with 20 m caisson for each wind turbine leg;
- leg structures 4 m in diameter relating to eight HVAC OSPs/Offshore convertor station platforms each comprising six legs;
- leg structures 5 m in diameter relating to two HVDC OSPs/Offshore convertor station platforms each comprising eight legs;
- scour protection 60 m diameter and 2 m in height associated with 15 m caissons for each OSP/Offshore convertor station platforms leg; and
- cable protection to a height of 3 m for 15% of inter-array/interconnector cables and areas along the Proposed Development export cable corridor with limited burial depth and at cable crossings.

60. The areas within the Proposed Development export cable corridor requiring cable protection were identified from the seabed classification data, Figure 4.42. The rocky outcrops where full burial depth may not be achieved are located within the eastern end of the corridor. Trenchless techniques would be used in the nearshore/inter-tidal areas. It should be noted that the scale of the model mesh meant that the general flow and sediment patterns around the structures could be observed on the wider scale. However, the localised nature of the scour meant that a detailed assessment of the effectiveness of the scour protection proposed at each foundation location was not undertaken as this was not the purpose of the computational modelling. The scour protection does not have implications on the global scale and is restricted to reducing sediment erosion in the vicinity of the foundations; there would be larger implications if scour protection were not provided (Whitehouse *et al.*, 2006).

61. The methodology implemented for the modelling used parameters selected from the project description outlined in volume 1, chapter 3 of the Offshore EIA Report, to ascertain the most influential and likely scenario for each coastal process aspect under examination. The indicative layout used within the modelling study is presented in Figure 5.1. For each stage of the following study, the maximum design scenario applied is outlined.

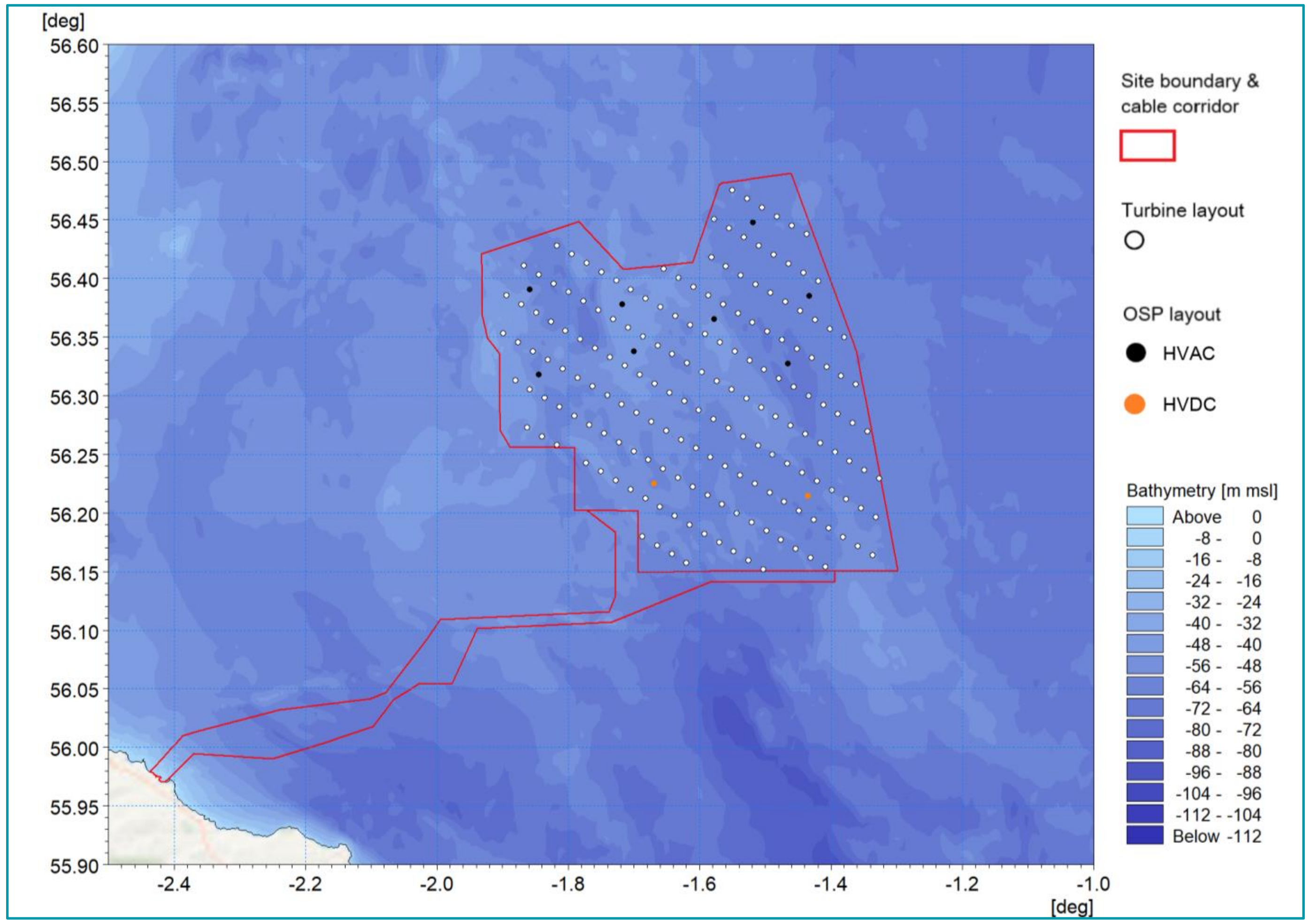


**Figure 5.1: Modelled Array Indicative Layout**

## 5.2. POST-CONSTRUCTION HYDROGRAPHY

### 5.2.1. TIDAL FLOW

62. The spring tide simulation was repeated with the addition of 780 structures (i.e. 716 wind turbine legs and 64 OSP/Offshore convertor station platforms legs). The wind turbine and HVDC OSP/Offshore convertor station platforms legs being of 5 m diameter and the remaining 48 HVAC OSP/Offshore convertor station platforms legs being 4 m in diameter; all with a circular plan form. This represented the largest obstruction to tidal flow as, although the 14 MW option has more elements in the water column, they are more slender in design. The bathymetry was also amended to take account of scour and cable protection. The following figures show the same mid flood and mid ebb steps from the simulation as were presented in Figure 4.22 and Figure 4.23 respectively, but with the Proposed Development foundation and structures in place. Where appropriate, the Proposed Development export cable corridor has been indicated on the figures along with the Proposed Development array area, to indicate the locality of the works without obscuring the model results. Due to the limited magnitude of the changes, difference plots have also been provided. These are the proposed minus the baseline condition, therefore increases in current speed will be positive. The same procedure for calculating differences and plotting figures has been implemented throughout this report.

63. Figure 5.2 shows the post-construction flood tide flow patterns with Figure 5.3 showing the changes and as the changes are limited to the vicinity of the development a more focused plot is provided in Figure 5.4. In the difference figures a log scale has been introduced to accentuate the values for clarity. Similarly Figure 5.5, Figure 5.6 and Figure 5.7 show the same information for the ebb tide. During peak current speed the flow is redirected in the immediate vicinity of the structures and cable protection at the south of the site. The variation is a maximum of 1 cm/s which constitutes less than 2% of the peak flows at 200 m from the structure and reduces considerably with increased distance from each structure.

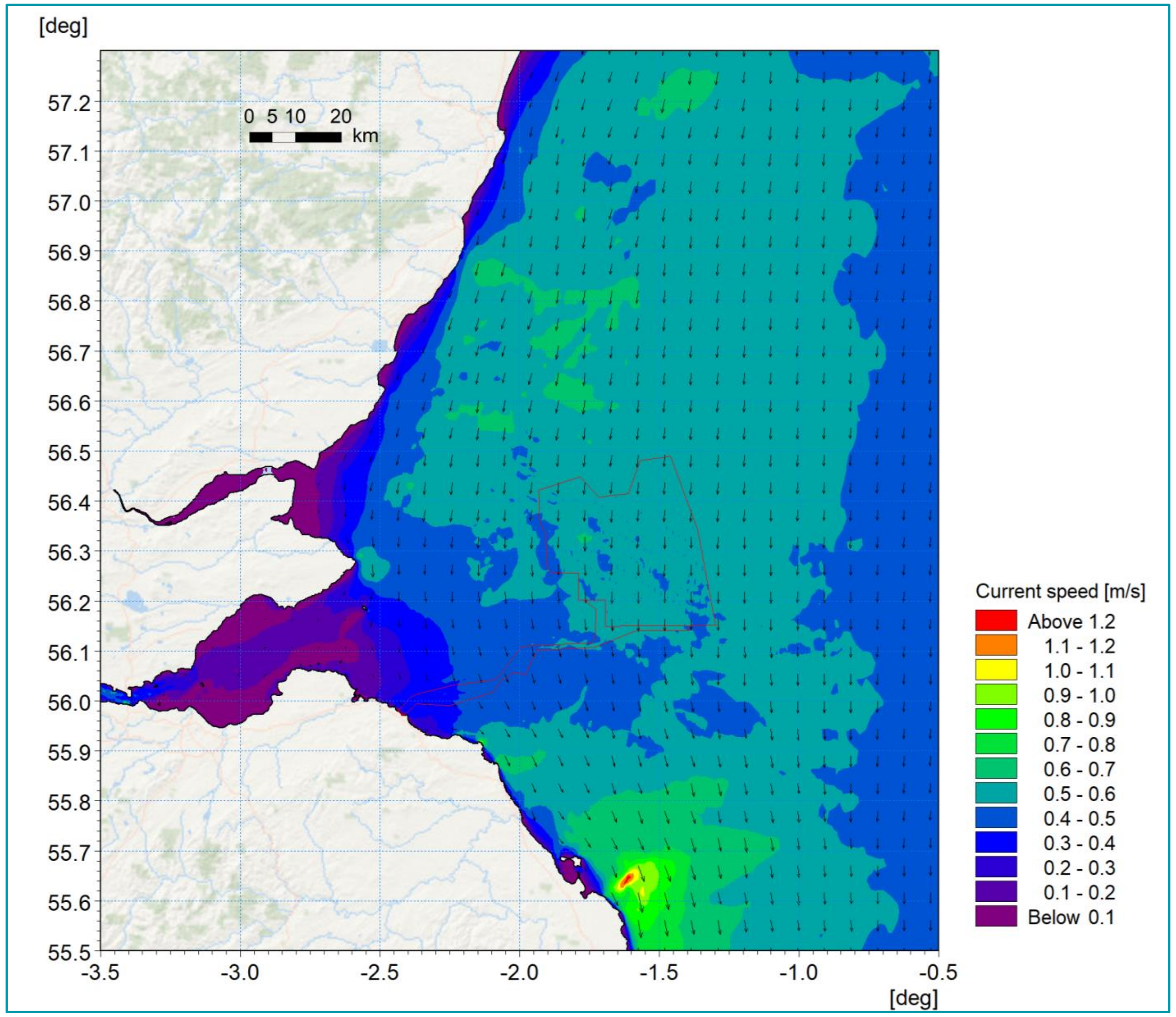


**Figure 5.2: Post-Construction Tidal Flow Pattern – Peak Flood (HW-1 Hour)**

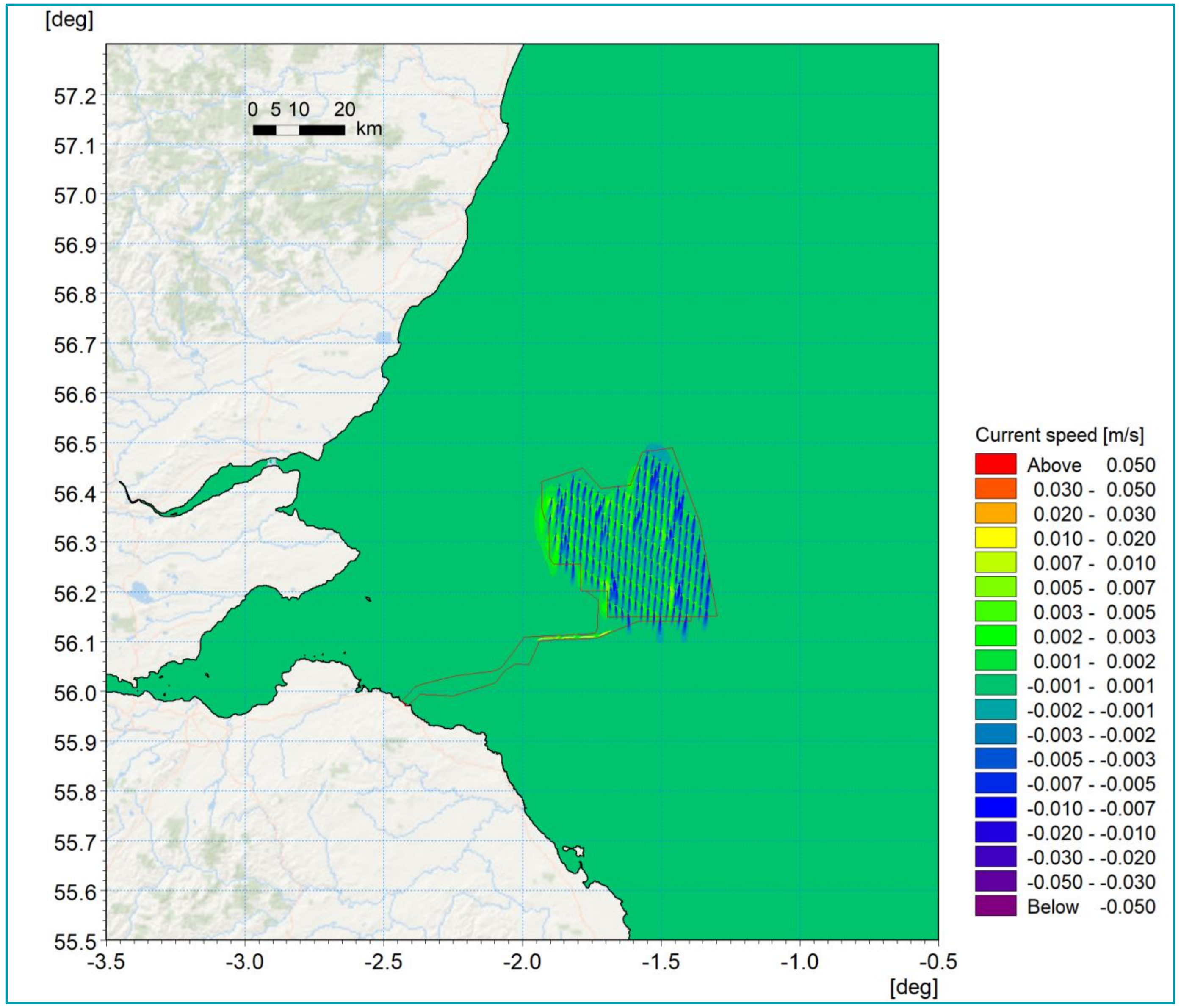


**Figure 5.3: Change in Tidal Flow (Post-Construction Minus Baseline) – Peak Flood (HW-1 Hour)**

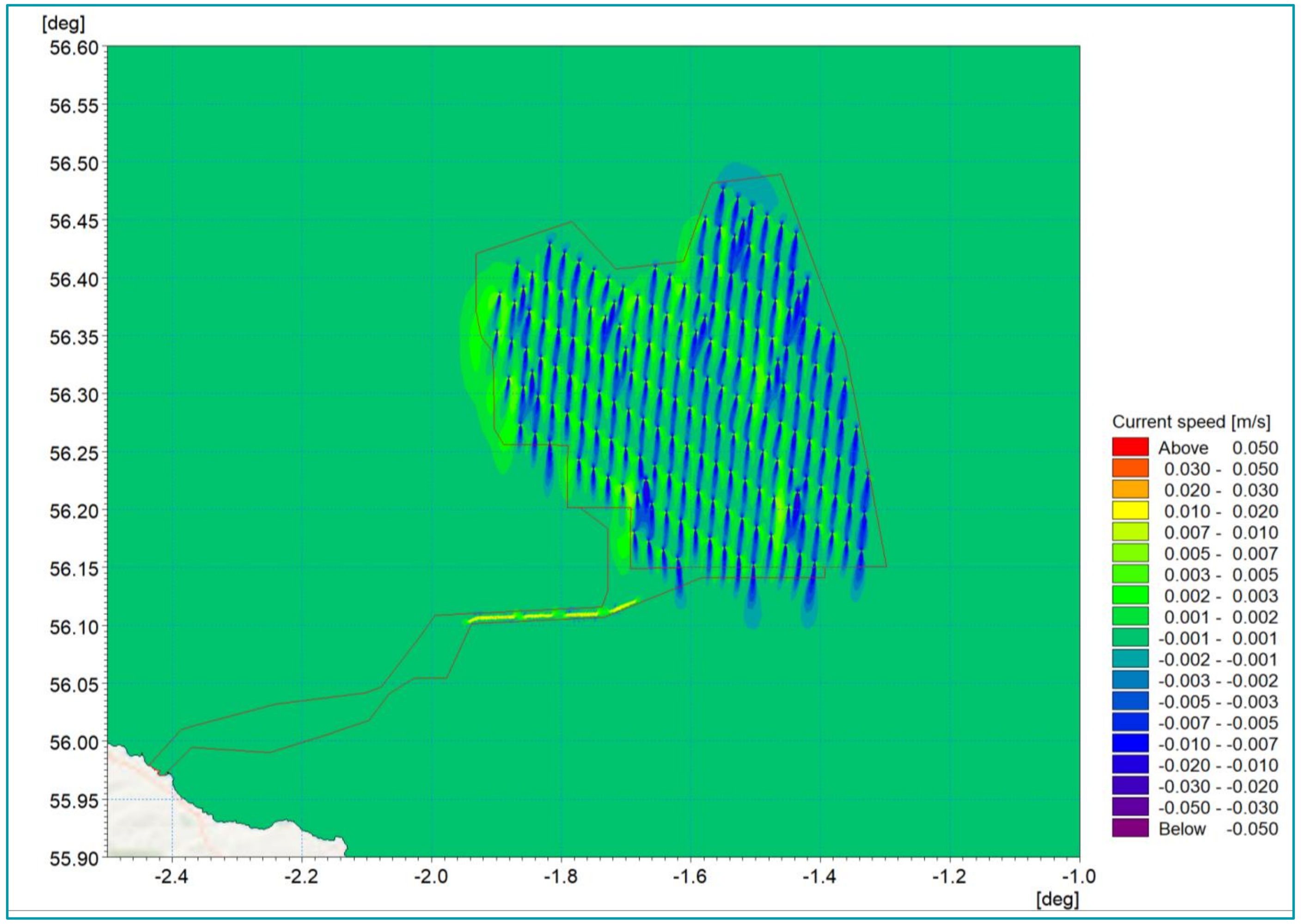


**Figure 5.4: Change in Tidal Flow (Post-Construction Minus Baseline) Proposed Development Array Area – Peak Flood (HW-1 Hour)**

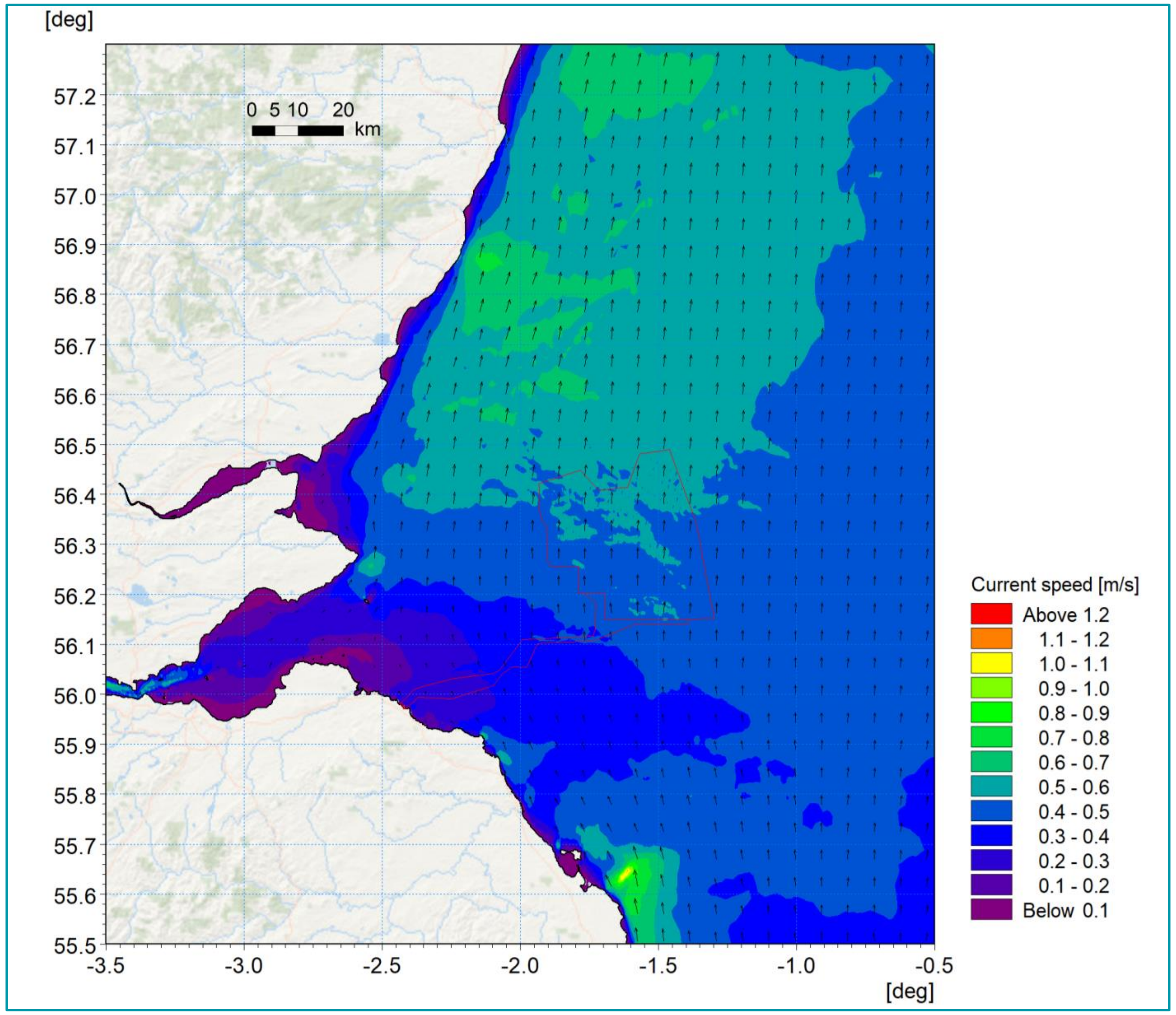


**Figure 5.5: Post-Construction Tidal Flow Pattern – Peak Ebb (LW-1 Hour)**

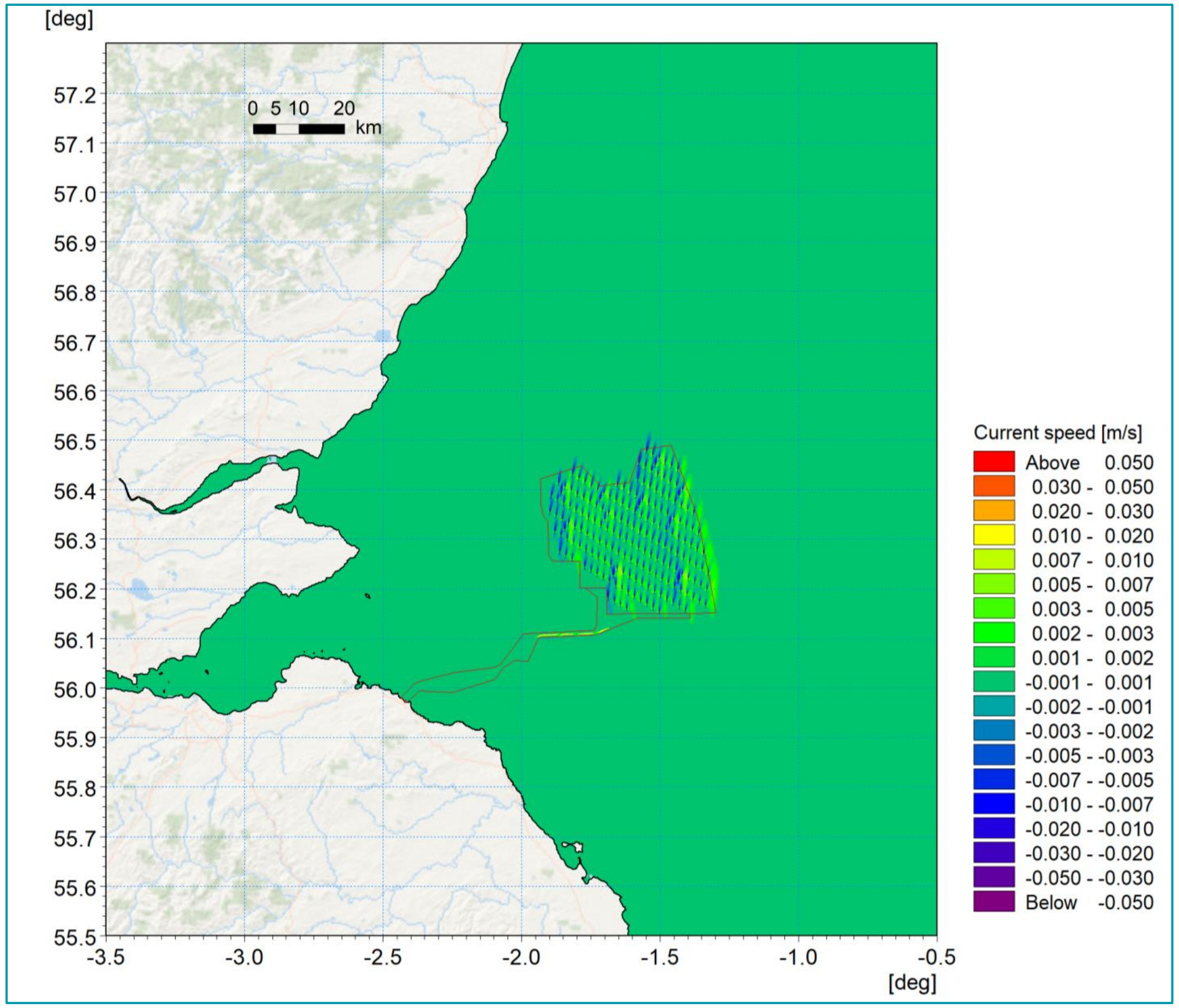


**Figure 5.6: Change in Tidal Flow (Post-Construction Minus Baseline) – Peak Ebb (LW-1 Hour)**

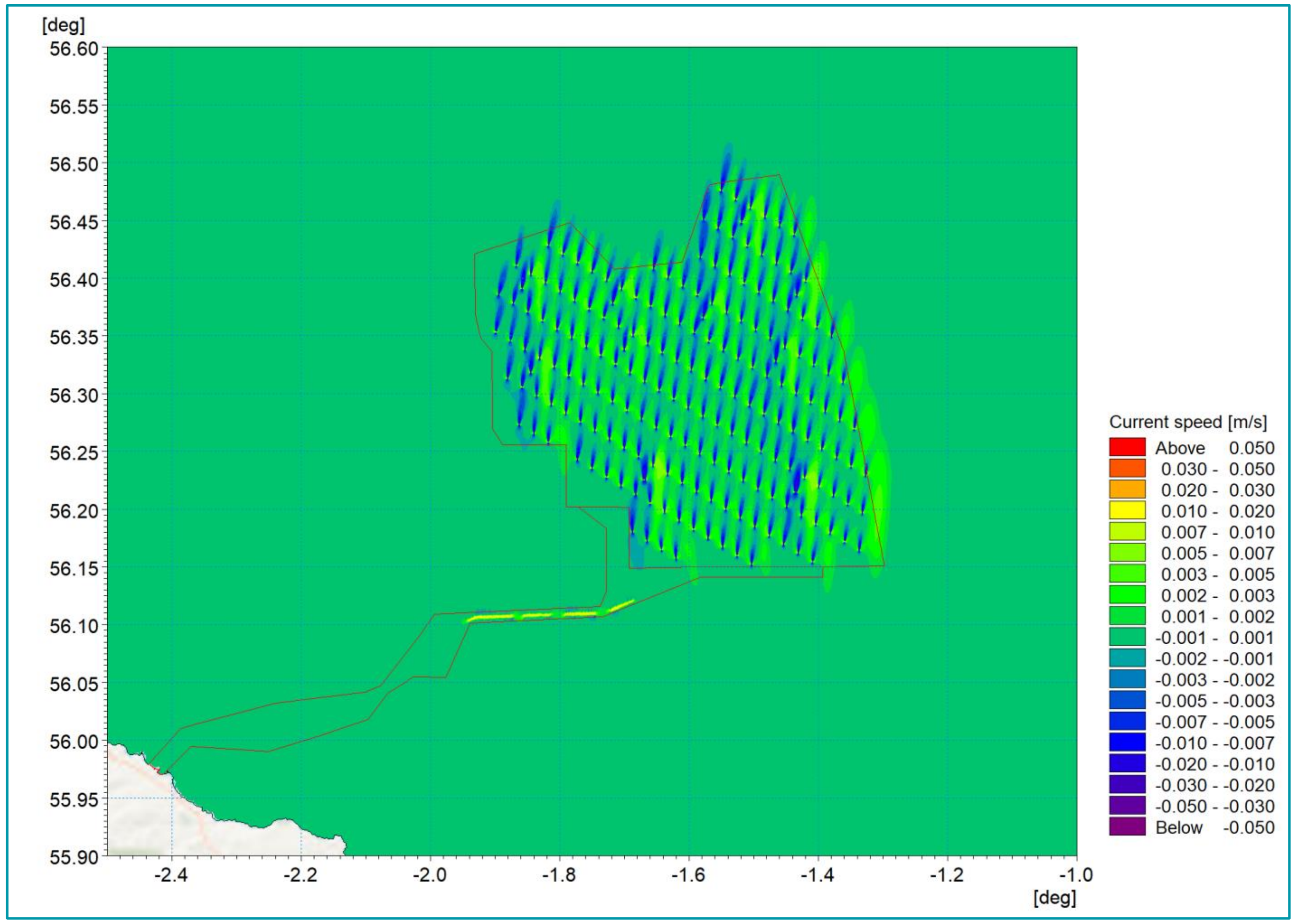


**Figure 5.7: Change in Tidal Flow (Post-Construction Minus Baseline) Proposed Development Array Area – Peak Ebb (LW-1 Hour)**

### 5.2.2. WAVE CLIMATE

64. Using the same principle as for the tidal modelling, the wave climate modelling was repeated with the inclusion of the Proposed Development structures, foundations and cable protection. Again, changes were found to be indiscernible from the baseline scenario by visual inspection therefore difference plots have been provided and a log scale was employed to highlight the variation.

65. The presence of the Proposed Development was seen to have the greatest influence when storms approached from the northerly sectors. The one in one year storm for the 000° direction for the mean sea level condition is presented in Figure 5.8 and corresponds to the baseline plot in Figure 4.27. The change in wave climate is presented in Figure 5.9. The changes are seen as reductions in the lee of the site and increases where the waves are deflected by the structures. These changes are in the order of 2 cm which represents less than 1% of the baseline significant wave height. A similar pattern was observed between

the one in one and 1 in 20 year return period storms from each direction therefore, for brevity, only the 1 in 20 year results are presented for the additional storm directions.

66. The more severe 1 in 20 year storm event results are presented in Figure 5.10 to Figure 5.17 for the four principal directions which effect the physical processes study area and coastal zone (000°, 045°, 090º and 135°). In each case, the post-construction wave climate is followed by the difference plot. It is apparent where the wave field interacts with either a wind turbine structure or a protection feature which reduces the water depth, the origin of the changes are focussed on specific locations. In the case of the 1 in 20 year storms, the changes are seen to follow the same pattern, with decreases in the lee of the Proposed Development and increases either side. However, it is noted that the changes are not considerably increased from the more frequent return period scenario and in the order of 2 cm to 4 cm whereas the baseline wave heights are increased for the greater return period events giving rise to a less marked overall impact on wave climate.

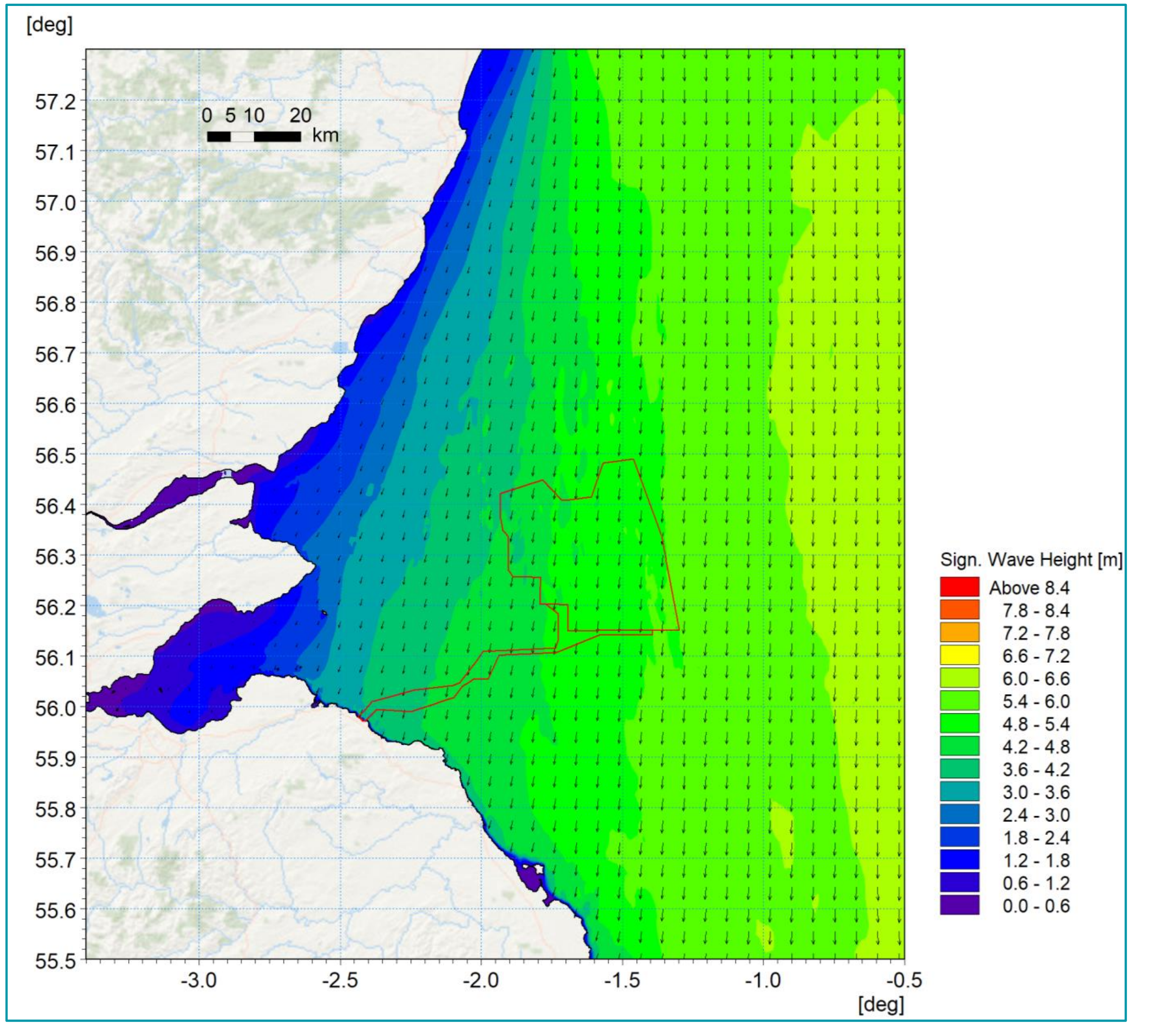


**Figure 5.8: Post-Construction Wave Climate 1:1 Year Storm 000° Mid-Tide**

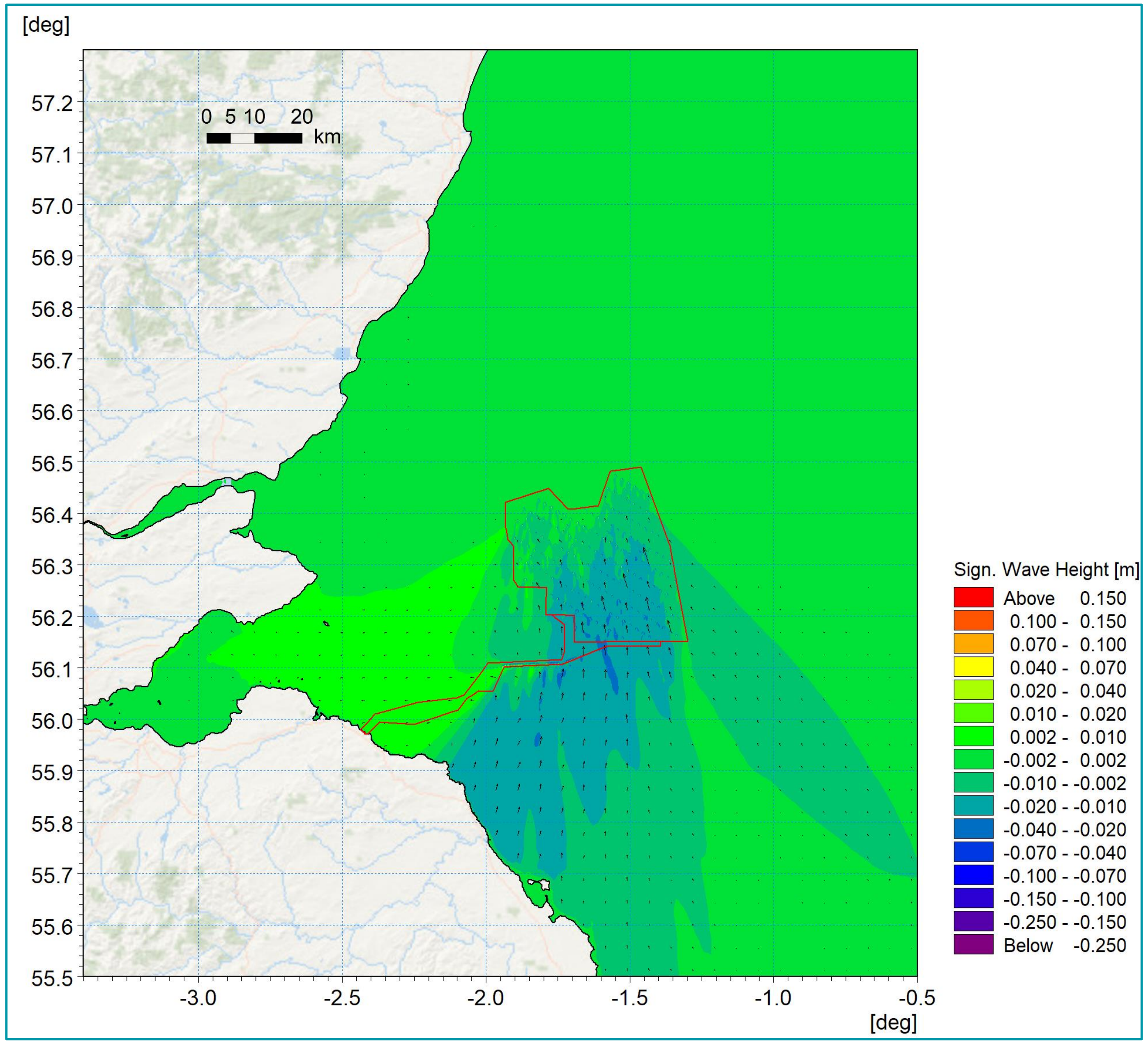


**Figure 5.9:** Change in Wave Climate 1:1 Year Storm 000° Mid-Tide (Post-Construction Minus Baseline)

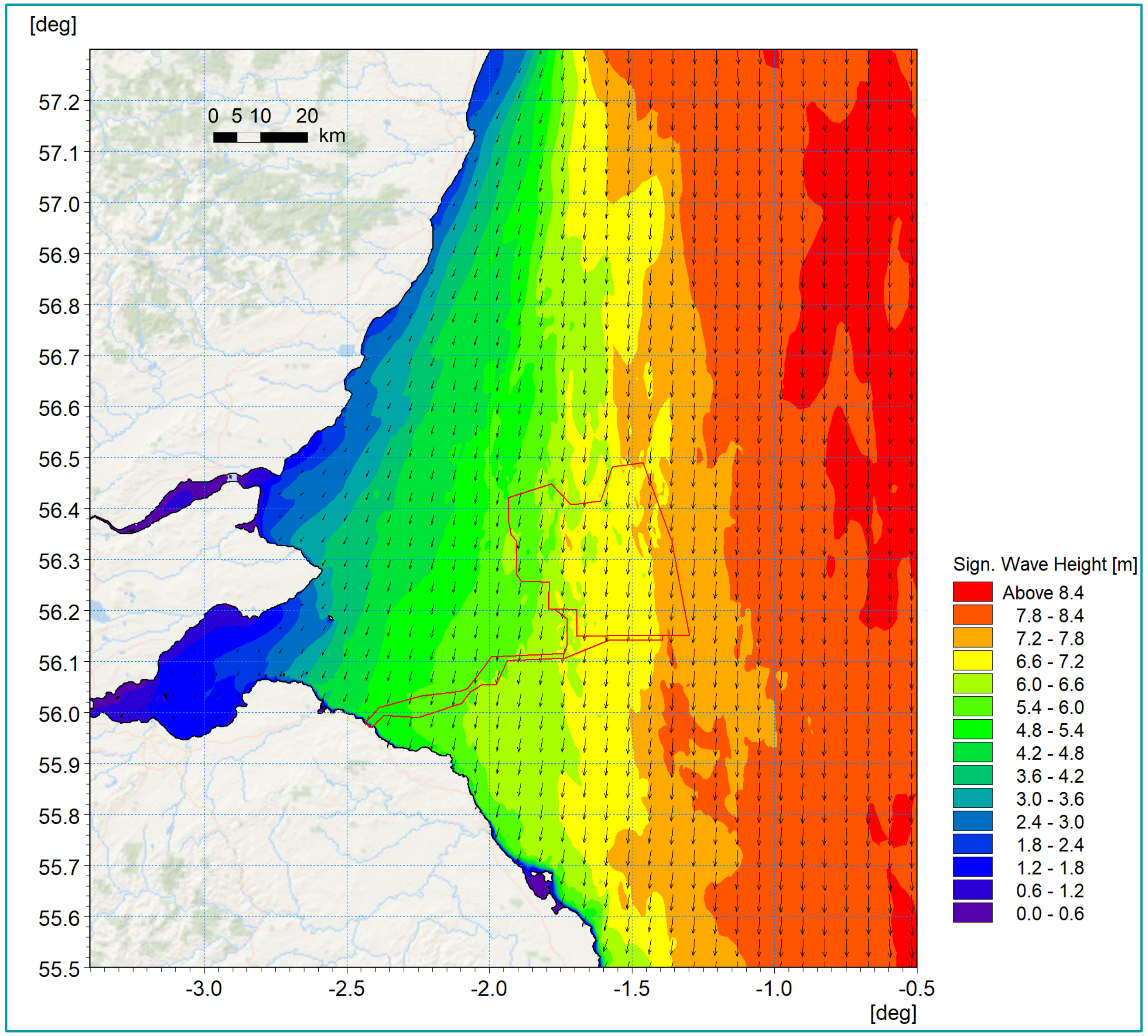


**Figure 5.10:** Post-Construction Wave Climate 1:20 Year Storm 000° Mid-Tide

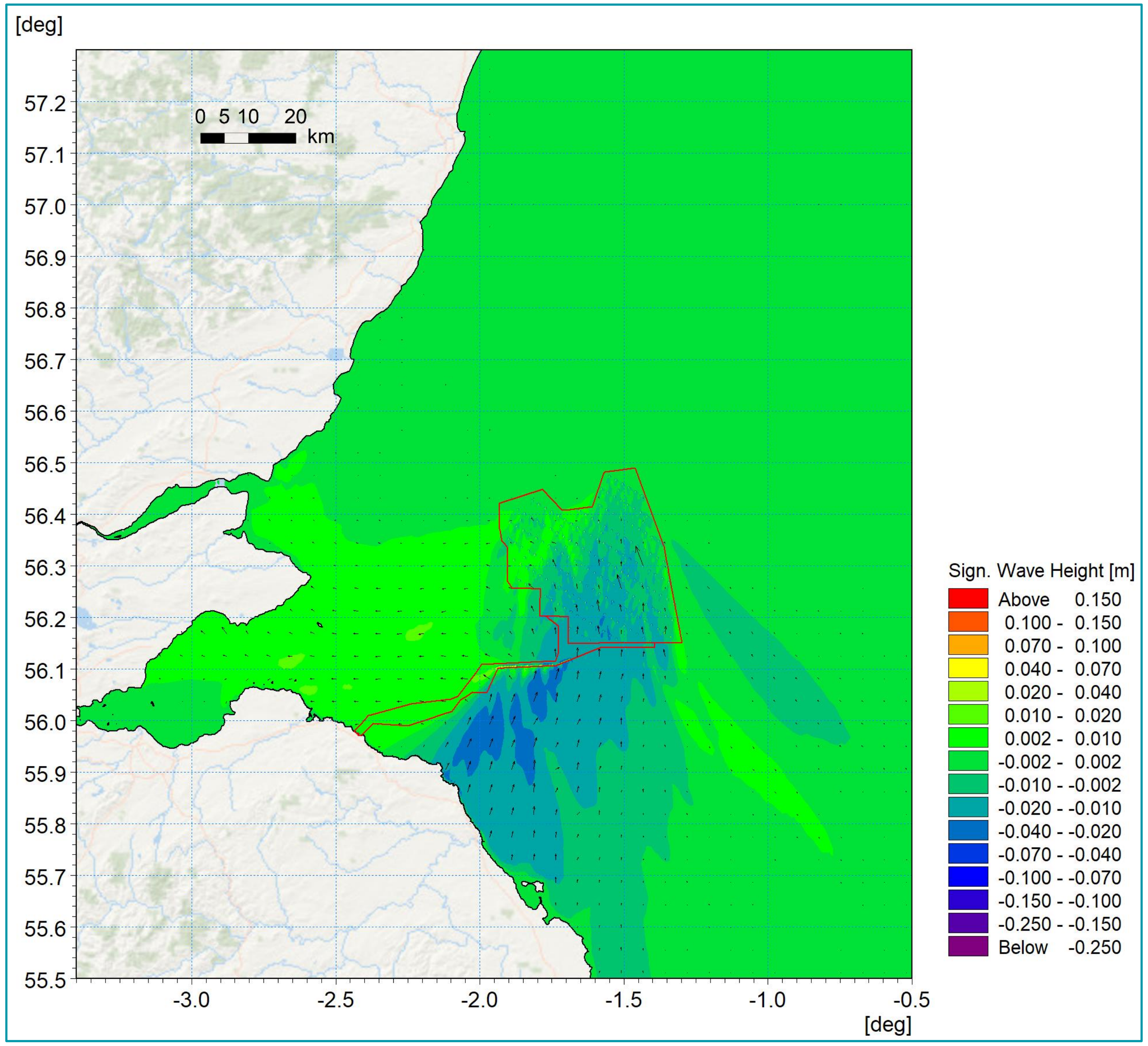


**Figure 5.11:** **Change in Wave Climate 1:20 Year Storm 000° Mid-Tide (Post-Construction Minus Baseline)**

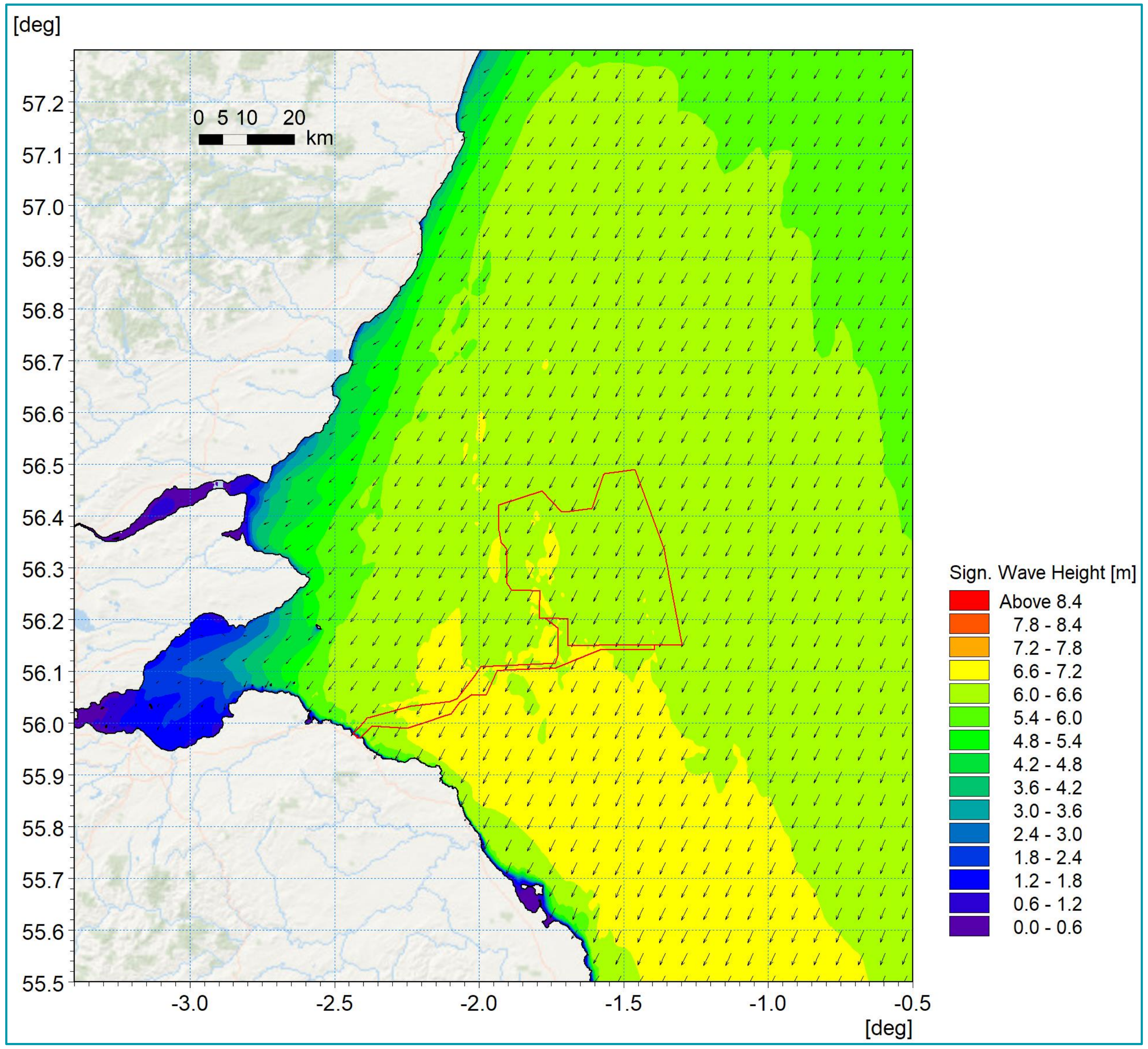


**Figure 5.12:** **Post-Construction Wave Climate 1:20 Year Storm 045° Mid-Tide**

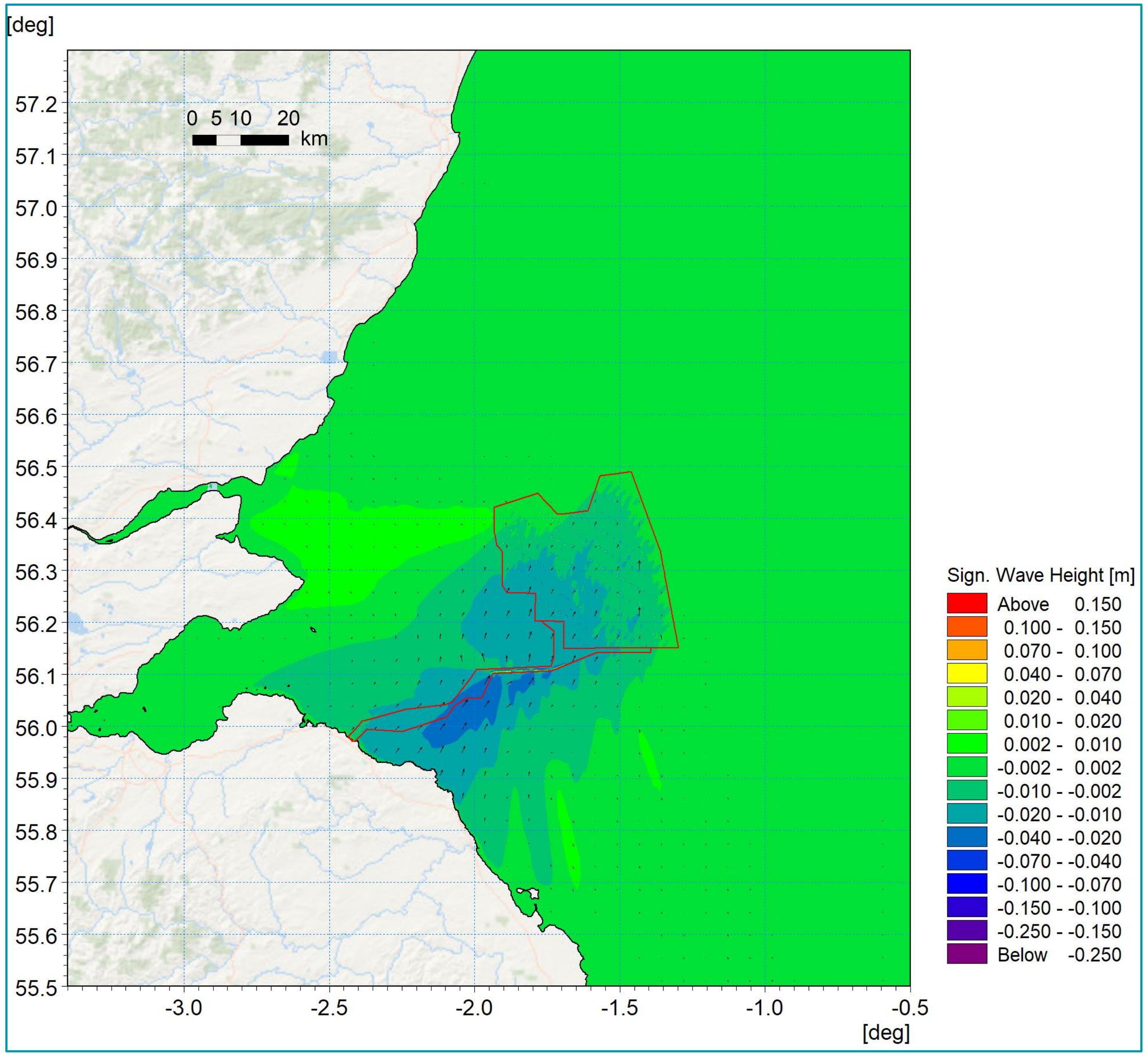


**Figure 5.13: Change in Wave Climate 1:20 Year Storm 045° Mid-Tide (Post-Construction Minus Baseline)**

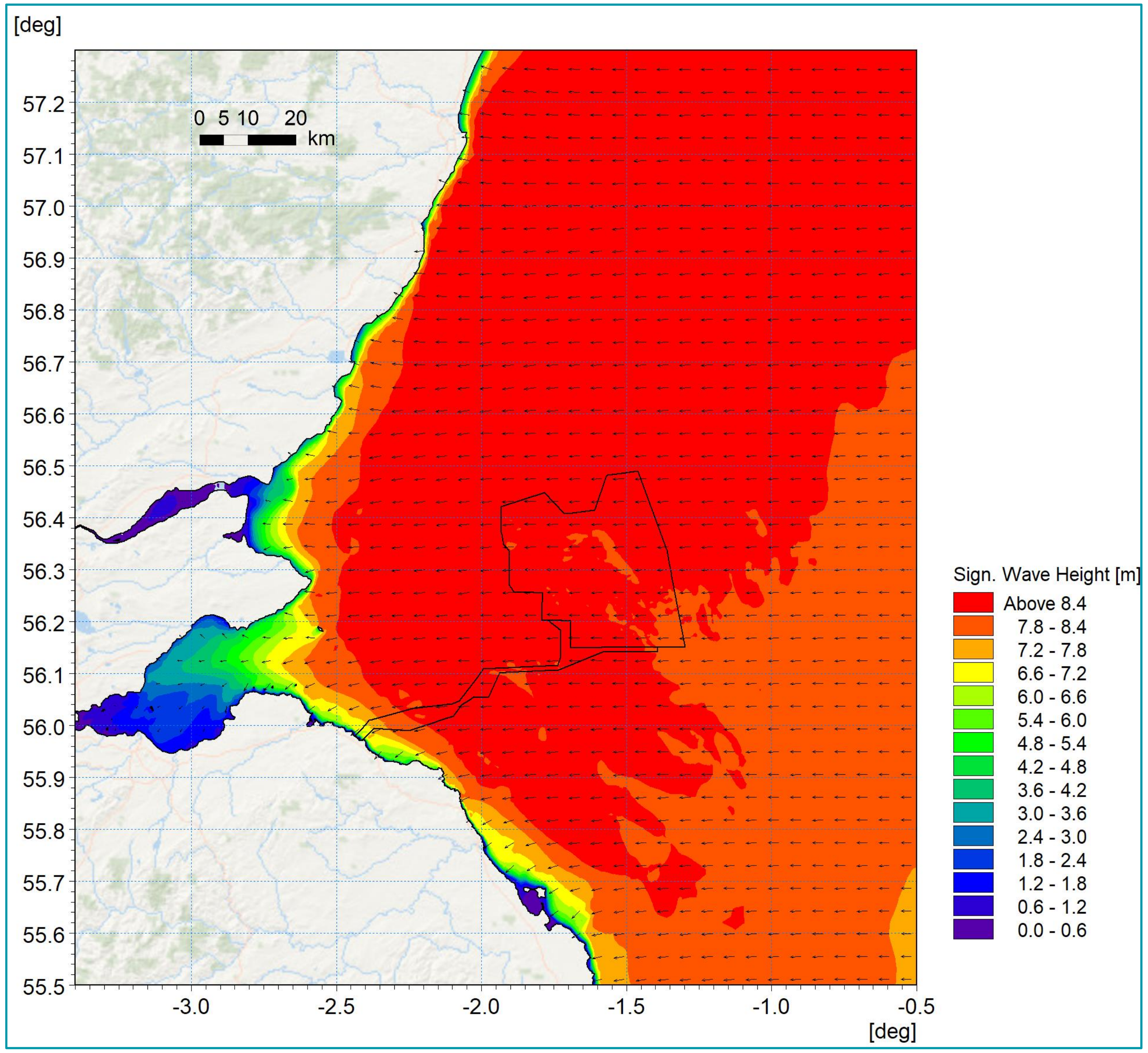


**Figure 5.14: Post-Construction Wave Climate 1:20 Year Storm 090° Mid-Tide**

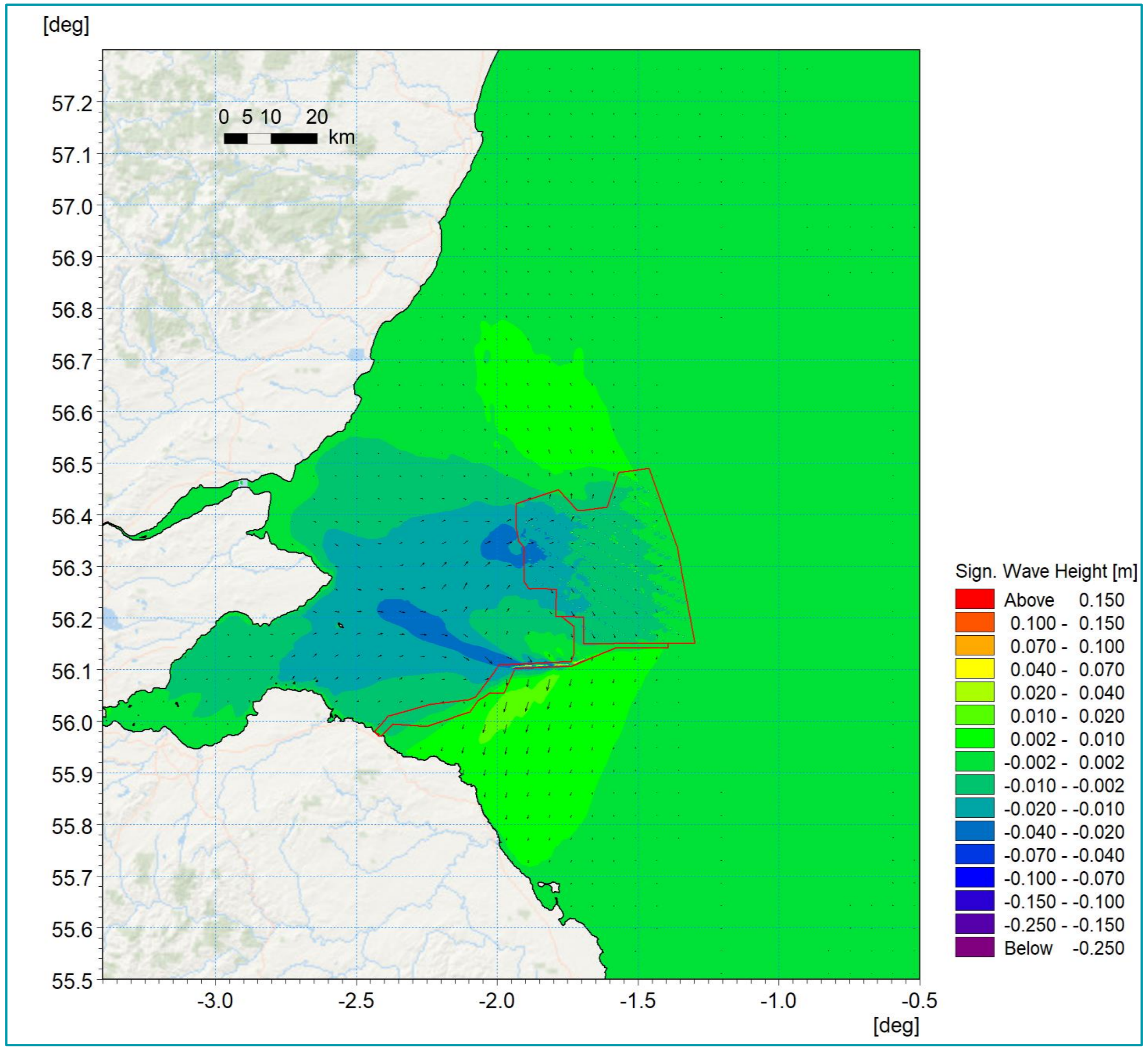


**Figure 5.15: Change in Wave Climate 1:20 Year Storm 090° Mid-Tide (Post-Construction Minus Baseline)**

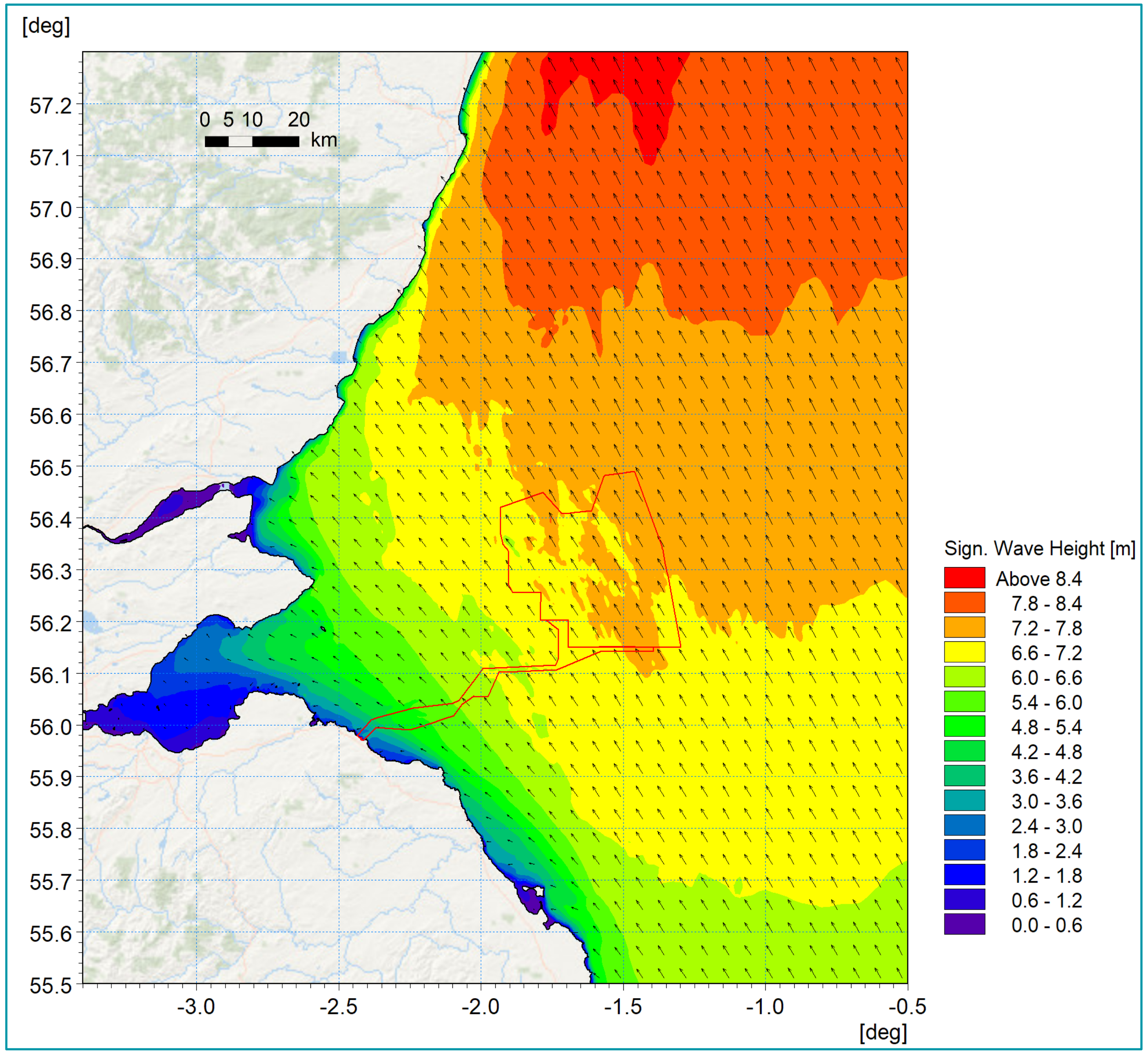


**Figure 5.16: Post-Construction Wave Climate 1:20 Year Storm 135° Mid-Tide**

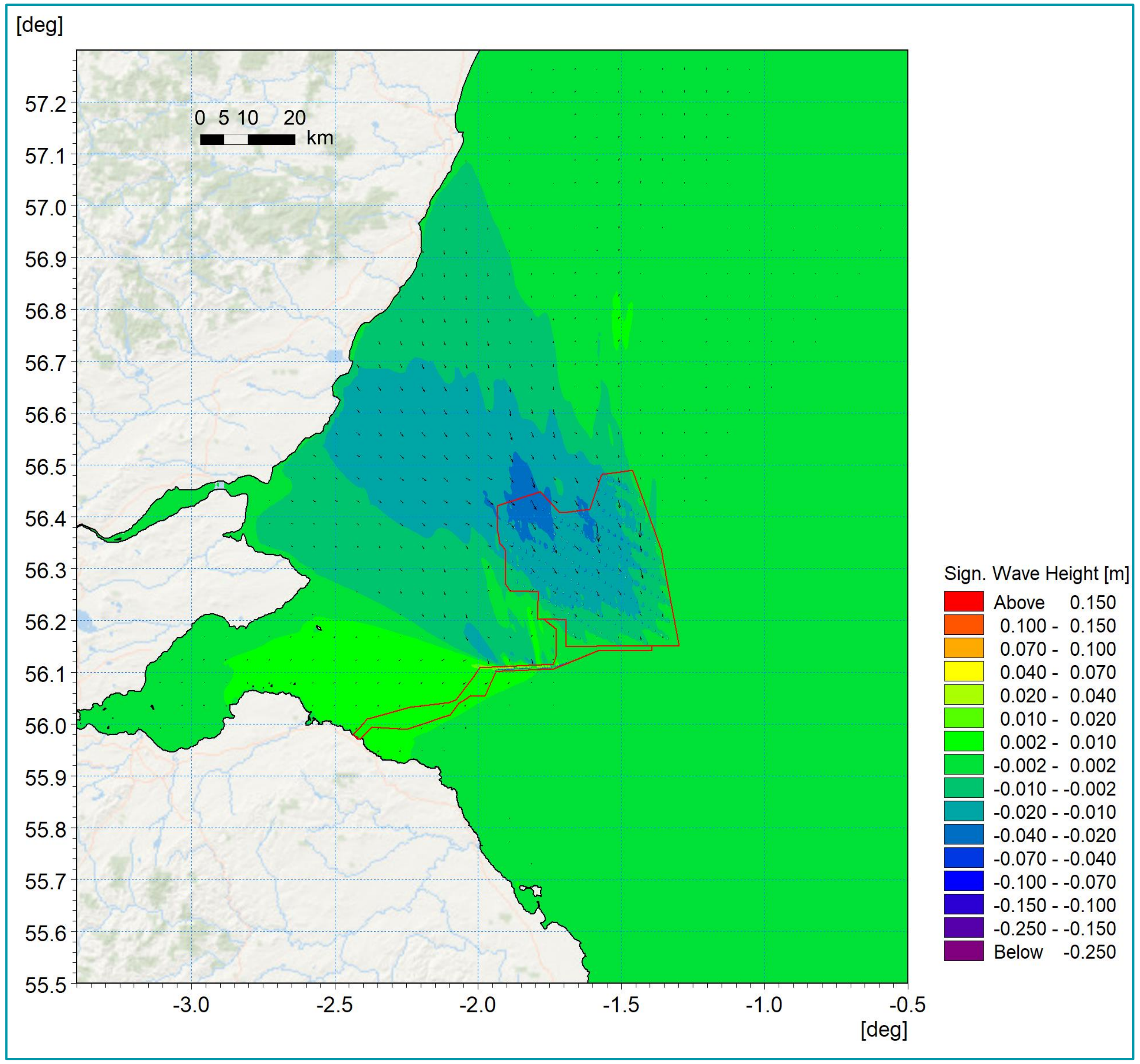


**Figure 5.17: Change in Wave Climate 1:20 Year Storm 135° Mid-Tide (Post-Construction Minus Baseline)**

### 5.2.3. LITTORAL CURRENTS

67. The previous sections established the magnitude of the changes in tidal currents and wave conditions individually, however sediment transport regimes are driven by a combination of these factors. Although the modelling has demonstrated that the principal contribution comes from tidal currents, for the sake of completeness, the influence on littoral currents was examined.

68. The modelling was extended to include the post-construction scenario (i.e. with 780 structures and associated scour protection relating to caisson foundations) for the one in one year storm from 000°. The baseline littoral currents for mid flood and mid ebb were presented in Figure 4.40 and Figure 4.41 respectively. The post-construction littoral currents are shown in Figure 5.18 and Figure 5.21 for the flood and ebb tides respectively. The corresponding changes for the flood tide are presented in Figure 5.19 with a more detailed plot in Figure 5.20 whilst for the ebb tide Figure 5.22 and Figure 5.23 show the corresponding information.

69. During the flood tide the influence of the wave climate is in concert with the tidal current and the tidal flow in the lee of each of the structures is further reduced. During the ebb tide, the tidal flow is in opposition to the wave climate and the resultant littoral current is reduced in magnitude. The presence of the structures has a limited influence on the wave induced reduction in flow and there is little difference between changes in littoral current magnitude and the tidal flows alone due to the installation. The magnitude of these changes remains limited to ±5% of the baseline currents at 200 m and reduces considerably with increased distance from each structure.

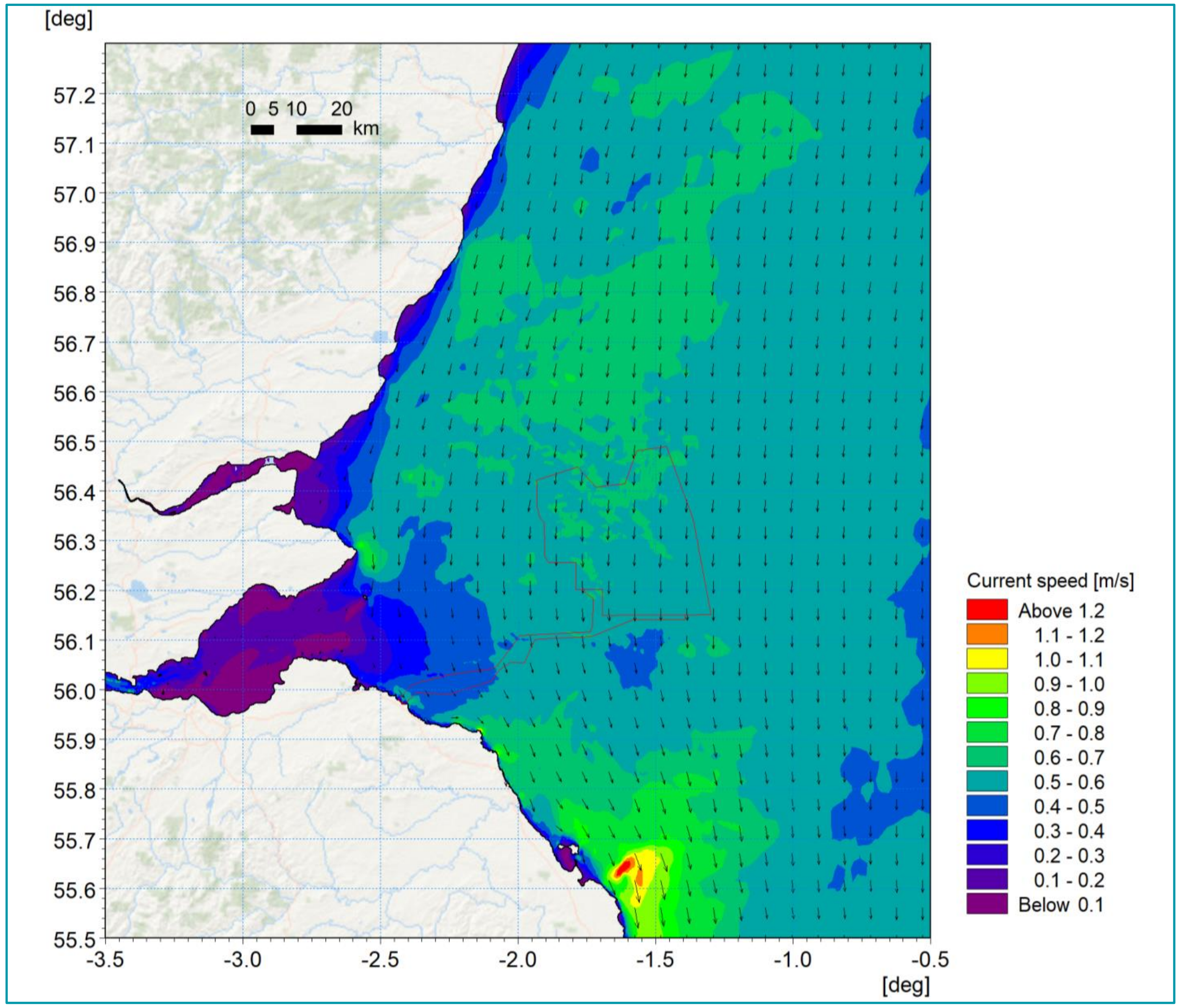


**Figure 5.18: Post-Construction Littoral Current 1:1 Year Storm from 000° - Flood Tide**

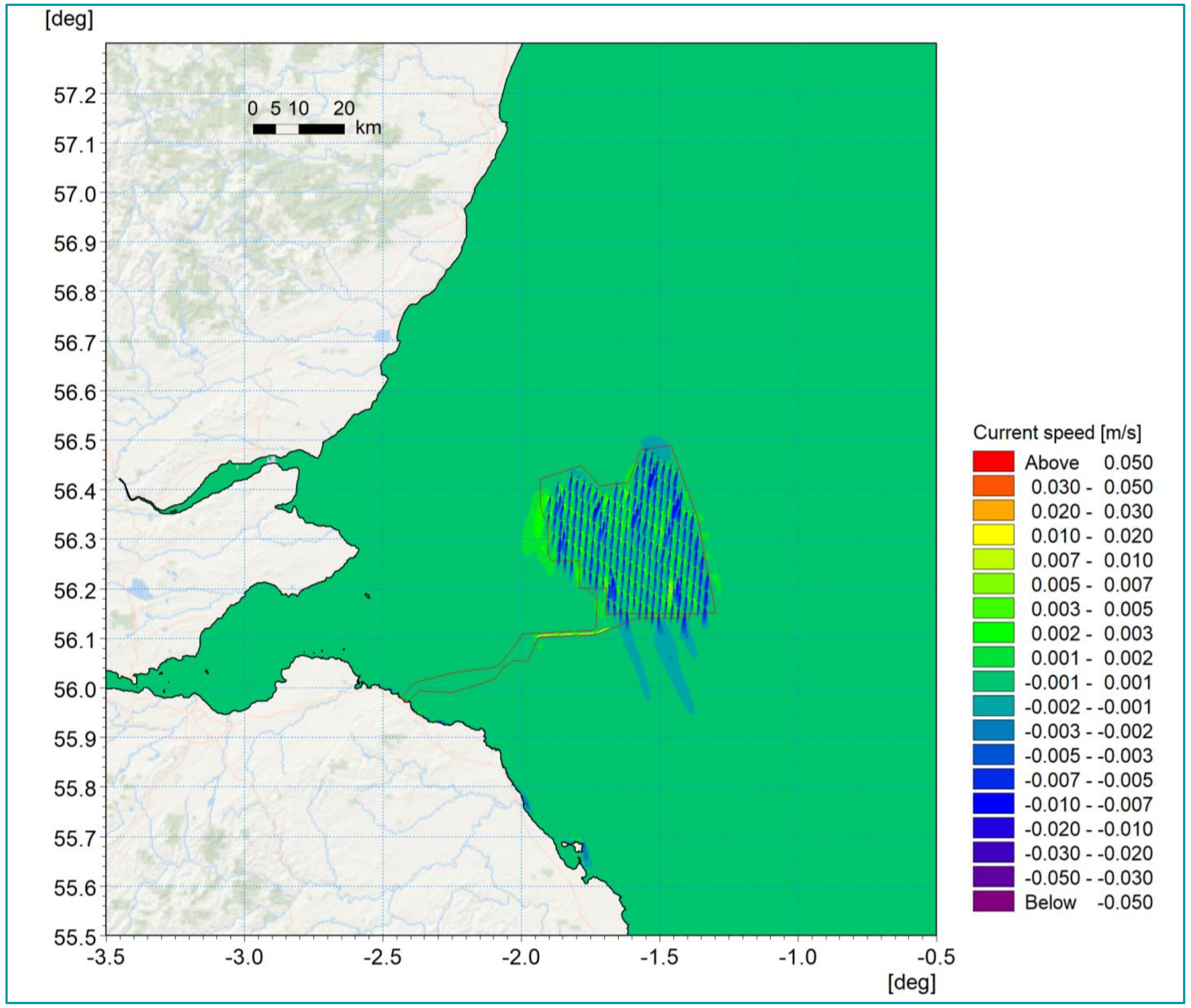


**Figure 5.19: Change in Littoral Current 1:1 Year Storm from 000° - Flood Tide (Post-Construction Minus Baseline)**

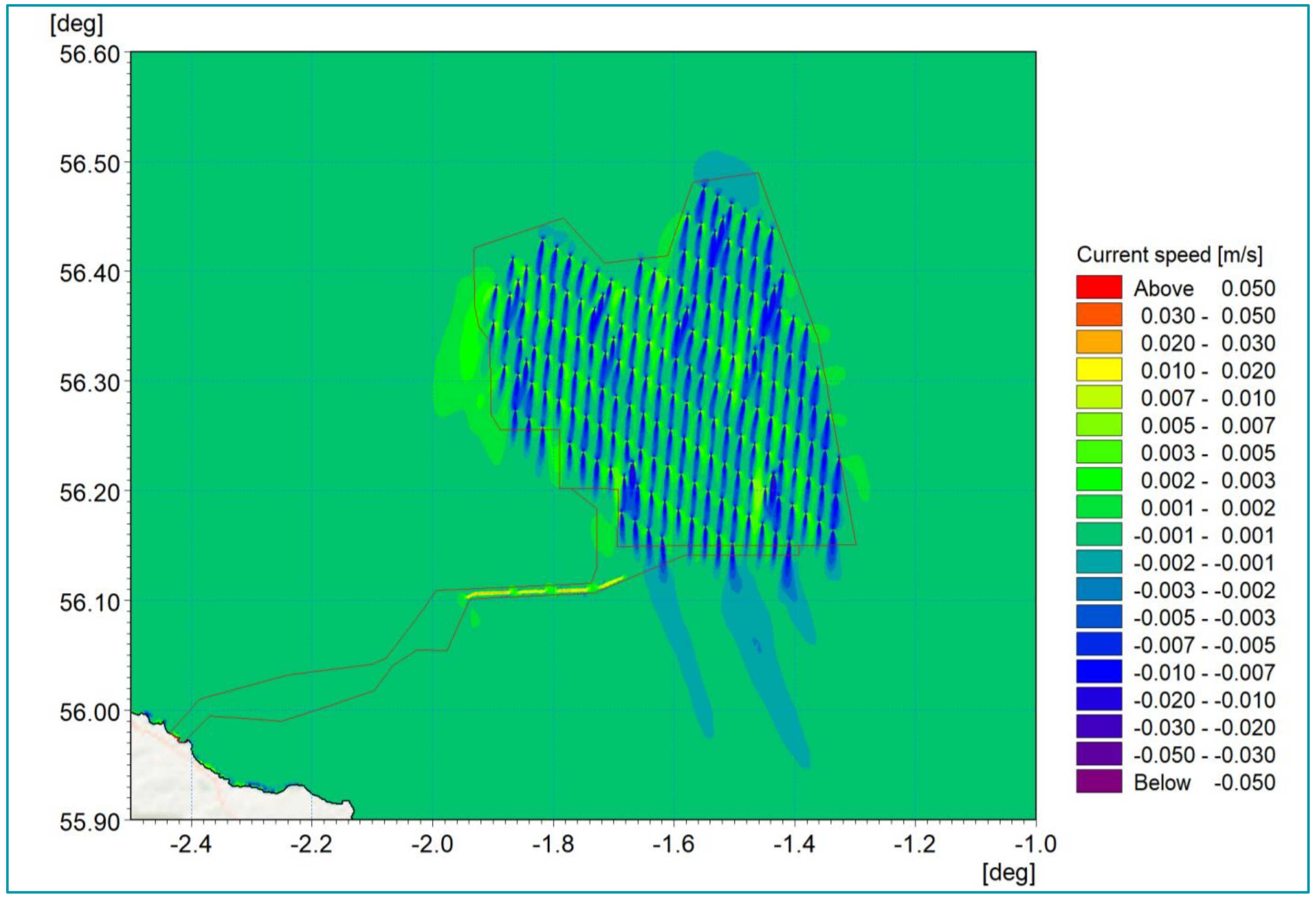


**Figure 5.20: Change in Littoral Current 1:1 Year Storm from 000° - Flood Tide (Post-Construction Minus Baseline) Proposed Development Array Area**

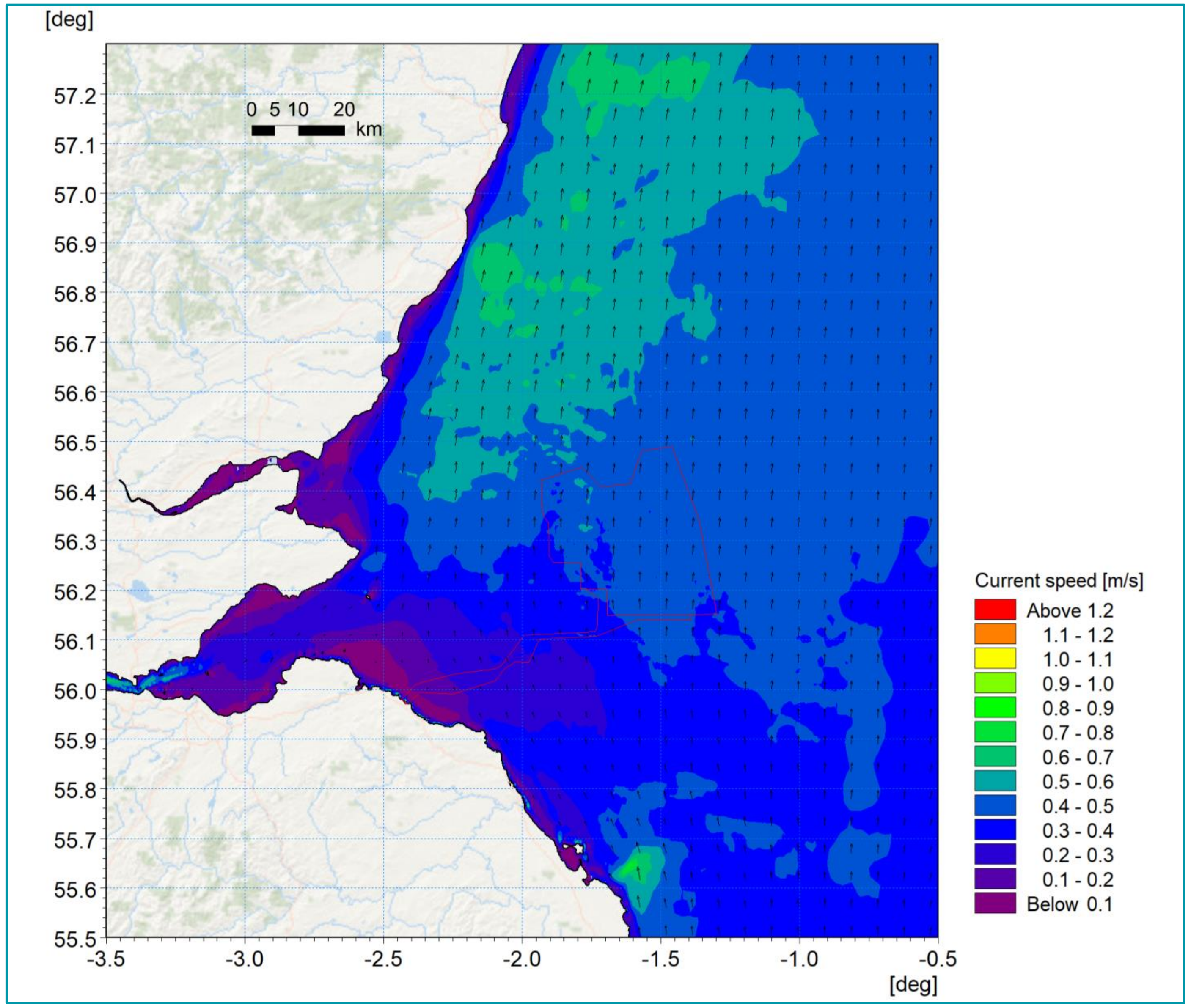


**Figure 5.21: Post-Construction Littoral Current 1:1 Year Storm from 000° - Ebb Tide**

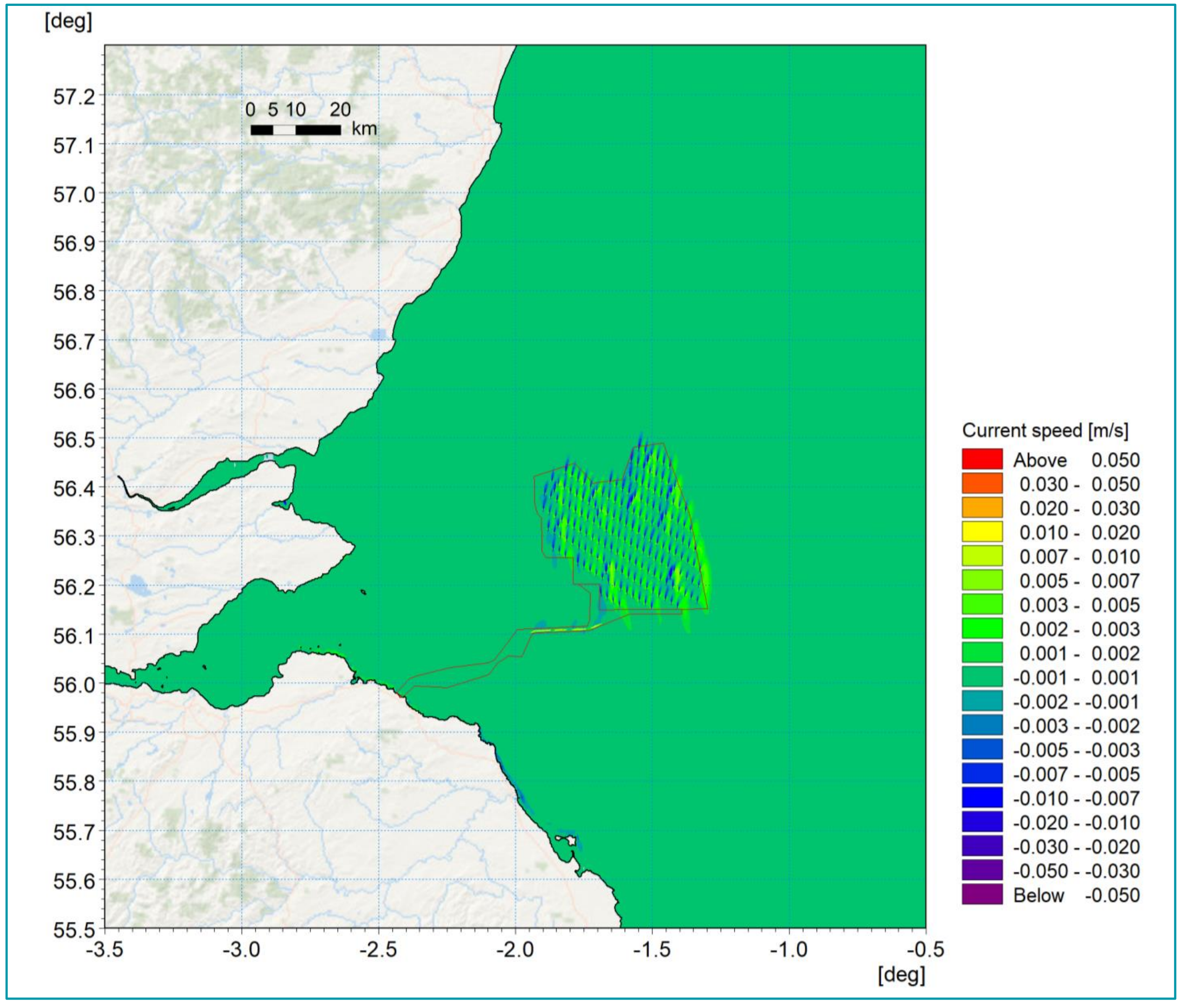


**Figure 5.22: Change in Littoral Current 1:1 Year Storm from 000° - Ebb Tide (Post-Construction Minus Baseline)**

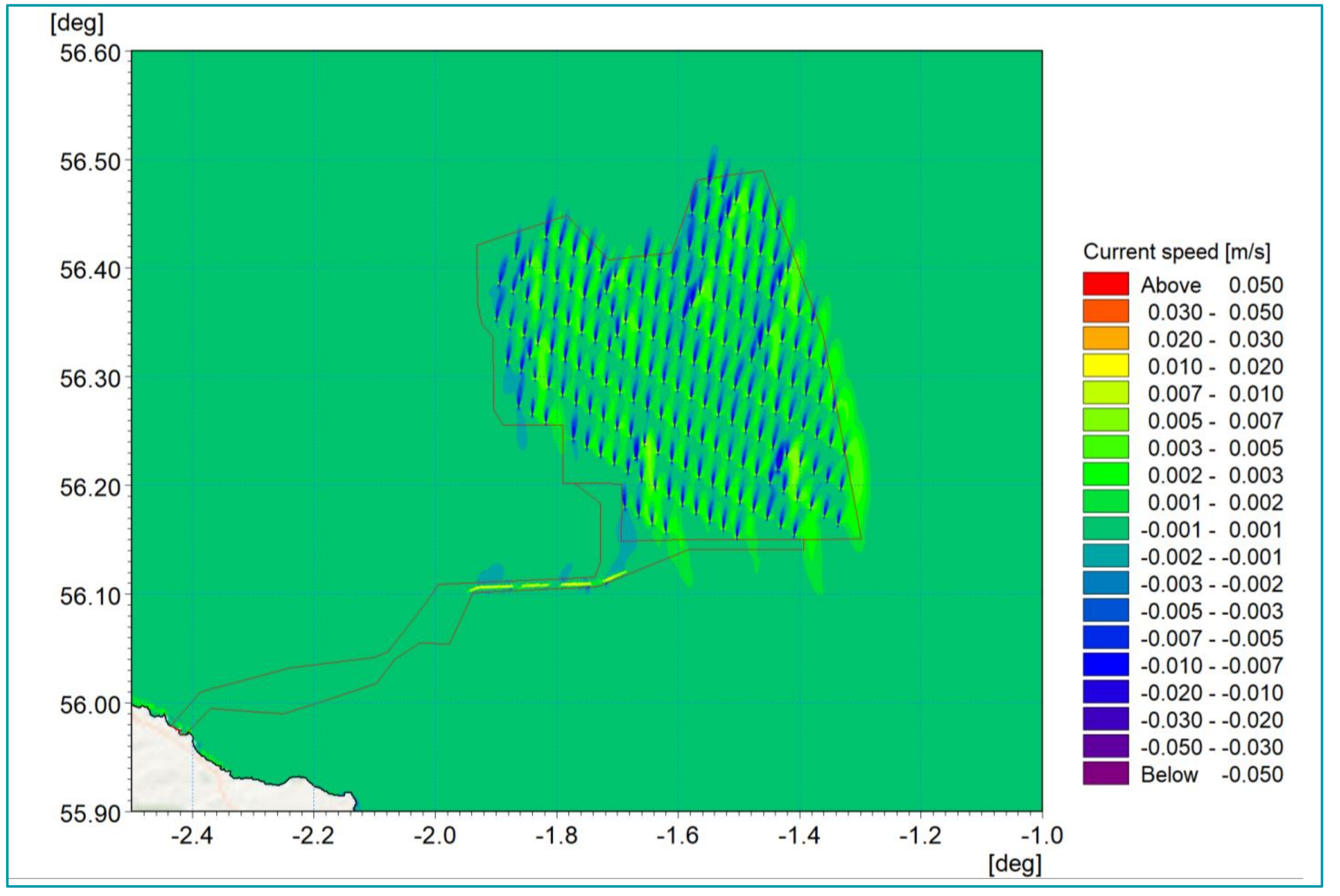


**Figure 5.23: Change in Littoral Current 1:1 Year Storm from 000° - Ebb Tide (Post-Construction Minus Baseline) Proposed Development Array Area**

## 5.3. POST-CONSTRUCTION SEDIMENTOLOGY

### 5.3.1. SEDIMENT TRANSPORT

70. The numerical modelling methodology for sediment transport was described in section 4.6, which indicated how the baseline information was discretised to form the basis of the modelled scenarios. For the post-construction scenario, in addition to the Proposed Development structures being included in the tide and wave models, the bed material map was edited to include the proposed additional scour and cable protection. In each case an area of fixed bed was applied overlain with a thin layer of sand to initialise the model and avoid instabilities. The scour protection was defined as the envelope of four times the 20 m caisson diameter for the wind turbine and four times the 15 m caisson diameter for the OSP/Offshore convertor station platforms legs. The models were then re-run for a spring tide under calm conditions and also for a one in one year storm from 000°.

71. There are a number of approaches for quantifying potential sediment transport, given that transport rates vary both across the area and due to tidal state and climate conditions. For this analysis, the residual current was calculated over the course of two tidal cycles (one day) with the structures in place and compared with that for the baseline (Figure 4.44) for the calm condition. The post-construction residual current and changes are shown in Figure 5.24 and Figure 5.25 respectively. As with previous results a more detailed plot is presented in Figure 5.26.

72. The corresponding sediment transport was simulated over the course of one day where the equivalent baseline daily sediment transport rate was shown in Figure 4.45. The post-construction daily sediment transport rate and differences are shown in Figure 5.27 and Figure 5.28 respectively. It should be noted that both the sediment transport and difference plots use a log palette as there is a large range in sediment transport potential across the domain and even so the changes in sediment transport rates are very small in the order of 0.01 $m^3/m$ over the course of a day.

73. This process was repeated for the 1 in 1-year storm. The baseline residual current (Figure 4.48) and daily potential sediment transport (Figure 4.49) were compared with the equivalent post-construction residual current pattern as shown in Figure 5.29; with the difference in Figure 5.30 and in more detail in Figure 5.31 whilst a similar comparison of the potential sediment transport is shown in Figure 5.32 and Figure 5.33.

74. This analysis shows that although there are changes as a result of the installation of the Proposed Development structures and associated scour and cable protection, the magnitude is limited in nature and log scales were required to illustrate values. As anticipated, in areas of reduced residual current in the lee of structures the sediment transport rate is also reduced and vice versa. Within the context of this comparative study there is a maximum change in residual current and sediment transport of circa ±15% which is largely sited within close proximity to the wind turbine foundation structures (less than 300 m elongated in the direction of principle tidal currents). It is noted that areas of reduced residual current and sediment transport are often accompanied by a similar increase in close proximity. This indicates that the residual current and resulting sediment transport paths are adjusted to accommodate the structures rather than transport pathways being cut off.

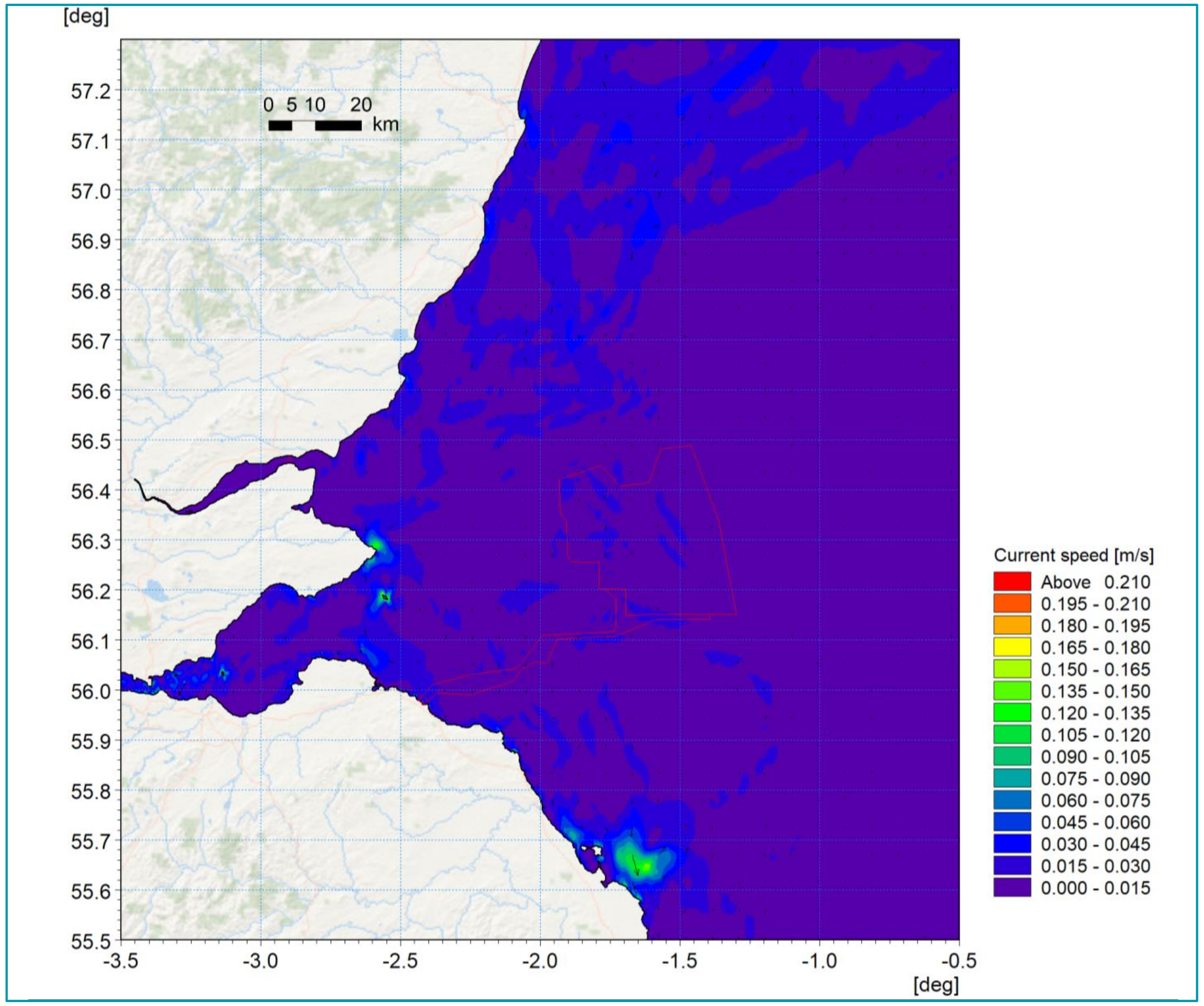


**Figure 5.24: Post-Construction Residual Current Spring Tide**

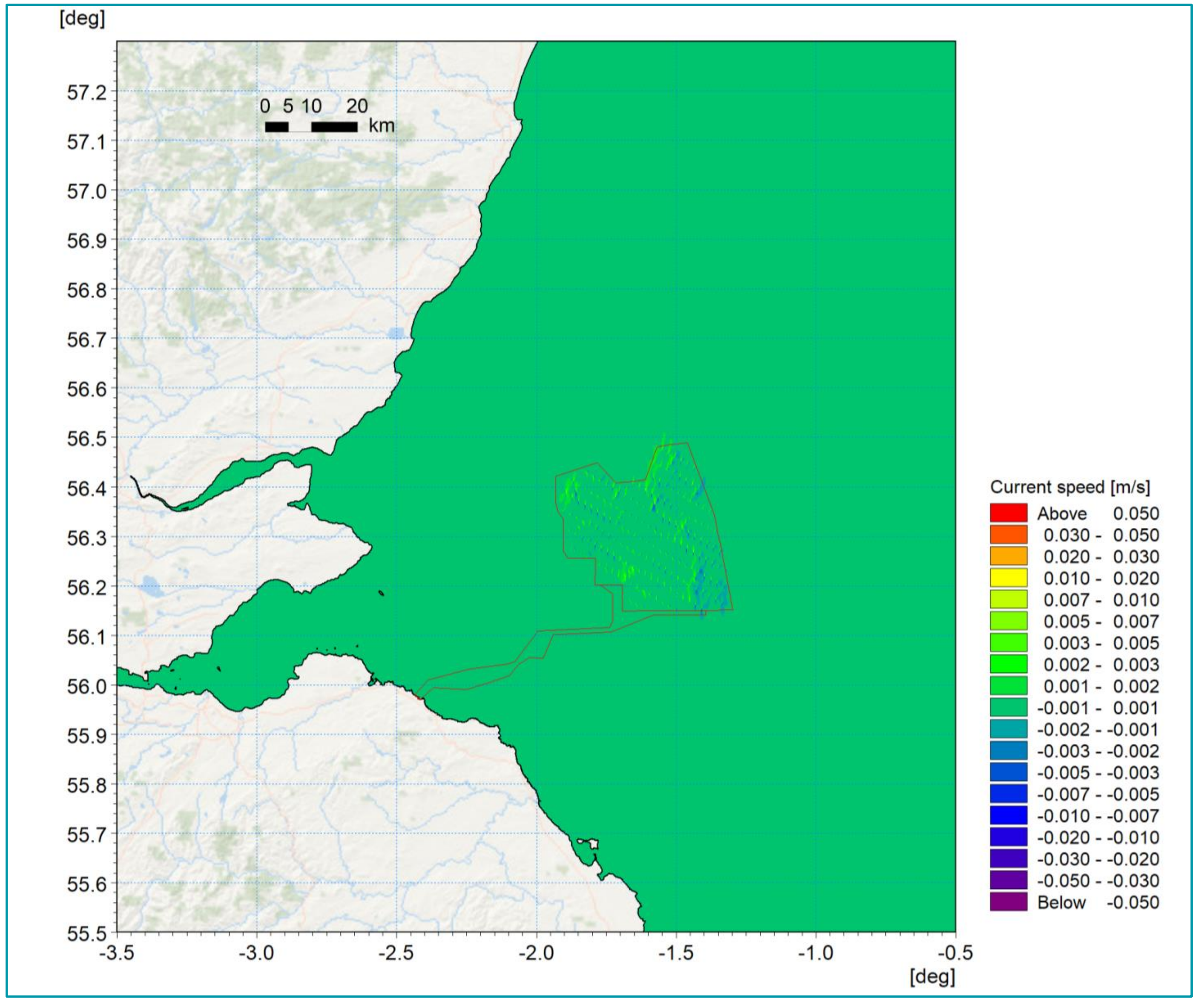


**Figure 5.25: Change in Residual Current Spring Tide (Post-Construction Minus Baseline)**

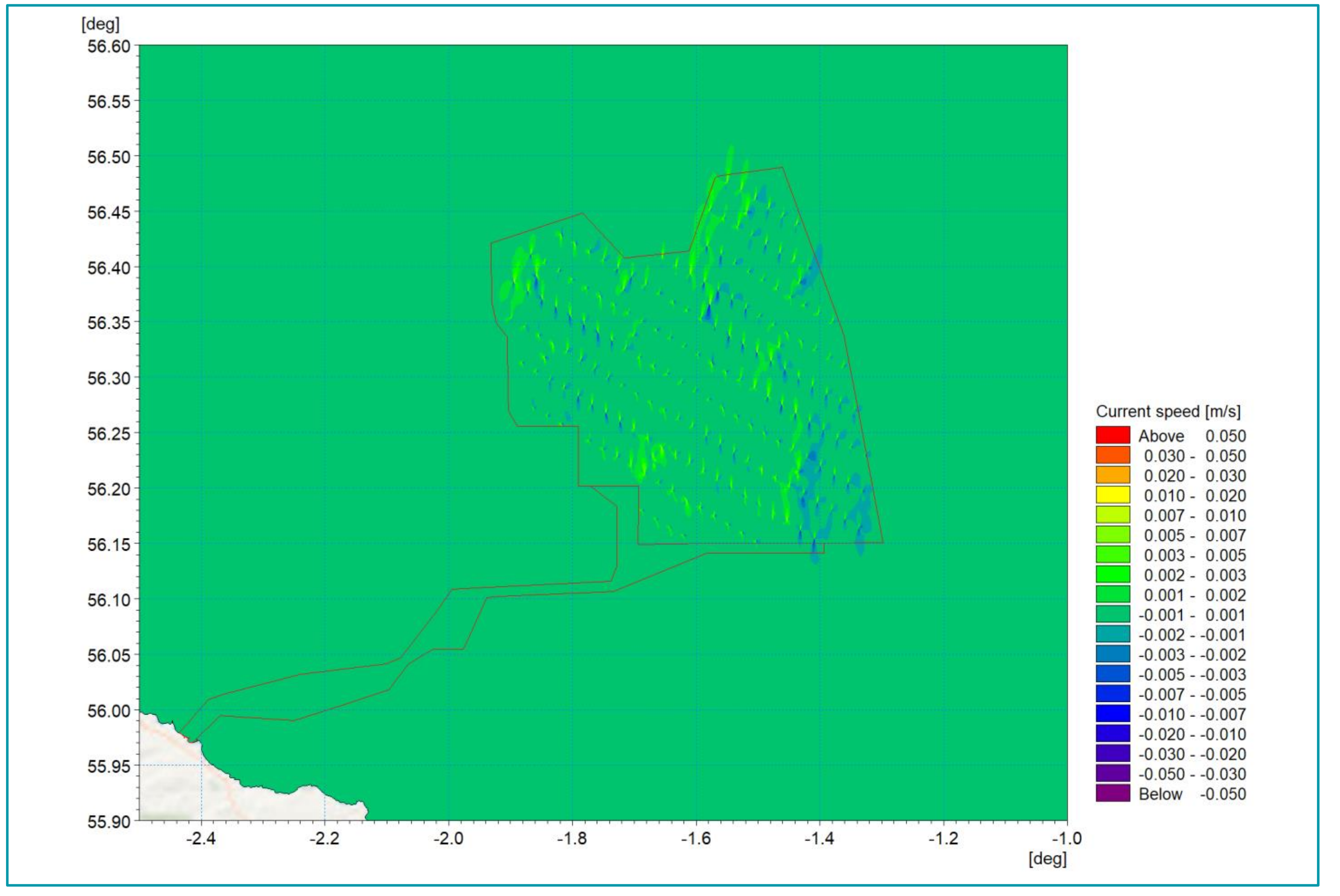


**Figure 5.26: Change in Residual Current Spring Tide (Post-Construction Minus Baseline) Proposed Development Array Area**

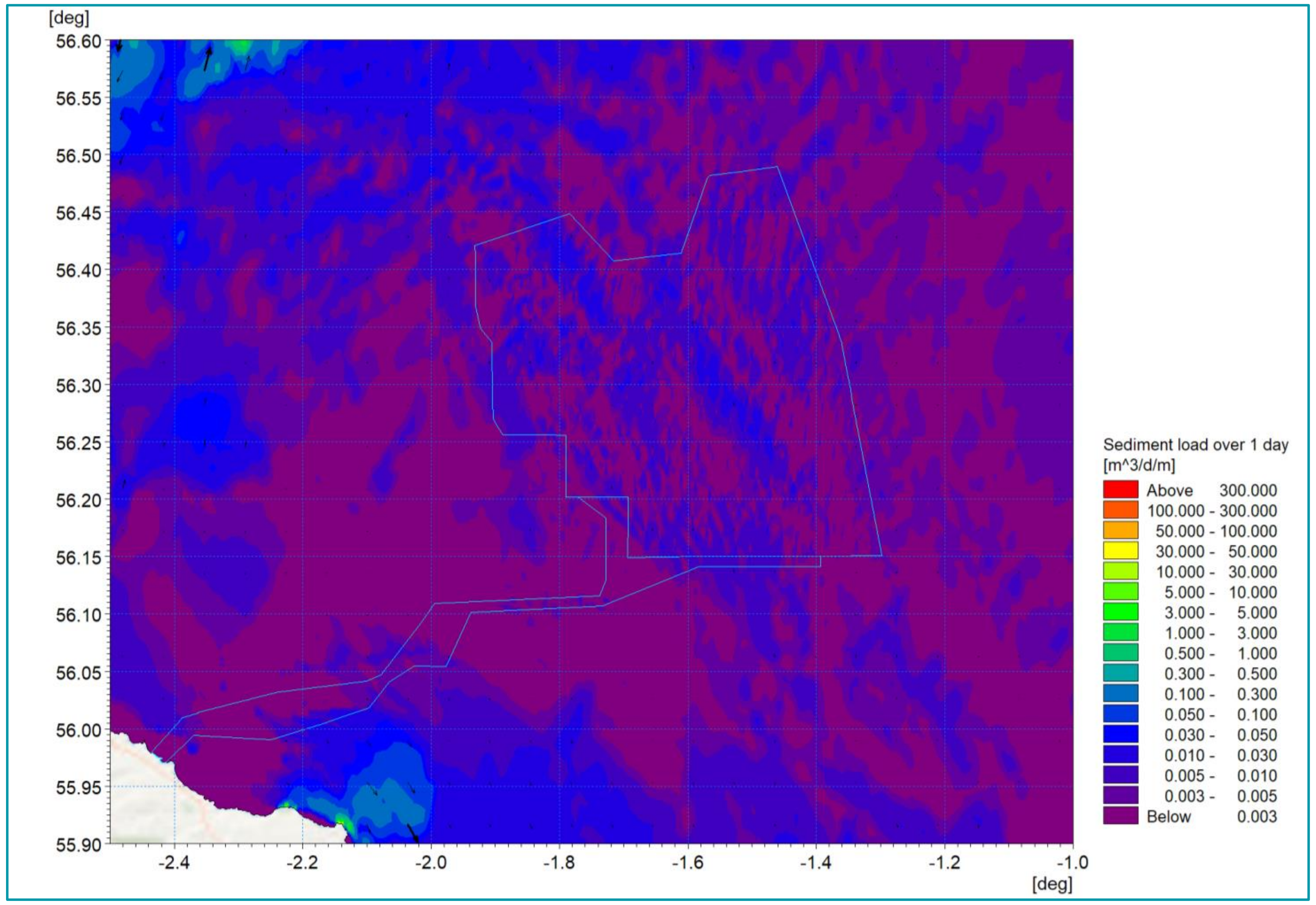


**Figure 5.27: Post-Construction Potential Sediment Over the Course of One Day (Two Tide Cycles)**

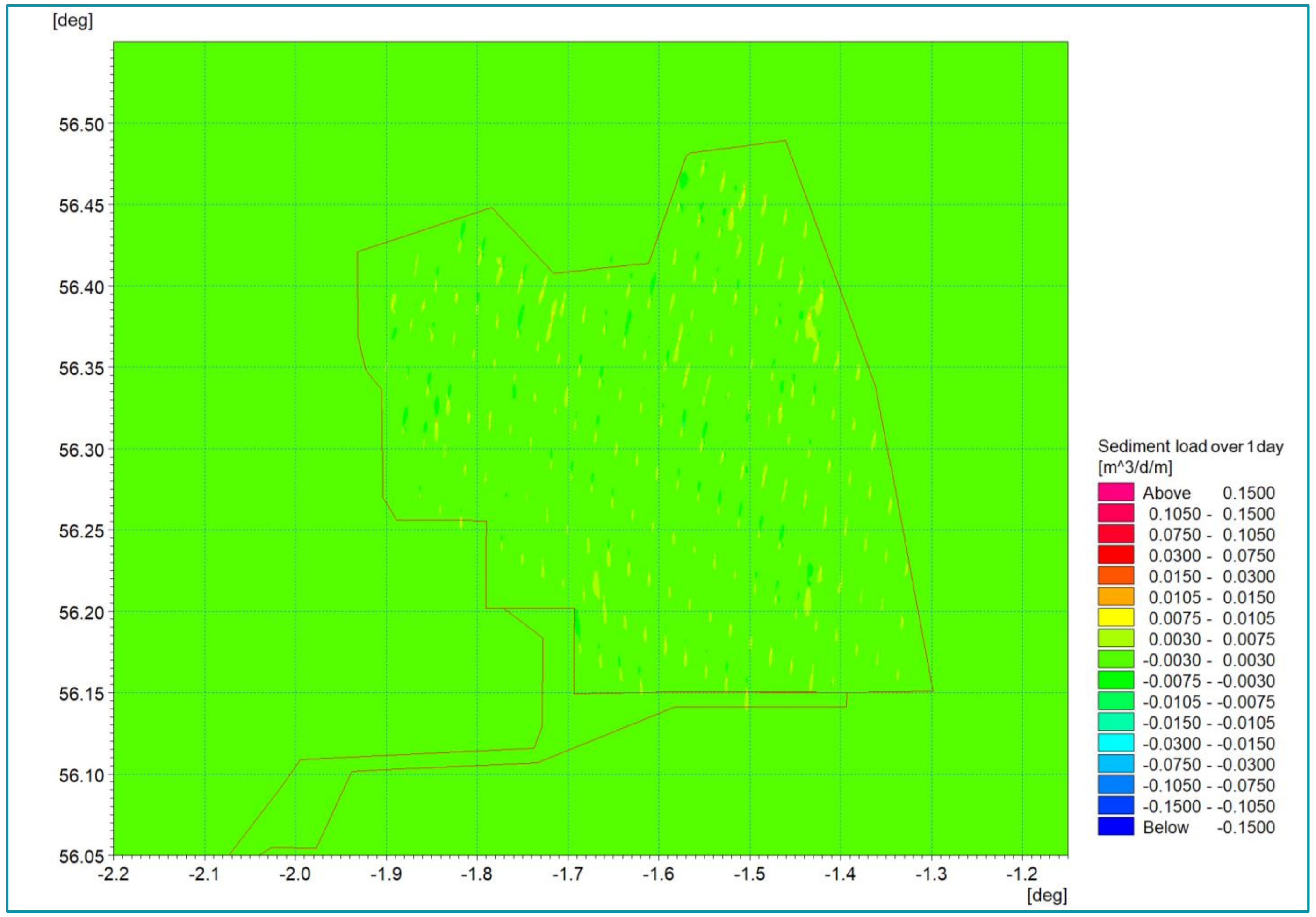


**Figure 5.28: Difference in Potential Sediment Transport Over the Course of One day (Post-Construction Minus Baseline)**

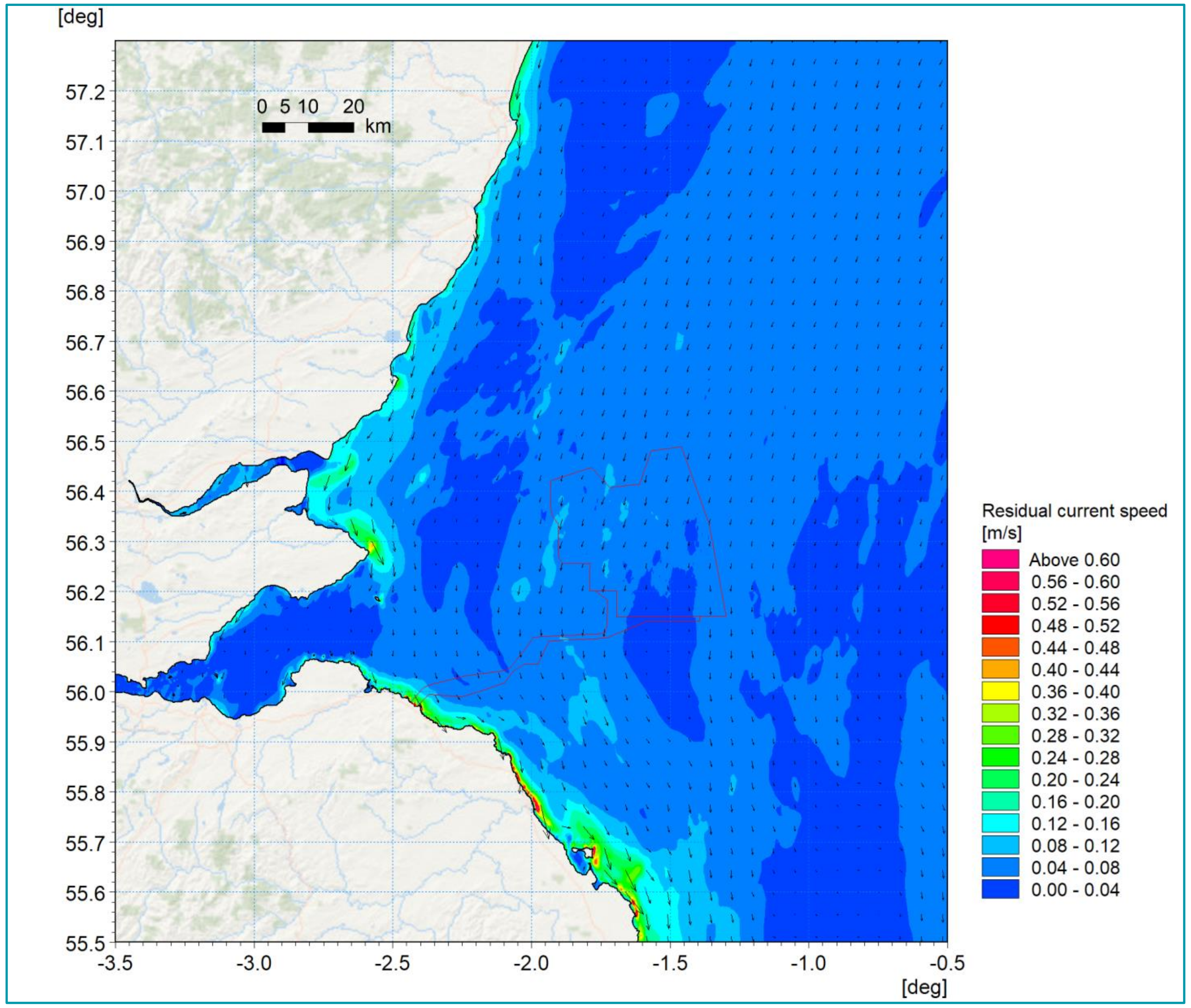


**Figure 5.29: Post-Construction Residual Current 1:1 Year Storm from 000° Spring Tide**

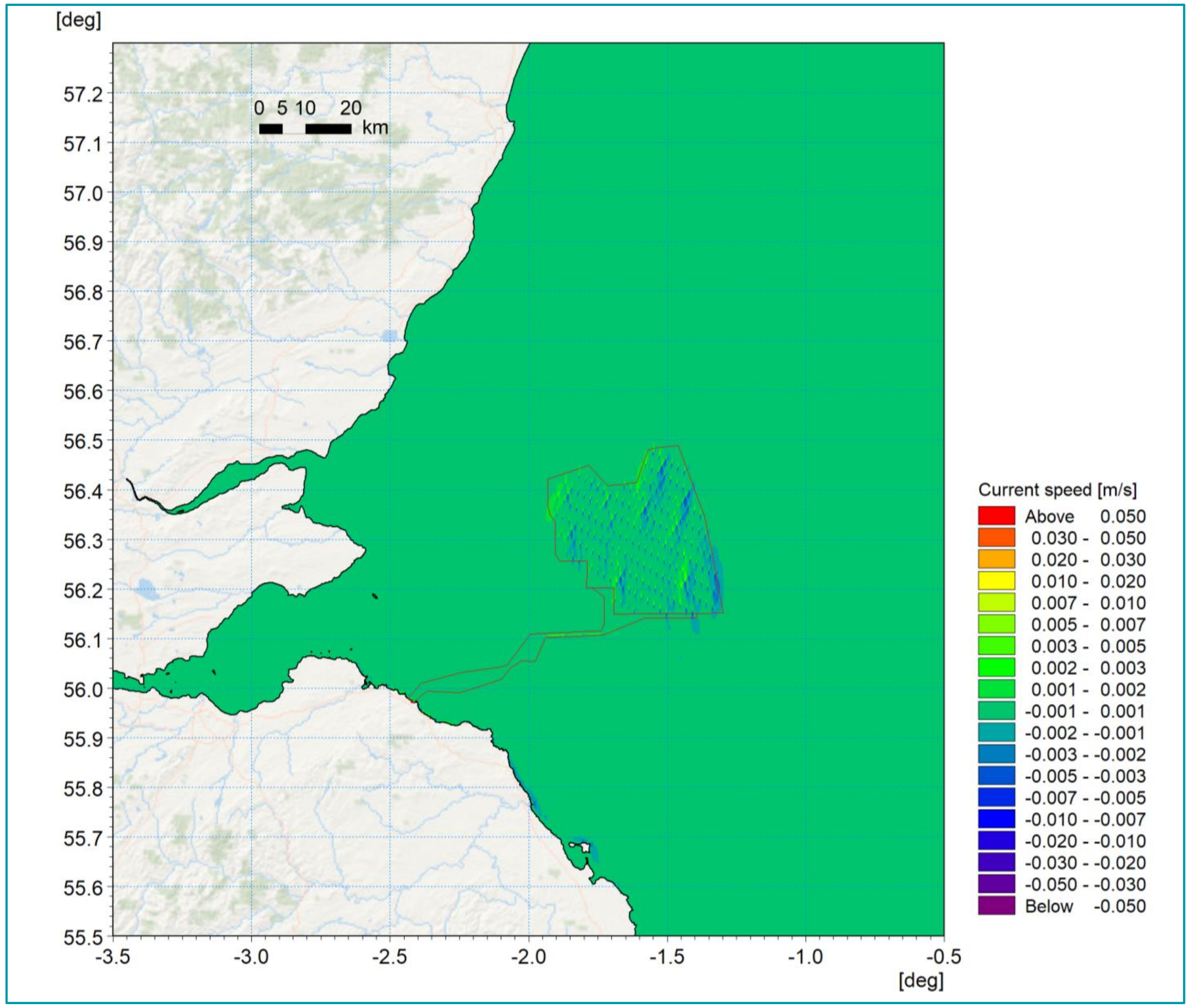


**Figure 5.30: Change in Residual Current 1:1 Year Storm from 000° Spring Tide (Post-Construction Minus Baseline)**

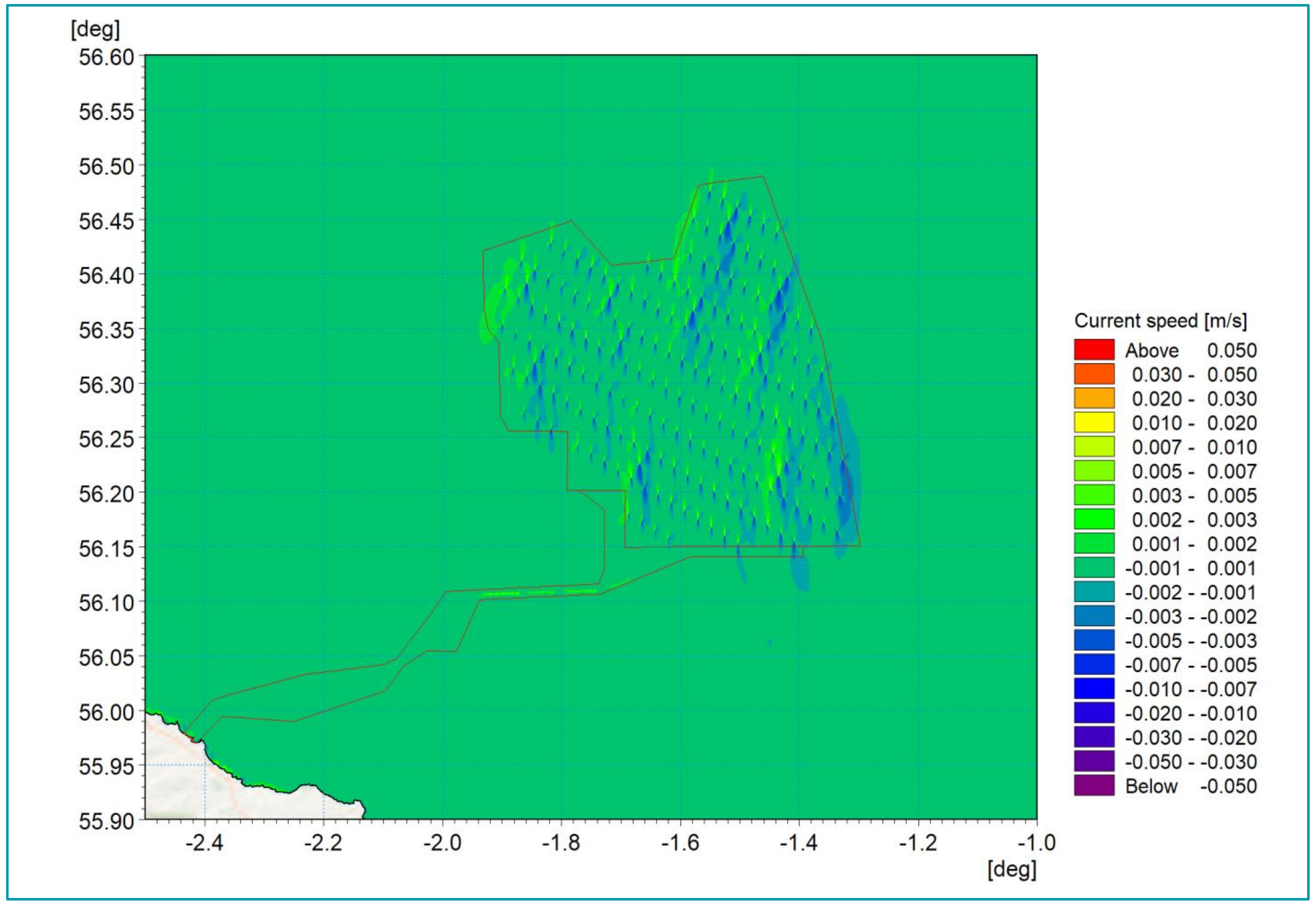


**Figure 5.31: Change in Residual Current 1:1 Year Storm from 000° Spring Tide (Post-Construction Minus Baseline) Proposed Development Array Area**

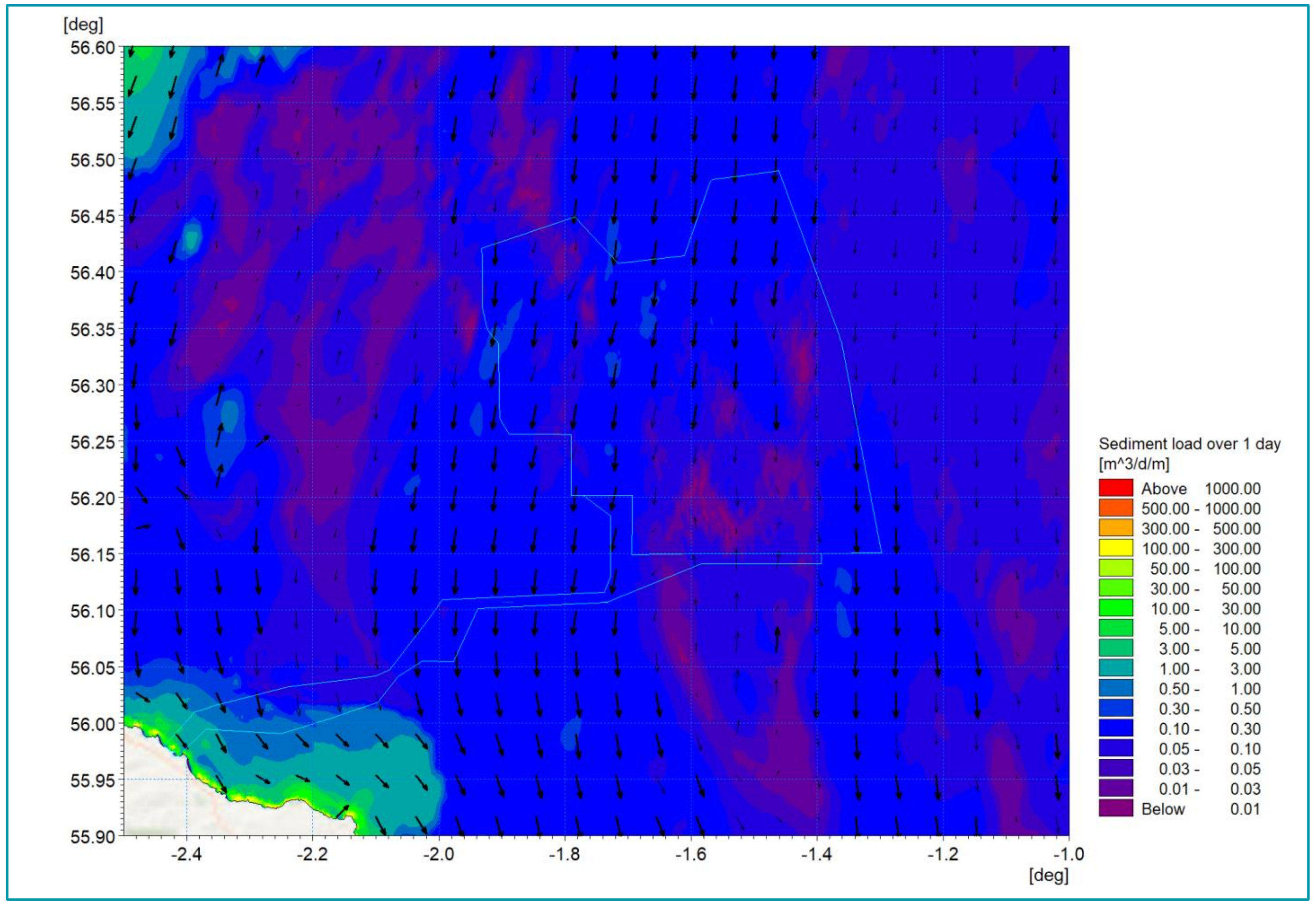


**Figure 5.32: Post-Construction Potential Sediment Transport over the Course of One day 1:1 Year Storm from 000°**

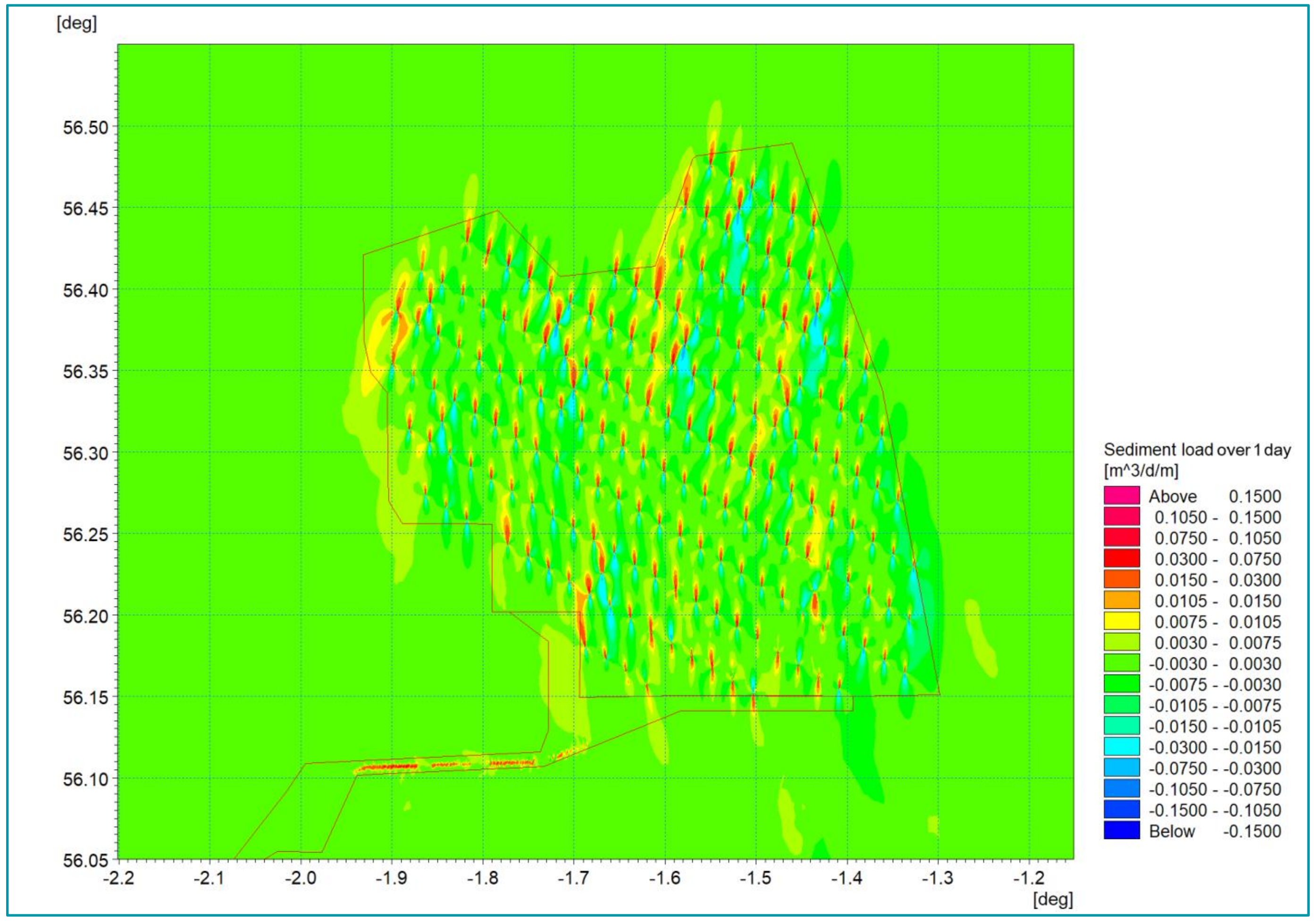


**Figure 5.33: Difference in Potential Sediment Transport over the course of One day (Post-Construction Minus Baseline) 1:1 Year Storm from 000°**

# 6. POTENTIAL CHANGES DURING CONSTRUCTION

75. In addition to the changes in coastal process resulting from the presence of the Proposed Development, the construction phase influences were quantified. The principal construction elements relate to the transport and fate of sediment brought into suspension due to seabed preparation, the installation of the foundation structures and the laying of inter-array/interconnector cables between the wind turbines/OSPs/Offshore convertor station platforms and the offshore export cables to shore. An overview of the modelling techniques implemented is provide in Table 3.1.

76. As with the post-construction aspects, the approach was to examine the construction technique which represents the maximum design scenario in terms of coastal processes. In practice, these changes are therefore likely to be of lesser magnitude. In each scenario the modelling examined excess SCC arising from the proposed activities (i.e. ambient SSC were not included). Baseline studies outlined in section 4.6 and section 4.7 indicate that turbidity levels are generally low, particularly in deep water areas, however sediment transport mechanisms are active with the associated bedload. Sedimented material arising from the construction phase activities would therefore be amalgamated into the sediment transport regime. The numerical modelling SSC provide depth average values and do not therefore differentiate between bed load and water column suspended sediment.

77. During each phase of the assessment the transport of suspended sediment was modelled by undertaking simulations which released sediment at a rate and location appropriate to each type of construction. The sediment released was defined according to the characteristics of grab samples collected at each specific location. Where a number of locations were encountered, such as a dredging path, then a representative grading was used. The sediment sample locations are presented in Figure 6.1.

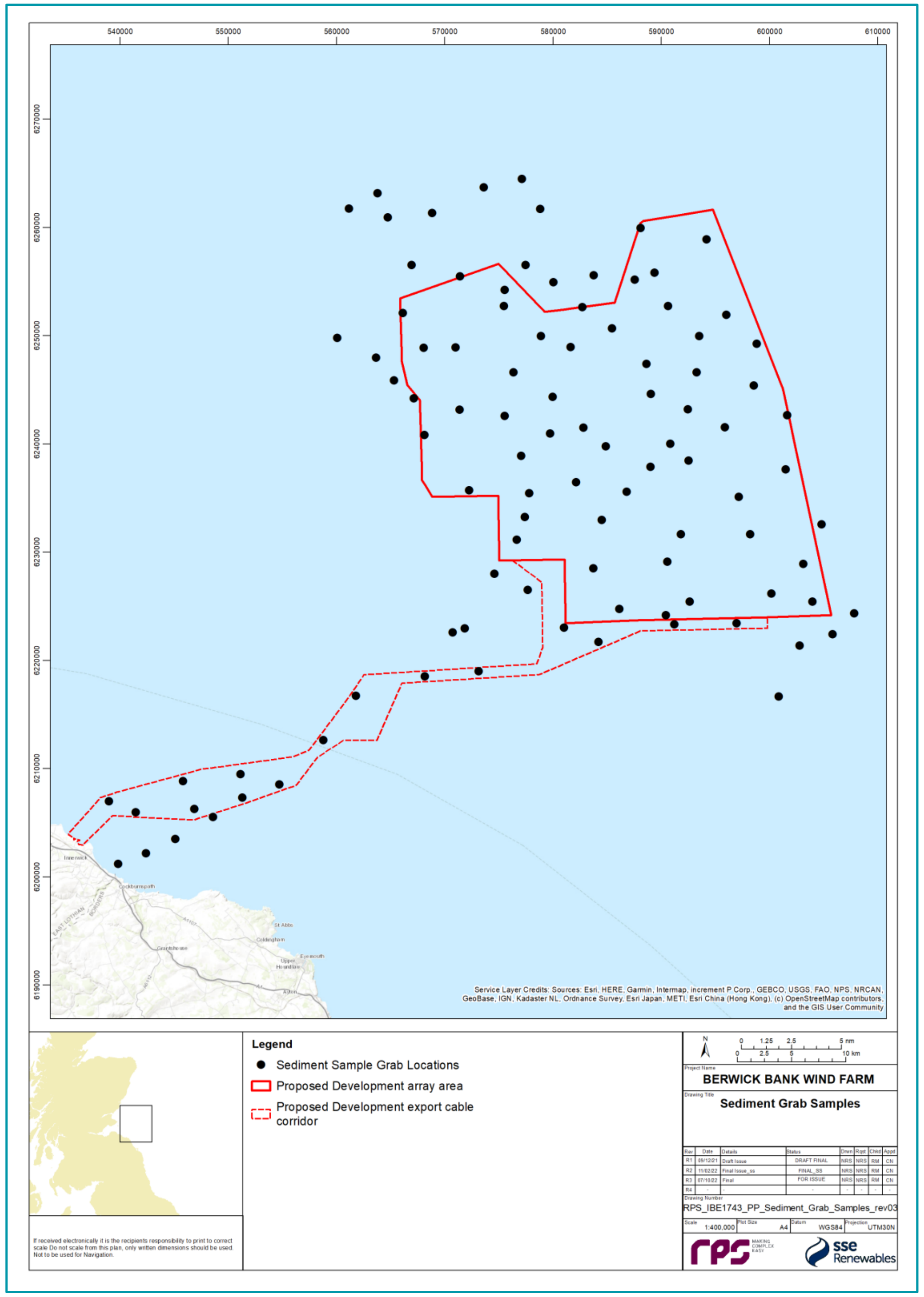


**Figure 6.1: Benthic Subtidal Survey Autumn 2020 - Grab Sample Locations**

## 6.1. SEABED PREPARATION

78. Due to the nature of the seabed in the Proposed Development array area and Proposed Development export cable corridor, the cable installation will require seabed preparation in the form of seabed features clearance. The Project Design Envelope (PDE) presented by the project description outlined in volume 1, chapter 3 of the Offshore EIA Report indicates that sand waves may be cleared for the offshore, inter-array and interconnector cabling along up to a 25 m wide corridor. Clearance activities may extend along circa 20% of the offshore cable route with an average clearance depth of up to 5 m and 30% of the inter-array cable route with an average clearance depth up to 1.3 m.

79. The modelling undertaken to quantify the potential increases in SSC and sedimentation simulated the use of a suction hopper dredger to remove material from the crest of sand waves and deposit material in the adjacent trough. In practice plough dredging may be undertaken however this type of operation would have less impact in terms of both SSC and sedimentation footprint.

80. Two representative clearance operations were assessed one relating to the offshore cabling and a second for the inter-array cables. The geophysical survey data was used to identify areas of sand waves and megaripples where the operations are most likely to be required. Figure 6.2 indicates these areas by grey shading and the clearance routes modelled are specified in yellow for the inter-array and green for the offshore cable. In each case the clearance was undertaken in a westerly direction with a dredging rate of 10,000 $m^3$/h with a spill of 3%.

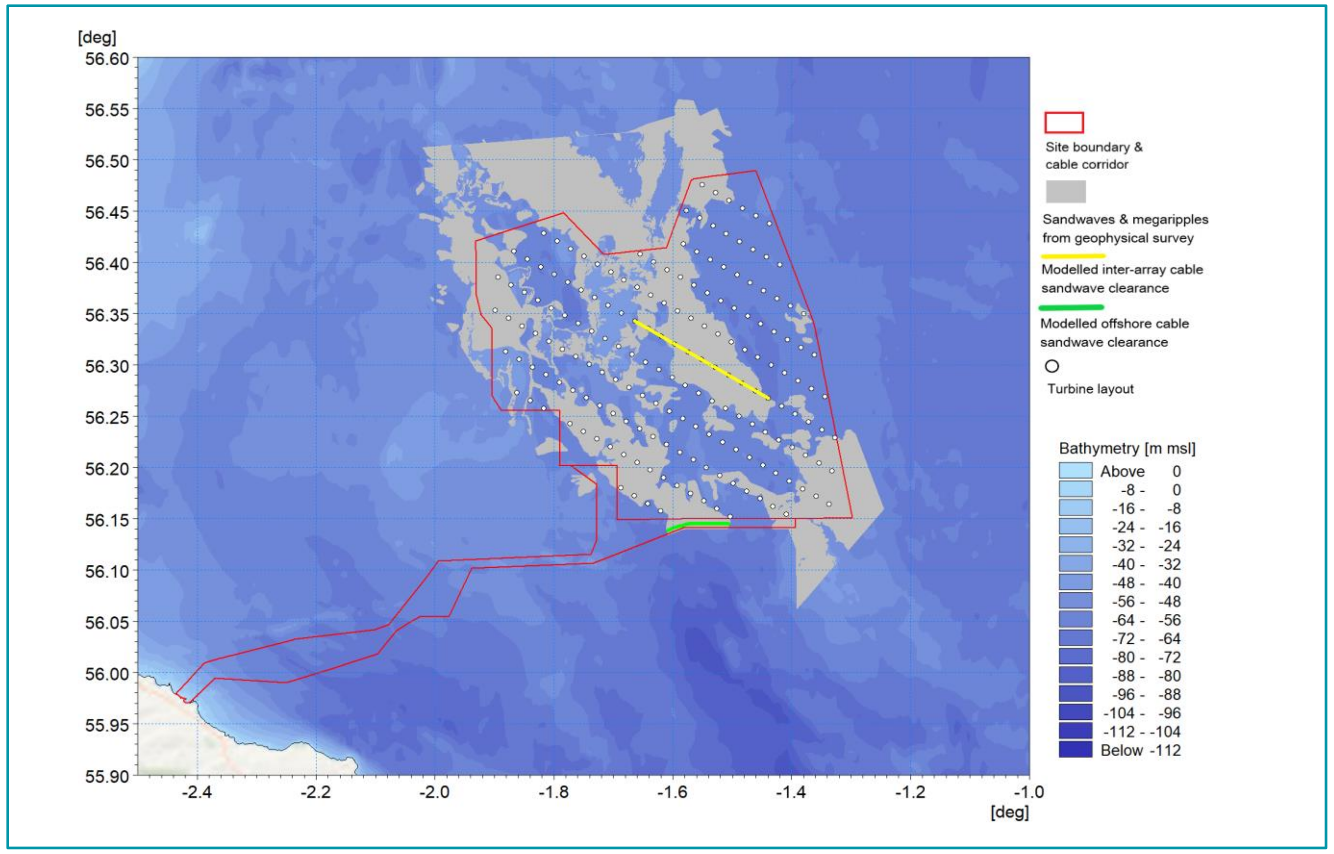


**Figure 6.2: Sand Wave Clearance Paths Modelled**

### 6.1.1. OFFSHORE CABLE SAND WAVE CLEARANCE

81. The offshore cable route was cleared at 80 m/h along the 25 m wide route for a period of two hours, in line with dredging rate and plant required to carry out the operation. The material was then deposited over a half hour period from the hopper with the modelled route taking 3.5 days to prepare. The redistributed material was classified using the properties identified from the sampling undertaken along the route simulated.

- coarse sand: 20%;
- medium sand: 33%;
- fine sand: 39%; and
- very fine sand: 8%.

82. The SSC vary greatly during the course of the dredge and disposal campaign. During the dredging phase when only 3% of the material is released the plume is very small with concentrations <100 mg/l as shown in Figure 6.3. During the disposal phase the plume is slightly larger (Figure 6.4) with concentrations reaching 2,500 mg/l at the release site. However, the most extensive increases are seen as the deposited material is redistributed on the successive tides, where sedimentation occurs on the slack tide reducing the SSC completely and resuspension and transport occurs when the tidal currents increase. Under these circumstance concentrations of 100 mg/l to 250 mg/l are seen as illustrated in Figure 6.5 which shows SSC arising at peak current speed. The average SSC during the course of the dredge and disposal campaign is presented in Figure 6.6 with values <100 mg/l with a plume width of 10 km which corresponds with the tidal excursion.

83. The average sedimentation depth is shown in Figure 6.7 and illustrates how the deposited material is focussed within 100 m of the site of release with a maximum depth 0.5 m to 0.75 m whilst the finer sediment fractions are distributed in the vicinity at much smaller depths circa 5 m to 10 mm. The dispersion of the released material would continue on successive tides and be incorporated into the baseline sediment transport regime. The sedimentation one day following the cessation of the clearance operation is presented in Figure 6.8 and is consistent with this mechanism.

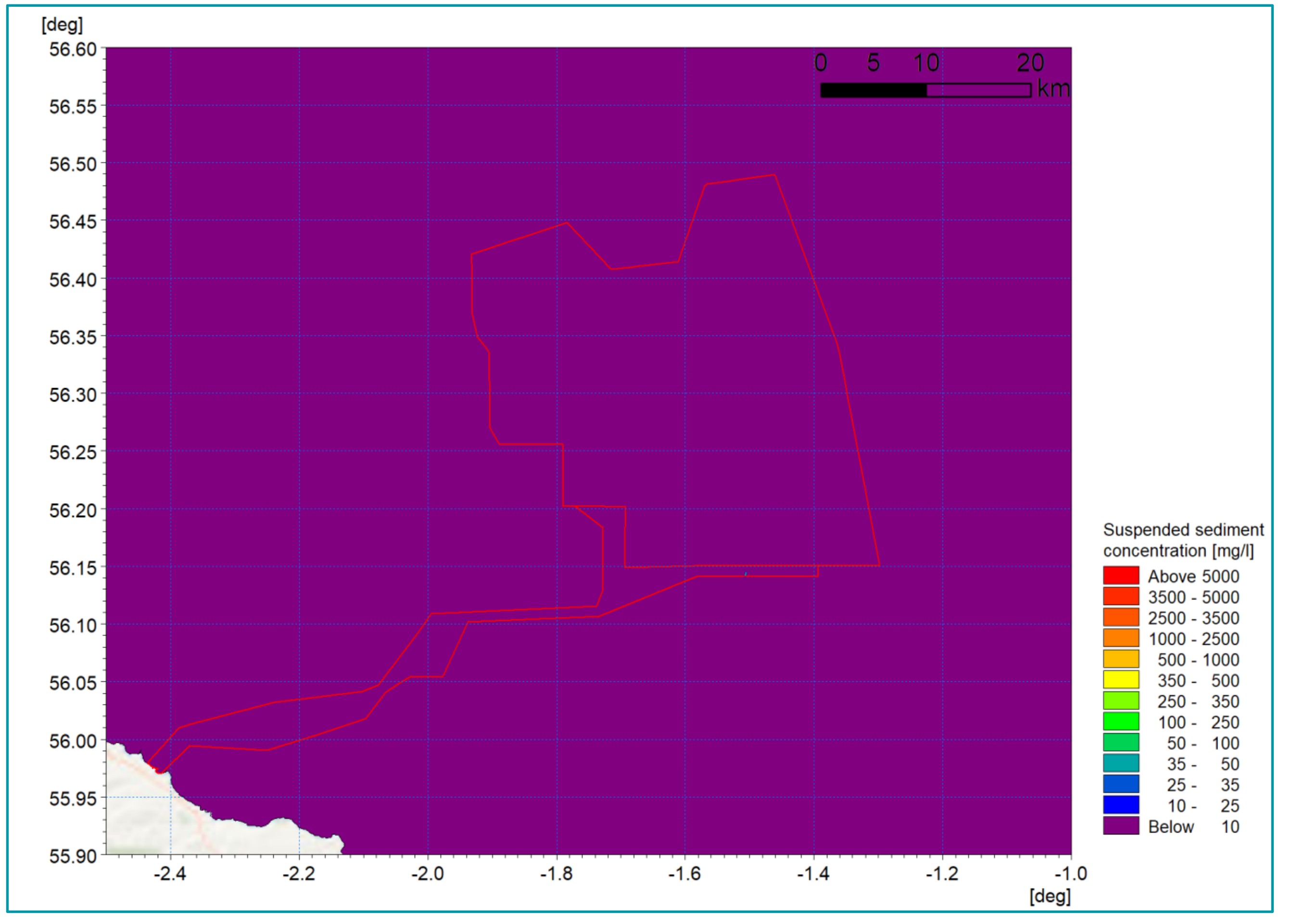


**Figure 6.3: Suspended Sediment Concentration During Dredging Phase – Offshore Cable Path**

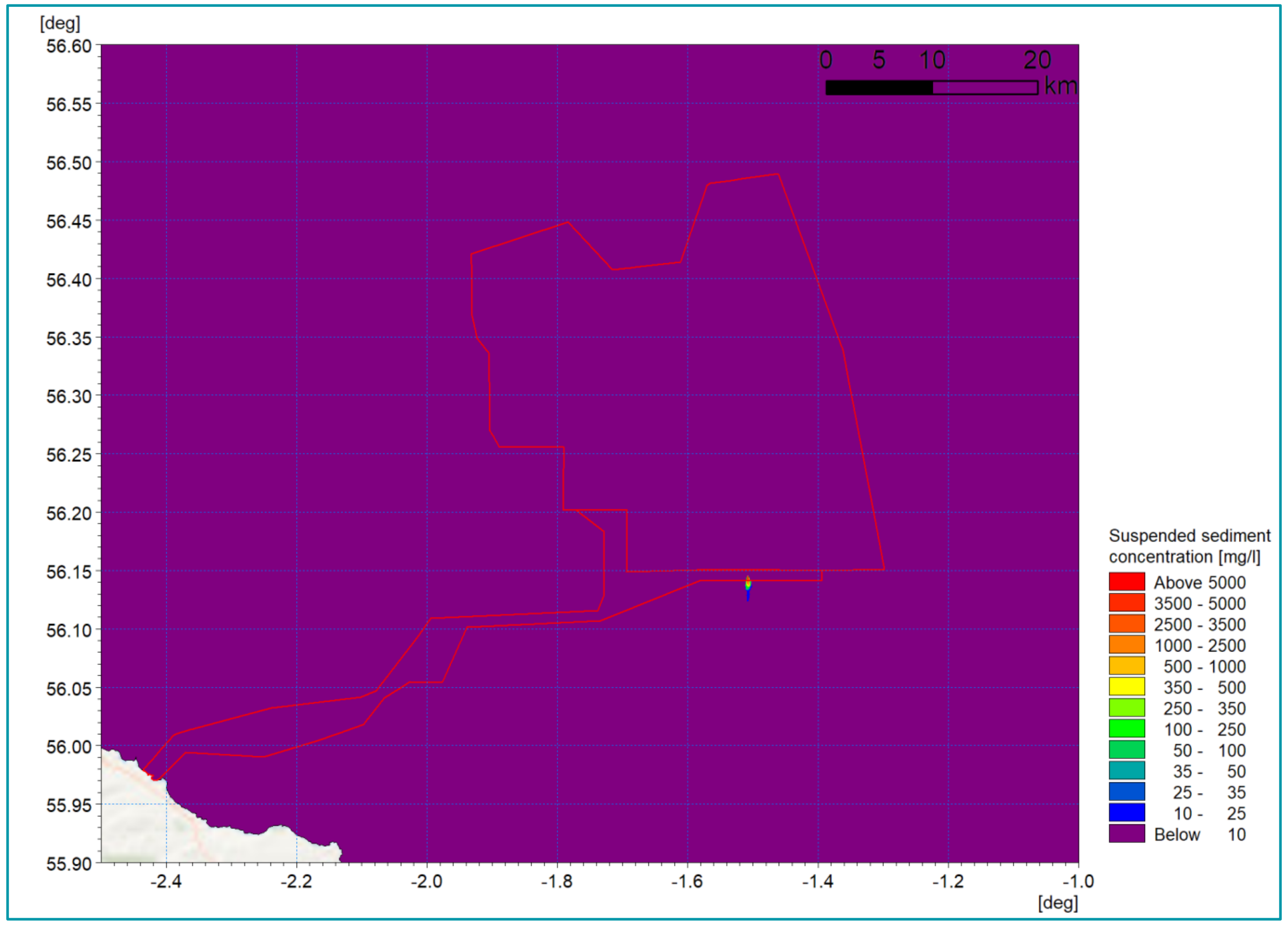


**Figure 6.4: Suspended Sediment Concentration During Disposal Phase – Offshore Cable Path**

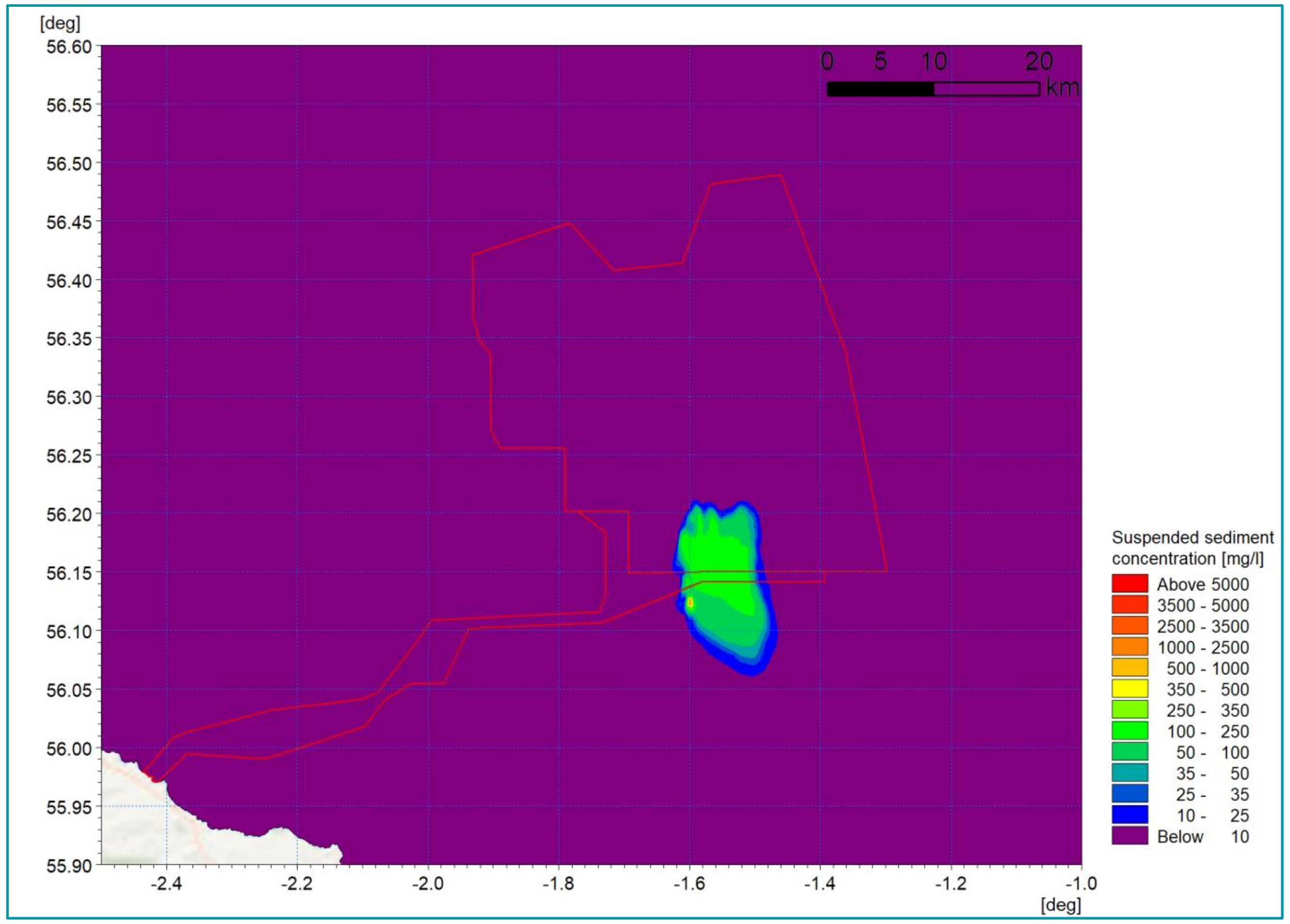


**Figure 6.5: Suspended Sediment Concentration with Sediment Re-Mobilisation – Offshore Cable Path**

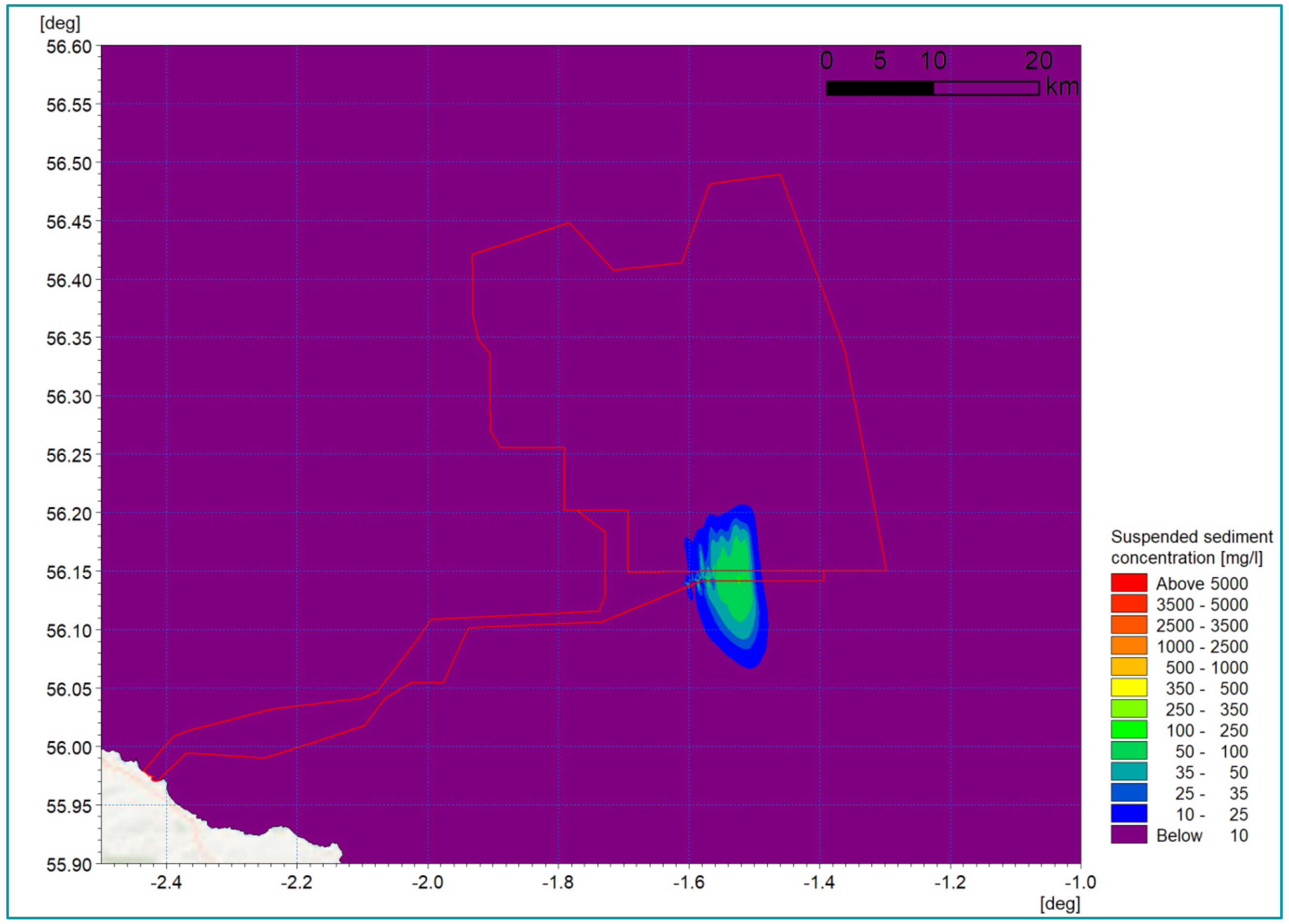


**Figure 6.6: Average Suspended Sediment Concentration During Dredge and Disposal Campaign – Offshore Cable Path**

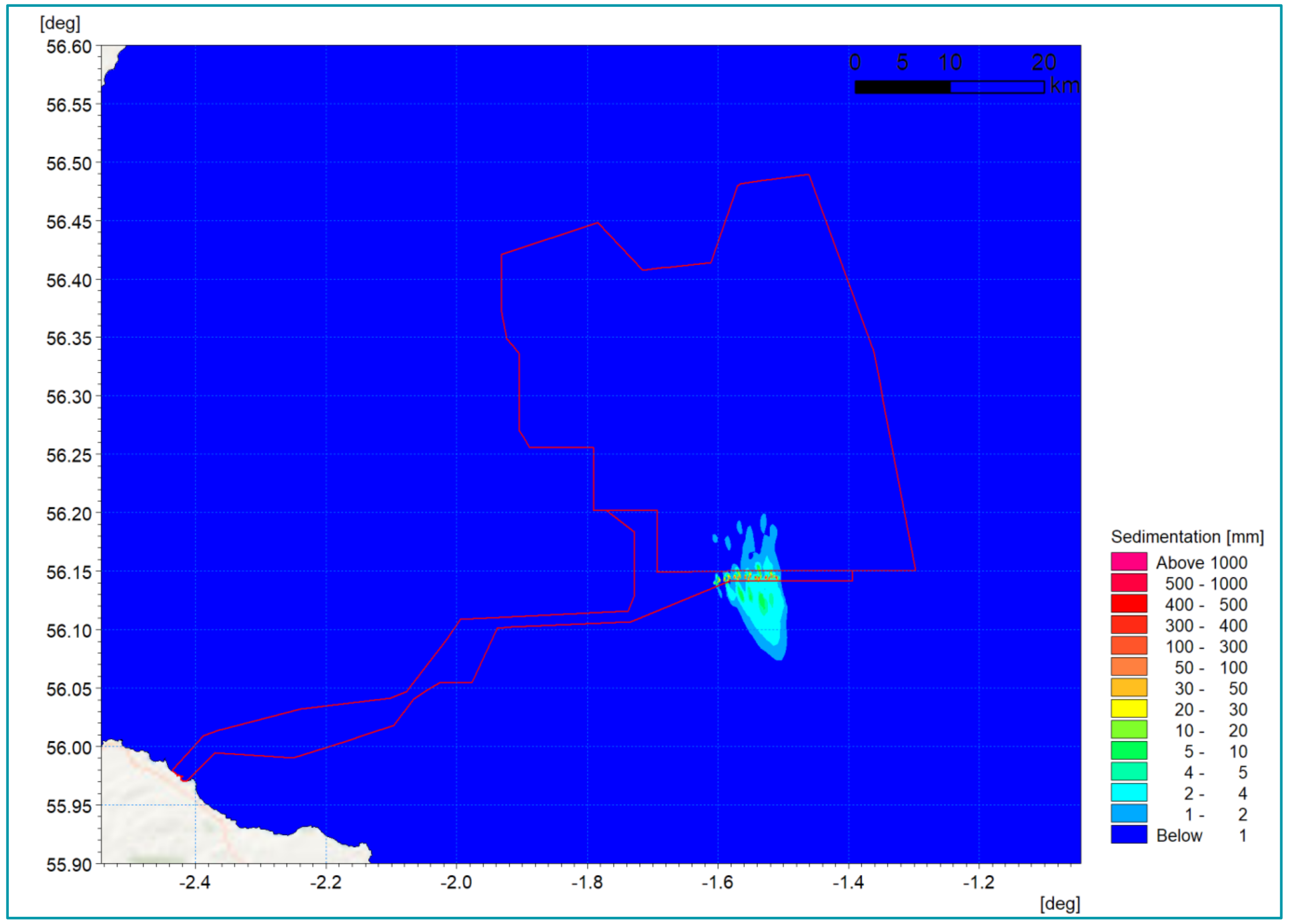


**Figure 6.7: Average Sedimentation During Dredge and Disposal Campaign – Offshore Cable Path**

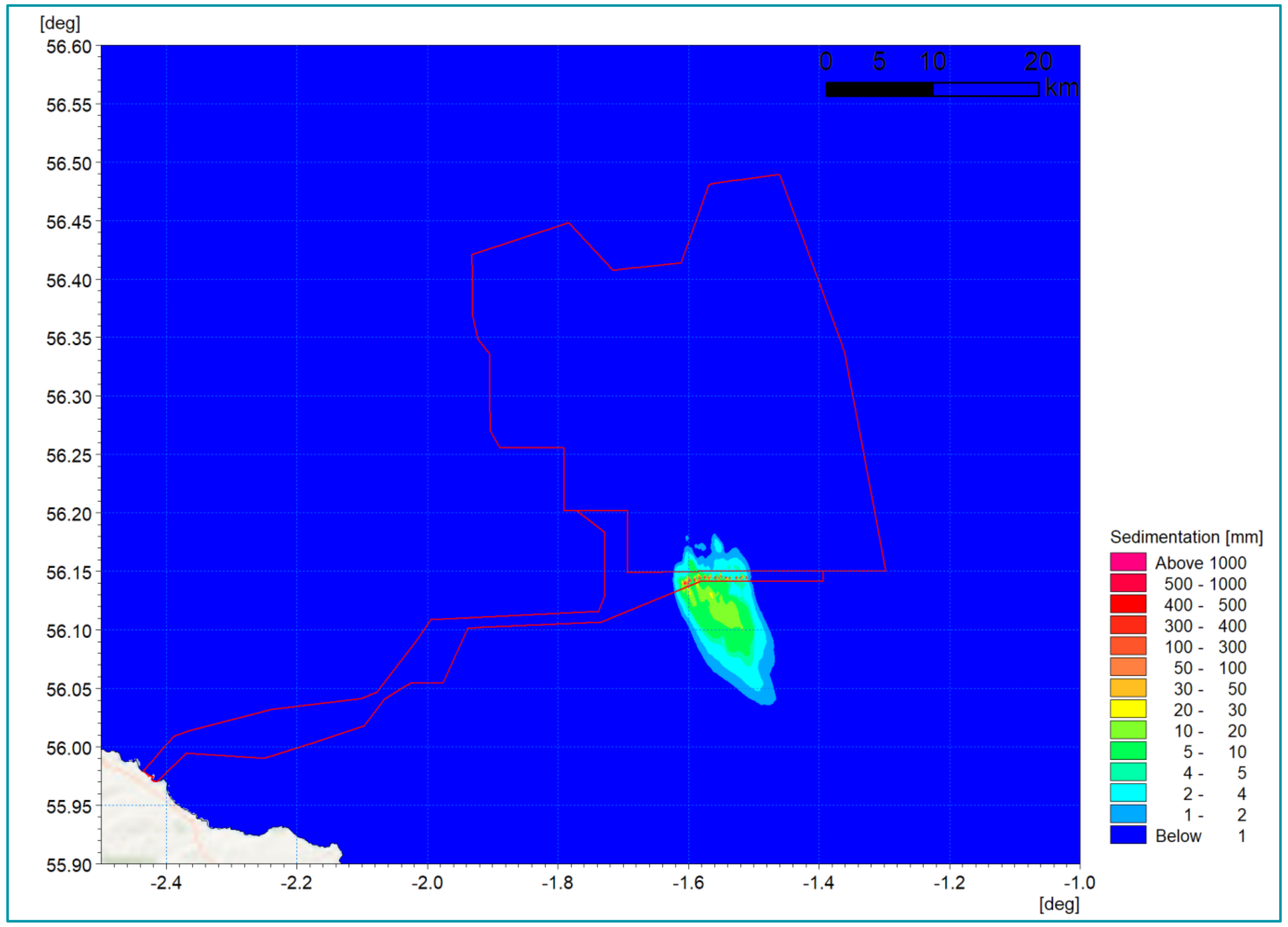


**Figure 6.8: Sedimentation One Day Following Cessation of Dredge and Disposal Campaign – Offshore Cable Path**

### 6.1.2. INTER-ARRAY CABLE SAND WAVE CLEARANCE

84. The inter-array cable route was cleared at 312 m/h along the 25 m wide route for a period of one hour, in line with the dredging rate and reduced removal depth. The material was then deposited over a 15 minute period from the hopper with the modelled route taking 2.1 days to prepare. As previously, the redistributed material was classified using the properties identified from the sampling undertaken along the route simulated.

- coarse sand: 28%;
- medium sand: 59%;
- fine sand: 10%; and
- very fine sand: 3%.

85. The resulting SSC showed similar characteristics to the offshore cable clearance. The dredging phase plumes were even smaller, as 3% spill of the material is released with faster progress along the route and again concentrations are <100 mg/l as shown in Figure 6.9. Similarly, the release phase plume is slightly larger than the dredging plume with concentrations reaching 2500 mg/l at the disposal site, Figure 6.10. At this site the greatest area of increased suspended sediment concentration, extending a tidal excursion circa 10 km from the site, is also associated with re-mobilisation of the deposited material on subsequent tides with concentrations of 100 mg/l to 250 mg/l whilst average levels <100 mg/l as illustrated in Figure 6.11 and Figure 6.12 respectively.

86. Due to the smaller volume the average sedimentation depth, shown in Figure 6.13, is typically half that of the offshore cable works. The sedimentation one day following the cessation of the clearance operation is presented in Figure 6.14 and shows deposited material at the site of release with depth 0.2 m to 0.4 m whilst in the locality lower depths, typically <5 mm, are present at 50 m distance from the release.

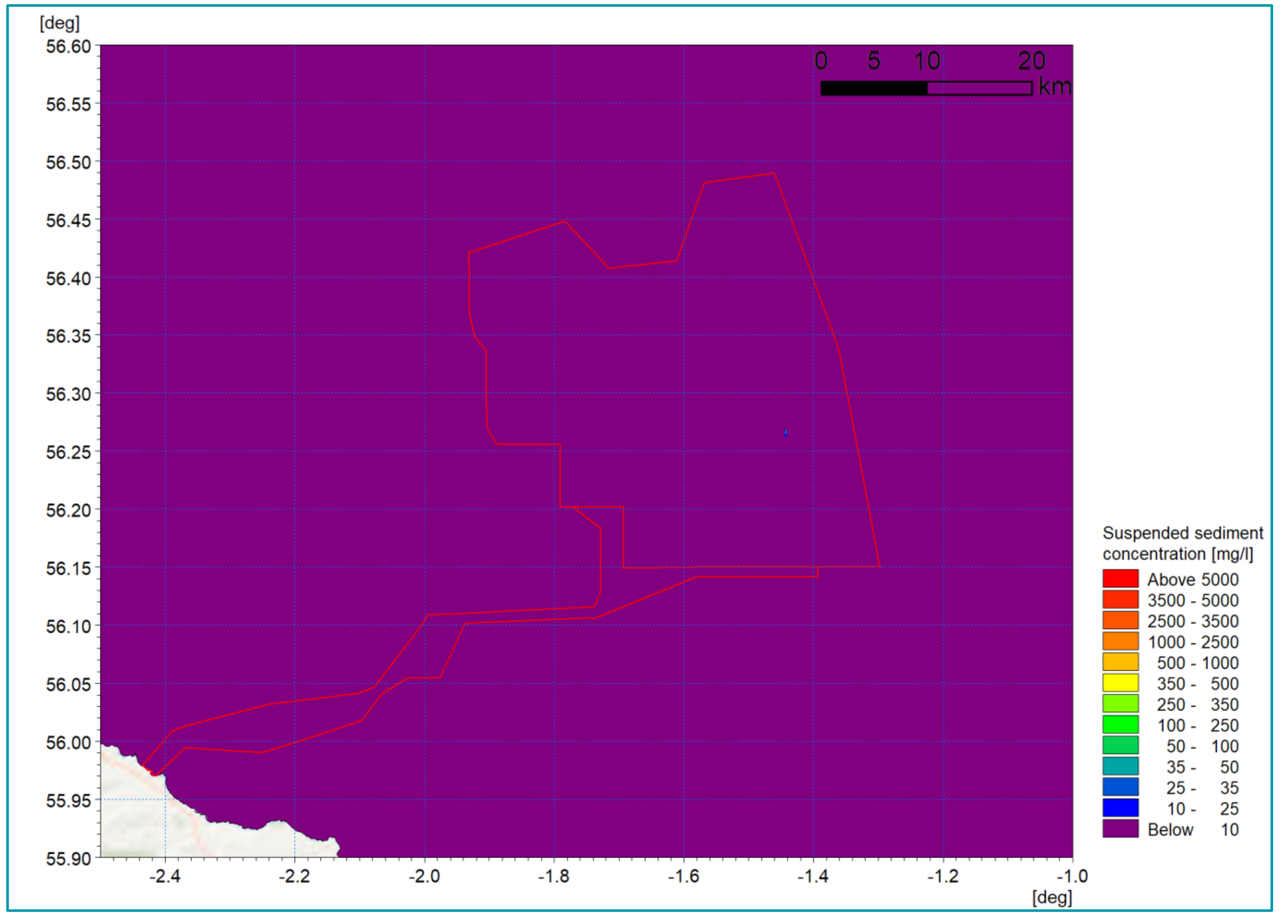


**Figure 6.9: Suspended Sediment Concentration During Dredging Phase – Inter-Array Cable Path**

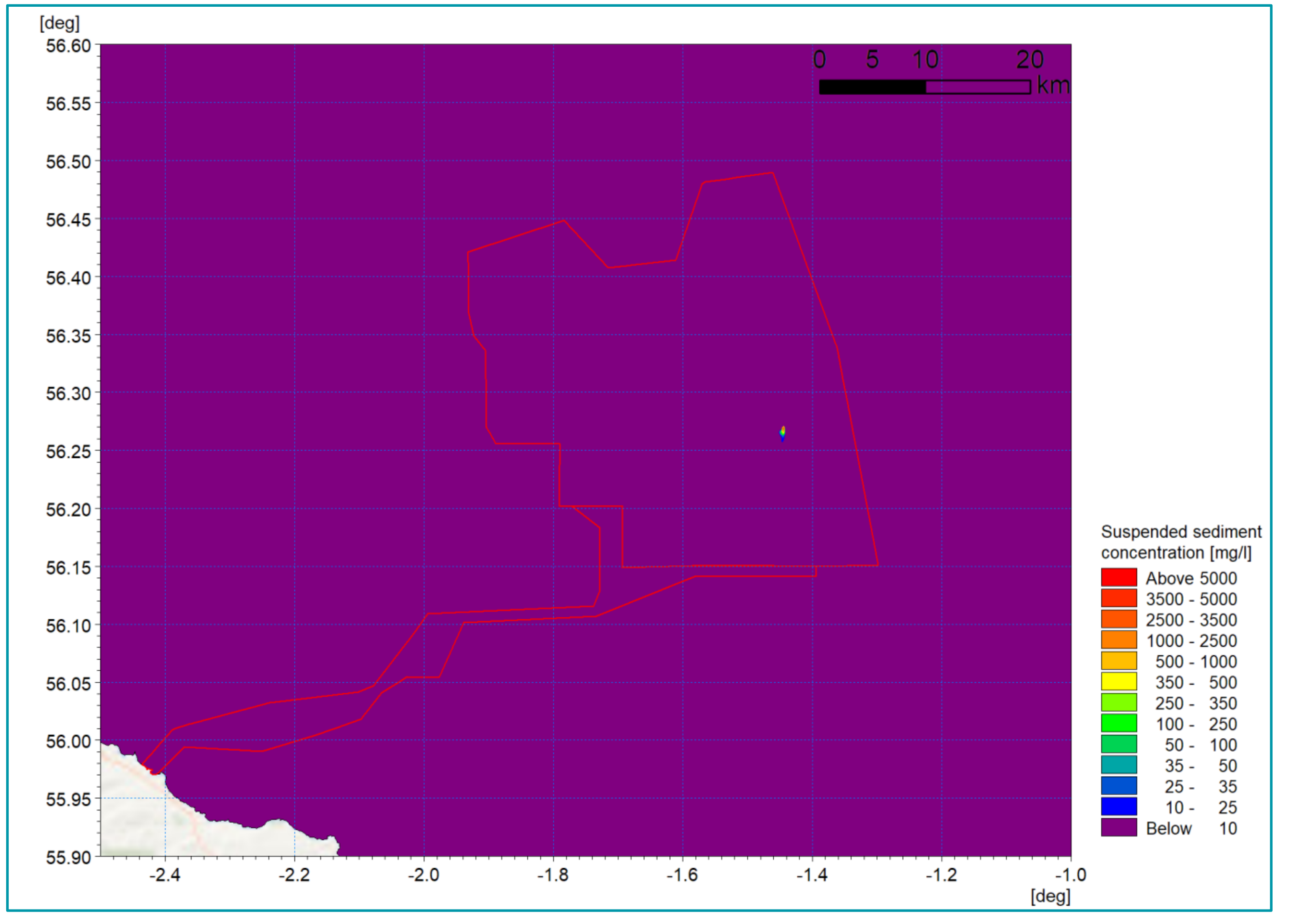


**Figure 6.10: Suspended Sediment Concentration During Disposal Phase– Inter-Array Cable Path**

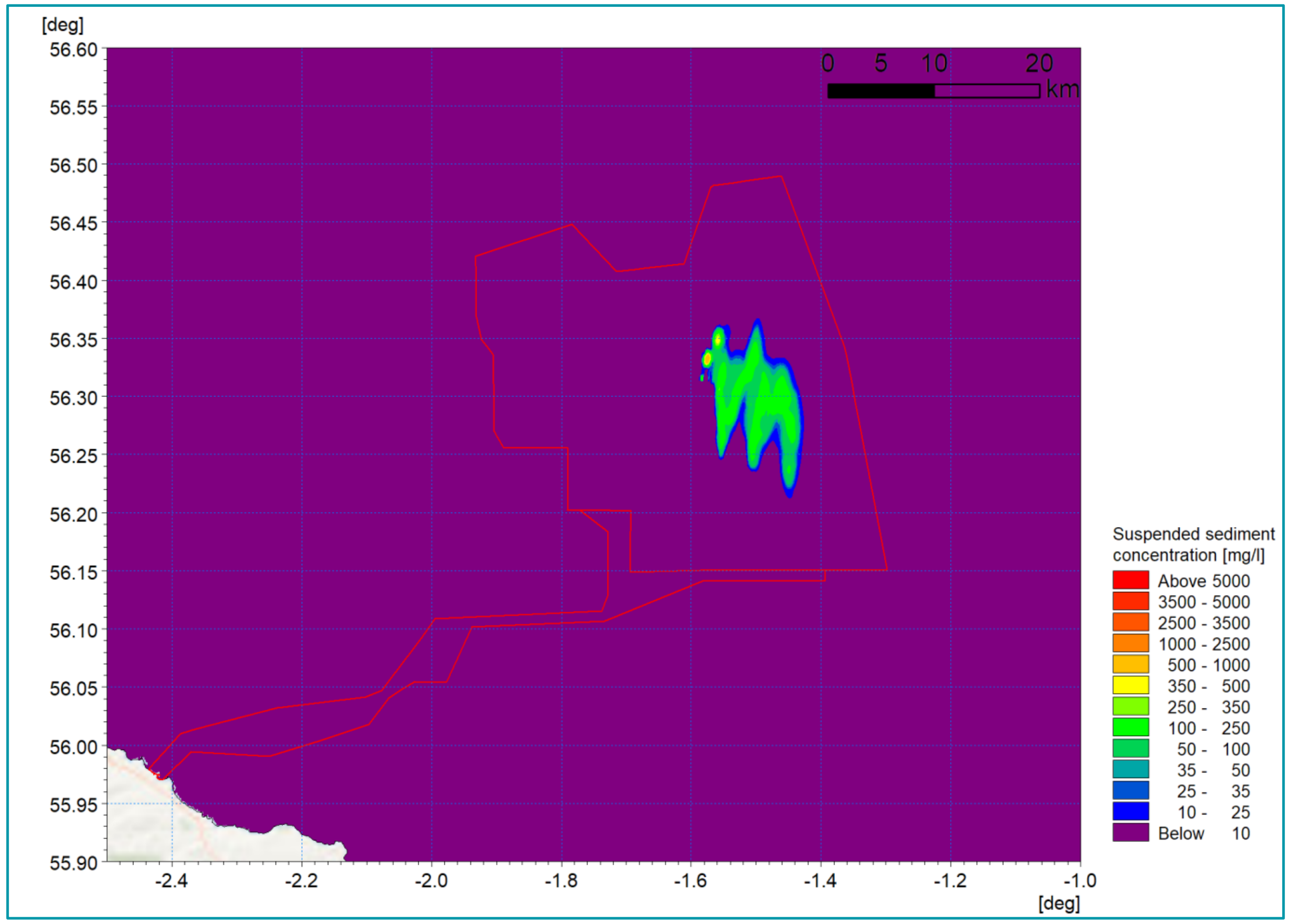


**Figure 6.11: Suspended Sediment Concentration with Sediment Re-Mobilisation – Inter-Array Cable Path**

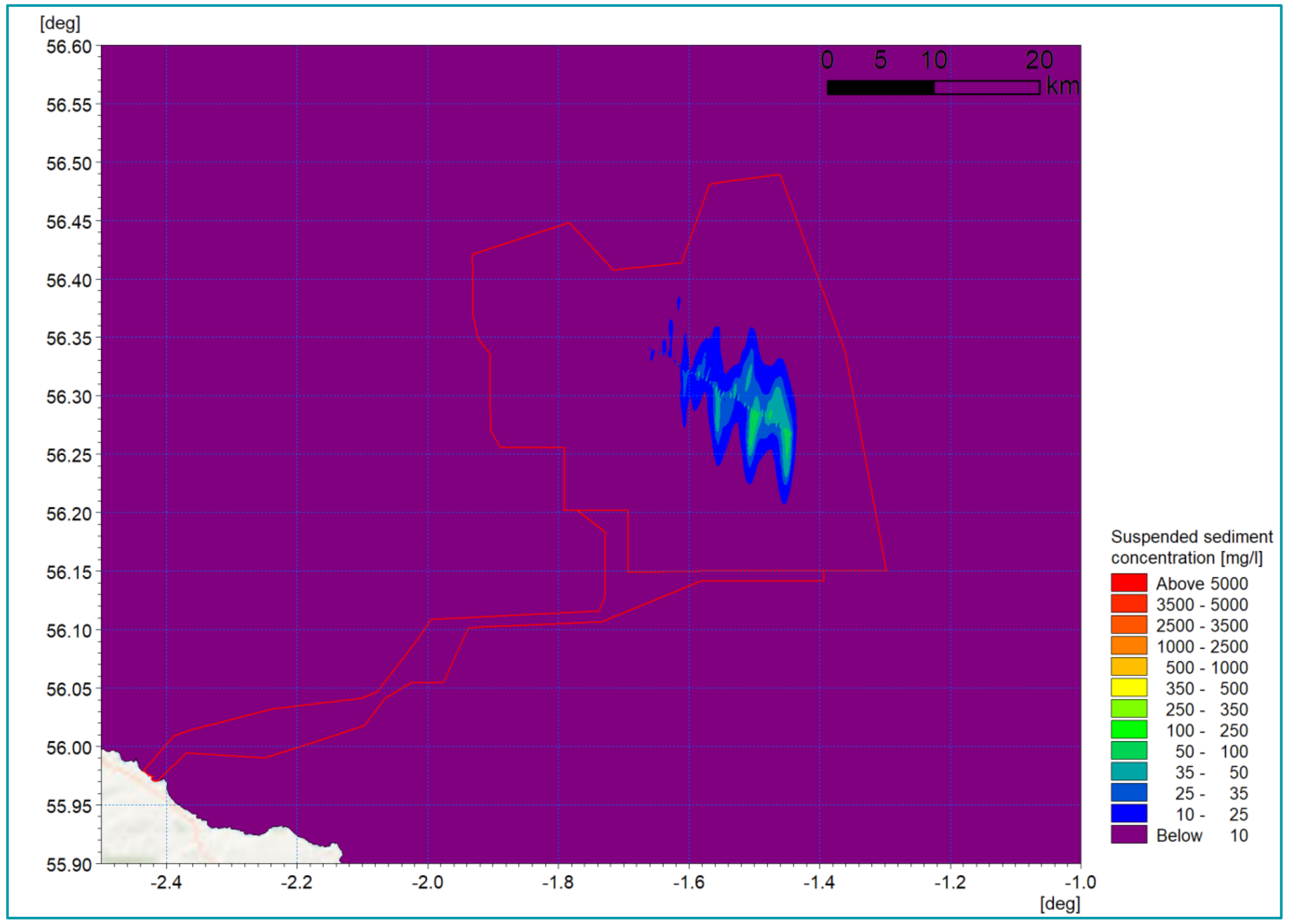


**Figure 6.12: Average Suspended Sediment Concentration During Dredge and Disposal Campaign – Inter-Array Cable Path**

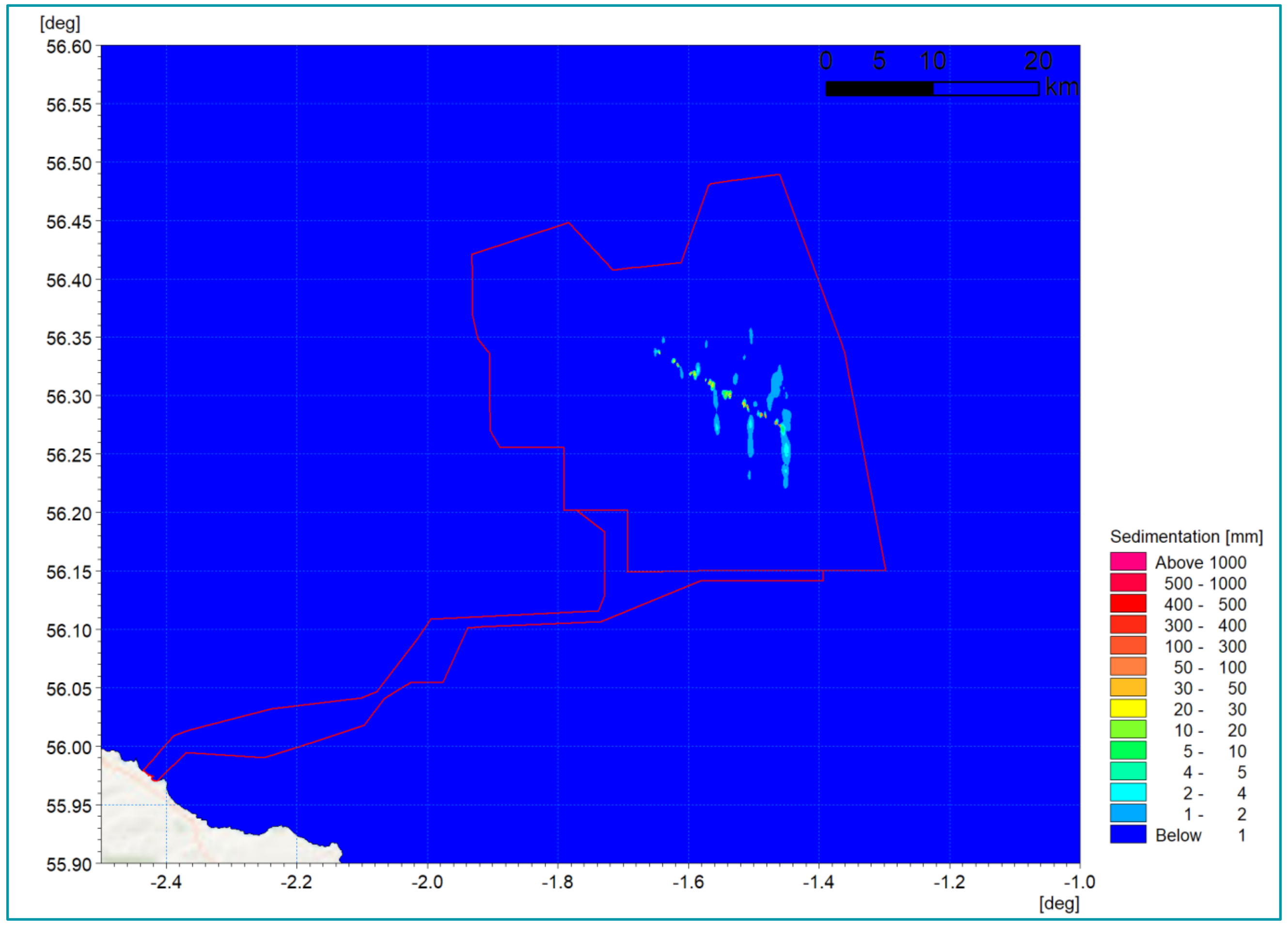


**Figure 6.13: Average Sedimentation During Dredge and Disposal Campaign – Inter-Array Cable Path**

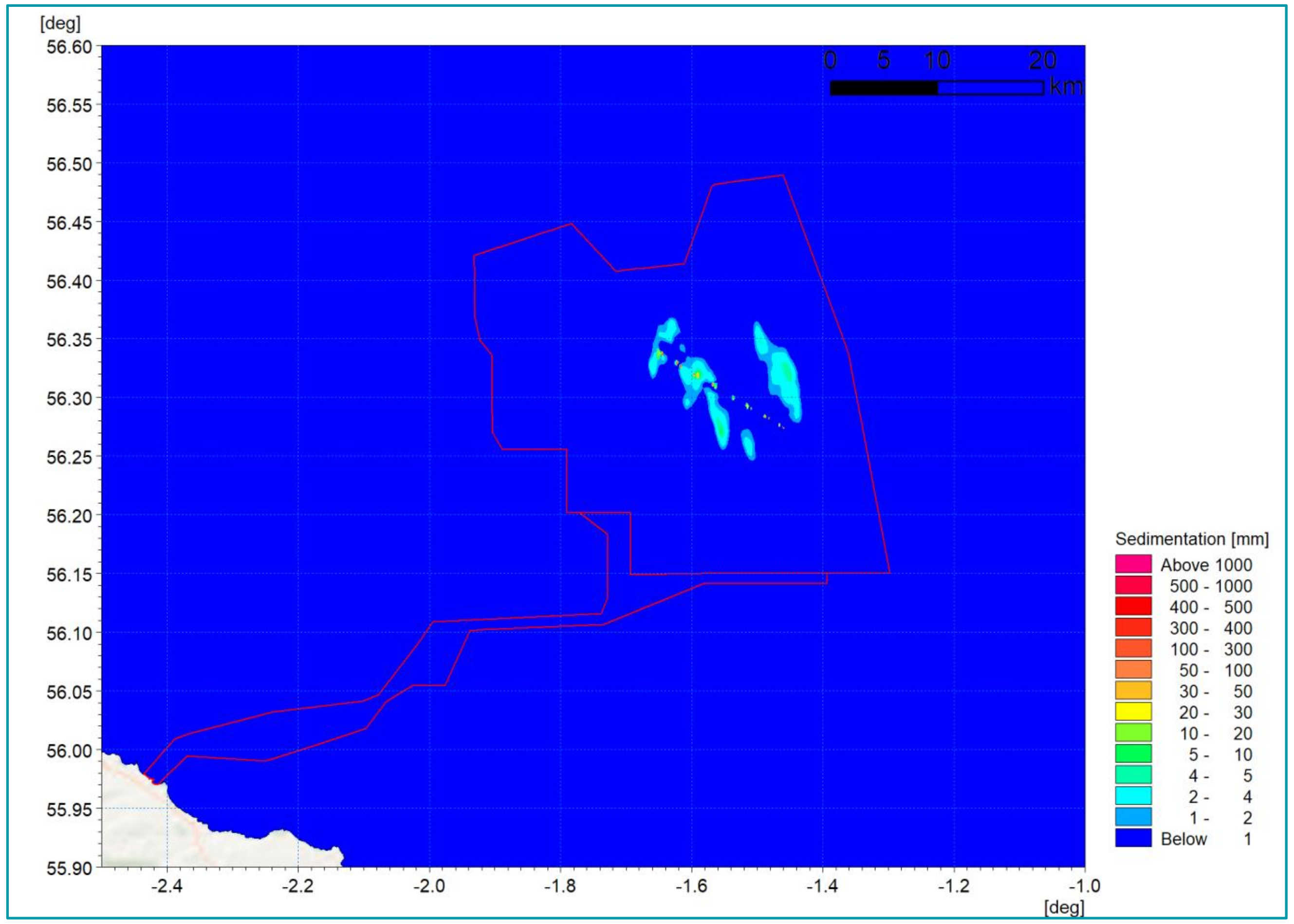


**Figure 6.14: Sedimentation One Day Following Cessation of Dredge and Disposal Campaign – Inter-Array Cable Path**

## 6.2. FOUNDATION INSTALLATION

87. The PDE presented in the project description outlined in volume 1, chapter 3 of the Offshore EIA Report includes two potential foundation types, piled and suction caissons foundations. The caissons were applied in the hydrographic assessments as they created the largest potential obstruction to tidal flow and sediment transport however the installation produces much less seabed disturbance than installation of piled foundations. Therefore, the piled structures were assessed in terms of potential increases in suspended sediment.

88. The largest potential release would be from augured (drilled) piles, where the material would be jetted and released to the water column as a plume. It is anticipated that 10% of piles across the site may require drilling of up to 20% of the pile depth. The modelling assumed that at each site the material which is released has a similar composition to the sampled sediment. In reality, to require drilling (rather than driving) the sediments are generally less granular and augured material would be less easily brought into suspension therefore the modelled scenario provides a conservative assessment in terms of suspended sediment concentration.

89. A sample of three representative pile installations were simulated to cover the range of conditions across the area both in terms of water depth, tidal currents and sediment grading; these locations are shown on an indicative layout in Figure 6.15. The sites were also selected in their proximity to the Firth of Forth Banks Complex MPA. The modelling was undertaken using the MIKE MT module which allows the modelling of erosion, transport and deposition of cohesive and cohesive/granular sediments. This model is suited to sediment releases in the water column and allows sediment sources which may vary spatially and temporally. In this case, the cohesive functions were not utilised as the material released comprised sand. The sediment grading was defined for each location and assumed two concurrent drilling operations located at separate legs of the same wind turbine location to provide the largest augmented sediment plume concentration.

90. At each location it was assumed that the auguring was required to the 16 m pile depth for an assumed 5.5 m diameter pile as a maximum design scenario (i.e. 380 $m^3$ per pile). The drilling rate was taken as 0.5 m/h which was both prescribed in the PDE and also allowed the release to cover the full range of tidal conditions (i.e. the auguring was undertaken continuously over a 32 hour period with material released throughout the water column).

91. For each location a set of results are presented. Firstly, the average suspended sediment plume during the course of the installation is shown. Due to the variation in suspended sediment levels, instantaneous plots of the sediment plumes are also presented during peak flood and ebb tides on each of the two days. It should be noted that all the plots require the use of a log scale to cover this range and provide clarity and during slack water SSC decrease to background levels.

92. The final set of plots relates to sedimentation. Due to the fine sandy nature of the material, it is clear that the sediment will be dispersed. It will be transported mid-tide, settle on slack water and be re-suspended and further dispersed on the resumption of tidal flow. For all three locations, sediment levels after the cessation of construction would not be discernible from the background sediments due to the limited magnitude of deposition and the similar nature of the material.

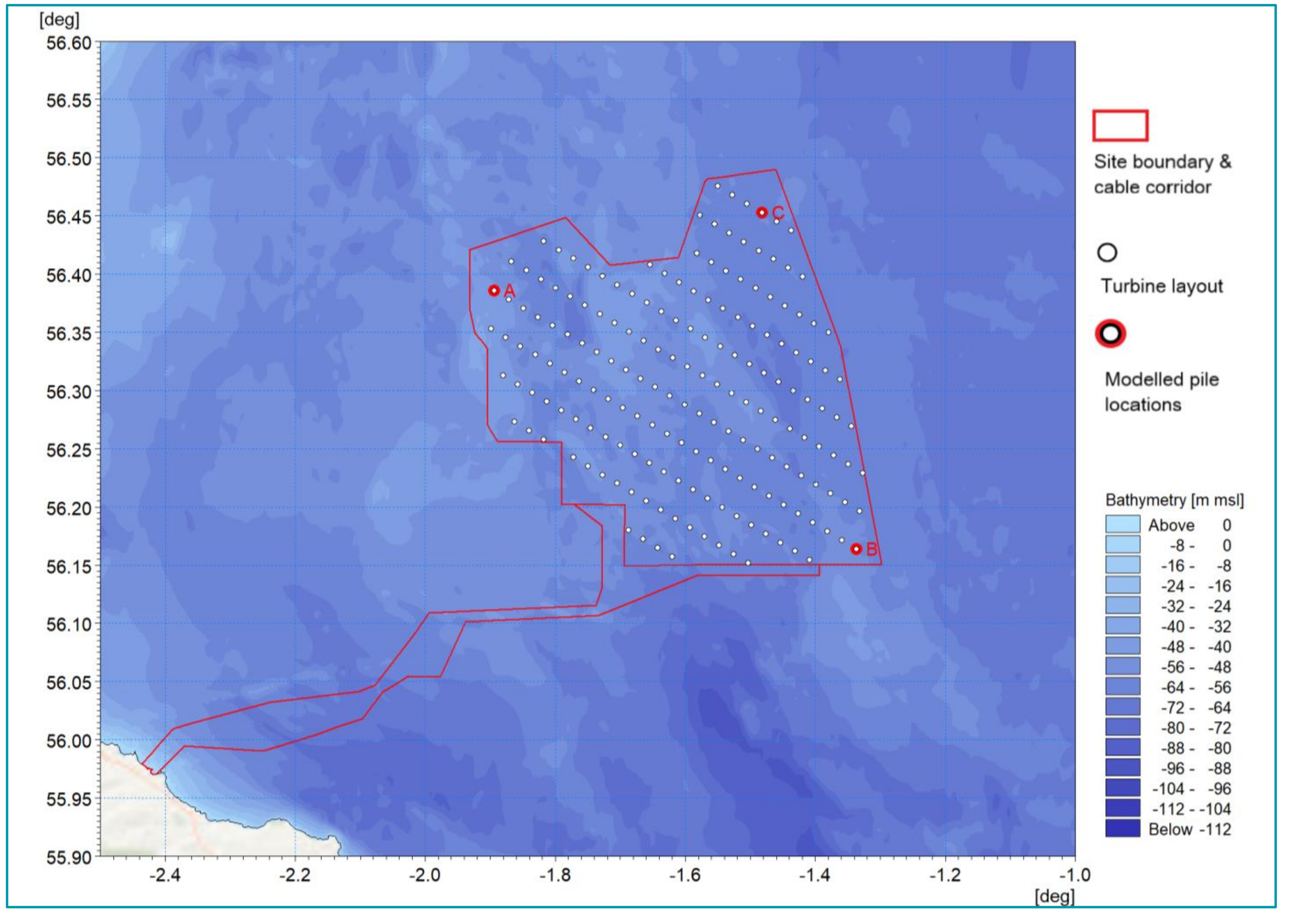


**Figure 6.15: Location of Modelled Piled Installations**

### 6.2.1. MODELLING LOCATION WIND TURBINE A

93. Wind turbine labelled A is located in the north-west of the Proposed Development array area within the Marr Banks with the following sediment composition derived from the seabed sample data.

- coarse sand: 3%;
- medium sand: 17%;
- fine sand: 66%; and
- very fine sand: 14%.

94. This location is sited between the Marr Banks at a relatively shallow point where current speeds are at their highest across the Proposed Development array area and, as a result, there is good dispersion potential. This is demonstrated in the average suspended sediment plot shown in Figure 6.16, where concentrations are <1 mg/l away from the immediate vicinity of the two discharge locations. The following figures illustrate this further; Figure 6.17 and Figure 6.18 show the instantaneous concentrations on the first auguring for peak flood and ebb tides respectively whilst, Figure 6.19 and Figure 6.20 show the instantaneous concentrations on the second day. In each case the plume related directly to the sediment releases is <5 mg/l and this drops to single figures within a very short distance, typically less than 500 m. Again, a log scale was required to illustrate low level of SSC. Some small areas of increased suspended sediment can be seen where material has been deposited on slack tides and subsequently re-suspended.

95. The sedimentation plots, shown in Figure 6.21 and Figure 6.22, present the average sedimentation and sedimentation one day following cessation of the works respectively. These demonstrate the dispersive nature of the site, dispersing material the full extent of the tidal excursion, and even using a very small contour interval this settlement would be imperceptible from the background sediment transport activity with plotted sediment depths less than typical grain diameters.

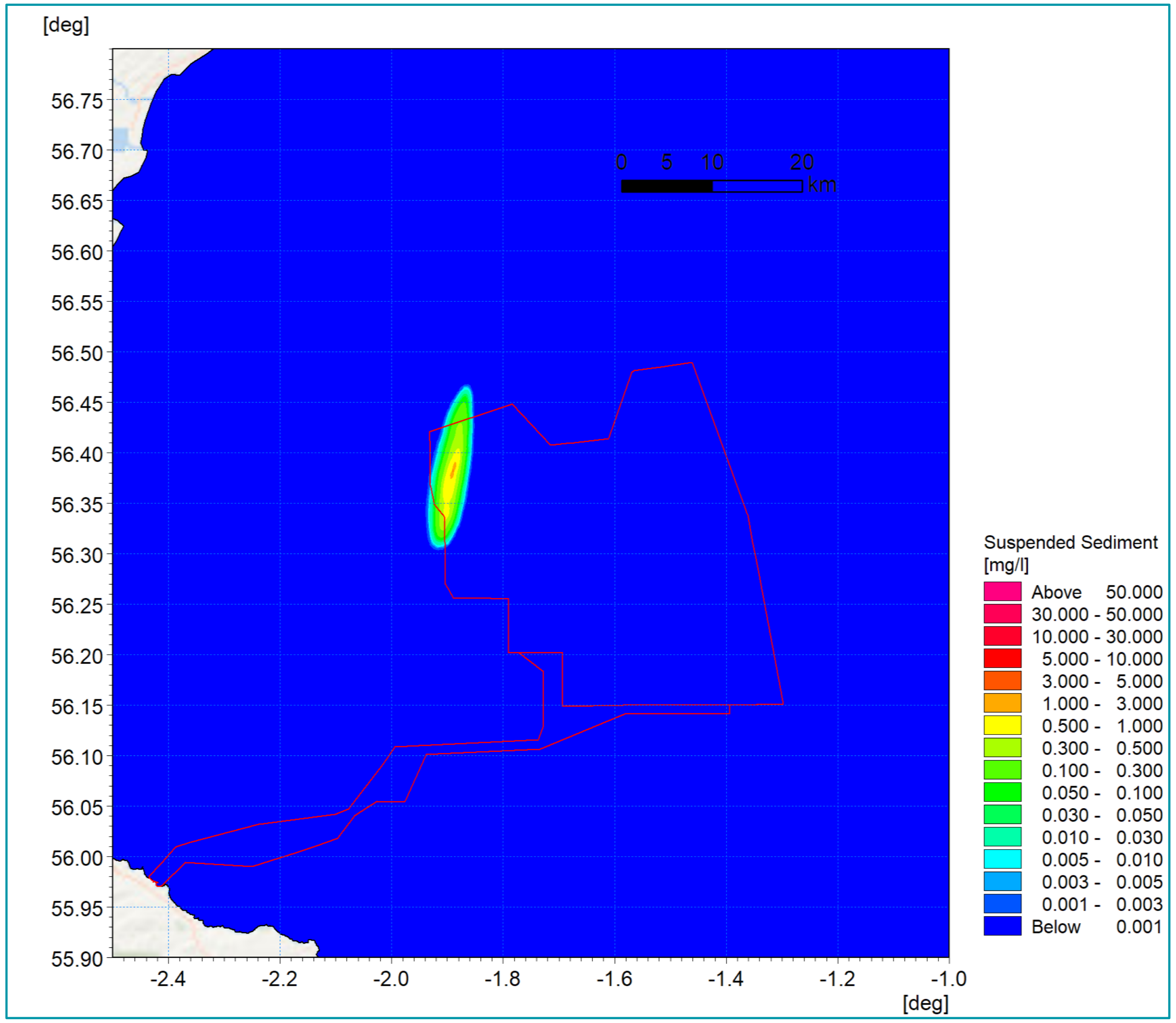


**Figure 6.16: Average Suspended Sediment Concentration – Pile Installation Wind Turbine A**

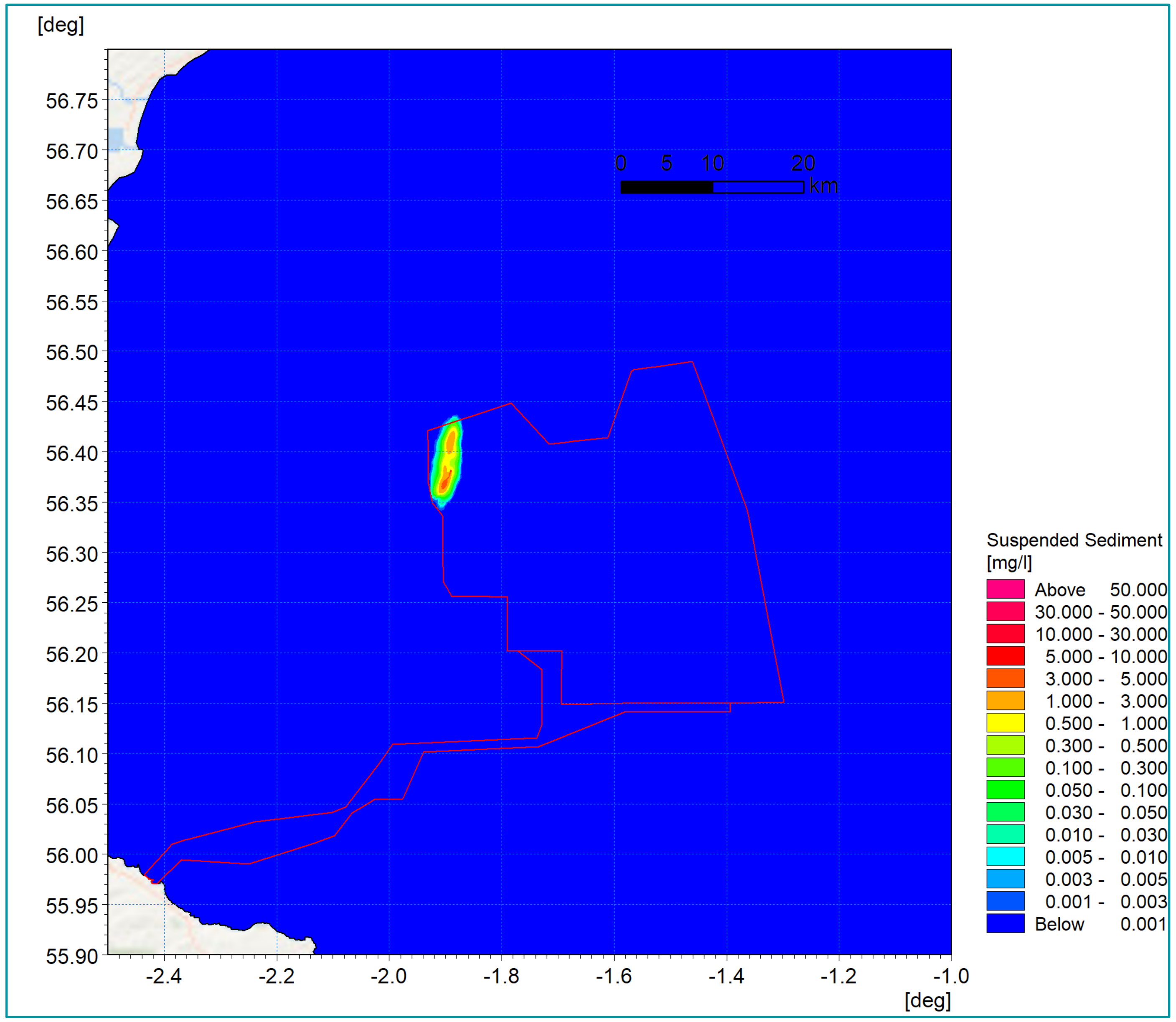


**Figure 6.17: Suspended Sediment Concentration Day One Peak Flood - Pile Installation Wind Turbine A**

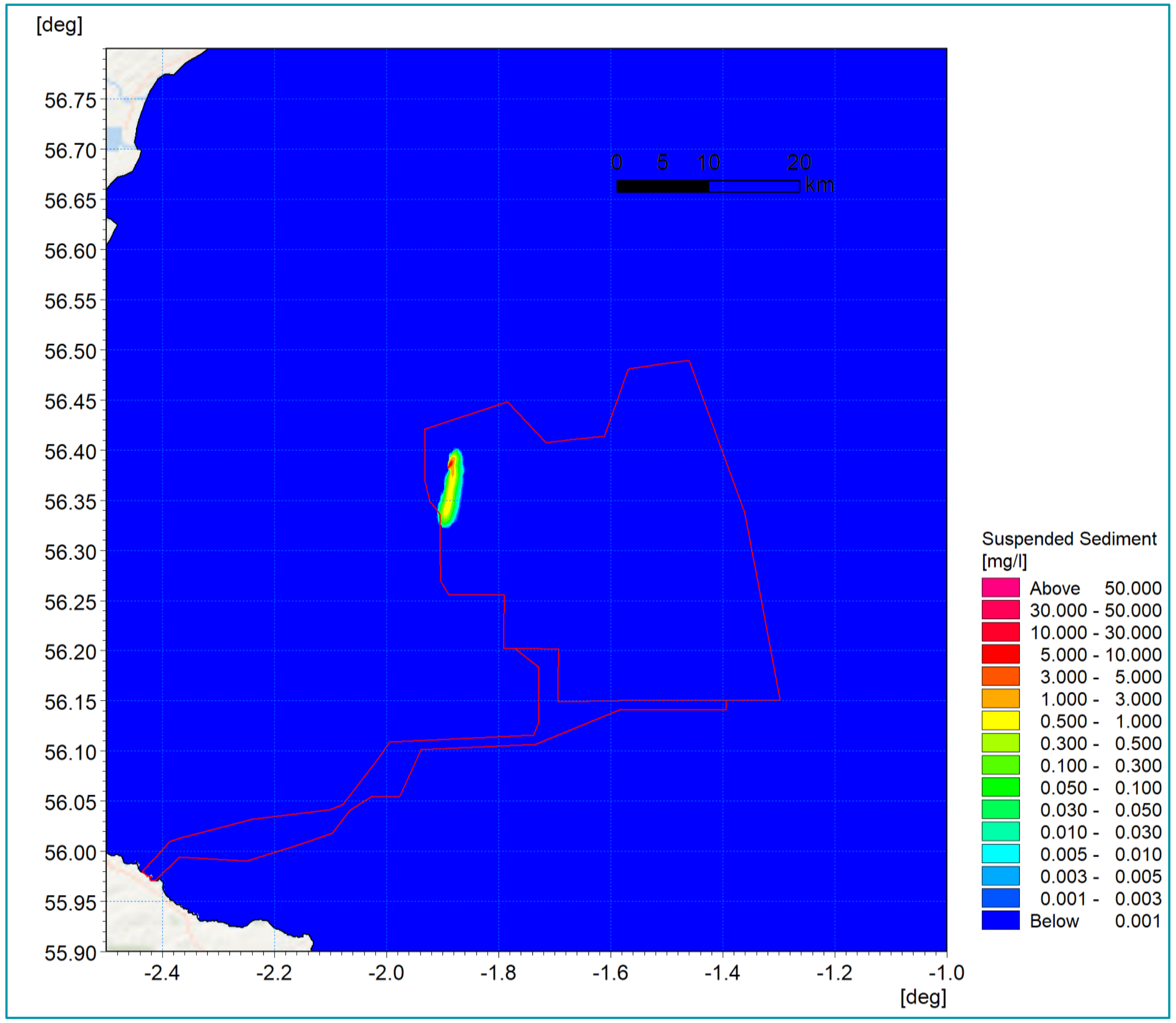


**Figure 6.18: Suspended Sediment Concentration Day One Peak Ebb - Pile Installation Wind Turbine A**

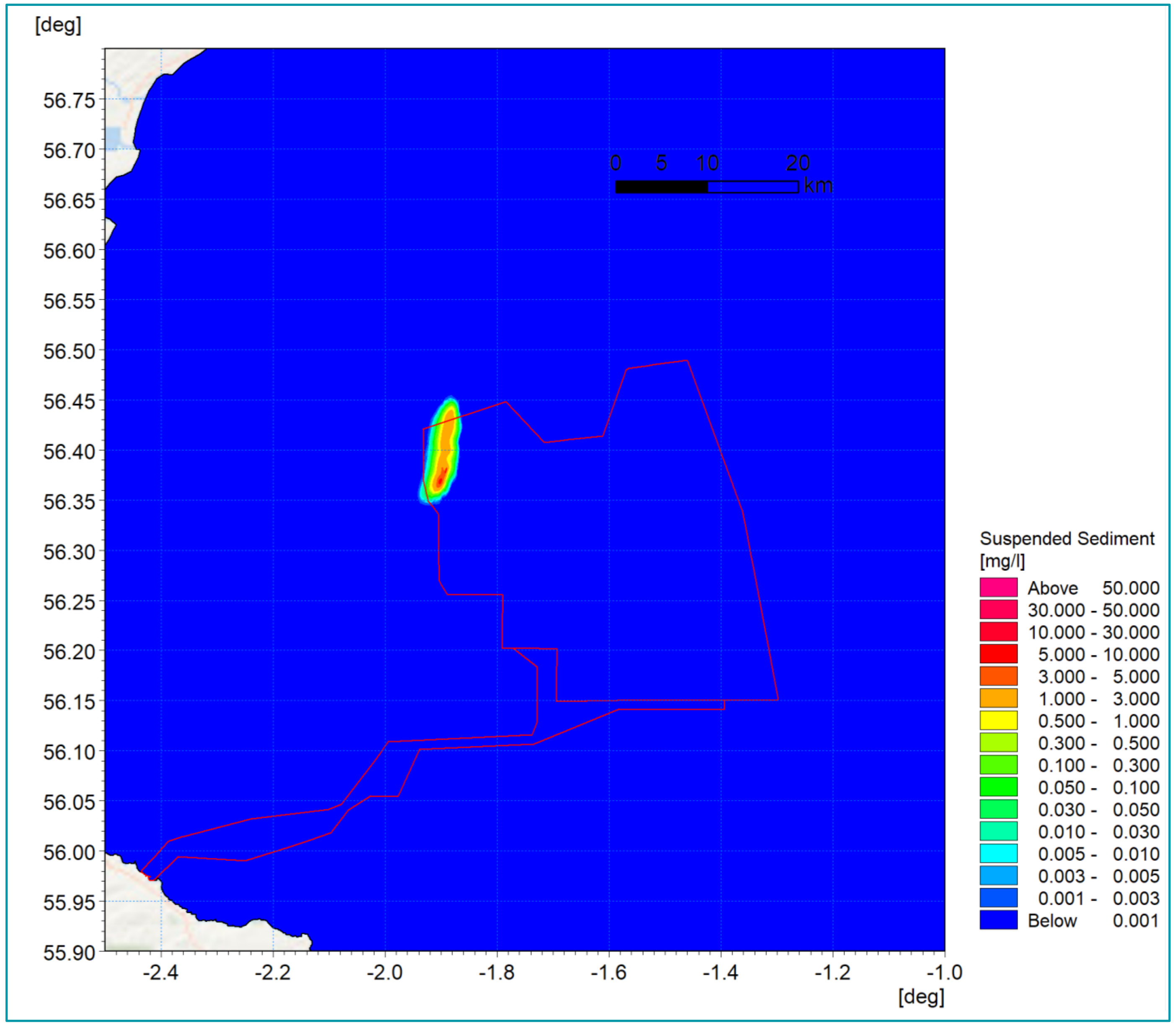


**Figure 6.19: Suspended Sediment Concentration Day Two Peak Flood - Pile Installation Wind Turbine A**

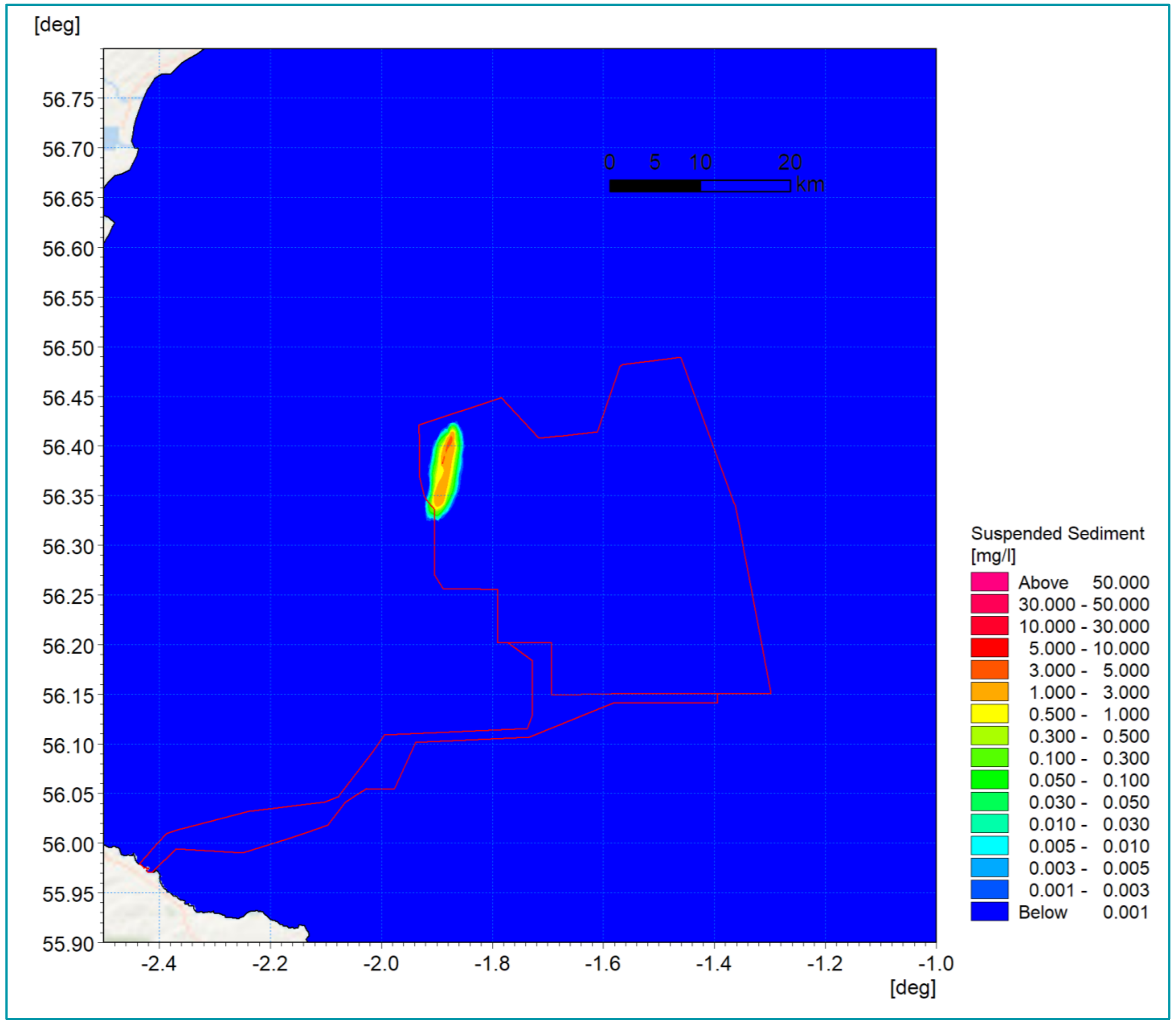


**Figure 6.20: Suspended Sediment Concentration Day Two Peak Ebb - Pile Installation Wind Turbine A**

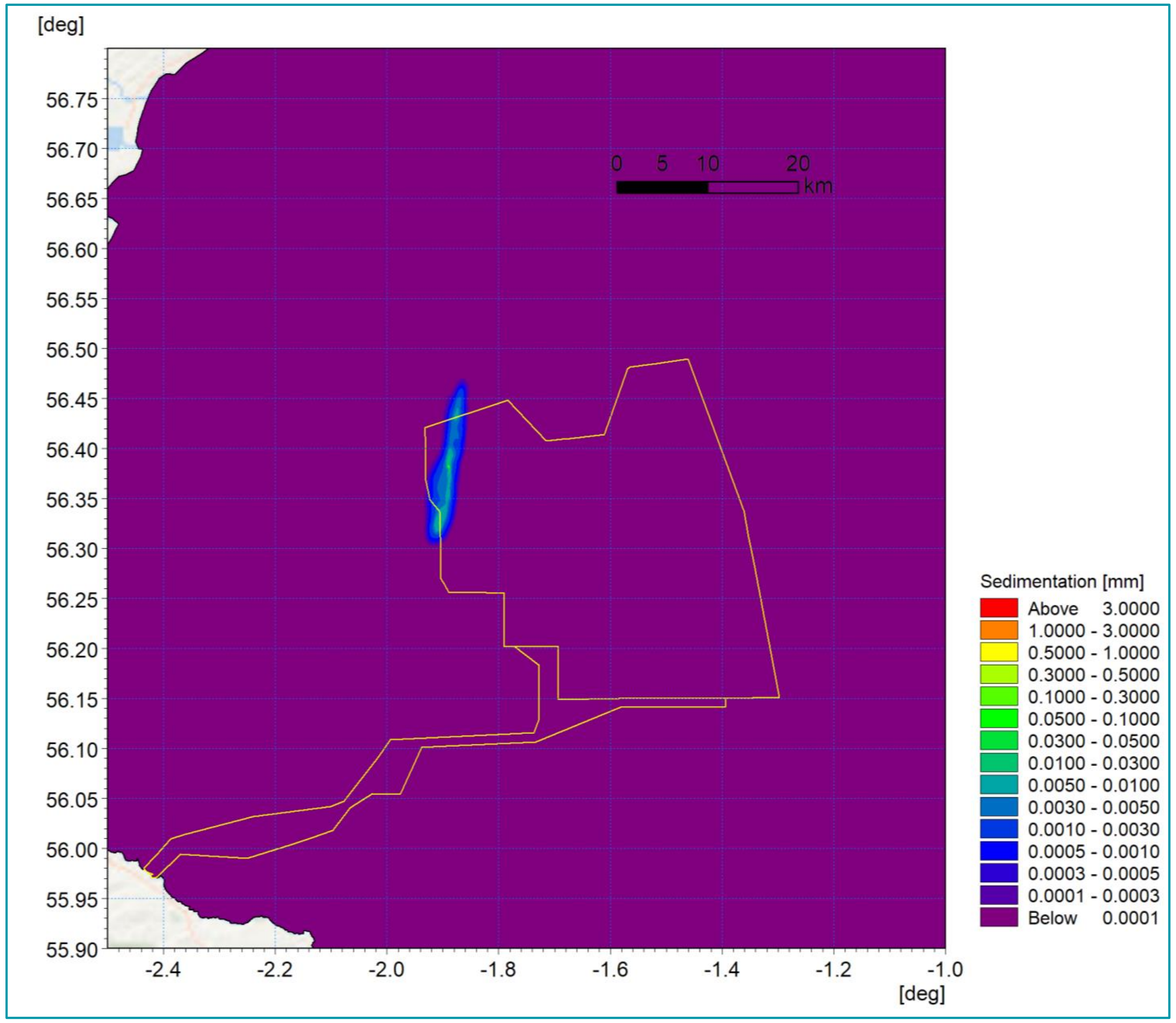


**Figure 6.21: Average Sedimentation During Pile Installation - Wind Turbine A**

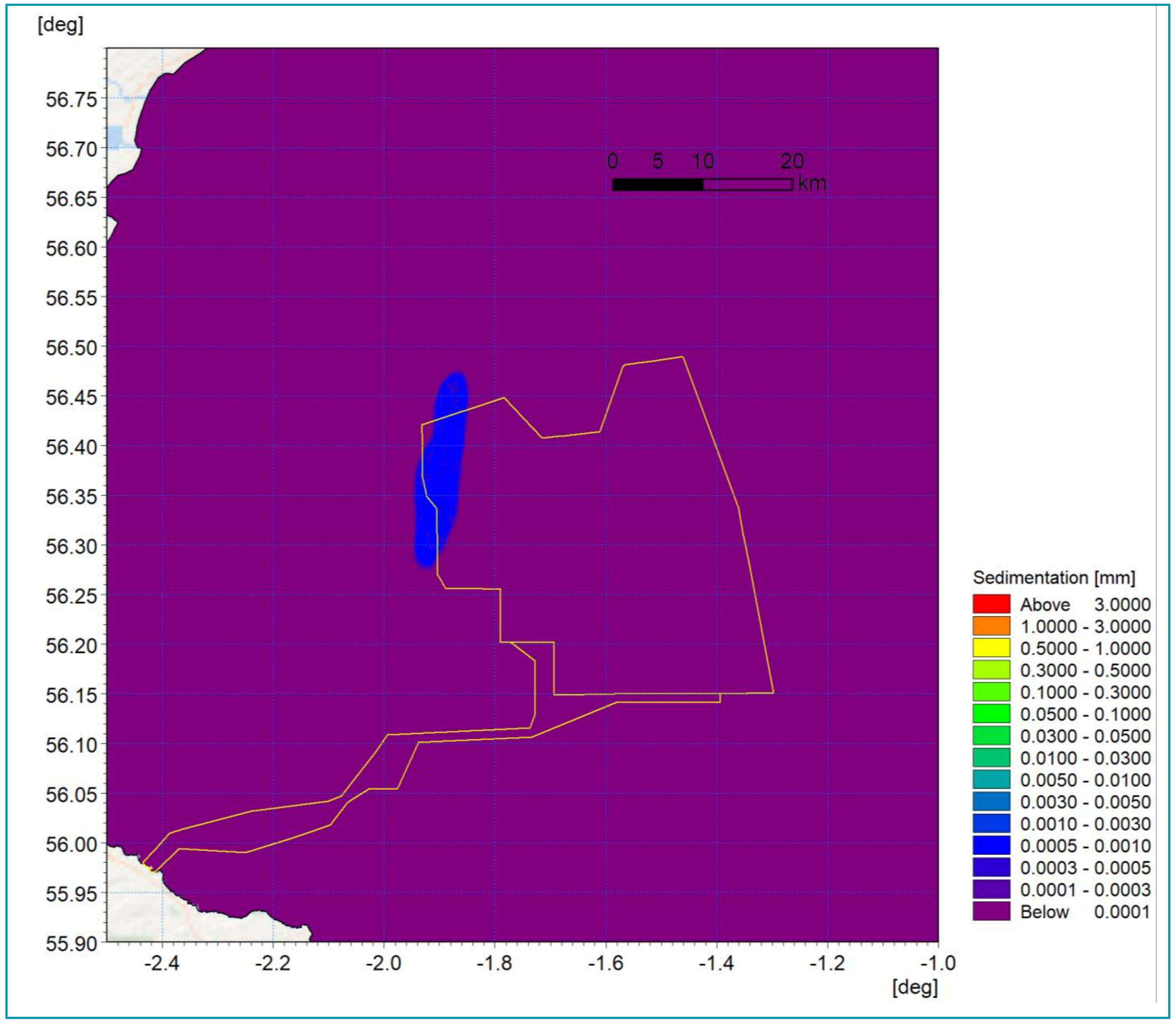


**Figure 6.22: Sedimentation One Day Following Cessation of Pile Installation - Wind Turbine A**

### 6.2.2. MODELLING LOCATION WIND TURBINE B

96. Wind turbine labelled B is located in the south-east of the Proposed Development array area on Berwick Bank with the following composition.

- very coarse sand: 6%;
- coarse sand: 10%;
- medium sand: 45%; and
- fine sand: 39%.

97. This location exhibits slightly coarser graded material and current speeds are slightly lower when compared to the site of wind turbine A previously examined. As anticipated the average suspended sediment plot shown in Figure 6.23, indicates a slightly smaller plume envelope however concentrations remain <1 mg/l a short distance, circa 400 m, from the two discharge locations. Figure 6.24 to Figure 6.27 illustrate the instantaneous concentrations on the peak flood and ebb tides on each day of the drilling. As with wind turbine A, areas of increased suspended sediment are evident where material has been deposited on slack tide and subsequently re-suspended. Typically, the plume concentration is <5 mg/l, and reduces with the distance from the site as the sediment is dispersed.

98. Figure 6.28 and Figure 6.29 show the average sedimentation and sedimentation one day following cessation of the drilling operation. In line with the slightly coarser material and lower current speeds the footprint is marginally smaller than site A however sedimentation levels remain very small due to the limited volume of material released.

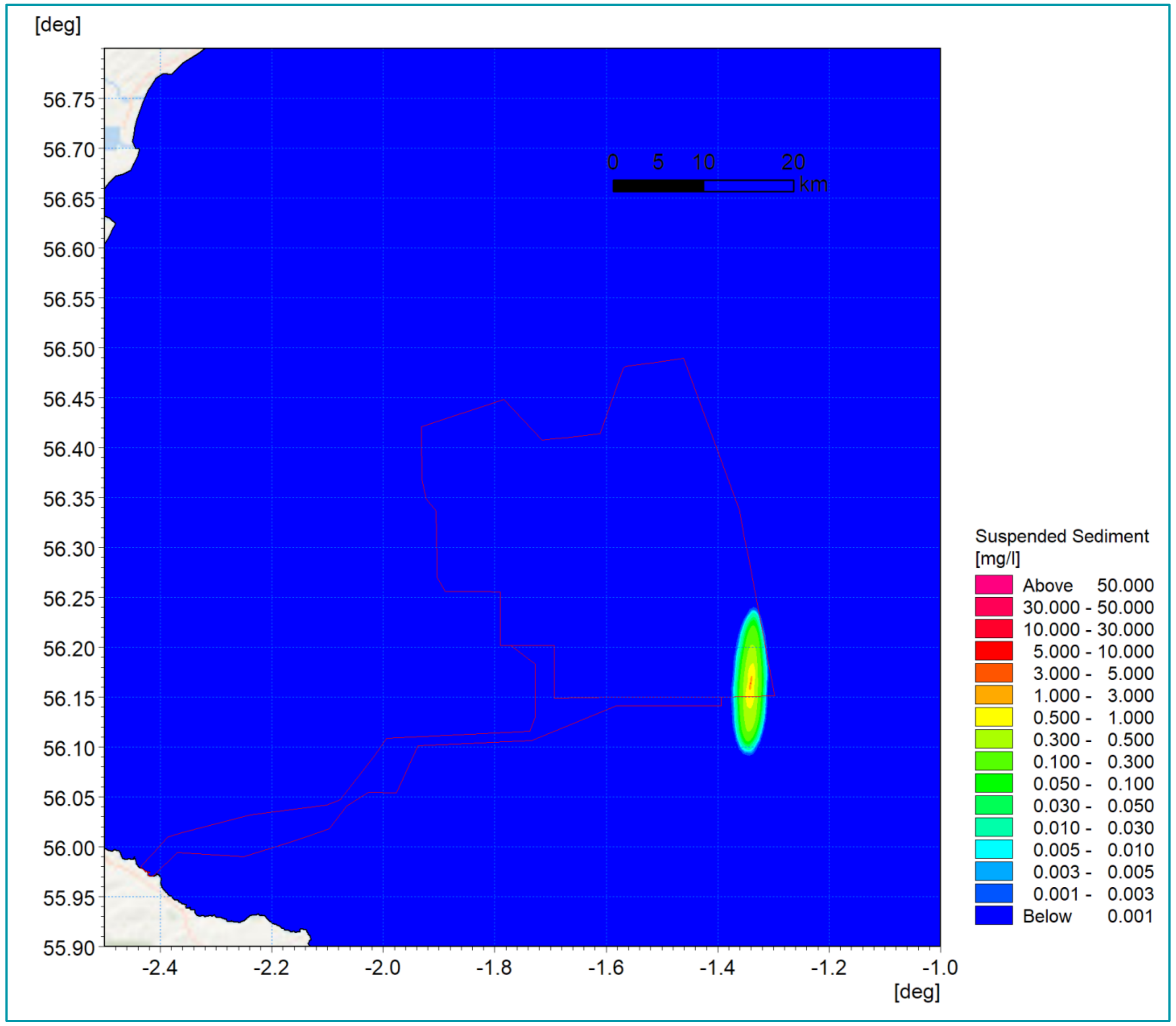


**Figure 6.23: Average Suspended Sediment Concentration – Pile Installation Wind Turbine B**

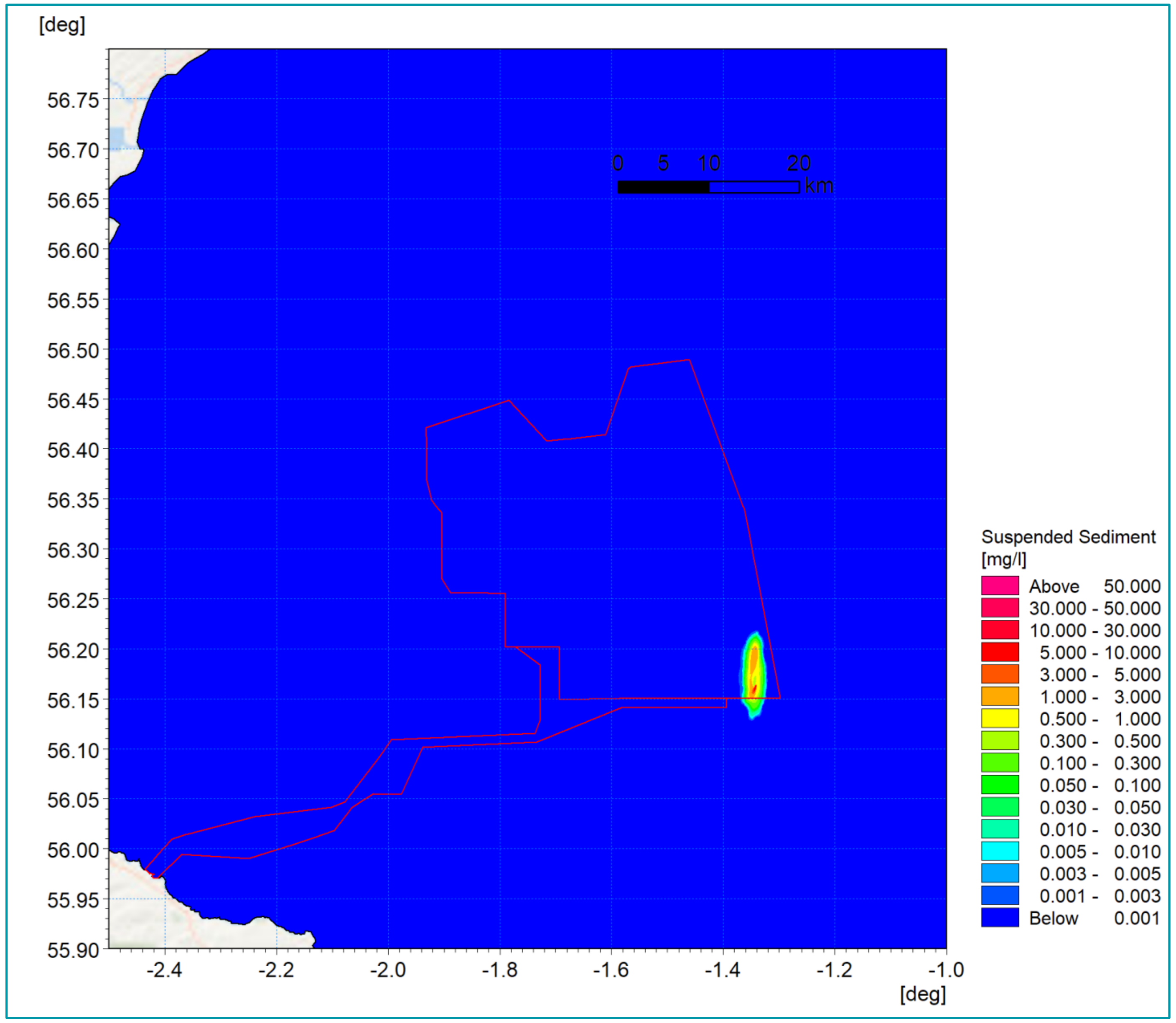


**Figure 6.24: Suspended Sediment Concentration Day One Peak Flood - Pile Installation Wind Turbine B**

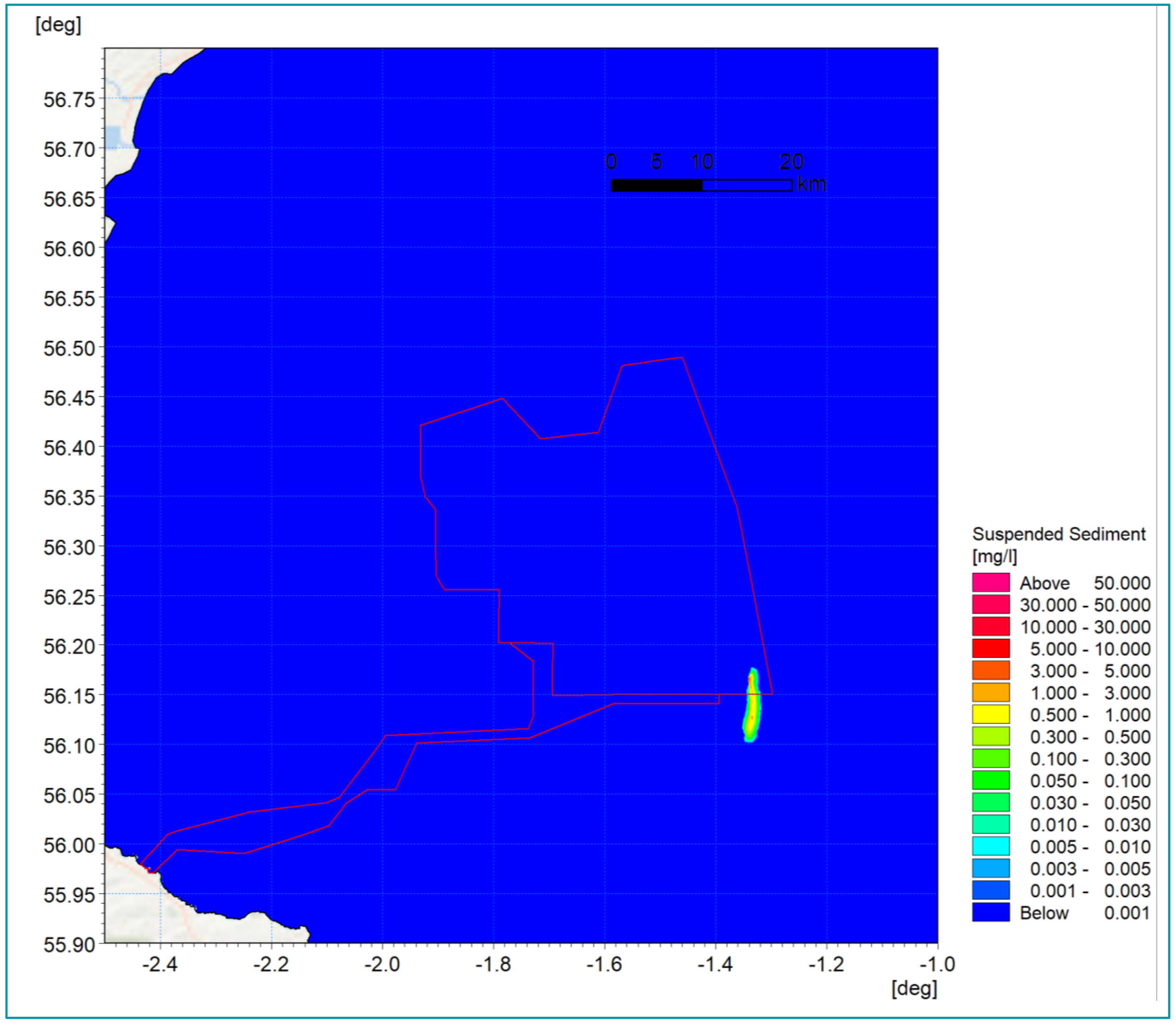


**Figure 6.25: Suspended Sediment Concentration Day One Peak Ebb - Pile Installation Wind Turbine B**

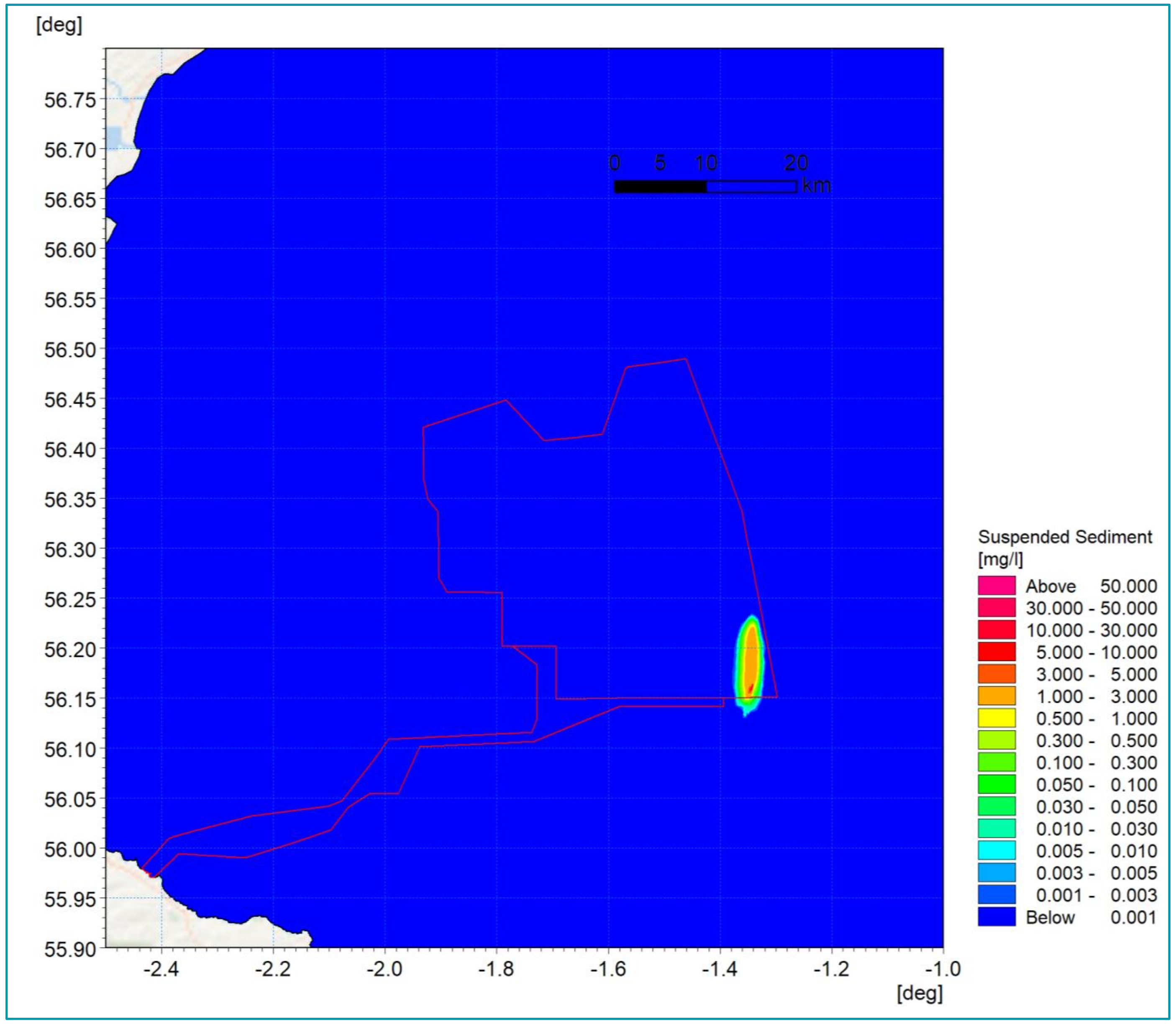


**Figure 6.26: Suspended Sediment Concentration Day Two Peak Flood - Pile Installation Wind Turbine B**

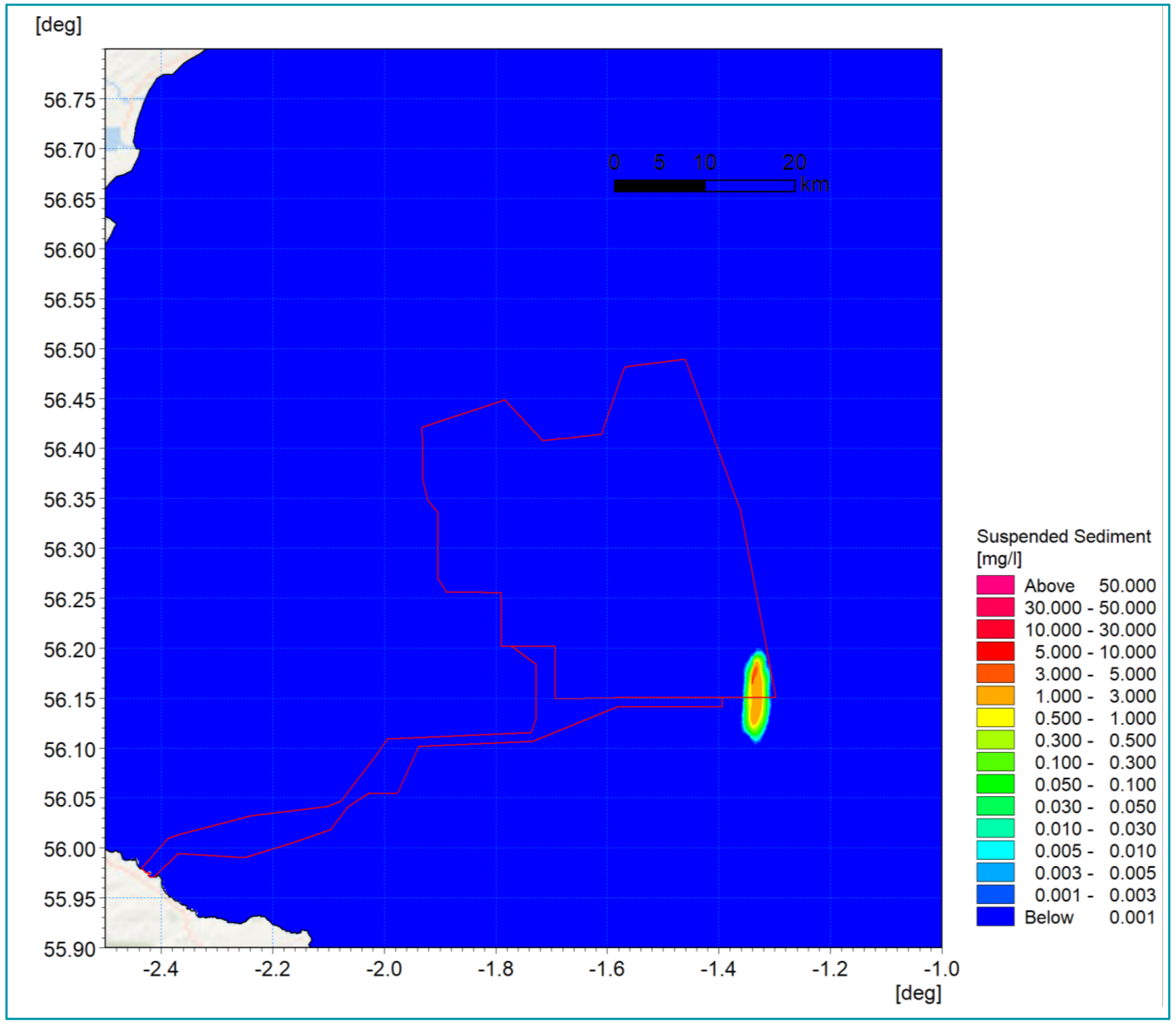


**Figure 6.27: Suspended Sediment Concentration Day Two Peak Ebb - Pile Installation Wind Turbine B**

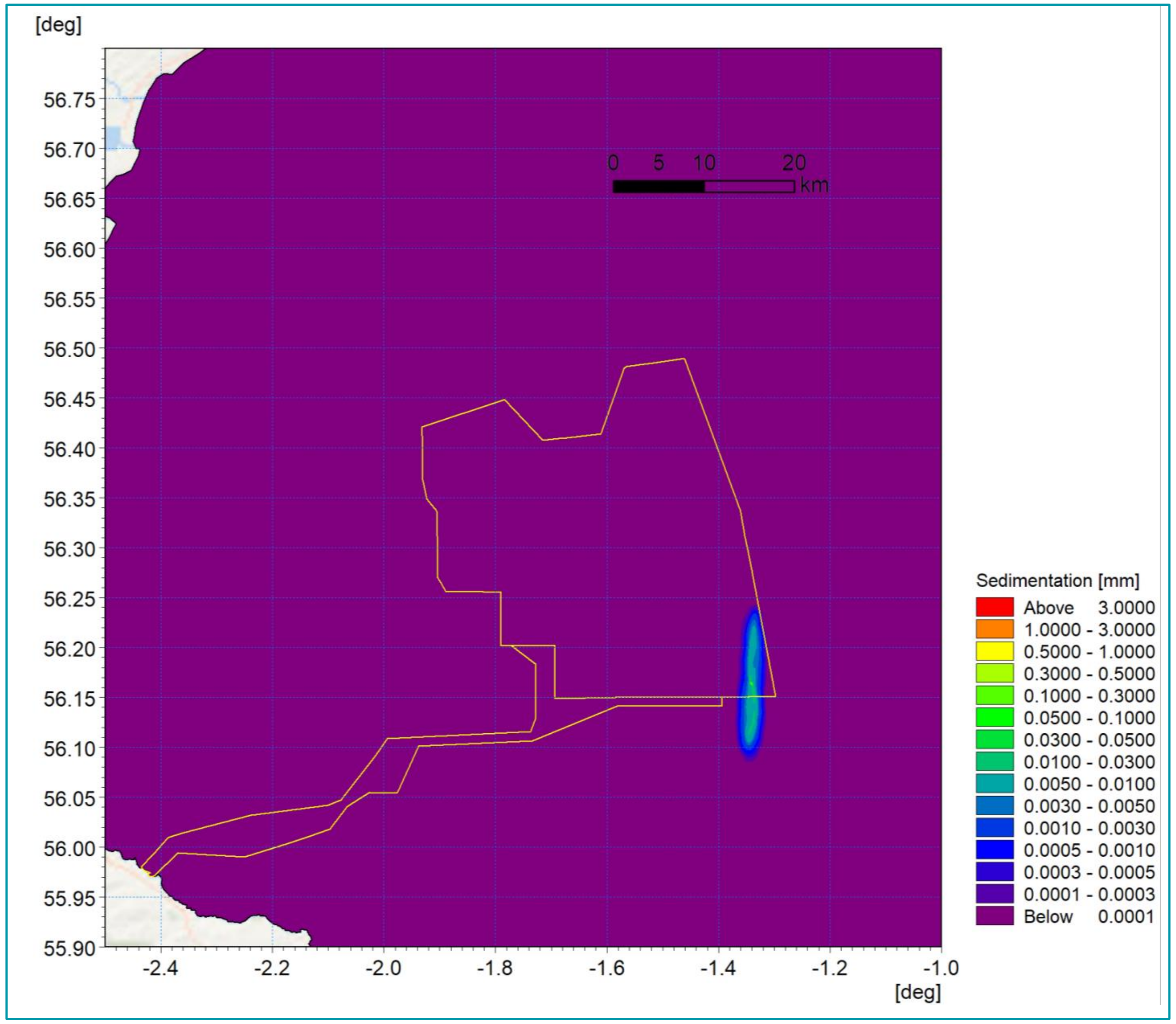


**Figure 6.28: Average Sedimentation During Pile Installation - Wind Turbine B**

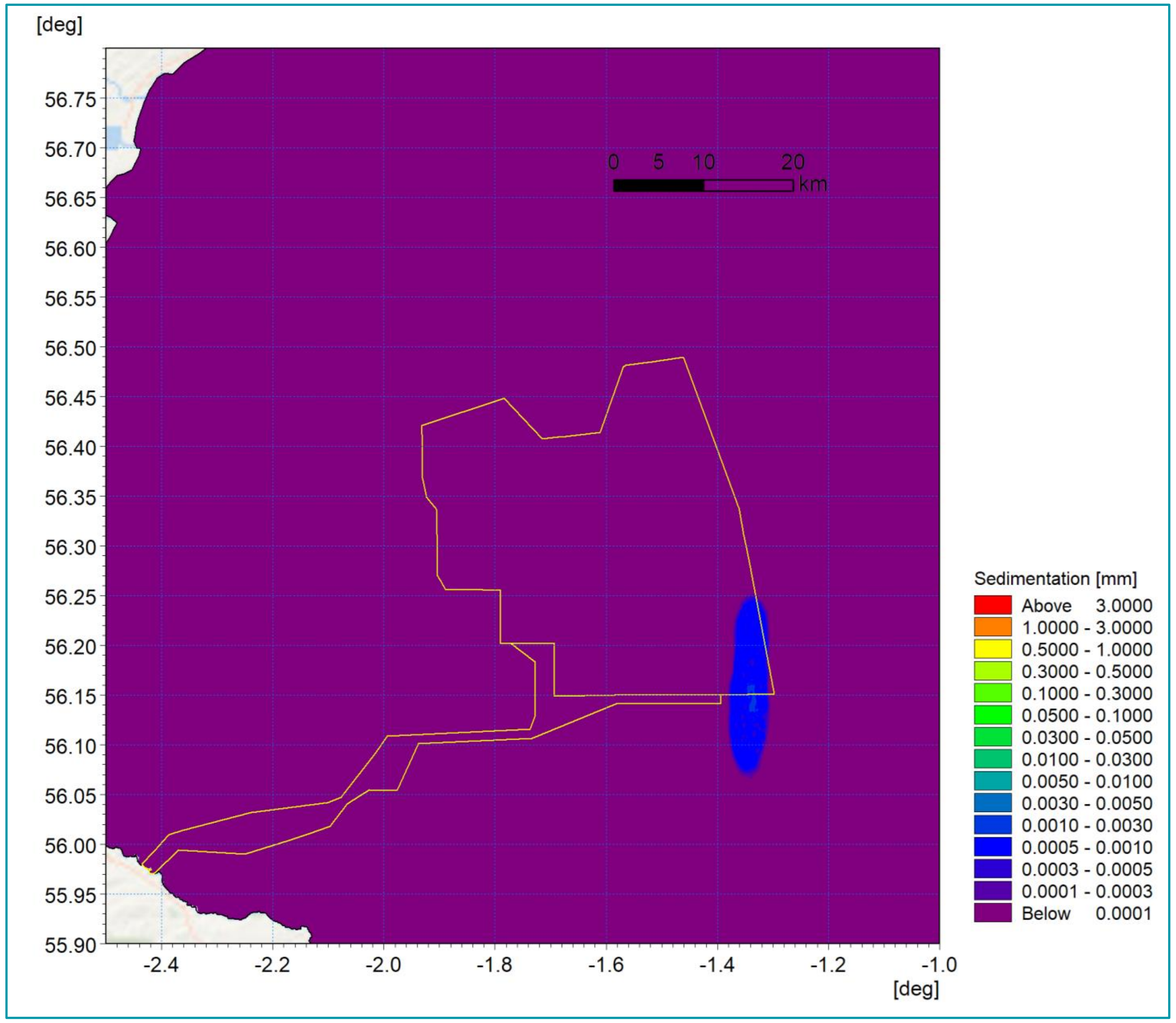


**Figure 6.29: Sedimentation One Day Following Cessation of Pile Installation - Wind Turbine B**

### 6.2.3. MODELLING LOCATION WIND TURBINE C

99. Wind turbine labelled C is located in the north-east of the Proposed Development array area south of Montrose Bank with the following composition.

- very coarse sand: 17%;
- coarse sand: 10%;
- medium sand: 28%; and
- fine sand: 45%.

100. This site was selected due to the proximity to Montrose Bank in the MPA close to the extent of the Proposed Development. The sediment composition and tidal flows are similar to site A and therefore the plume extent and subsequent footprint are of a similar scale and form. This is demonstrated in the average suspended sediment plot shown in Figure 6.30 and instantaneous figures Figure 6.31 to Figure 6.34, where peak concentrations are <5 mg/l and average values are typically less than one fifth of this. At this location the transport cycle is also evident with material settling out on slack tides and re-suspended with increasing current speeds.

101. The average sedimentation shown in Figure 6.35 also indicates this transport cycle with the material being dispersed further following the end of the operation as illustrated in Figure 6.36. The resulting sedimentation depths are <0.001 mm from the two drilling operations and demonstrates that this settlement would be imperceptible from the background sediment transport activity.

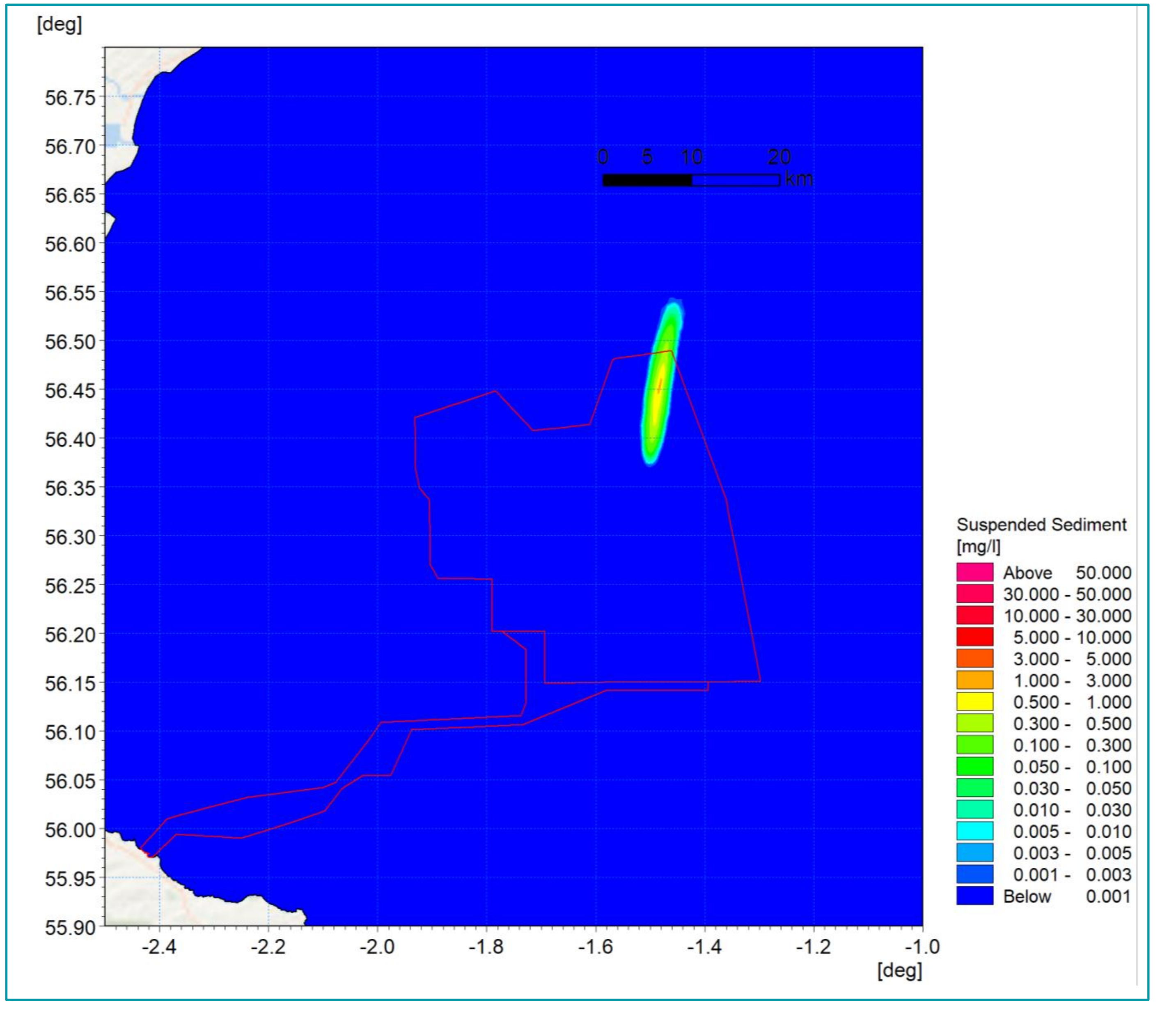


**Figure 6.30: Average Suspended Sediment Concentration – Pile Installation Wind Turbine C**

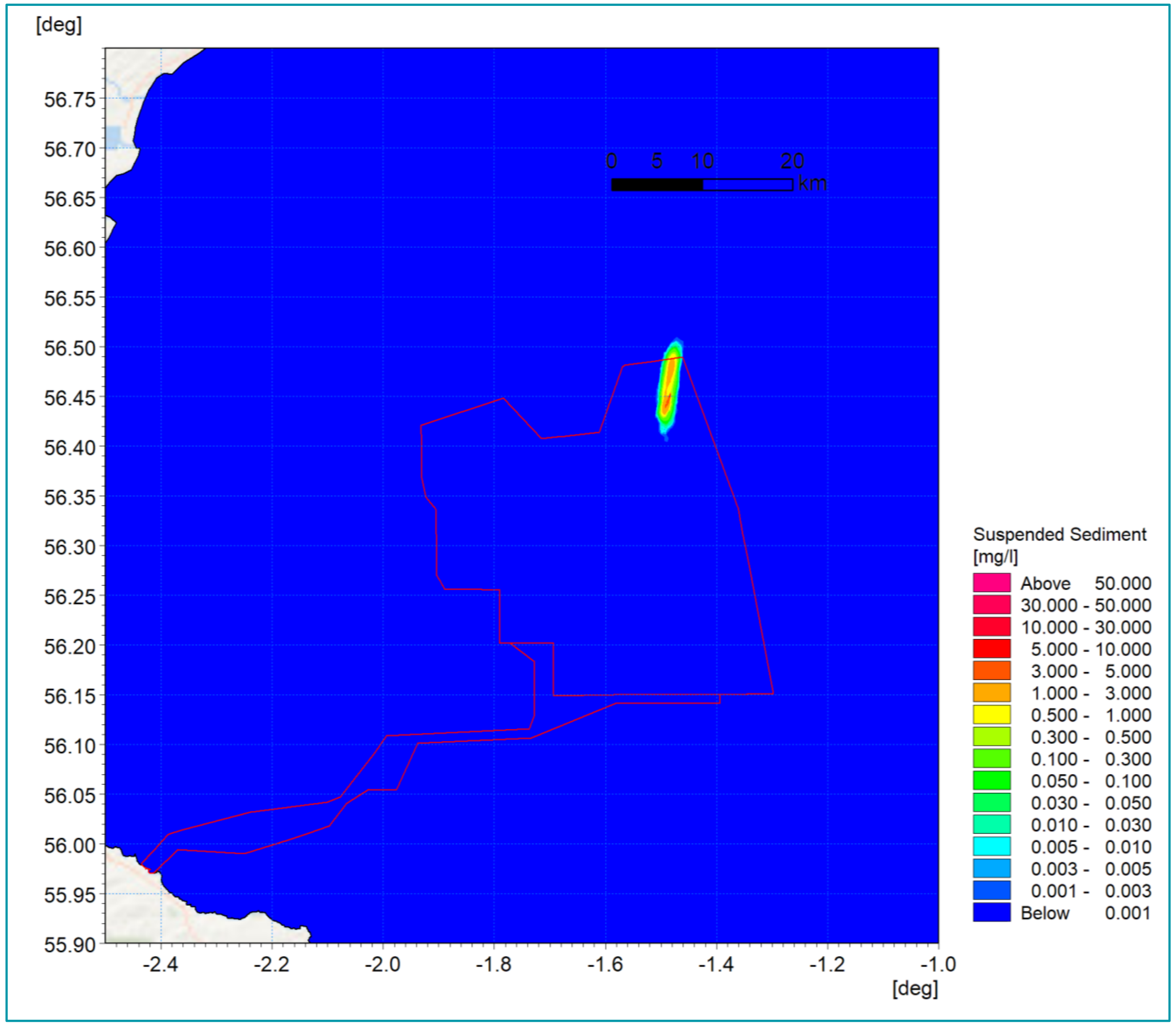


**Figure 6.31: Suspended Sediment Concentration Day One Peak Flood - Pile Installation Wind Turbine C**

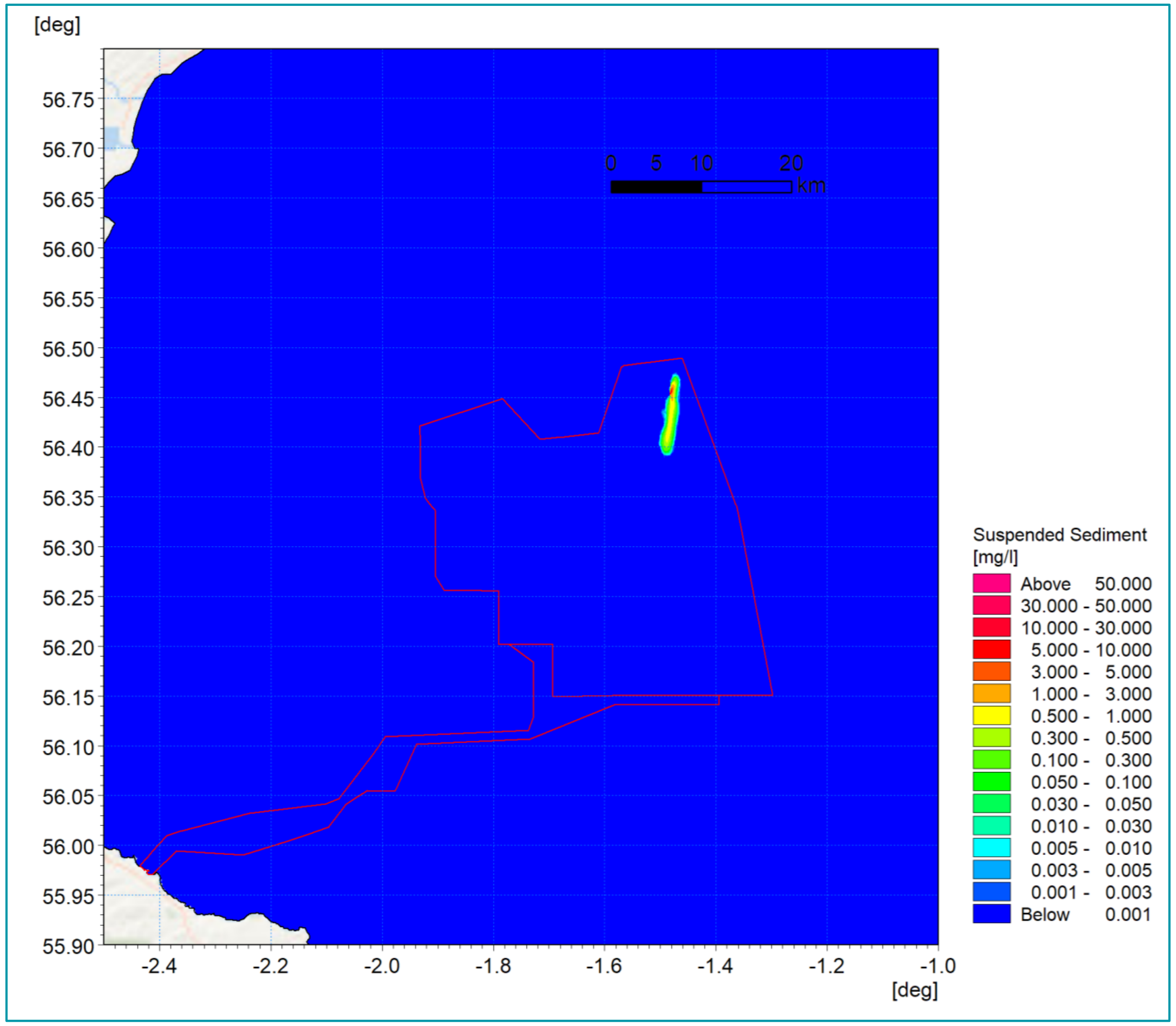


**Figure 6.32: Suspended Sediment Concentration Day 2 Peak Ebb - Pile Installation Wind Turbine C**

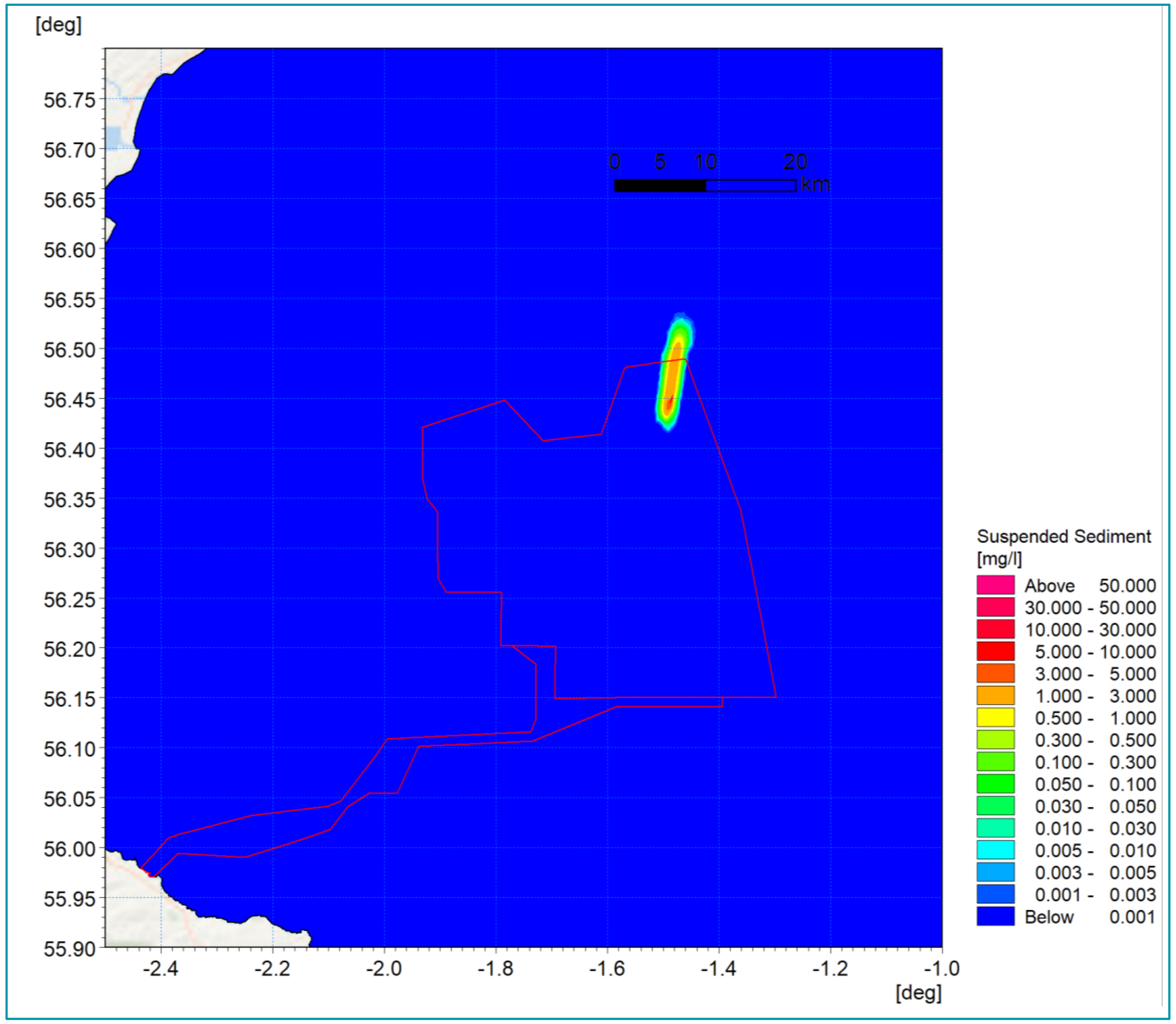


**Figure 6.33: Suspended Sediment Concentration Day Two Peak Flood - Pile Installation Wind Turbine C**

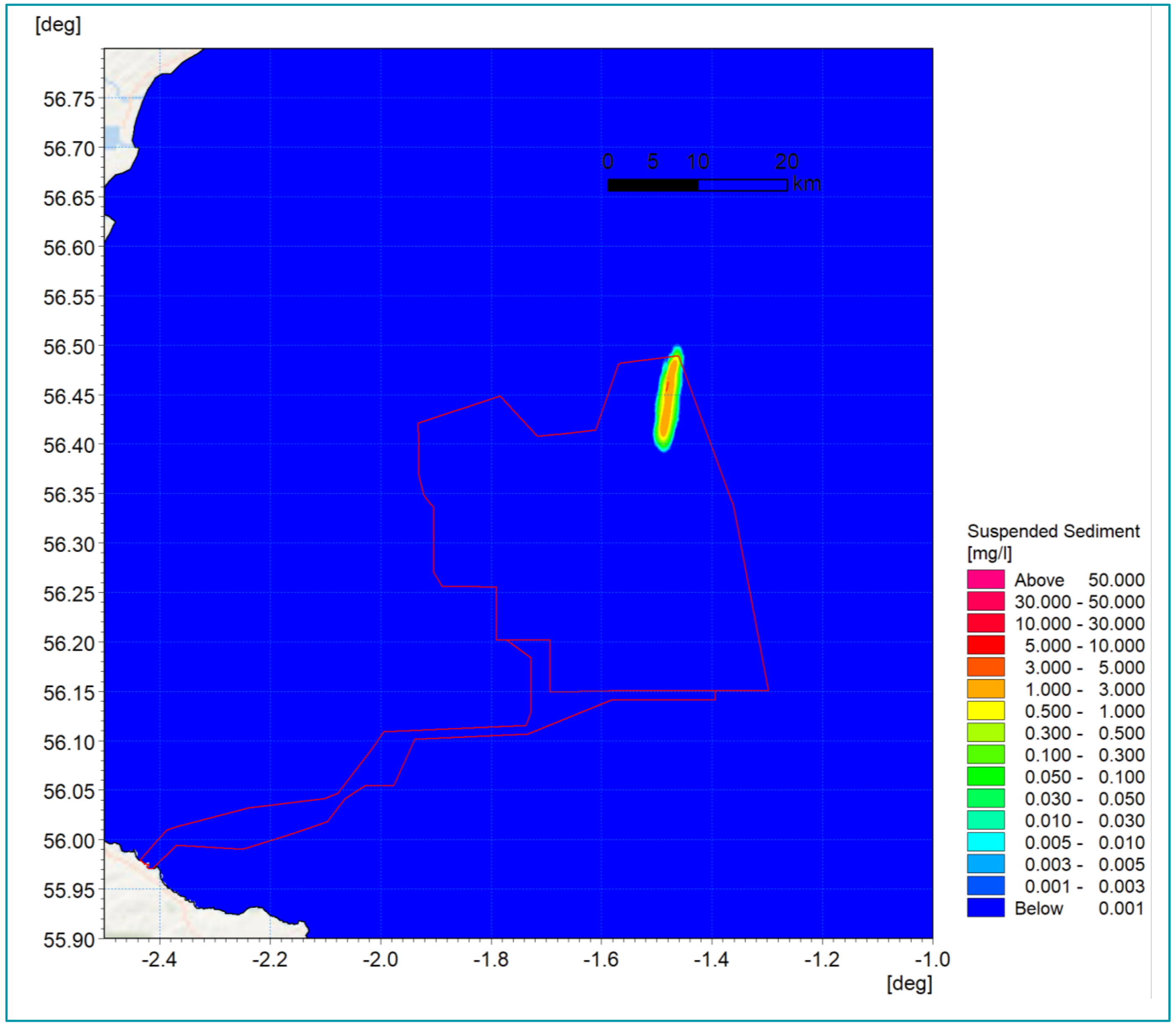


**Figure 6.34: Suspended Sediment Concentration Day Two Peak Ebb - Pile Installation Wind Turbine C**

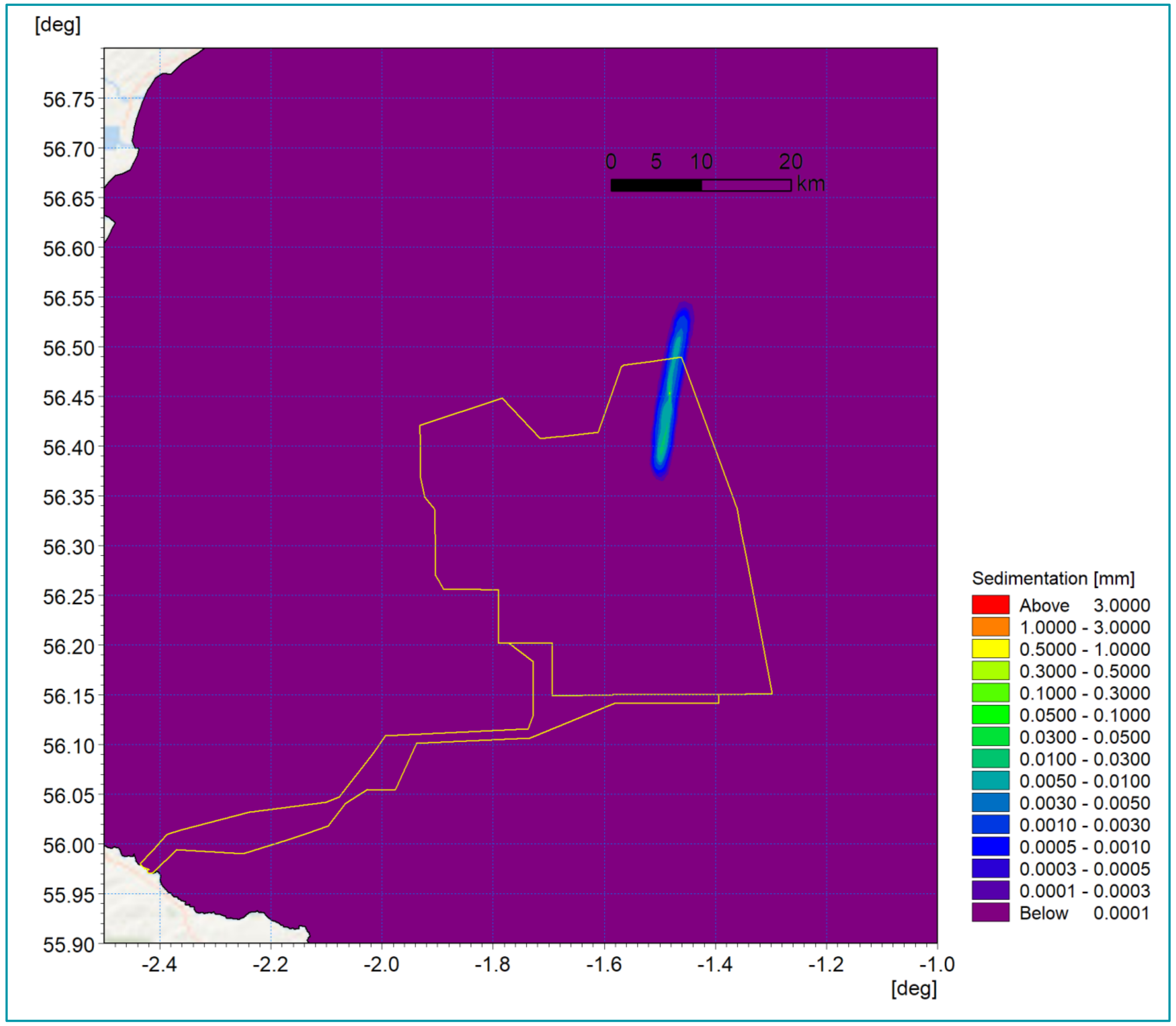


**Figure 6.35: Average Sedimentation During Pile Installation - Wind Turbine C**

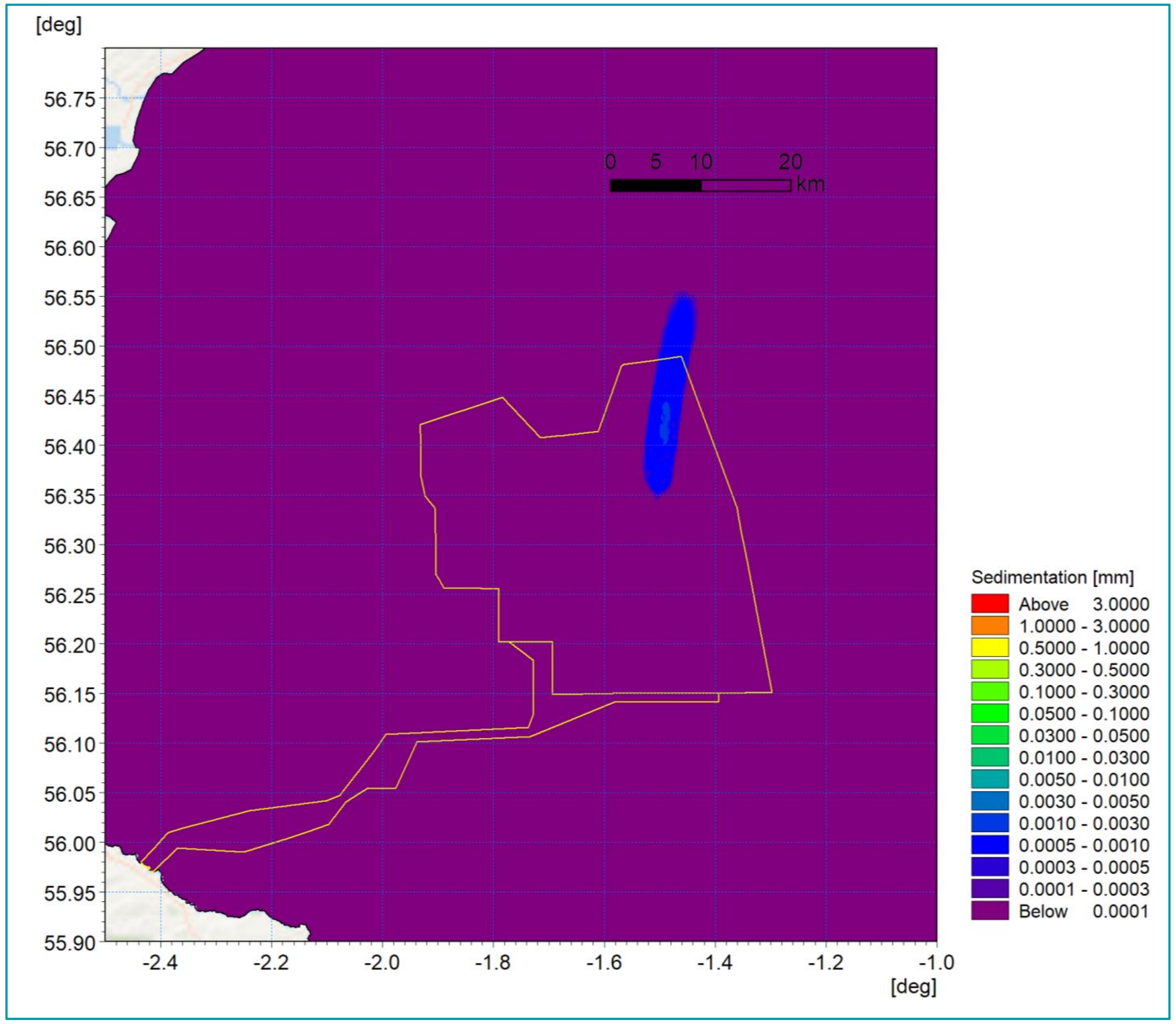


**Figure 6.36: Sedimentation One Day Following Cessation of Pile Installation - Wind Turbine C**

## 6.3. CABLE INSTALLATION

102. The third aspect of the construction phase is cable installation, including the inter-array cables, interconnector cables and offshore export cables to shore. For the maximum design scenario in terms of release of sediment into the water column, cables were assumed to be trenched. A number of trenching techniques may be suited to the ground conditions; however, it was assumed within the modelling that a trench of material of the maximum depth presented in the project description outlined in volume 1, chapter 3 of the Offshore EIA Report was mobilised into the lower water column as a result of the burial process, in line with the Business Enterprise and Regulatory Reform (BERR) guidelines (BERR, 2008). In reality the preferred scenario would be jet trenching and the maximum depth may not always be achieved with a corresponding reduction in the amount of material mobilised.

103. Similar to the pile installation, the model simulations used the sediment grading determined from sediment sampling. However, the modelling was undertaken using the MIKE PT module. This module was implemented as it had the advantage that it could be used to describe the transport of material released in a specific part of the water column. In this way, the dispersion would not be over-estimated or the corresponding sedimentation under-estimated by the application of a current profile through the water column.

104. Trenching rates can vary widely depending on the bed material and equipment used; typically, rates are between 25 m/h and 780 m/h. For the simulation, a relatively high rate of 500 m/h was used over an extensive sample route ensuring that material was released at all tidal states over a number of tides and ensuring initial concentrations were not underestimated.

### 6.3.1. INTER-ARRAY/INTERCONNECTOR CABLES

105. Inter-array and interconnector cable installation will be undertaken along a number of paths which connect groups of wind turbines to a local hub (i.e. the OSP/Offshore convertor station platforms) or which connect two OSPs/Offshore convertor station platforms to each other. Each route would be undertaken as a separate operation and thus a single example has been selected to quantify the potential suspended sediment levels during the installation. Figure 6.37 shows an indicative wind turbine layout with the modelled inter-array cable route shown in yellow. This route was run from the south-east corner of the site, perpendicular to the tidal flow to the west, then in line with tidal flows in a northerly direction before re-crossing the site. This ensured that the full extent of the site and tidal conditions were incorporated into the simulation.

106. The inter-array cabling was undertaken along the indicated route with a trench 2 m wide and 3 m in depth thus circa 469,000 m$^3$ of material was mobilised during the seven day simulation. The sediment grading characteristics were derived from sediment sampling along the route and defined by the following sand fractions.

- very coarse sand: 22%;
- coarse sand: 12%;
- medium sand: 36%; and
- fine sand: 30%.

107. The model results presented follow the same format as those for the wind turbine installation described in paragraphs 91 and 92. Figure 6.38 shows the average suspended sediment concentration over the course of the trenching phase. It is clear that the sediment is re-suspended and dispersed on subsequent tides as the plume envelope is most extensive towards the start of the route to the south-east of the site with peak values of 100 mg/l.

108. Figure 6.39 to Figure 6.44 shows the suspended sediment patterns over the course of this operation, day two, four and five peak flood and ebb tides respectively. Whilst Figure 6.45 and Figure 6.46 show the flood and ebb tides at the end of the trenching. The volume of material mobilised is relatively large, and elevated tidal currents disperse the material giving rise to concentrations of up to 500 mg/l. As was evident in the previous operations, the material settles during slack water and then is re-suspended to form an amalgamated plume. This is further illustrated in Figure 6.47 and Figure 6.48 which show the average sedimentation and the sedimentation one day following cessation at slack water. The sedimentation is greatest at the location of the trenching and may be up to 30 mm in depth however within close proximity, circa 100 m, the depths reduce considerably which is indicated by the use of a log scale in all figures. Although the material is dispersed, it remains within the sediment cell and is therefore retained within the transport system.

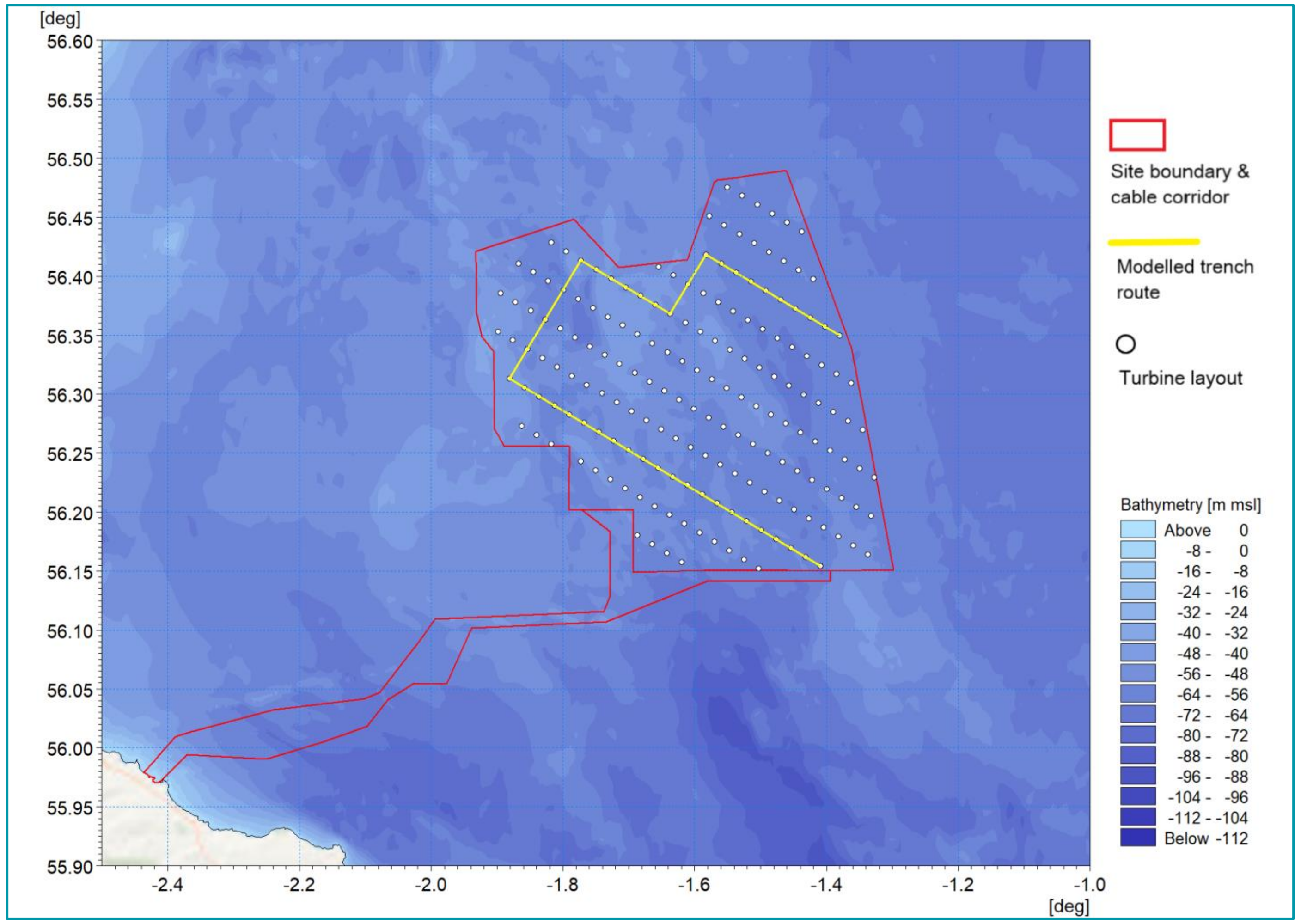


**Figure 6.37: Modelled Inter-Array Cable Route**

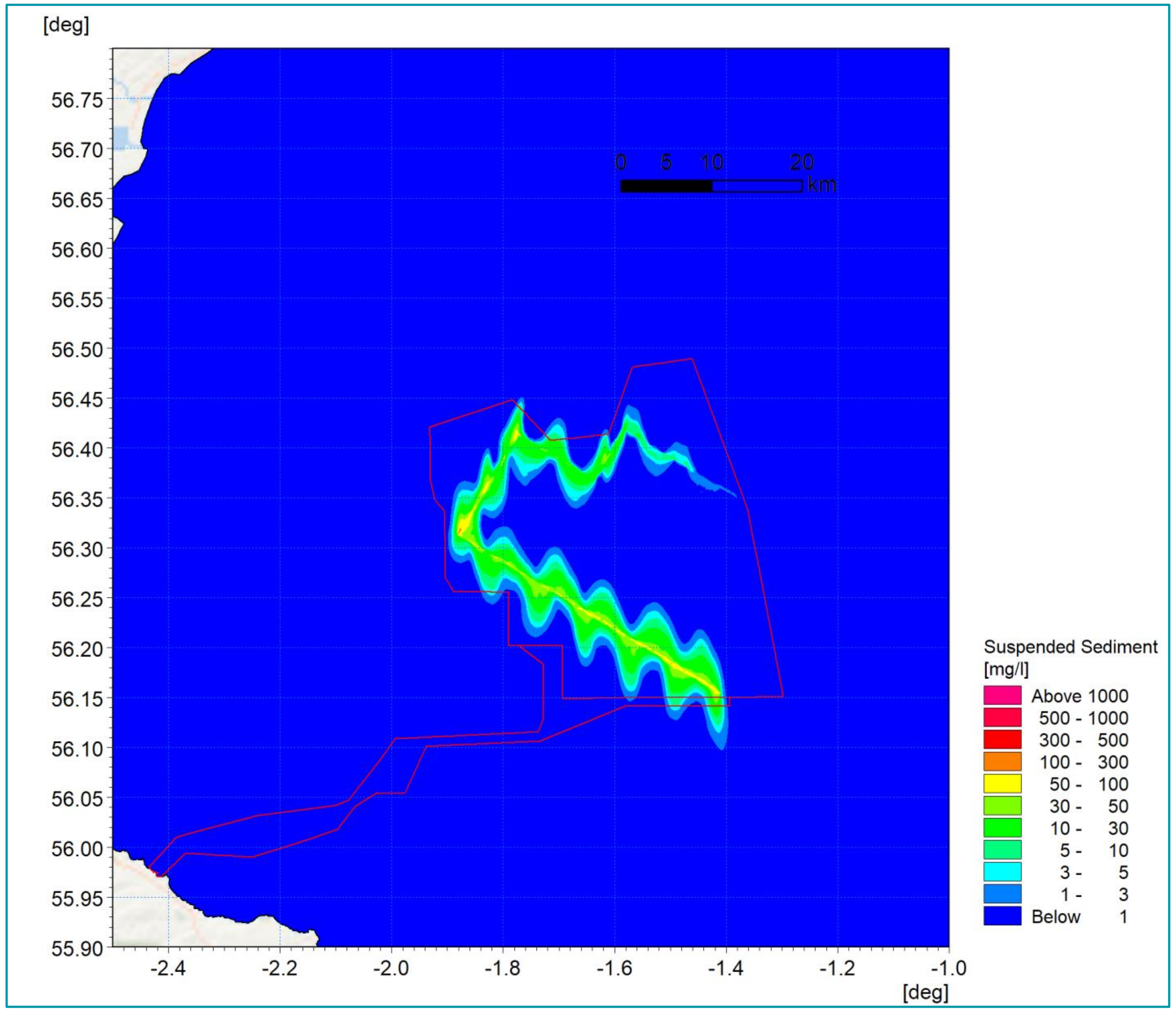


**Figure 6.38: Average Suspended Sediment Concentration During Inter – Inter-Array Cable Trenching**

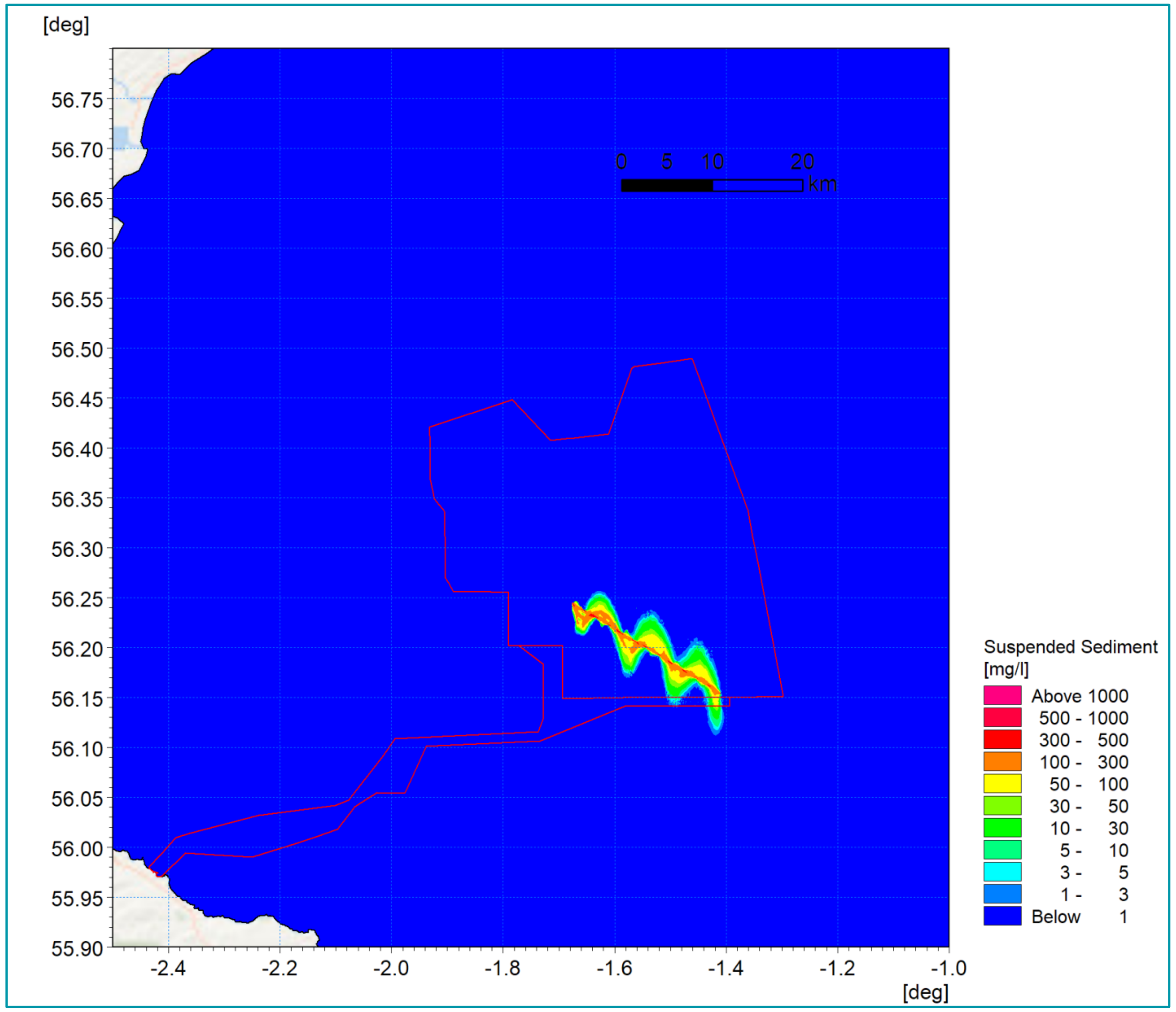


**Figure 6.39: Suspended Sediment Concentration Day Two Peak Flood – Inter-Array Cable Installation**

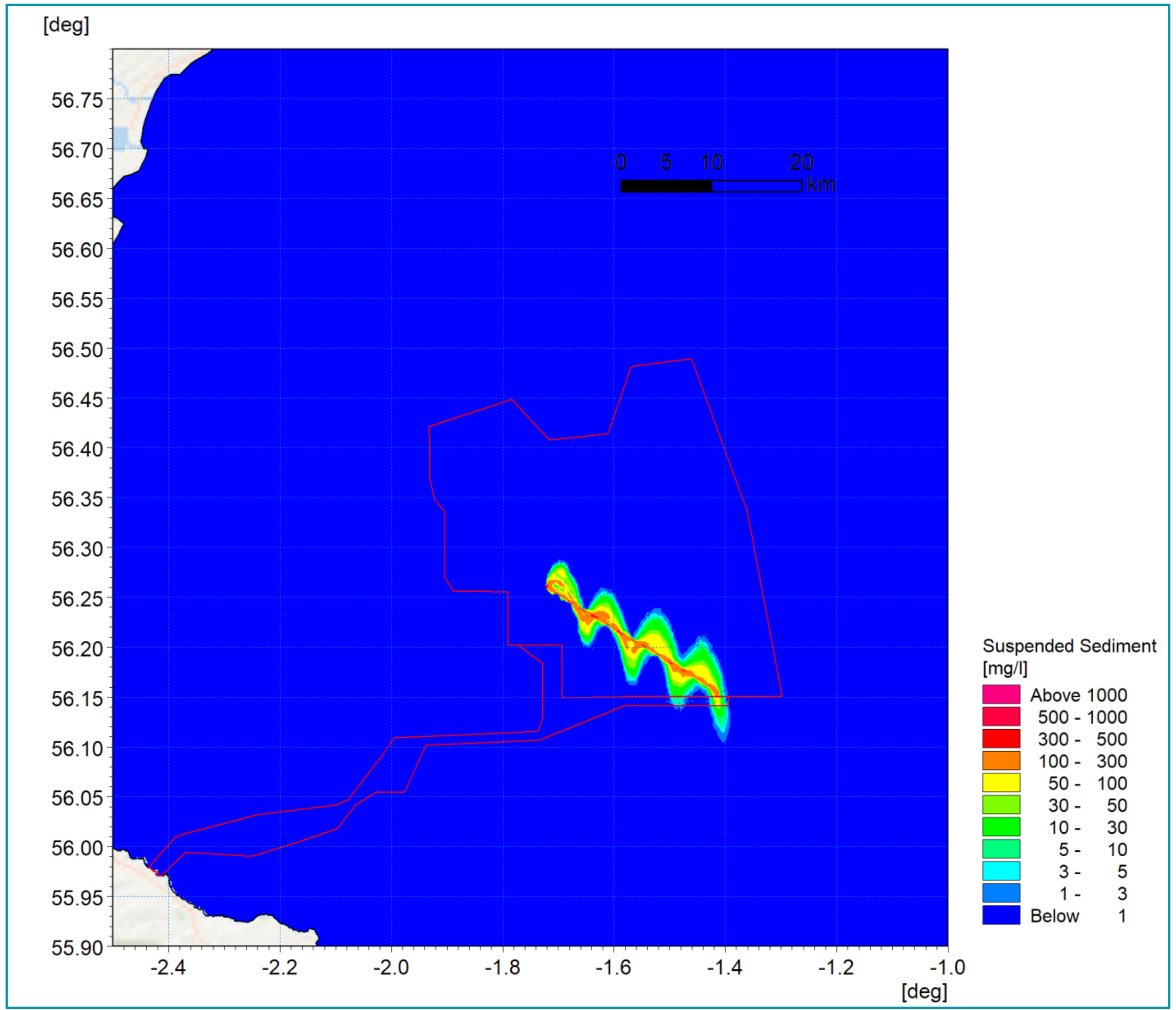


**Figure 6.40: Suspended Sediment Concentration Day Two Peak Ebb – Inter-Array Cable Installation**

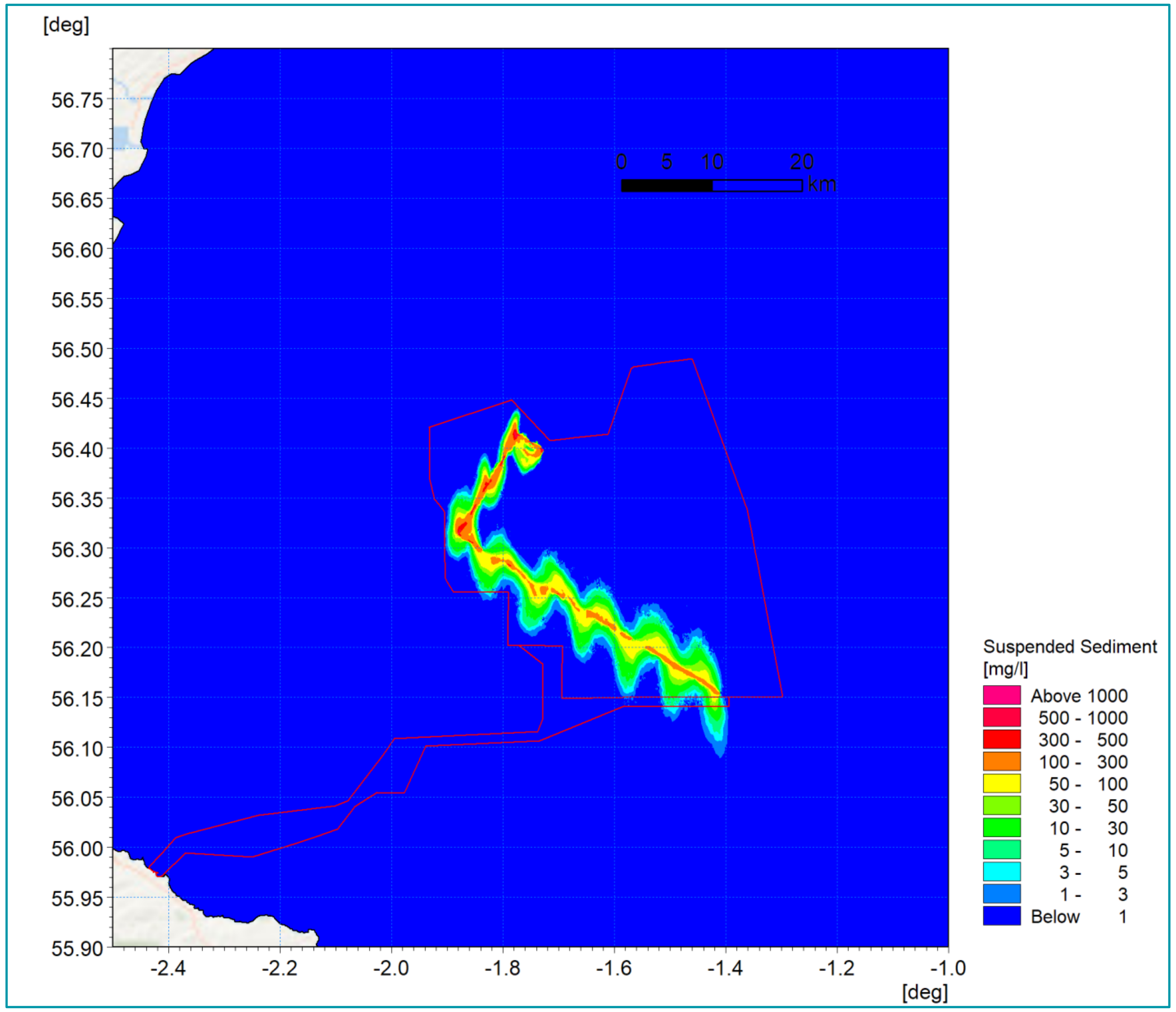


**Figure 6.41: Suspended Sediment Concentration Day Four Peak Flood – Inter-Array Cable Installation**

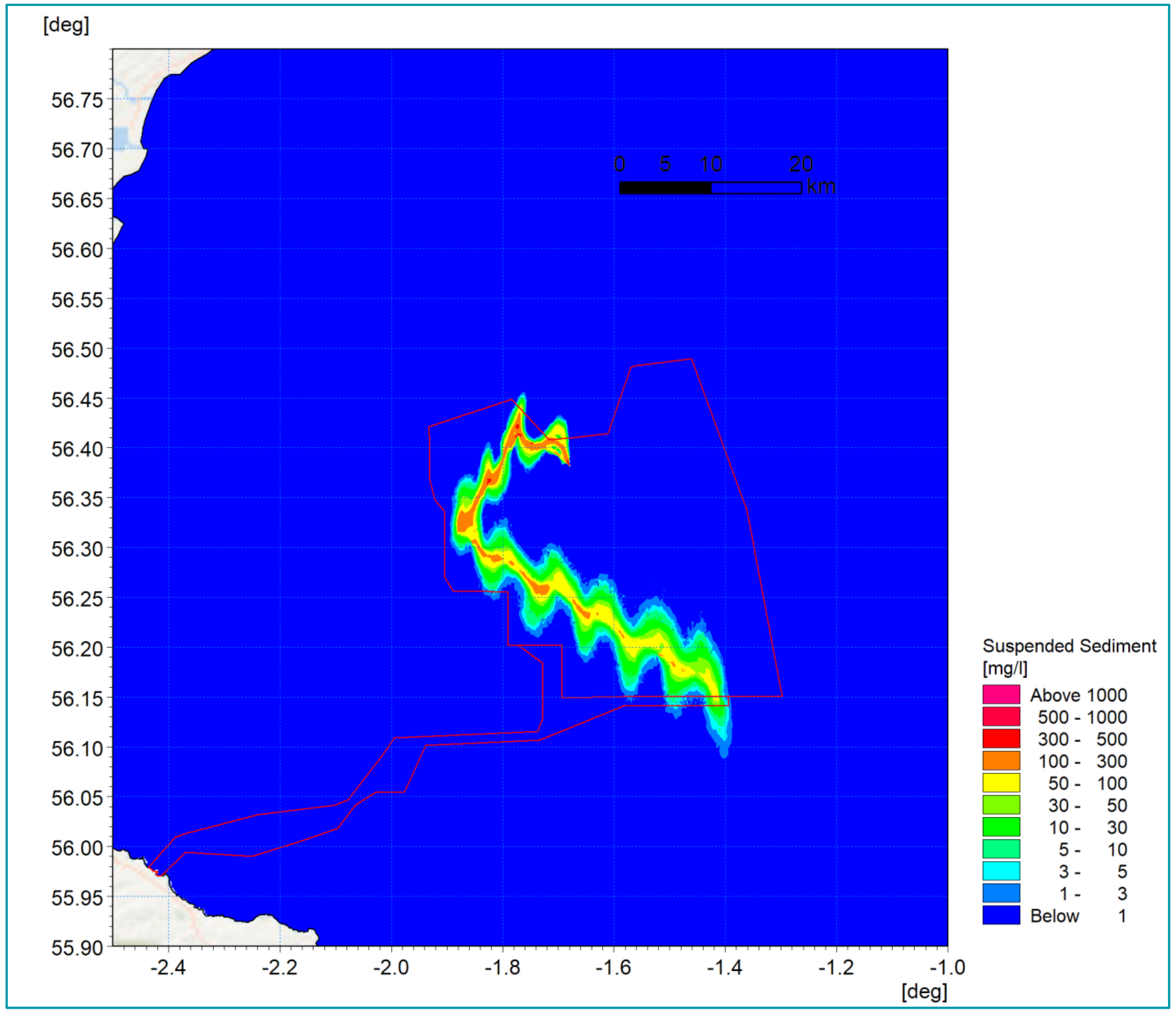


**Figure 6.42: Suspended Sediment Concentration Day Four Peak Ebb – Inter-Array Cable Installation**

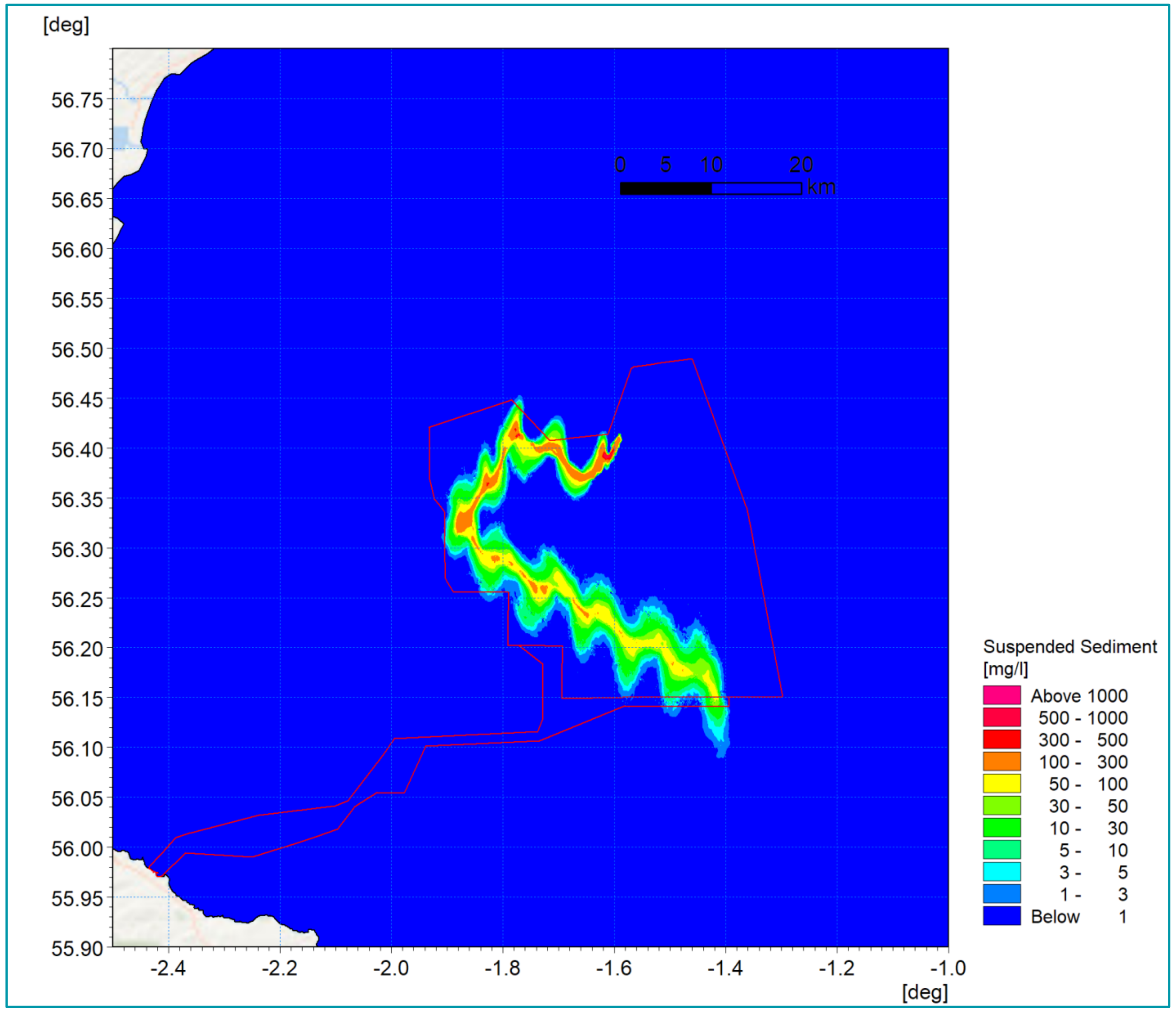


**Figure 6.43: Suspended Sediment Concentration Day Five Peak Flood – Inter-Array Cable Installation**

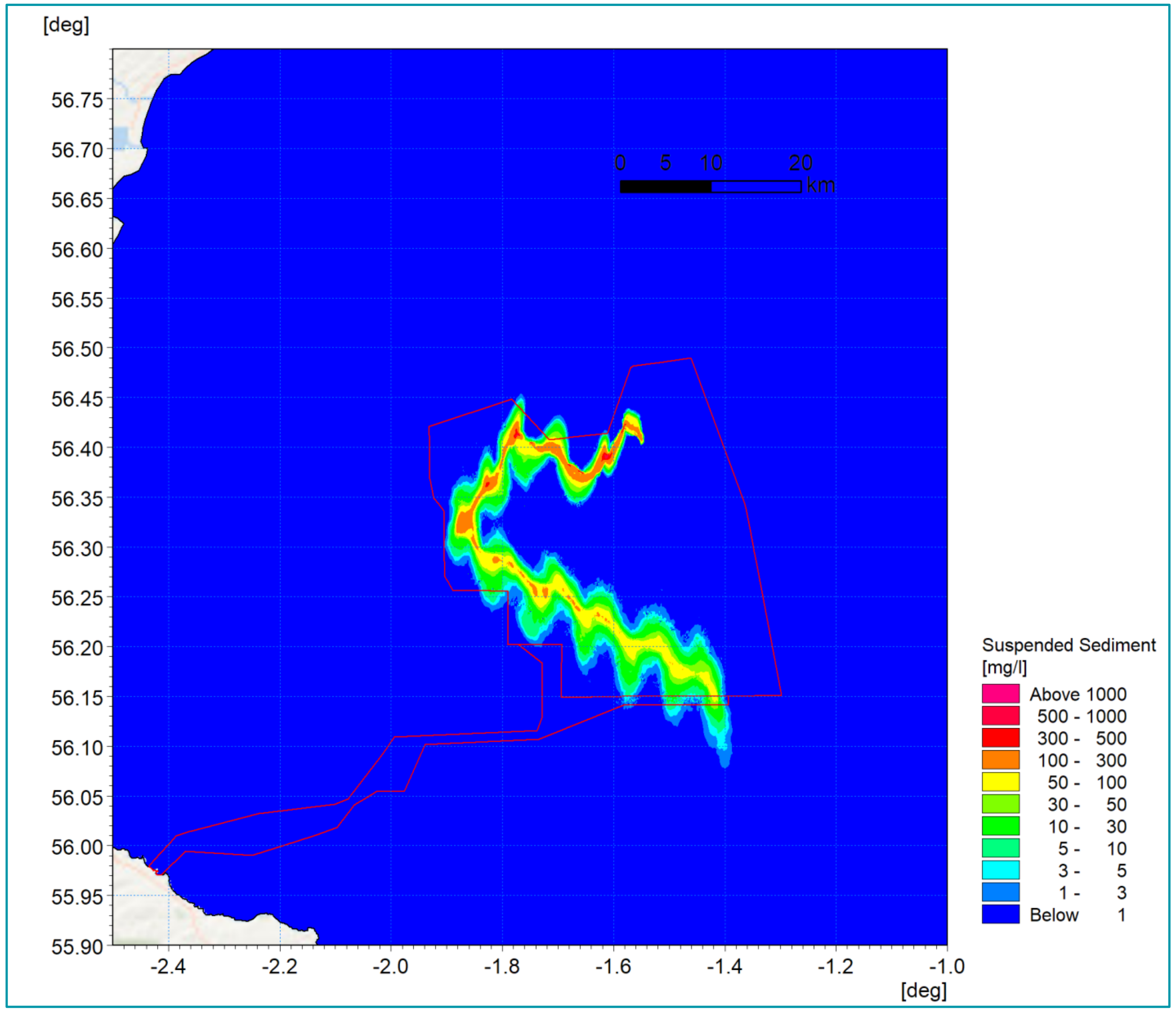


**Figure 6.44: Suspended Sediment Concentration Day Five Peak Ebb – Inter-Array Cable Installation**

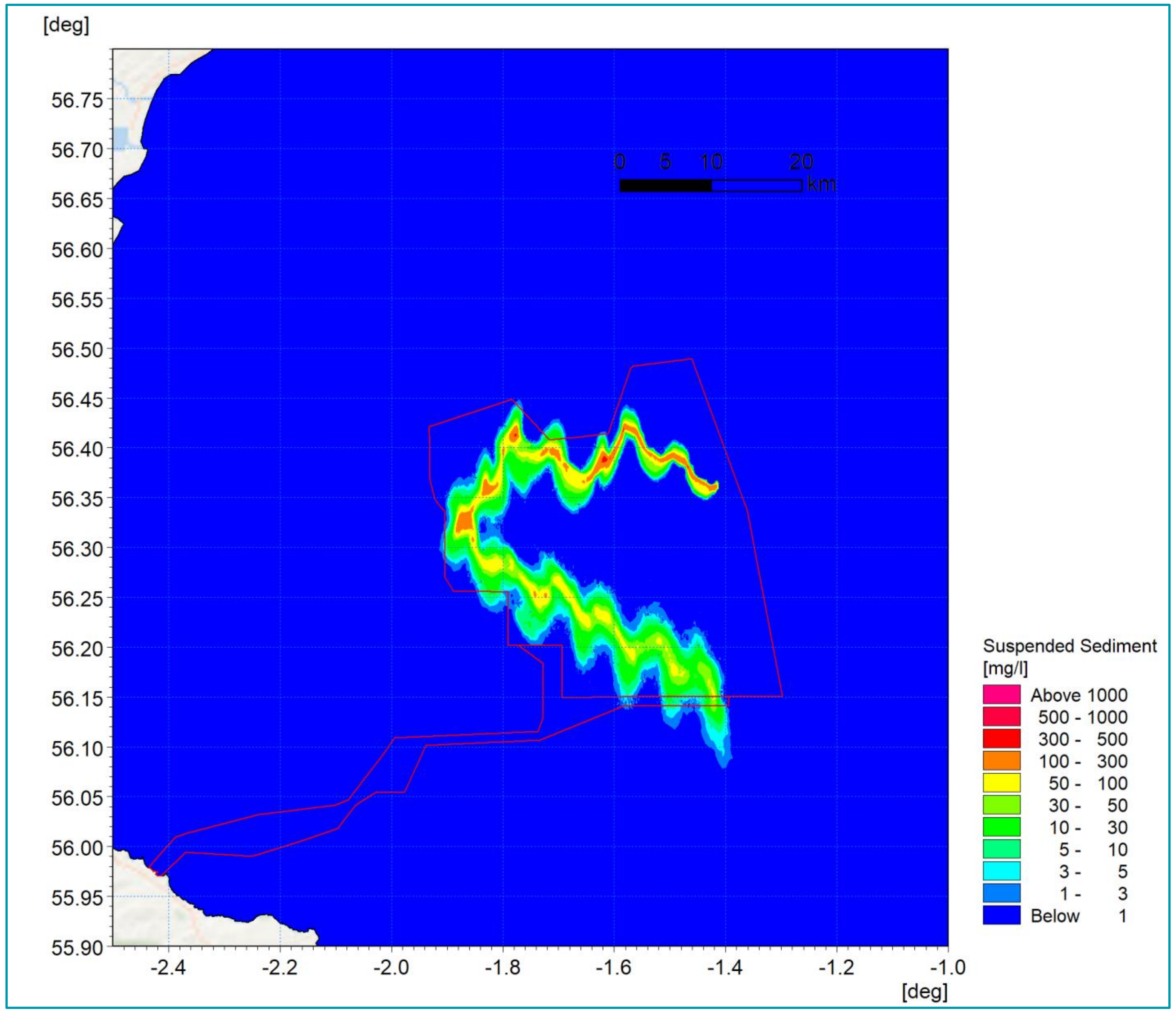


**Figure 6.45: Suspended Sediment Concentration Final Day Peak Flood – Inter-Array Cable Installation**

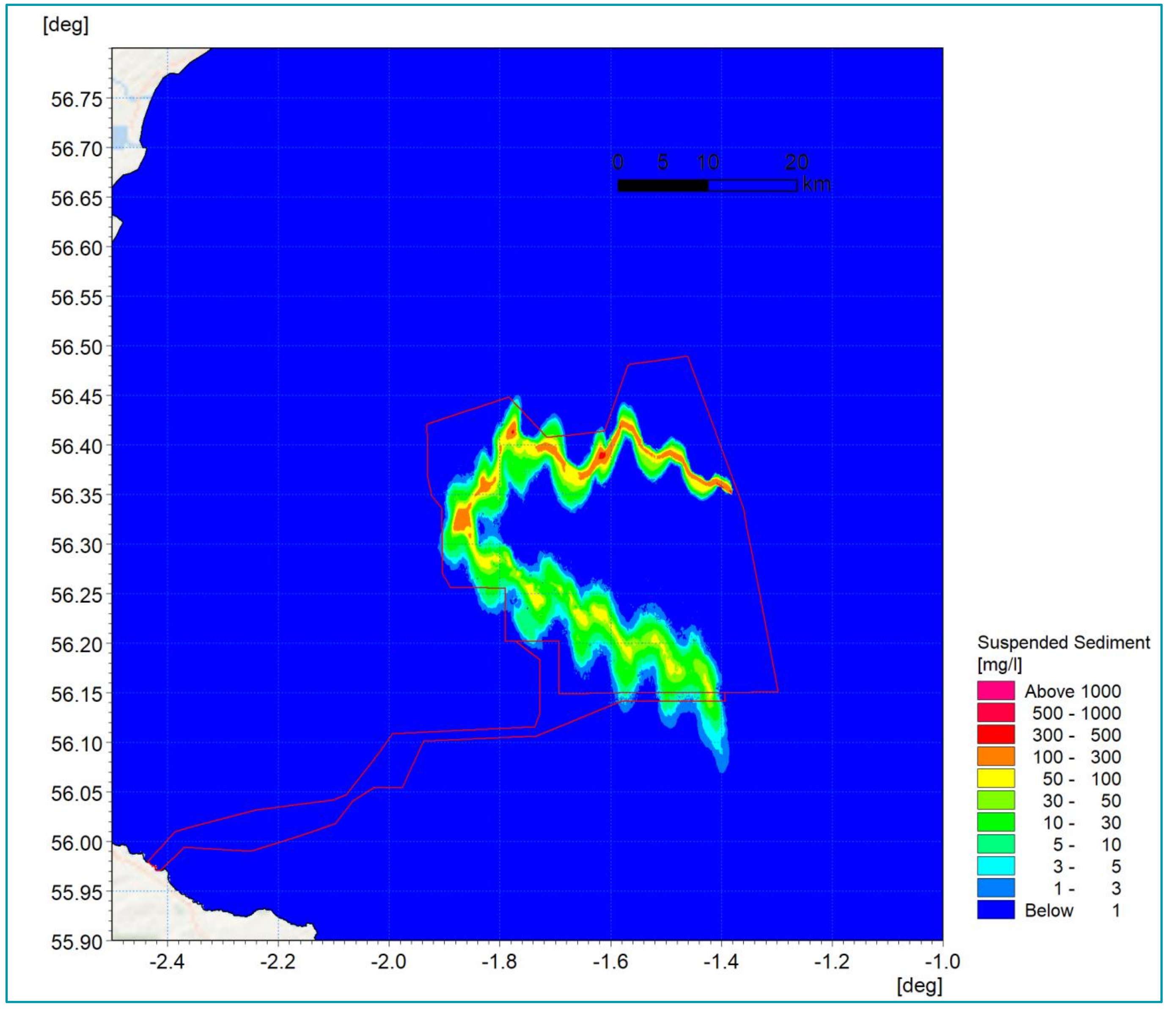


Figure 6.46: Suspended Sediment Concentration Final Day Peak Ebb – Inter-Array Cable Installation

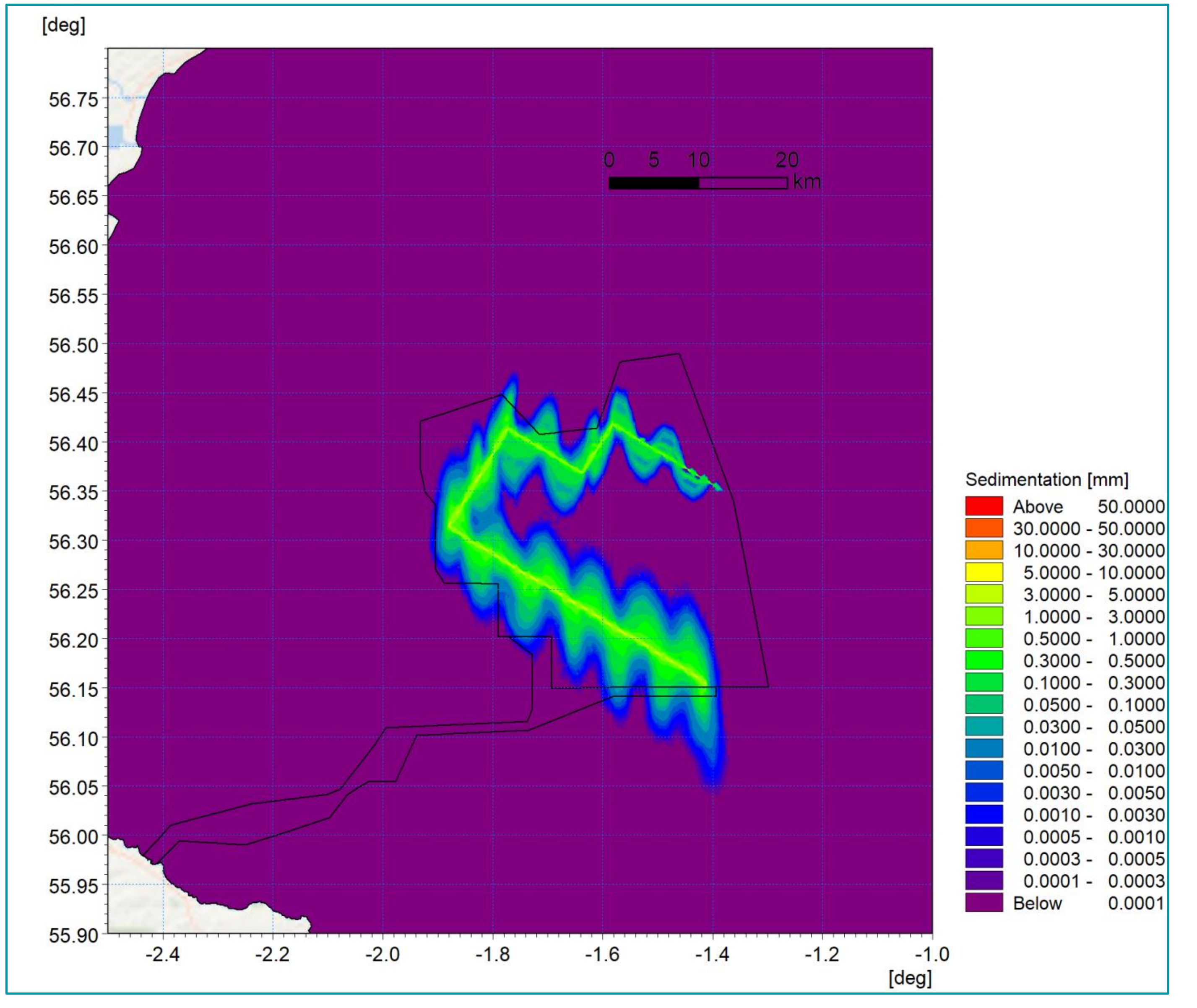


Figure 6.47: Average Sedimentation during Inter-Array Cable Installation

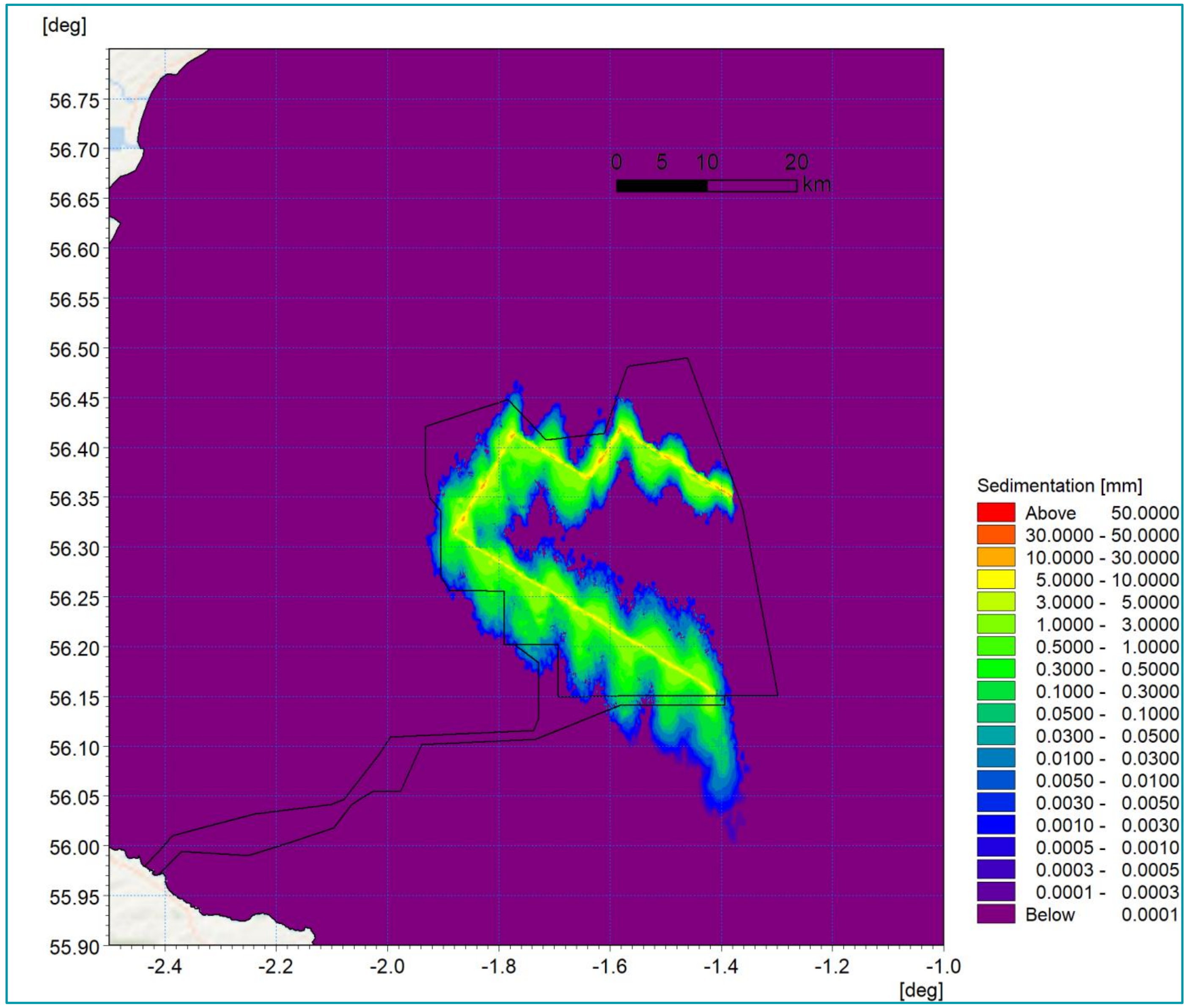


**Figure 6.48: Sedimentation One Day Following Cessation of Inter-Array Cable Installation**

### 6.3.2. OFFSHORE EXPORT CABLES

109. The proposed Skateraw offshore cable route was examined using numerical modelling. The simulation assumed the same trenching rate as with the inter-array cables (i.e. 500 m/h), and that installation began from offshore and continued to the nearshore region of the proposed trenchless landfall. Each trench was 2 m at the surface extending to a depth of 3 m (i.e. the greatest burial depth proposed). The operation took approximately 5.5 days to complete encompassing a range of tidal conditions and mobilised 400,000 $m^3$ of material. The composition was determined from the sampling data and was of generally more finely graded material than the inter-array material:

- medium sand: 22%;
- fine sand: 46%;
- very fine sand: 18%; and
- coarse silt: 14%.

110. The landfall trenching route modelled is illustrated by the yellow trace in Figure 6.49 and the average suspended sediment plume during the course of the operation is shown in Figure 6.50. The figure shows how the plume travels north and south on the tide as the release progresses along the route perpendicular to the tidal flow. This gives rise to average SSC <50 mg/l.

111. The instantaneous SSC for peak flood and ebb tides are presented for day two, day four and the final day in Figure 6.51 to Figure 6.56 respectively. They show increases where sediment is released at the cable location but also at the extent of each tidal cycle as material is re-suspended. The plume travels north and south on the tide as the release progresses along the route perpendicular to the tidal flow and sediment concentrations reduce to background levels on slack tides. Average SSC along the route range between 50 mg/l and 500 mg/l.

112. Finally, Figure 6.57 shows the average sedimentation whilst Figure 6.58 illustrates sedimentation levels one day following cessation of the sediment release. Tidal patterns indicate that although the released material migrates both north and south by settling and being re-suspended on successive tides, the sedimentation level is small. Although there is some migration of material, sediment remains within the cell and would be drawn into the baseline transport regime with small increases in bed sediment levels, typically <3 mm at the coastline.

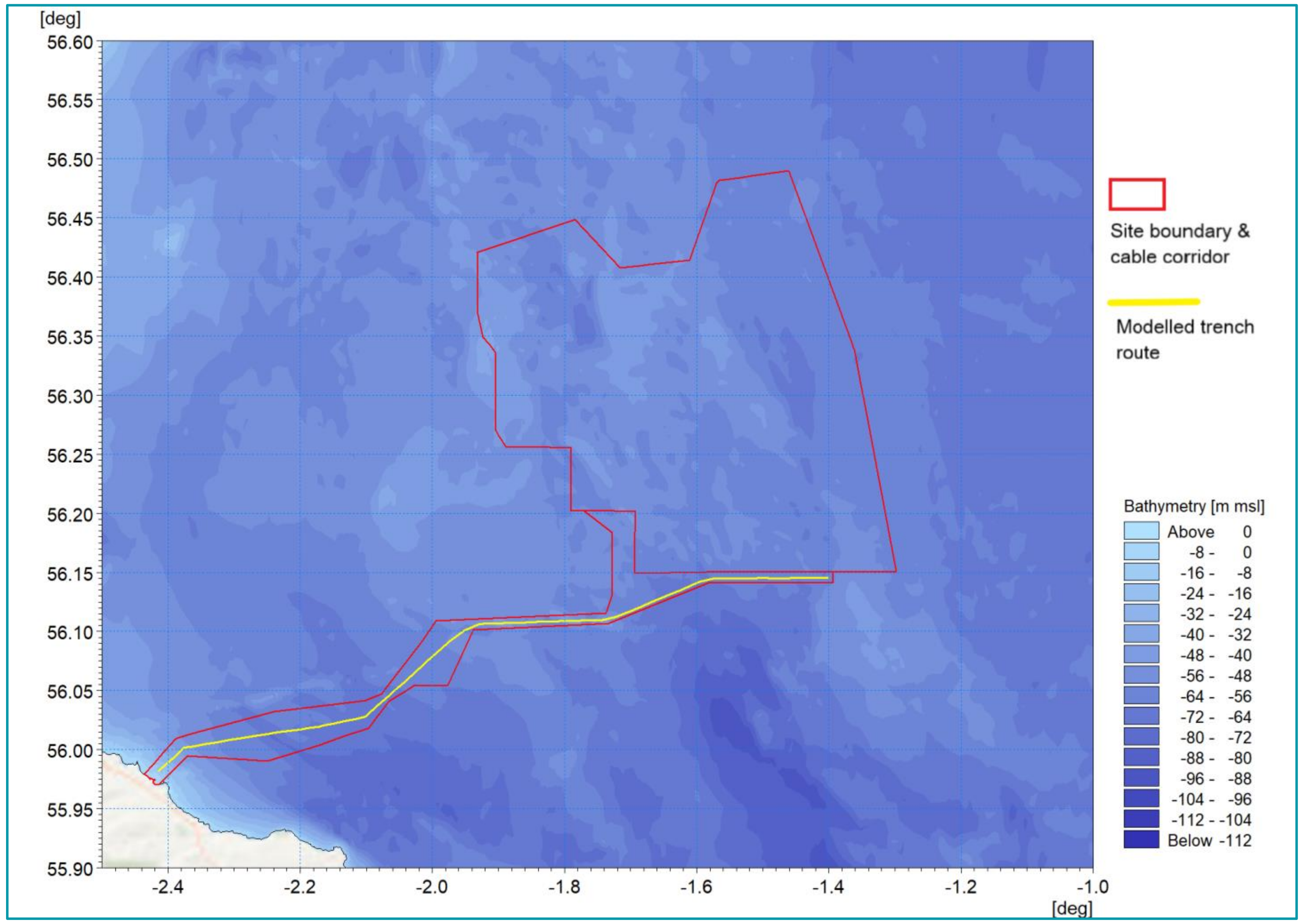


**Figure 6.49: Modelled Offshore Cable Route**

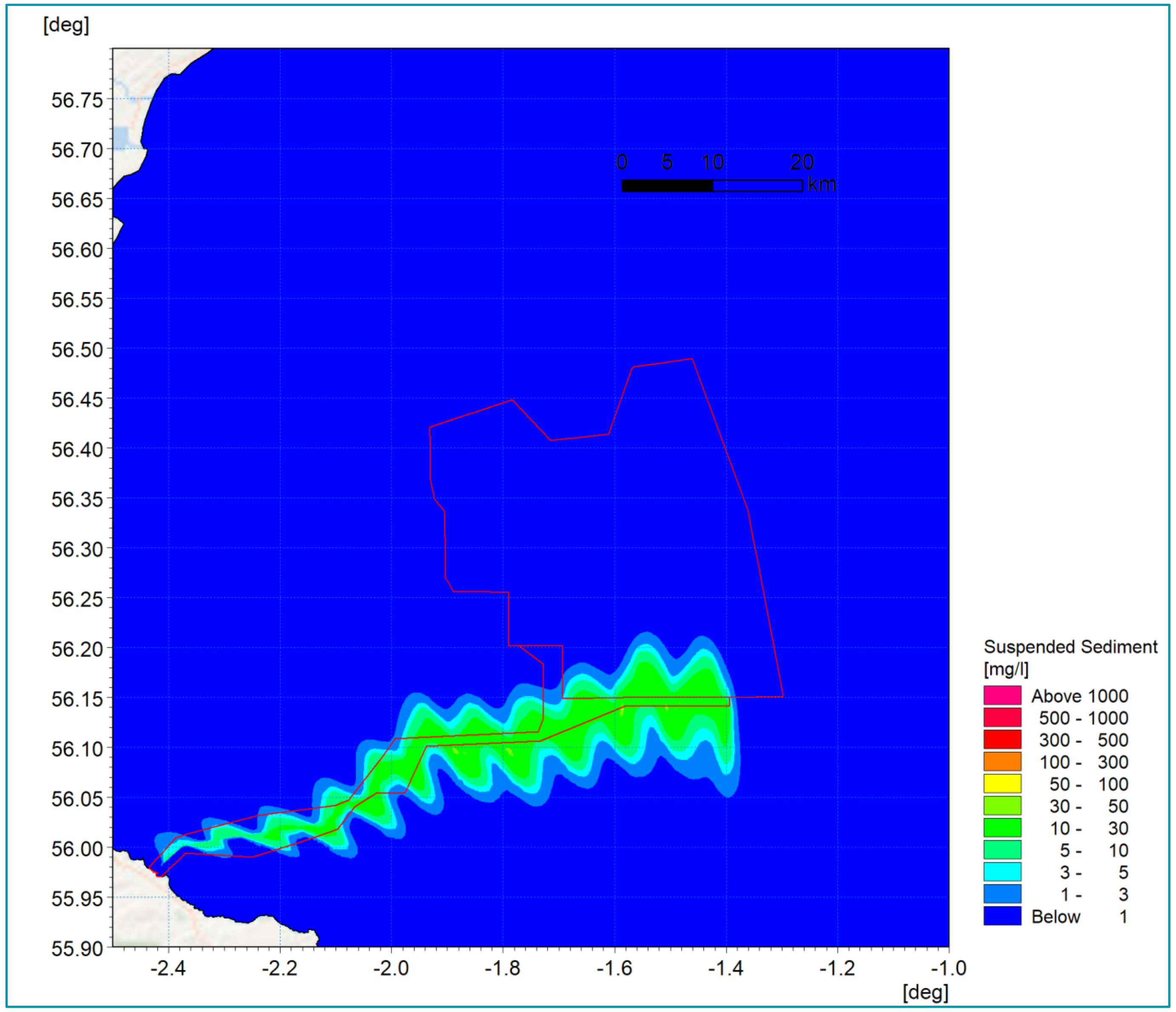


**Figure 6.50: Average Suspended Sediment Concentration During Offshore Export Cable Trenching**

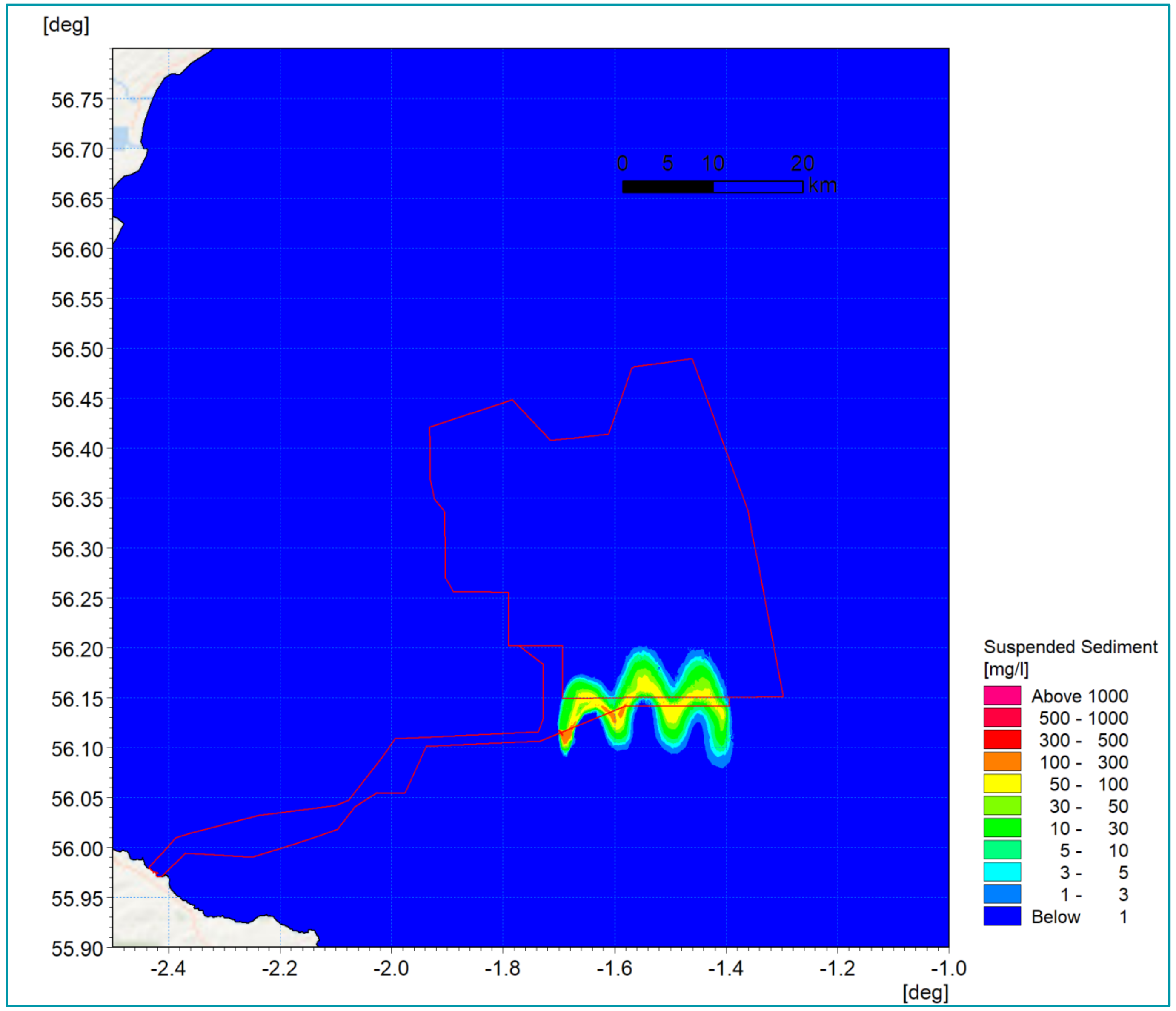


**Figure 6.51: Suspended Sediment Concentration Day Two Peak Flood – Offshore Export Cables Installation**

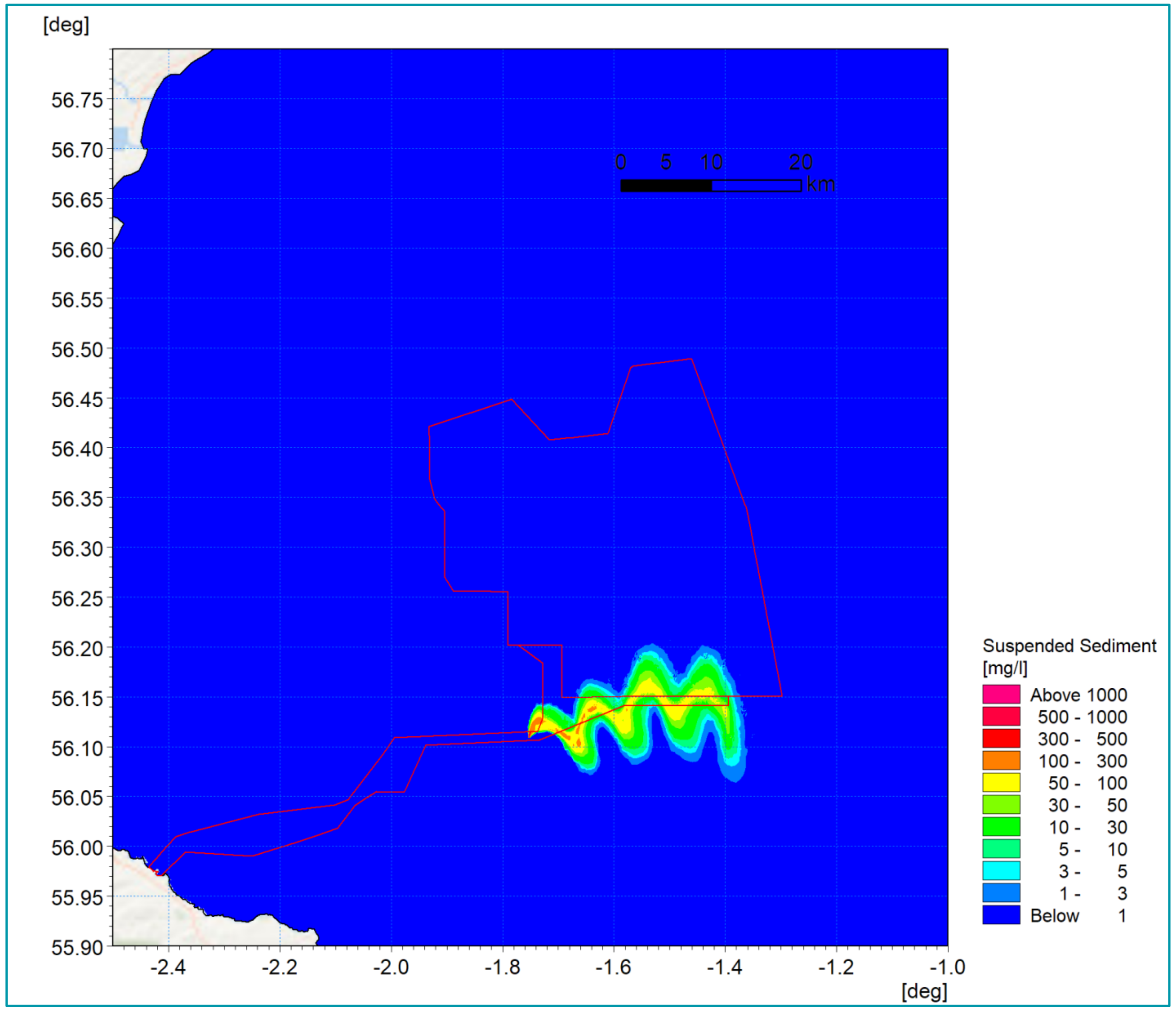


**Figure 6.52: Suspended Sediment Concentration Day Two Peak Ebb – Offshore Export Cables Installation**

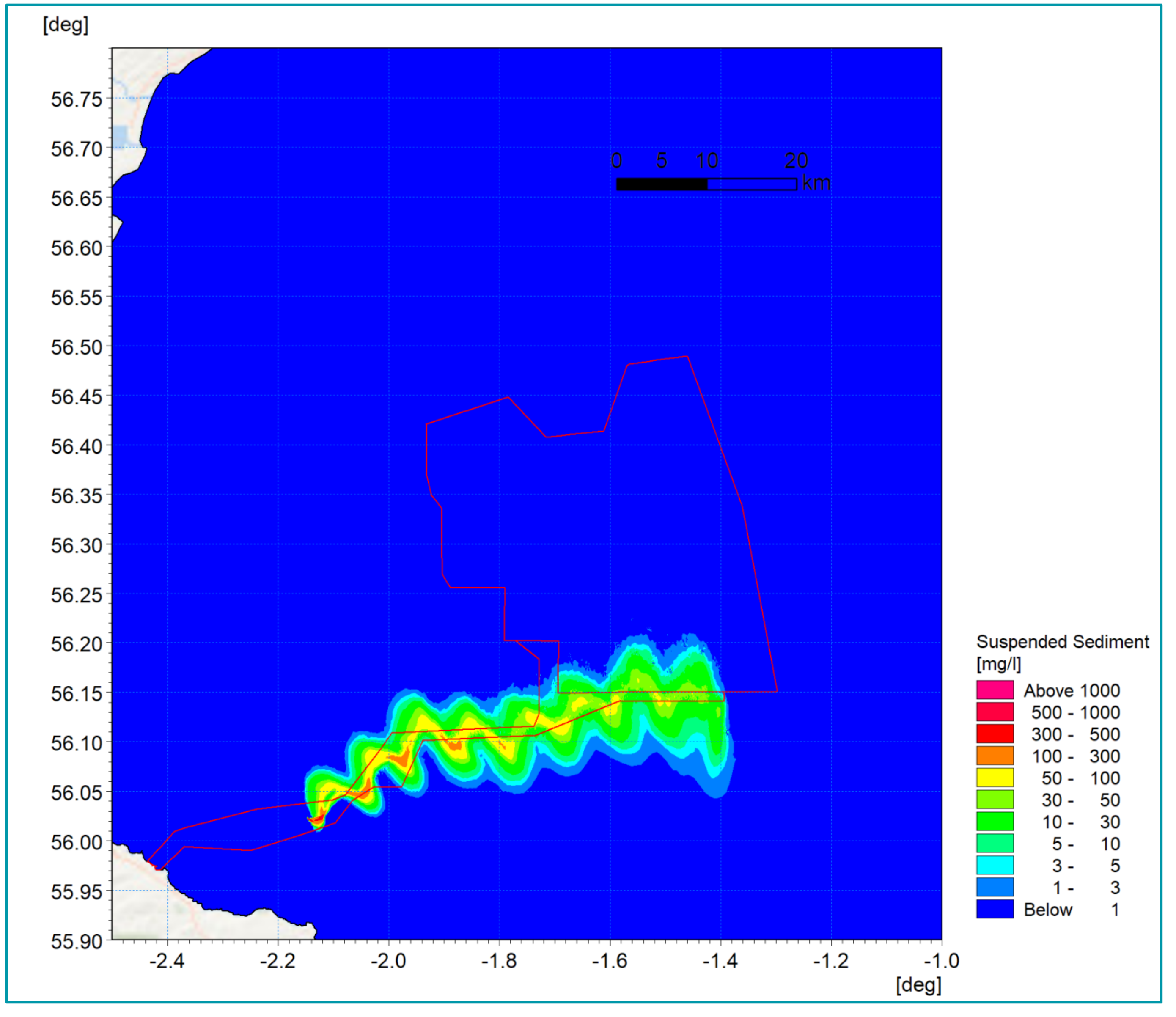


**Figure 6.53: Suspended Sediment Concentration Day Four Peak Flood – Offshore Export Cables Installation**

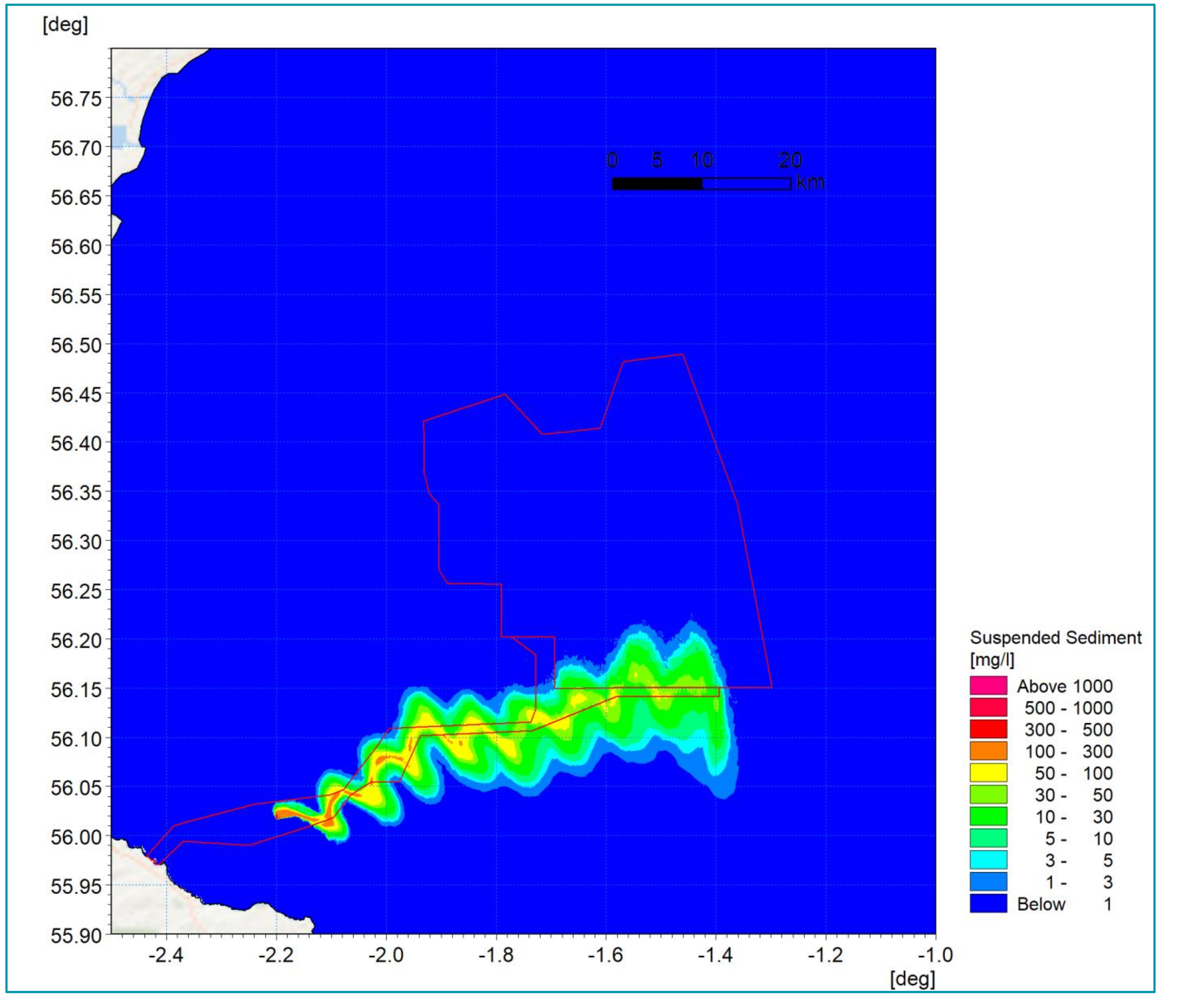


**Figure 6.54: Suspended Sediment Concentration Day Four Peak Ebb – Offshore Export Cables Installation**

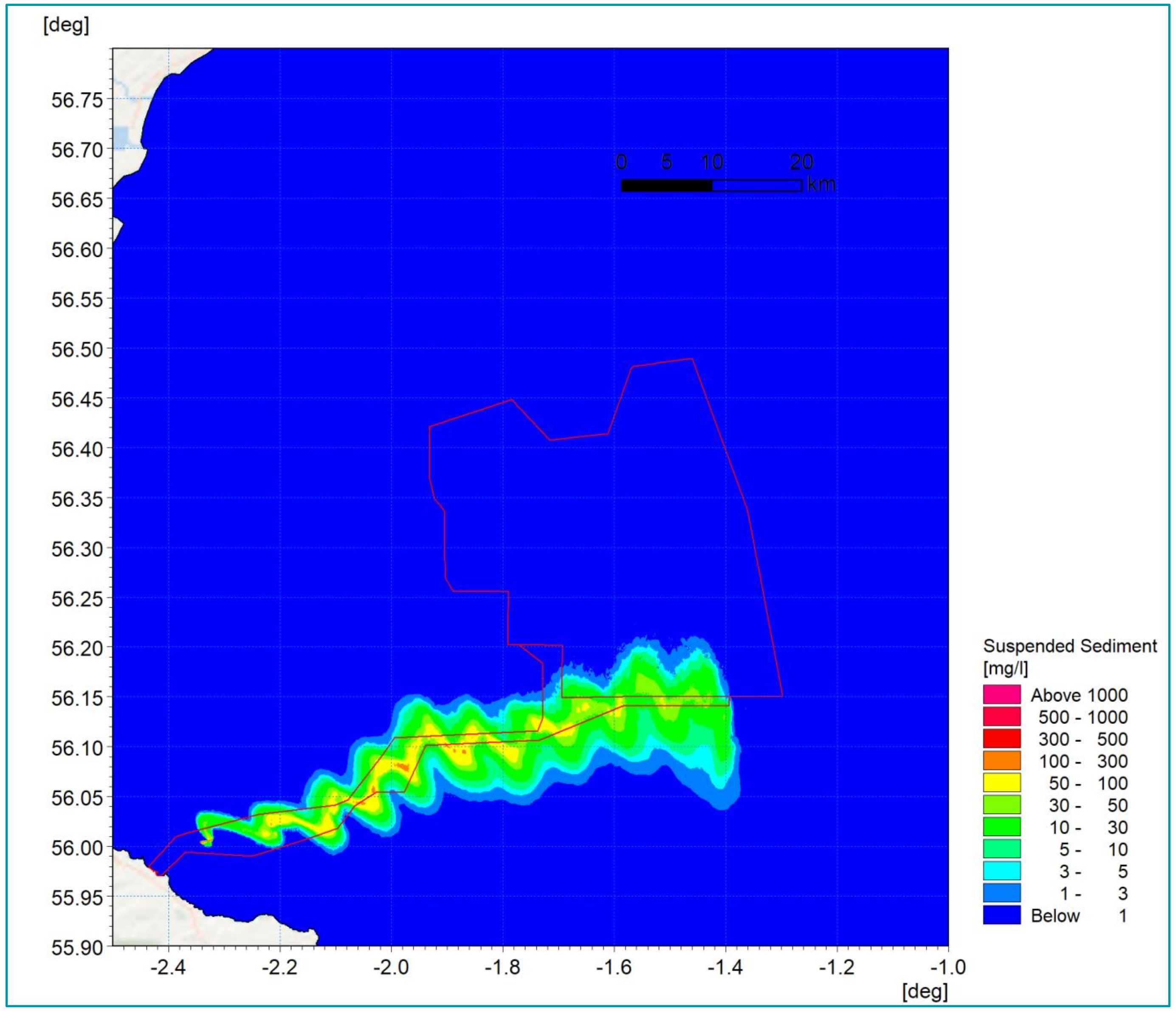


**Figure 6.55: Suspended Sediment Concentration Final Day Peak Flood – Offshore Export Cables Installation**

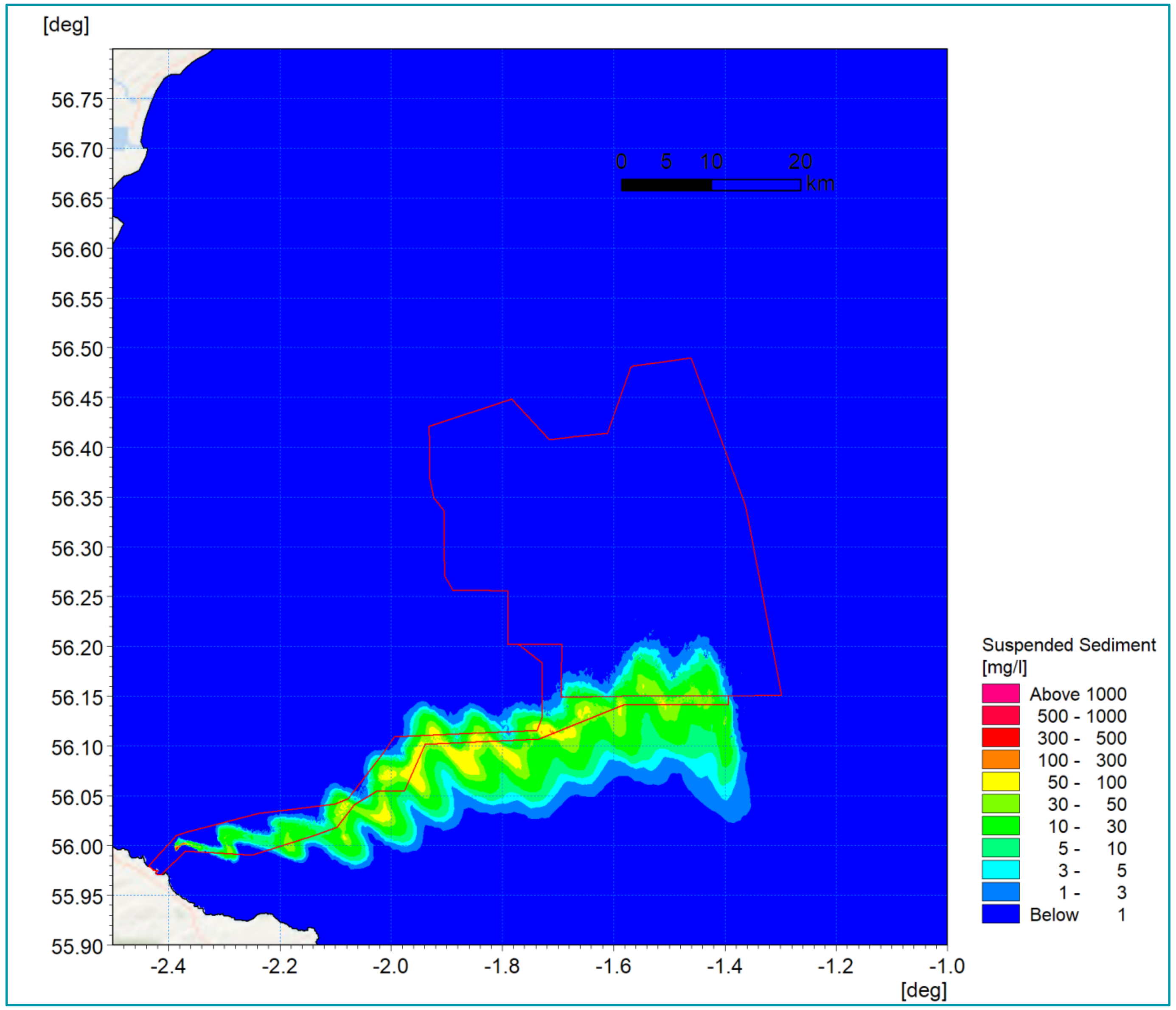


**Figure 6.56: Suspended Sediment Concentration Final Day Peak Ebb – Offshore Export Cables Installation**

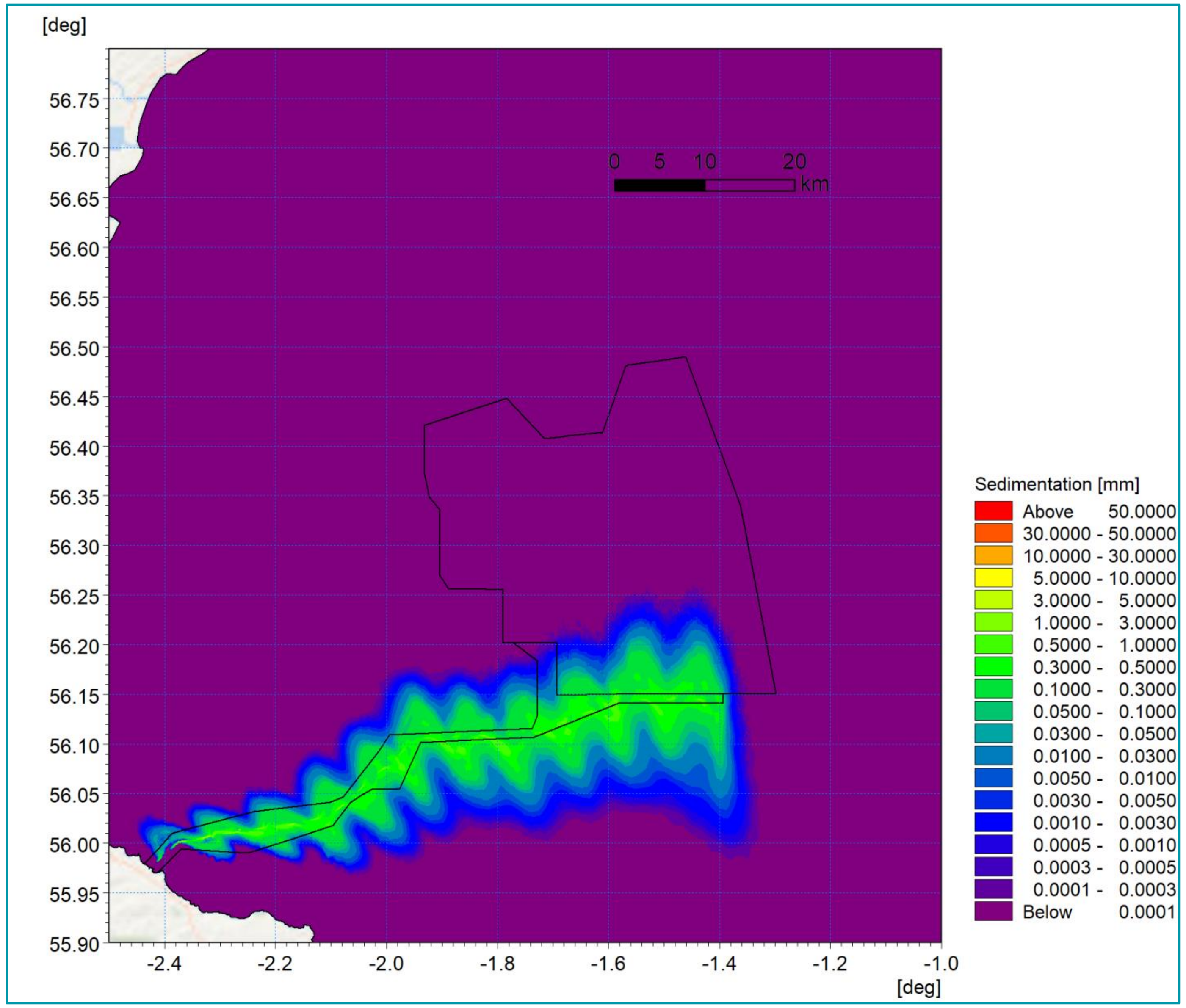


Figure 6.57: Average Sedimentation During Offshore Export Cables Installation

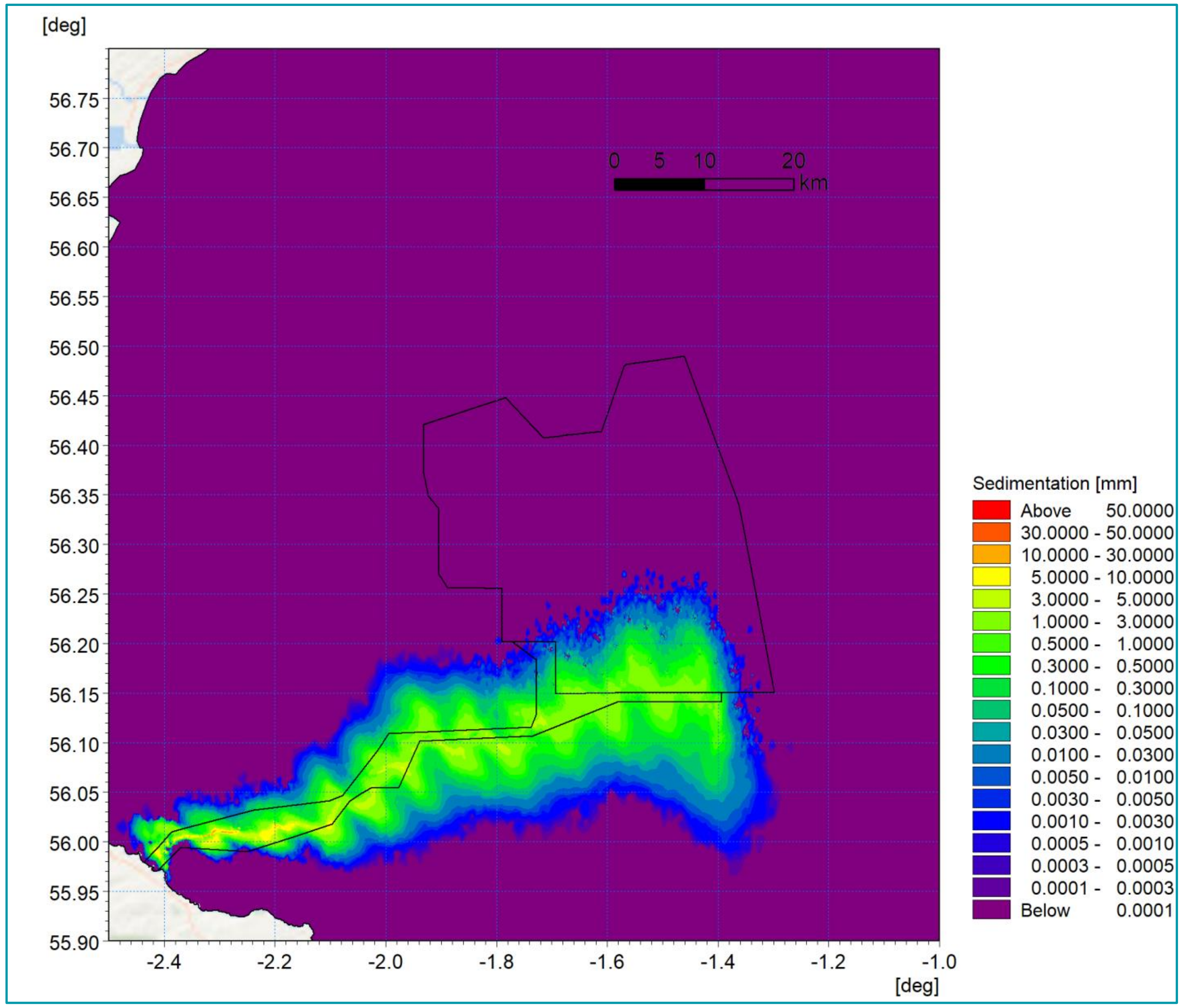


Figure 6.58: Sedimentation One Day Following Cessation of Offshore Export Cables Installation

# 7. SUMMARY

113. The Proposed Development is located within an area which encompasses the Firth of Forth Banks Complex MPA and a range of designations including bathing waters therefore the impact on physical processes is important in the assessment of the potential environmental impact. This report has outlined the baseline characteristics of the region in terms of coastal processes. This includes tidal current, wave climate and sediment transport under both calm and storm conditions. Numerical modelling has been used to quantify the changes in physical processes due to the installation of the Proposed Development. The presence of the wind turbine foundations redirects both waves and tidal flow and although some changes in sediment transport were revealed, these were limited in magnitude and represented an adjustment in the transport path alignment.

114. The installation of the Proposed Development was seen to marginally reduce wave heights in the lee of the structures whilst a marginal increase was noted at the periphery, however during larger storm events these effects were less marked. Any considerable changes in tidal currents and wave climate would not extend to the coastline and there would be no change in coastal processes in this area.

115. Finally, suspended sediment plumes for construction activities were quantified. In all cases, the material released was native to the bed sediments and, although there are short periods of increased turbidity, the material was retained in the sediment cell and would be subsequently assimilated into the existing sediment transport regime.

# 8. REFERENCES

BERR (2008). *Review of Cabling Techniques and Environmental Effects applicable to the Offshore Windfarm Industry. Technical Report*, Department for Business Enterprise and Regulatory Reform (BERR), in association with Defra, 164pp.

Berx, B, Hughes, S. (2009). *Climatology of Surface and Near-bed Temperature and Salinity on the North-West European Continental Shelf for 1971–2000.* Elsevier.

Centre for Environment, Fisheries and Aquaculture Science (Cefas) (2016). *Suspended Sediment Climatologies around the UK,* CEFAS.

Fugro (2012). *Seagreen Wind Energy Limited: Firth of Forth Zone Development – Metocean Study*.

Fugro (2020a). *Seagreen 2 and 3 Windfarm Zones Geophysical Survey – Final Survey Results Report – Export Cable Route*. Unpublished report for SSE Seagreen Wind Energy Limited, Fugro Document No: P906089-RESULTS-008 (01).

Fugro (2020b). *Seagreen 2 and 3 and ECR Windfarm Zone Geophysical Survey – Final Survey Results Report – Seagreen 2 and Seagreen 3*. Unpublished report for SSE Seagreen Wind Energy Limited, Fugro Document No: P906089-RESULTS-012 (01).

Graham, A. G. C., Lonergan, L. and Stoker, M. S. (2009). *Seafloor glacial features reveal the extent and decay of the last British Ice Sheet, east of Scotland*. J. Quaternary Sci., Vol. 24 pp. 117–138. ISSN 0267-8179.

HR Wallingford (2009). Firth of Forth and Tay Developers Group, Collaborative Oceanographic Survey, Specification and Design. *Work Package 1. Review of existing information*.

HR Wallingford (2012). *Appendix E3 – Geomorphological Assessment*. Seagreen Wind Energy. Available at: http://marine.gov.scot/datafiles/lot/SG_FoF_alpha-bravo/SG_Phase1_Offshore_Project_Consent_Application_Document%20(September%202012)/006%20ES/Volume%20III_Technical%20Appendices/Part%201_Technical%20Appendices/Appendix%20E3.pdf. Accessed September 2021.

Partrac Ltd (2020) *P1936.05.03.01.D01v1- SG1 SSE Berwick & Marr Bank Metocean*.

Partrac Ltd (2020) *P1936.05.03.01.D02v01- SG2 SSE Berwick & Marr Bank Metocean*.

Partrac Ltd (2020) *P1936.05.03.01.D03v01- SG3 SSE Berwick & Marr Bank Metocean*. Ramsay and Brampton (2000). *Coastal Cells in Scotland: Cell 1 - St Abb's Head to Fife Ness*. Available at: http://www.dynamiccoast.com/resources. Accessed September 2021.

SSER (2021a) *Berwick Bank Offshore Scoping Report.* Available at: BERWICK BANK WIND FARM Offshore Scoping Report - Introduction (berwickbank-eia.com)

XOCEAN Ltd (2021) *00338 SSE Berwick Bank Lot 1 & 2 Operations and Results Report*. Unpublished report for SSER

sse | For a better world of energy